

Multidecker assemblies from Porphyrin and Phthalocyanine derivatives

Norah Ali Alsaiari

This thesis is submitted in partial fulfilment of the requirements of the degree of Doctor of
Philosophy at the University of East Anglia



Supervised by Prof Andrew N. Cammidge.

July 2022

©This copy of the thesis has been supplied on condition that anyone who consults it is understood to recognise that its copyright rests with the author and that use of any information derived there from must be in accordance with current UK Copyright Law. In addition, any quotation or extract must include full attribution.

Declaration

The research described in this thesis is, to the best of my knowledge, original and my own work except where due reference has been made.

Norah Alsaiari

Dedication

This thesis is dedicated to my father's soul

My father who was waiting for this moment, passed away unexpectedly on

14 Feb 2020.

Abstract

The work set out in this thesis focuses on the synthesis and investigations of linked heteroleptic triple deckers (TD) based on porphyrin-phthalocyanine-porphyrin analogues. They are interesting materials because of the potential applications of lanthanide-bridged triple and double deckers in molecular devices. Research on their synthesis has taken huge steps forward in recent years. They also have low oxidation potentials, as well as reversible electrochemistry. Such remarkable features give these complexes great potential for their use in several applications, for example, molecular magnets, multibit molecular information storage, sensors, nonlinear optical materials, nanomaterials and field effect transistors that cannot be achieved by their mono- metallic macrocycle counterparts. A number of multidecker systems have previously been synthesised by Cammidge group.

Firstly, this current research focuses on phthalocyanine and related macrocycles by attempting to synthesise unsymmetrical systems that could be inserted in a triple-decker formed by the reaction with linked porphyrins, with a view to preparing higher order structures through linking this unsymmetrical central macrocycle. However, insertion of the selected phthalocyanines proved challenging. Triple decker structures were formed and isolated, but characterisation proved challenging, and the spectroscopic results could not prove that simple porphyrin-phthalocyanine-porphyrin were formed.

Secondly, we switched to the synthesis of alternative macrocycles such as tetrabenzotriazaporphyrins (TBTAPs) which are hybrid structures that lie between the parent phthalocyanine and tetrabenzoporphyrin macrocycles. Importantly, the meso carbon opens up a variety of possibilities in the TBTAPs. The synthesis of triple deckers with different meso- substituted TBTAPs has been achieved but the spectroscopic characterisation was much more complicated as compared to the previous symmetric phthalocyanine derivatives. Rotation is hindered (NMR) in these cases. Finally, the decision was taken to investigate a different class of multichromophore assemblies. We aimed to synthesise a compound that bears a more rigid element to the bridge that could be further functionalised or dimerised. Triple deckers of compounds that bear a more rigid element (such as benzene and porphyrin) to the bridge were successfully synthesised using the developed procedure for the selective formation of linked closed triple deckers, and overall, this appears to be a very promising strategy for building up more complex arrays of TDs.

Access Condition and Agreement

Each deposit in UEA Digital Repository is protected by copyright and other intellectual property rights, and duplication or sale of all or part of any of the Data Collections is not permitted, except that material may be duplicated by you for your research use or for educational purposes in electronic or print form. You must obtain permission from the copyright holder, usually the author, for any other use. Exceptions only apply where a deposit may be explicitly provided under a stated licence, such as a Creative Commons licence or Open Government licence.

Electronic or print copies may not be offered, whether for sale or otherwise to anyone, unless explicitly stated under a Creative Commons or Open Government license. Unauthorised reproduction, editing or reformatting for resale purposes is explicitly prohibited (except where approved by the copyright holder themselves) and UEA reserves the right to take immediate 'take down' action on behalf of the copyright and/or rights holder if this Access condition of the UEA Digital Repository is breached. Any material in this database has been supplied on the understanding that it is copyright material and that no quotation from the material may be published without proper acknowledgement.

Acknowledgements

I would like to express my sincere gratitude to my supervisor, Prof. Andrew N. Cammidge for all his support both personally and professionally. Also, for this great opportunity and all the motivation that he has provided all the way. This thesis would not have been possible without his guidance and supporting during all the time of research and writing up of this thesis.

I would like to extend my thanks to the past and present of my supervisory team for their valuable comments and supports Dr. Chris Richards, Dr. Maria Paz Muñoz-Herranz., and Dr. Isabelle Fernandes. I also thank Dr. Joseph Wright and Dr. David Hughes for X-Ray crystallography service.

I would especially like to thank Dr. Faeza Alkorbi, Dr. Ahad Alsahli and Shazia Soobrattee for their valuable support and friendship. I would like to thank all previous and current colleagues and friends with whom I have shared lab 3.08 for their support during my PhD. Also, a special thanks to my friends from other labs 3.17 and 3.10 with whom I have had a great time and will carry with me the great memories of our time spent together.

I am also grateful to the teaching, technical and administrative staff of the school of chemistry at UEA for their help throughout my degree.

I am very thankful to my husband, Marie, for his support and endless encouragement and for doing everything possible to help every step of the way, along with my wonderful children Omar, Fatimah, Saleh and Tamim who supporting and understanding all the time, give me the strength and the motivation to complete this journey. Without my family and their never-ending love, this research would not have survived. I would like to express my sincere gratitude to my parents and my brothers and sisters for encouraging and supporting me throughout my study in the UK. Although my father is no longer physically present in my life, I still feel his impact every day and grateful to him

I would also like to thank Saudi Culture Bureau and Najran University who provided full funding for this work.

List of abbreviations

acac	Acetylacetonate
Ar	aryl
BINAP	2,2'-bis(diphenylphosphino)-1,1'-binaphthyl
b.p	Boiling point
C ₁₀	Decane
C ₁₂	Dodecane
°C	Degrees Celcius
cm	Centimetre
COSY	Correlation spectroscopy
δ	Chemical Shift
DABCO	1,4-diazabicyclo [2.2.2] octane
DBU	1.8-diazabicyclo [5.4.0] undec-7-ene
d	Doublet
d-	Deuterated
dd	Doublet of doublets
DCM	Dichloromethane
DDQ	2,3-Dichloro-5,6-dicyano-1,4-benzoquinone
DMF	Dimethyl formamide
DMSO	Dimethyl sulfoxide
dt	Doublet of triplets
Et ₂ O	Diethyl ether
EtOAc	Ethyl acetate
ε	Extinction coefficient
eq	Equivalent
g	Grams
h	Hours
HOMO	Highest occupied molecular orbital
Hz	Hertz
IR	Infrared
<i>J</i>	Coupling constant
K	Kelvin

L	Ligand
Ln	Lanthanide
TD(La)	Lanthanum linked Triple deckers
LUMO	Lowest unoccupied molecular orbital
m	Multiplet
M (in structures)	Metal (any)
M	Molarity
MALDI-ToF-MS	Matrix-assisted laser desorption/ionization (time of flight)
Me	Methyl
MHz	Megahertz
min	Minutes
mg	Milligrams
ml	Millilitres
mm	Millimetres
mmol	Millimol
m.p.	Melting point
MS	Mass spectrometry
Mwt	Molecular weight
nm	Nanometres
NMR	Nuclear Magnetic Resonance
OMe	methoxy
oi	<i>Ortho</i> -inside
oo	<i>Ortho</i> -outside
Pc	Phthalocyanine
PDT	Photodynamic therapy
Pet.	Petroleum
Ph	phenyl
pm	Picometre
Por	Porphyrin
ppm	Parts per million
py	Pyridine
pyr	Pyrrole

q	Quadruplet
r.t.	Room temperature
λ	wavelength
s	Singlet
S	Solvent
SMM	Single-Molecule Magnets
t	Triplet
^t Bu	<i>tert</i> -butyl
TD	Triple decker
THF	Tetrahydrofuran
TLC	Thin Layer Chromatography
TPP	Tetraphenyl porphyrin
TPPOH	5,10,15-tris-phenyl-20-(<i>p</i> -hydroxyphenyl) porphyrin
tt	Triplet of triplets
UV-Vis	Ultraviolet-Visible

Table of Contents

1 Introduction	2
1.1 History of Porphyrins.....	2
1.1.1 Structure of porphyrin.....	2
1.1.2 Porphyrin nomenclature.....	4
1.1.3 Spectroscopic characteristics.....	5
1.1.3.1 Porphyrins' UV-Vis Spectroscopy.....	5
1.1.3.2 Porphyrins' NMR Spectroscopy.....	7
1.1.4 The synthesis of symmetric porphyrins.....	7
1.1.4.1 Rothmund synthesis.....	8
1.1.4.2 Adler synthesis.....	8
1.1.4.3 Lindsey synthesis.....	9
1.1.4.4 Conclusions.....	10
1.1.5 Synthesis of unsymmetrically substituted porphyrins.....	10
1.1.6 The reaction of porphyrins with metal ions.....	12
1.2 Phthalocyanine.....	13
1.2.1 History of Phthalocyanine.....	13
1.2.2 Structure of Phthalocyanines.....	14
1.2.3 Metallated Phthalocyanine.....	15
1.2.4 Absorption spectra of Phthalocyanine.....	16
1.2.5 Chemistry of formation of phthalocyanine.....	18
1.2.6 Synthesis of symmetrical Phthalocyanine.....	20
1.2.7 Synthesis of unsymmetrical Pcs (A3B type).....	21
1.3 Introduction to TBTAPs.....	22
1.3.1 Synthesis of TBTAPs.....	23
1.4 Dyads, triad and Sandwich type complexes.....	27
1.5 Synthesis of (porphyrin) (phthalocyanines) triple-decker complexes.....	28
1.5.1 Synthesis of Homoleptic complexes.....	28
1.5.2 Synthesis of heteroleptic complexes.....	30
1.6 Application of porphyrin, phthalocyanine and their triple decker.....	33

1.6.1 Photodynamic therapy.....	33
1.6.2 Detection of gaseous Nitric oxide.....	34
1.6.3 single-molecule magnet (SMM).....	35
References.....	37
2. Results and discussion.....	43
2.1 Introduction of the aims of project.....	43
2.2 Synthesis of the unsymmetrical tetrasubstituted porphyrin precursor TPP-OH 64	45
2.3 Synthesis of Porphyrin dyad 58	47
2.3.1 Optimisation of reaction conditions for C ₁₀ porphyrin dyad formation.....	49
2.4 Synthesis of metal-free phthalocyanine 13	51
2.5 Triple decker formation using unsubstituted phthalocyanine.....	52
2.5.1 Improvement attempts with low boiling point solvents.....	53
2.6.1 Synthesis of 6, 7-dicyano-1, 1, 4, 4-tetramethyltetralin.....	56
2.6.2 Synthesis of 4-hydroxyphthalonitrile 69	58
2.6.3 attempt of synthesis of unsymmetrical mono-hydroxy phthalocyanine.....	58
2.6.4 Metal-free phthalocyanine 79	59
2.7 Synthesis of closed triple decker 80 from symmetrical Pc 79	60
2.8 Synthesis of closed triple decker 86 from t butyl phthalonitrile 85	64
2.9 Synthesis of phthalocyanine- phthalocyanine dimer.....	68
2.9.1 Synthesis of Pc-Pc dimer 91	68
2.9.2 Attempt to synthesis of Pc-Pc dimer 92	71
2.10 Conclusion.....	72
2.11 Porphyrin and tetrabenzotriazaporphyrin arrays.....	72
2.11.1 Background and aims.....	72
2.11.2 Synthesis of aminoisoindoline 48	75
2.11.3 Synthesis of meso-substituted TBTAPs.....	77
2.11.4 Attempts of synthesis of triple decker with meso-substituted TBTAP 50	79
2.11.5 Attempts of synthesis of triple decker with meso-substituted TBTAP 102	84
2.11.6 Attempts of synthesis of triple decker with meso-substituted TBTAP 104	86
2.11.7 Synthesis of aminoisoindoline 107	87
2.11.8 Synthesis of meso-substituted TBTAP 104	89

2.11.9 Synthesis of TBTAP 104 by the intermediate 109	93
2.11.10 Attempts of synthesis of triple decker with meso-substituted TBTAP.....	95
2.11.11 Synthesis of closed triple decker with C ₁₂ porphyrin dyad.....	97
2.11.12 Conclusion.....	99
2.13 Multiple chromophores with a more rigid element to the bridge.....	99
2.13 Synthesis of dyad porphyrin with substituted benzene in the bridge.....	101
2.13.1 Synthesis of bromoalkoxyporphyrin 117	101
2.13.2 Synthesis of dyad 119	103
2.13.3 Synthesis of closed triple decker 120	105
2.13.3.1 ¹ H NMR characterization of closed triple decker 120 complex.....	107
2.13.4 Synthesis of trimeric porphyrin with porphyrin in the bridge.....	111
2.13.5 Synthesis of unsymmetrically substituted porphyrin.....	112
2.13.5.1 Synthesis of 5-(3,5-dimethoxyphenyl)-10,15,20-triphenylporphyrin 122	112
2.13.5.2 Synthesis of 5-(3,5-dihydroxyphenyl)-10,15,20-triphenylporphyrin 123	114
2.13.5.3 Synthesis of Zinc porphyrin 124	114
2.13.5.4 Synthesis of bromoalkoxyporphyrin 126	115
2.13.5.5 Synthesis of trimer 125	116
2.13.5.6 Synthesis of closed triple decker 127	118
2.13.5.7 Conclusion and future work.....	120
References.....	122
3. Experimental	125
3.1 General Methods.....	125
3.2 Synthesis of TPP-OH 64	126
3.3 Synthesis of tetraphenylporphyrin (TPP) 4	127
3.4 Synthesis of Porphyrin C ₁₀ dyad 58	127
3.5 Synthesis of Porphyrin C ₁₂ dyad 112	128
3.6 Synthesis of Substituted Phthalonitrile.....	129
3.6.1 Synthesis of 2, 5-Dichloro-2, 5-dimethylhexane 72	129
3.6.2 Synthesis of 1, 1, 4, 4-Tetramethyl-1, 2, 3, 4-tetrahydronaphthalene 73	129
3.6.3 Synthesis of 6, 7-dibromo-1,1,4,4-tetramethyl-1,2,3,4-tetrahydronaphthalene 74	130
3.6.4 Synthesis of 6,7-Dicyano-1,1,4,4-tetramethyl-1,2,3,4-tetrahydronaphthalene 68	130

3.7 Synthesis of 4-hydroxyphthalonitrile 69	131
3.8 Synthesis of bisphthalonitrile 89	131
3.9 Synthesis of bisphthalonitrile 90	132
3.10 Synthesis Metal free phthalocyanine 13	133
3.11 Synthesis of Metal-free phthalocyanine 79	133
3.12 Synthesis of Tetra-tert-butyl-phthalocyanine 85	134
3.13 Closed triple decker dyad 59	134
3.14 Synthesis of 2-bromobenzamidine hydrochloride 46	135
3.15 Synthesis of aminoisindol 48	136
3.16 Synthesis of aminoisindol 101	137
3.17 Synthesis of aminoisindol 107	137
3.18 Synthesis of Aza-dipyrromethene 108	138
3.19 Synthesis of compound 109	139
3.20 Synthesis of MgTBTAP.....	140
3.20.1 Synthesis of MgTBTAP-(4-OMe-Ph) 50	141
3.20.2 Synthesis of MgTBTAP-(thiophenyl) 104	142
3.20.3 Synthesis of MgTBTAP-(phenyl) 102	143
3.21 Synthesis of metal-free TBTAPs.....	143
3.22 Closed triple decker	144
3.22.1 Closed triple decker 86	144
3.22.2 Closed triple decker formulated as 96	145
3.22.3 Closed triple decker formulated as 103	146
3.22.4 Closed triple decker formulated as 111	146
3.23 Synthesis of homoleptic double decker 82 from symmetrical Pc 79	147
3.24 Synthesis of homoleptic double decker 82 from symmetrical Pc 79	148
3.25 Synthesis of double decker 115	148
3.26 Synthesis of 5-(3,5-dimethoxyphenyl)-10,15,20-triphenylporphyrin 122	149
3.27 Synthesis of 5-(3,5-dihydroxyphenyl)-10,15,20-triphenylporphyrin 123	150
3.28 Synthesis of Zinc 5-(3,5-dihydroxyphenyl)-10,15,20-triphenylporphyrin 124	151
3.29 Synthesis of bromoalkoxyporphyrin.....	151
3.30 Synthesis of dimer porphyrin 119	154

3.31 Synthesis of dimer porphyrin 125	155
3.32 Synthesis of closed triple decker 120	156

Chapter 1: Introduction

1. Introduction

1.1 History of Porphyrins

The word porphyrin is derived from *porphura*. They are a large class of deeply coloured pigment, with both natural and artificial origin. Porphyrins consist of four pyrrole rings linked by four methine bridges.^[1]

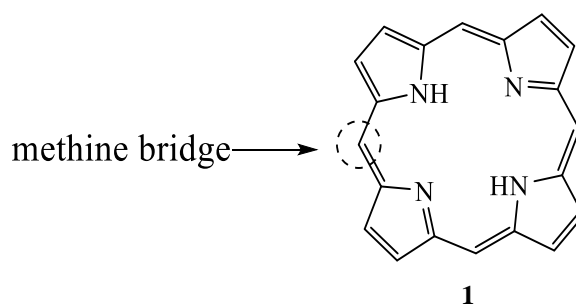


Figure 1.1: The structure of porphyrin

The porphyrins are an essential class of naturally occurring macrocyclic compounds formed in biological systems that assume a vital part in the metabolism of living beings. Some of the best examples are the iron-containing porphyrin found as heme **2** (of haemoglobin) and the magnesium-containing reduced porphyrin (or chlorin) found in chlorophyll **3**.^{[2], [3]}

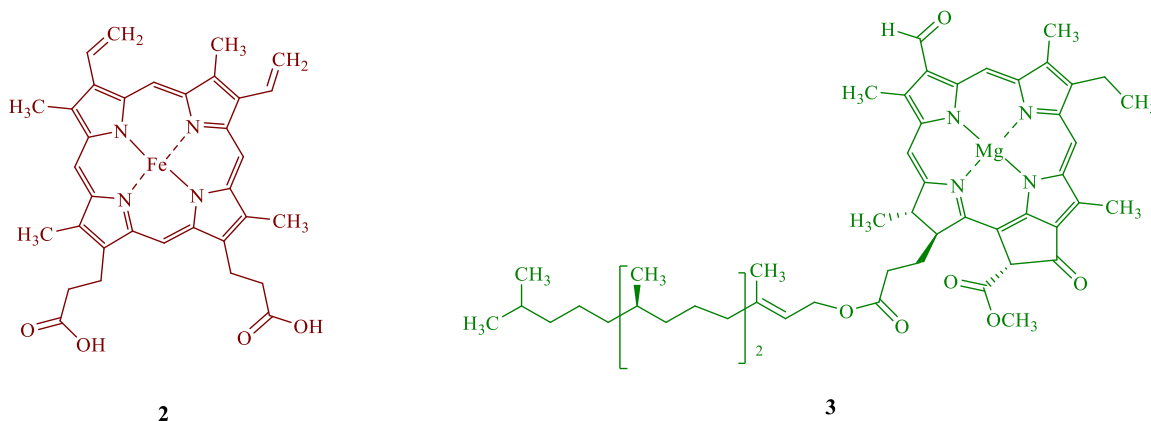


Figure 1.2: Naturally occurring porphyrins.

1.1.1 Structure of porphyrin:

Porphyrins are aromatic macrocyclic systems and have a π system of 22 π electrons, 18 of which are incorporated into the delocalised system on the ring in accord with Hückel's rule of aromaticity $[4n+2]$ where $n=4$.^[4] Hollingsworth has stated that there are six distinct delocalised porphyrin pathways containing 18π electrons.

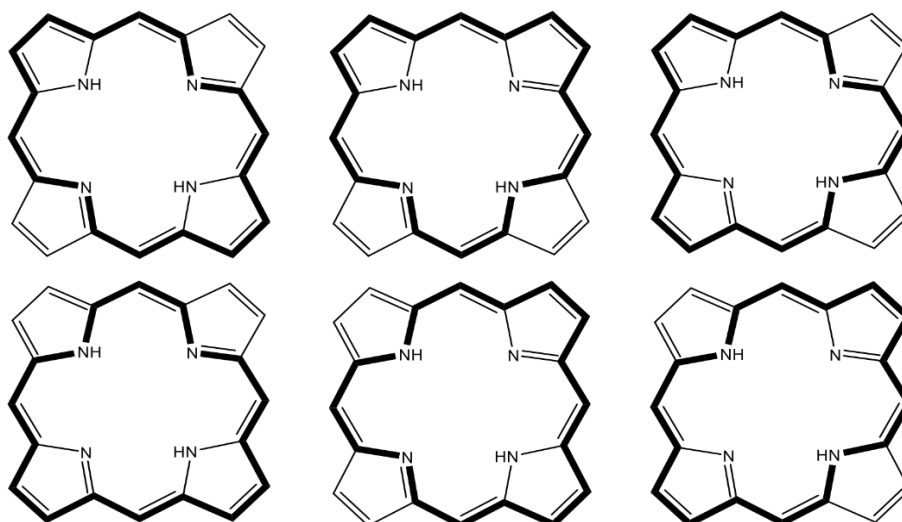


Figure 1.3: Six porphyrin cores illustrating the different delocalisation of 18π electrons.

Some research from ^{13}C NMR and X-Ray analysis suggests that the 16 membered ring of the 18π electrons systems is more favoured for the delocalisation pathway in the porphyrin.^{[4],[5]}

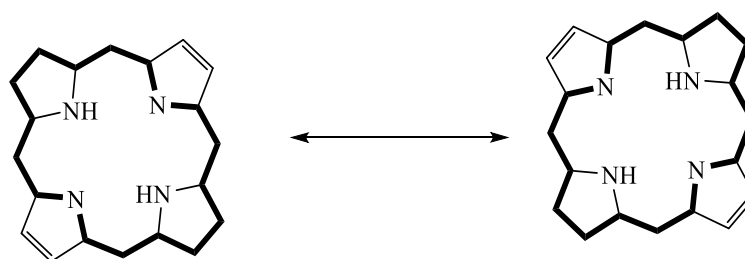


Figure 1.4: Delocalisation of 18π electrons on porphyrin ring system.

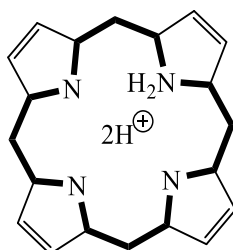


Figure 1.5: The favoured π electron delocalisation pathway.

There are two types of porphyrin substitution, β -substituted porphyrins and *meso*-substituted porphyrin. The β -substituted porphyrins are naturally found in many forms and *meso*-substituted porphyrins are the most interesting in synthetic chemistry.^[6]

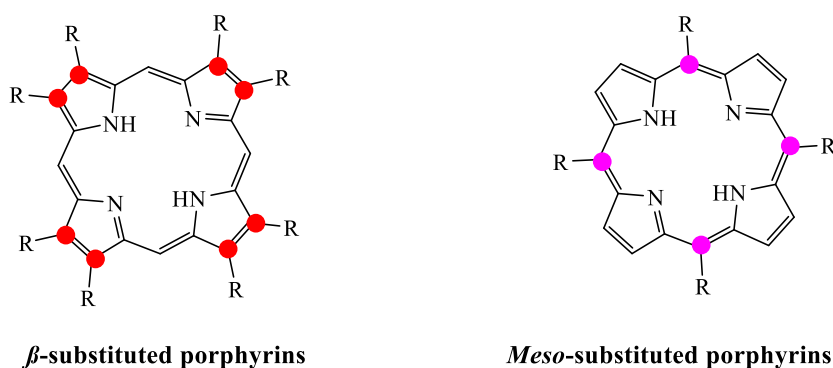


Figure 1.6: Structure of β - substituted and *meso*-substituted porphyrins.

Unsubstituted porphyrins can exist in two different tautomeric structures. NMR studies show that tautomer **A**, which carries two H on two opposite pyrrole rings, is more stable than tautomer **B** which carries 2H at adjacent pyrrole rings. The exchange between trans tautomers **A** and **C** is rapid at room temperature (figure 1.7).^[7]

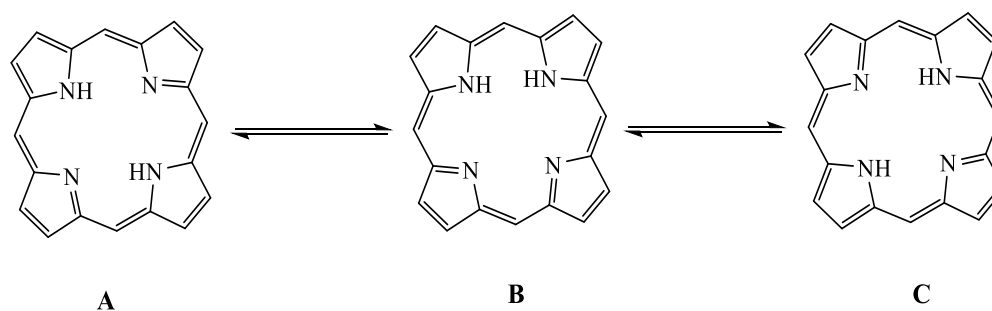


Figure 1.7: Tautomerisation of porphyrins

1.1.2 Porphyrin nomenclature:

According to IUPAC rules, positions 5, 10, 15 and 20 are referred to as *meso*, positions 2, 3, 7, 8, 12, 13, 17 and 18 are called β -pyrrole positions while 21 and 23 indicate the two nitrogen atoms bonded to the hydrogen atoms (figure 1.8). As indicated earlier the first kind of compound (*meso* -substituted porphyrin) are artificially made while the second kind (β -substituted porphyrin) are widely present in natural products.^[8]

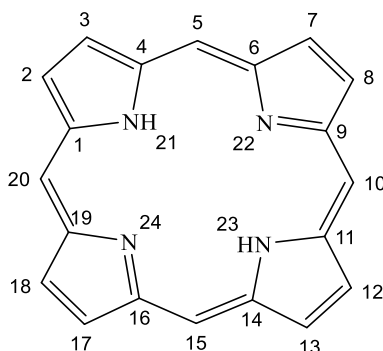


Figure 1.8: Porphyrin numeration

1.1.3 Spectroscopic characteristics:

1.1.3.1 Porphyrins' UV-Vis Spectroscopy:

The spectrum of absorption of porphyrins has been widely studied in terms of the four-orbital model [two highest occupied π orbitals and two lowest unoccupied π^* orbitals] which was first introduced by Gouterman.^[9] It shows that charge localisation is important in the electronic properties of these materials. The absorption bands of porphyrins are formed which is caused by the transitions between two different orbitals, namely, the two LUMOs and the two HOMOs. The energy of these orbitals is influenced by the ring's metal centre and the substituents.

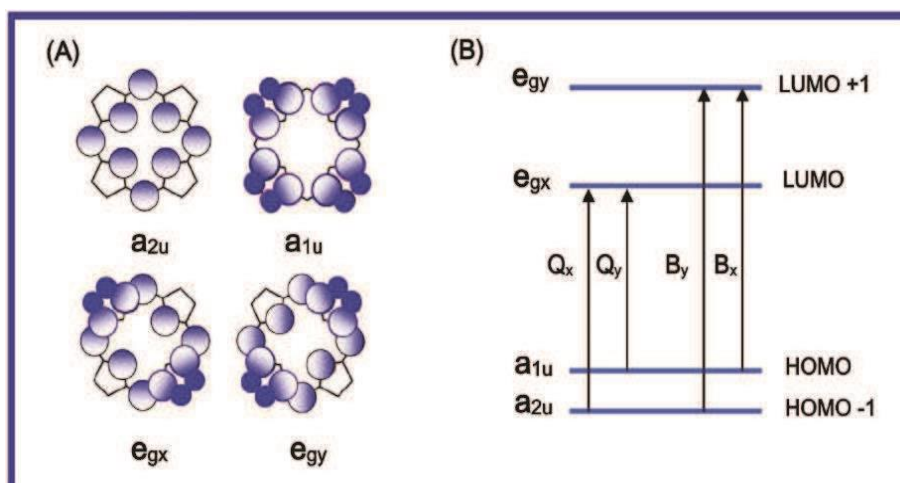


Figure 1.9: Porphyrin HOMOs and LUMOs. A) The illustration of the Gouterman orbitals. B) Energy level transitions of the orbitals according to Gouterman's theory.

Porphyrins show very characteristic absorption spectra because of their highly conjugated π system and the intensity and colour of porphyrins come from their absorption in two regions

of UV-Visible spectrum, in the near Ultraviolet and in the visible region.^[10] They show intense absorption from 380 to 420 nm called the Soret band or B band which is the transition from the ground state to the second excited state (S_0-S_2) and weaker absorption bands in the longer wavelength region (500-700nm) of visible light called Q band which corresponds to the transition from ground state to the first excited state (S_0-S_1).^[10] Metalloporphyrins are more symmetrical than metal-free porphyrins and therefore have only two Q bands. Metal-free porphyrins have four smaller Q bands between 500-700 nm (figure 1.10) and metalloporphyrins have two smaller Q bands between 500-700 nm (figure 1.11).^[11]

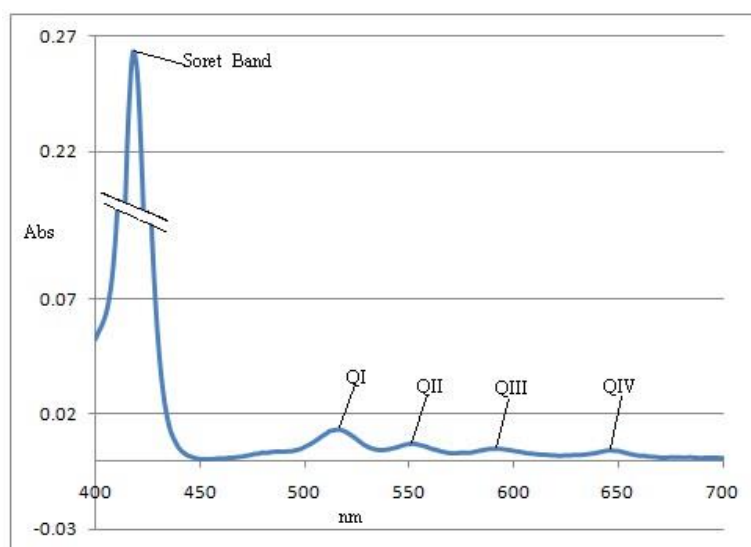


Figure 1.10: Typical H₂-Porphyrin UV-Vis Spectrum.^{[11],[10]}

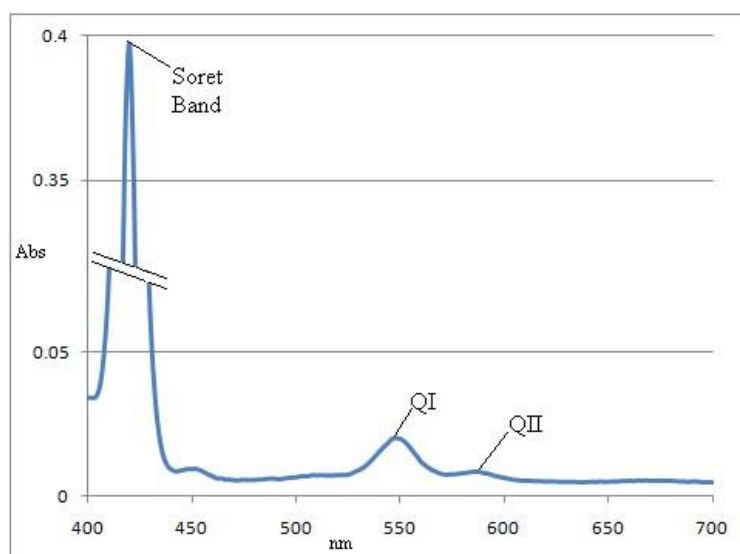


Figure 1.11: Typical Zinc-Porphyrin UV-Vis Spectrum.^[10]

The difference between the spectrum of metalloporphyrins and the metal-free porphyrin occurs because they have two different symmetry point groups. metal-free porphyrins have D_{2h} symmetry and metalloporphyrins have D_{4h} symmetry. As a result, this causes some of the energy levels to become degenerate and decreasing the number of Q bands.

1.1.3.2 Porphyrins' NMR Spectroscopy:

The porphyrin macrocycle has 22 π electrons and 18 of which are involved in the conjugated aromatic system (supported by Hückel's rule). It can be seen that there are strongly shifted downfield signals of the β -pyrrole and *meso*-protons due to the paramagnetic ring current which causes de-shielding effect. Additionally, the N-H protons of the rings are shifted upfield in the spectrum at the negative region, resulting from the shielding effect for the ring current as shown below in figure 1.12.

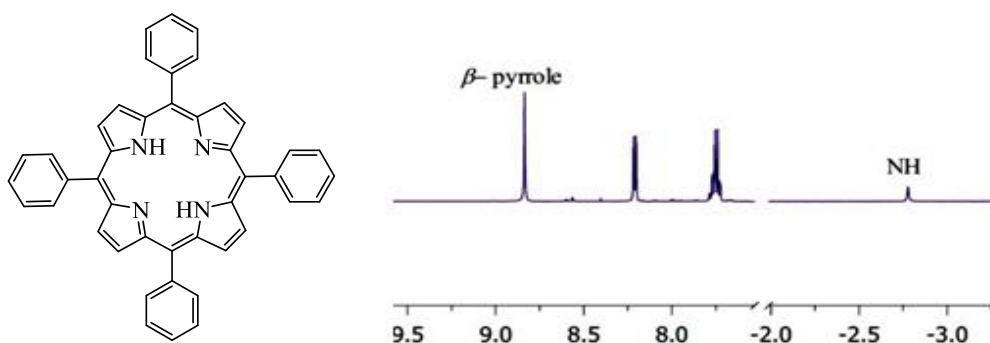


Figure 1.12: ¹H NMR spectrum of tetraphenyl porphyrin (TPP) **4**.

1.1.4 The synthesis of symmetric porphyrins:

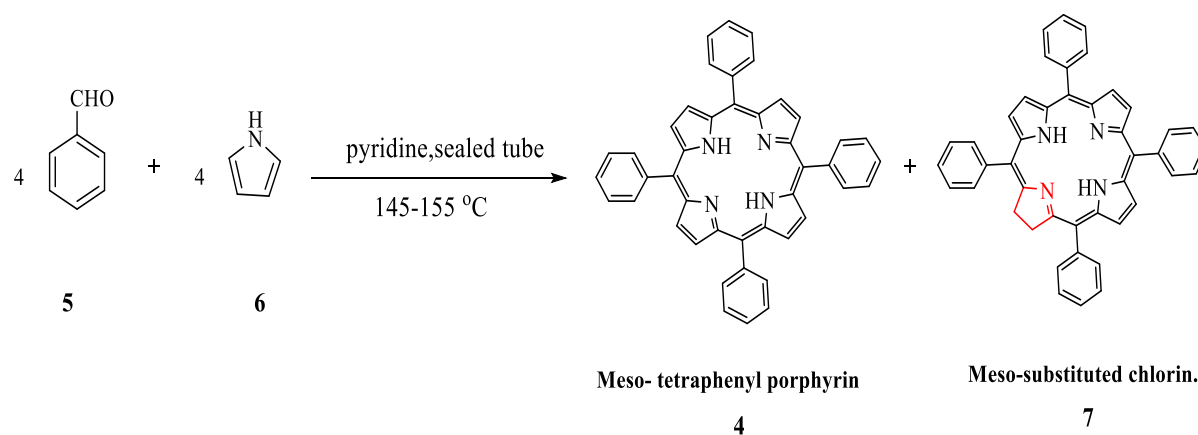
There are different strategies to obtain porphyrins which have many different positions where substituents can be placed.

The first simple synthesis of a porphyrin was confirmed by Fisher then after that a large number of synthetic methods have improved the preparation of porphyrin and its derivatives- especially for *meso* and β -substituted porphyrin, where the preparation of *meso*-substituted porphyrin is achieved by different strategies.^[12]

There are three main methods for the synthesis of *meso*-substituted porphyrins:

1.1.4.1 Rothemund synthesis:

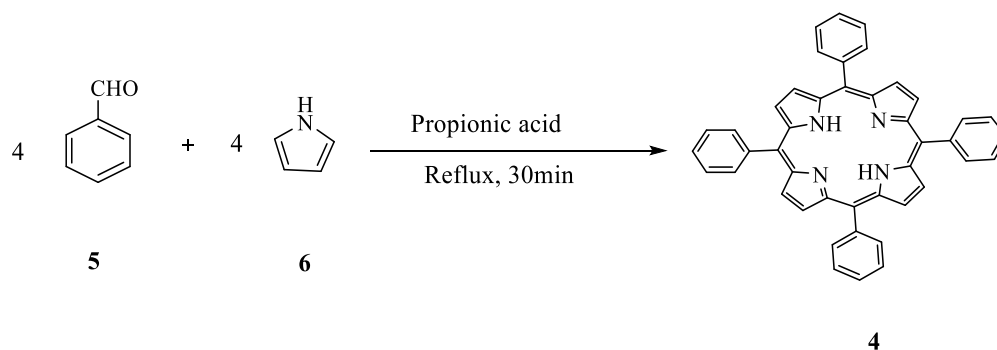
In 1935 Rothemund achieved the synthesis of *meso*-tetra substituted porphyrins by reacting pyrrole and acetaldehyde in methanol. Then in 1941 he mixed pyrrole with benzaldehyde in pyridine and this reaction was done in a sealed tube at 145-155 °C under nitrogen for 48h (Scheme 1.1).^[13] However, the yield obtained for the blue crystals of the *meso*-tetraphenyl porphyrin was less than 10%, as the main by-product of reaction was *meso*-substituted chlorin.^{[6],[14]} To understand the formation of this by-product, in 1946 Calvin and co-workers discovered when metal salts such as zinc acetate was added to the reaction mixture, the yield of porphyrin increased and the amount of chlorin compound decreased.^[14]



Scheme 1.1: Rothemund procedure.

1.1.4.2 Adler synthesis:

In the mid-1960's the synthesis of *meso*-substituted porphyrin was modified by the Adler-Longo method, by refluxing pyrrole and aldehyde at low concentrations in propionic acid for half an hour and open to air (Scheme 1.2).^[15] Propionic acid is ideal to use because many aldehydes are soluble in it and the porphyrin product crystallises out easily with relatively high yield. It was found that the yields of prepared porphyrin could be significantly improved under these acidic conditions. The yield of porphyrin was 30-40 %, and the chlorin contamination was lower than that obtained with the Rothemund methodology.

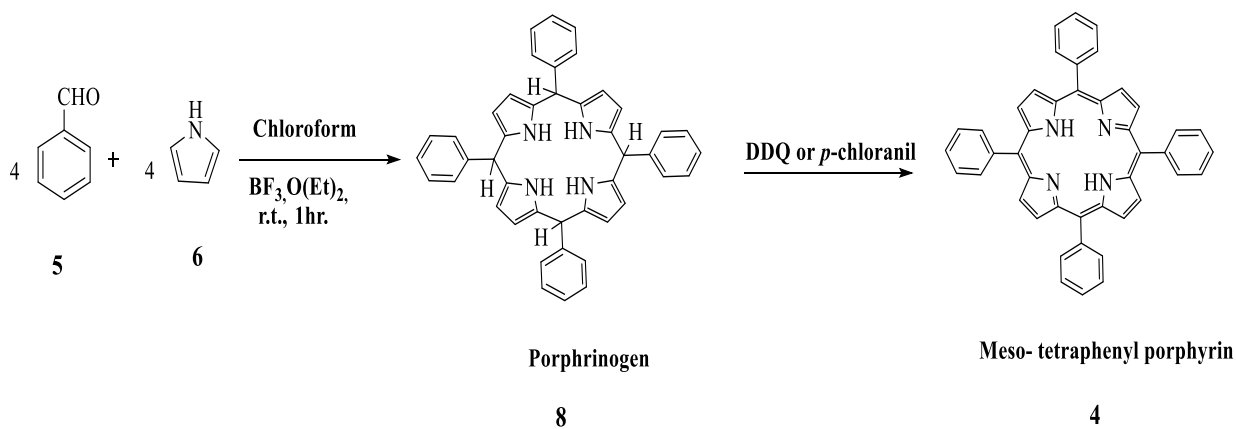


Scheme 1.2: Adler's procedure.

1.1.4.3 Lindsey synthesis:

Over the period 1979 -1986 Lindsey developed a new two step one flask method to synthesise porphyrins, in order to increase the number of porphyrins produced from using various aldehydes.^[16]

The synthesis used a process of condensation and oxidation steps. To achieve equilibrium and avoid side reactions, in all steps of the preparation of porphyrins the reaction was carried out under mild conditions. The reaction requires a condensation of pyrrole with aldehydes in chloroform or dichloromethane in the presence of acid catalyst, TFA or borontrifluoride etherate and under inert atmosphere and room temperature (Scheme 1.3).^[17] A stoichiometric amount of DDQ or *p*-chloranil is then added to oxidise the initially formed porphyrinogen to porphyrin,^[17] to yield 35-40 % of the product (meso-tetraphenyl porphyrin).^[17]



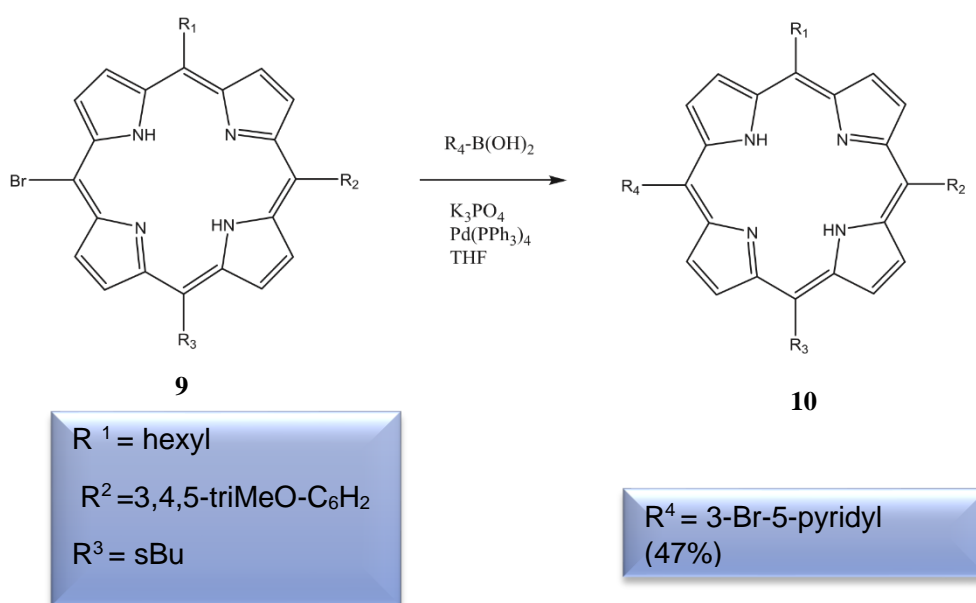
Scheme 1.3: Lindsey's two-step, one-flask synthesis of meso-substituted porphyrins.

1.1.4.4 Conclusions:

In conclusion there are three main methods for making meso-substituted porphyrins, and a comparison of porphyrin synthesis methods proves that the Rothmund synthesis produced a low yield, and it has no preference while Adler's method produce better yield of porphyrin, but it still has some disadvantages for benzaldehydes bearing substituents that are unstable in high temperature and acidic conditions which failed with this method. Also, there are purification problems because of using propionic acid. However, Lindsey method gave a higher yield of porphyrin than Rothmund and Adler methods. Also, purification of porphyrin is easier due to fewer by-products that are formed. Drawbacks to this method is that the purification usually involves chromatography and the high volume of solvent used restricts the reaction scale. In this case, it may be better to use the Adler method.

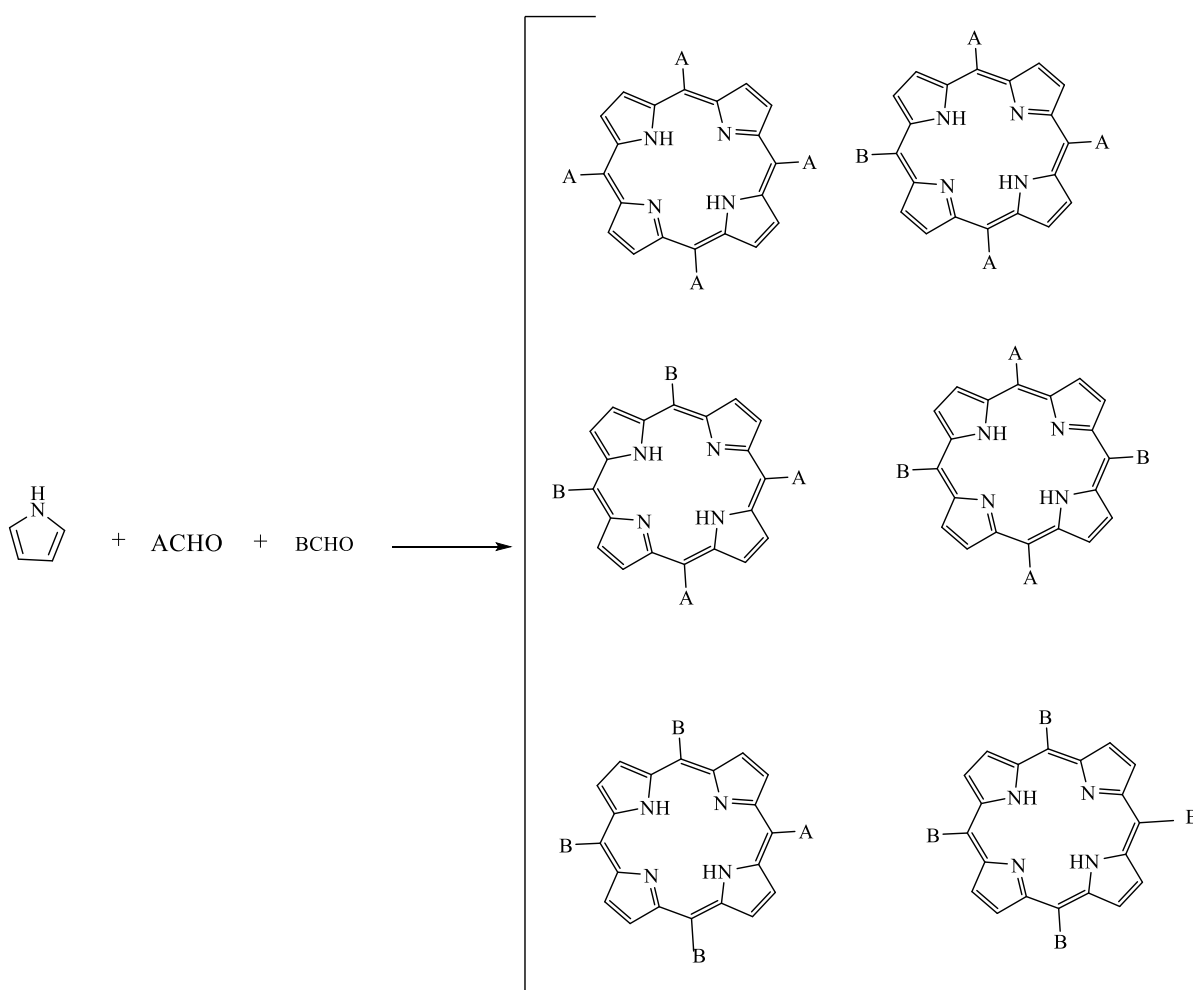
1.1.5 Synthesis of unsymmetrically substituted porphyrins:

A typical example of the unsymmetrically meso-substituted porphyrins is the ABCD-type porphyrins where four different substituents are found at the meso-position.^{[18],[19]} There are different pathways to synthesise the unsymmetrical substituted porphyrin, but no ideal method is known. Senge and co-workers^[19] achieved a new route for the synthesis of ABCD-type porphyrins through bromination of the ABC porphyrins, followed by Pd-catalyzed C–C-couplings as shown in the scheme below.



Scheme 1.4: ABCD-type porphyrin synthesis.^[19]

Amongst the numerous methods is the synthesis of AAAB porphyrin via mixed aldehyde condensation involving a mixture of two aldehydes with pyrrole as precursors to obtain a statistical mixture of products, or similarly using a combination of different pyrrole building blocks.^[20] Scheme 1.5 shows the synthesis using two different aldehydes. More elegant methods are known, such as those involving pre-synthesis of pyrrole-aldehyde intermediates. However, an acid-catalysed environment is required for such condensations. This can be problematic as it has the potential to scramble the pyrrole units, which puts a limit to the reaction's scope.



Scheme 1.5: Example of mixed condensation to give unsymmetrical porphyrins.

1.1.6 The reaction of porphyrins with metal ions:

Generally porphyrins are synthesized in a metal free form and metal ions incorporated into the structure when a metal ion M^{n+} is inserted into the porphyrin H_2P to form $MPor^{(n-2)+}$ and the two N-H protons in H_2P are replaced.^[3]



The size of the porphyrin-macrocycle is perfectly matched to many metal ions and an extensive number of metals can be embedded in the center of macrocycle (e.g., Zn, Cu, Ni, Co, etc.). Metalloporphyrins play important roles in many biochemical processes. Depending on the size of metal ions and charge, they can fit into the center of the cavity. As a result regular metalloporphyrins are formed which are kinetically inert complexes.^[3]

Most of the naturally occurring metalloporphyrins are regular types in which metal ions are located within the plane of tetrapyrrolic ligand due to their size match, where the ionic radii is between 55-80 pm figure 1.13.^[21]



Figure 1.13: Schematic representation of regular metalloporphyrin.

However, the metal ions whose ionic radius between 80-90 pm are too large to locate into the center of macrocycle, and therefore they are located out of the ligand plane, thus forming sitting atop (SAT) metalloporphyrins as illustrated in figure 1.14.^[21]

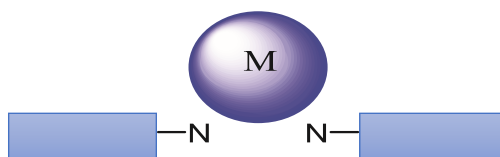


Figure 1.14: Schematic representation of SAT porphyrin.

The affinity of the ligand to the metal will determine whether or not it can combine with the metal ion in the porphyrin core. In general, the tetracoordinate complex has a poor affinity

for additional ligands since divalent metal ions like Co (II), Ni (II), and Cu (II) are already bonded to it. When combined with a fourth ligand, chelates of Mg (II), Cd (II), and Zn (II) easily form penta coordinate complexes with square-pyramidal structures. In the presence of metals such as Ru(II), Fe(II), and Mn, metalloporphyrins with two additional ligands resulted in a deformed octahedral geometries.^[22]

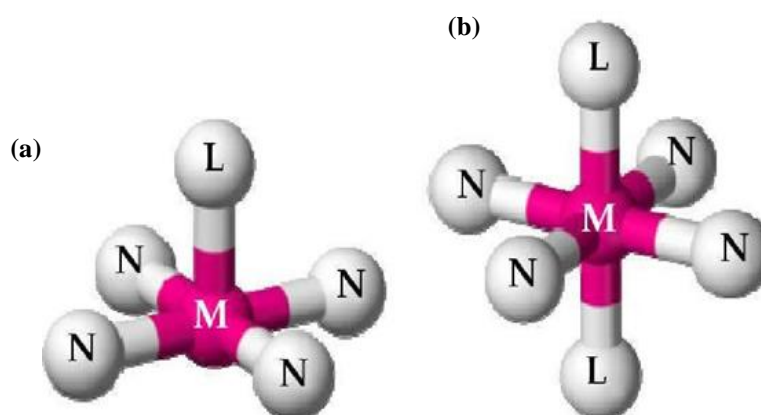
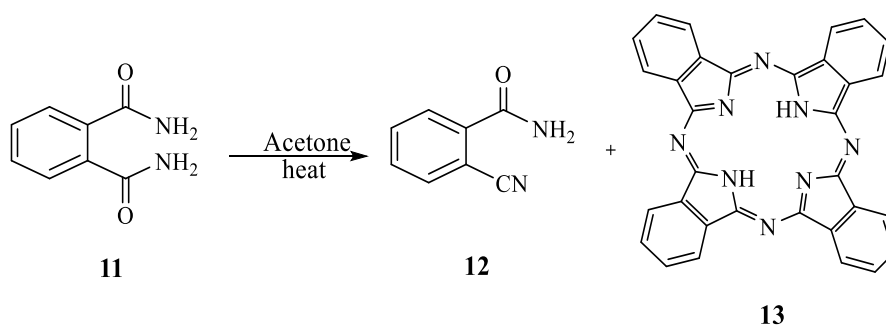


Figure 1.15: Schematic pictures of square-pyramidal (a) and octahedral structures (b) (only enclose nitrogen N, metal M and extra ligands L).^[22]

1.2 Phthalocyanine:

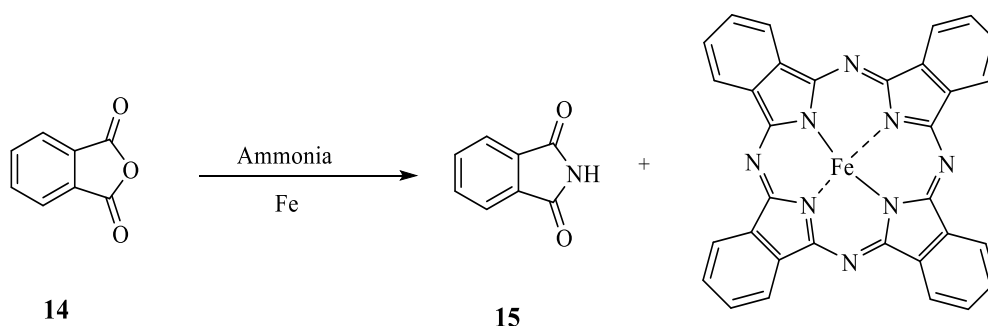
1.2.1 History of Phthalocyanine:

In 1907, an unidentified blue compound was discovered by Braun and Tcherniac as by-product during the preparation of *o*-cyanobenzamide from phthalamide in acetone (scheme 1.6) known as Phthalocyanines.^{[23],[24]}



Scheme 1.6: First synthesis of metal-free phthalocyanine.

In 1927, Swiss researchers accidentally discovered copper phthalocyanines, copper naphthalocyanine and copper octamethyl phthalocyanine when attempting to make phthalonitriles.^[25] Also, in the same year iron phthalocyanine was discovered at Scottish dyes of Grangemouth during the preparation of phthalimide from phthalic anhydride and ammonia (scheme 1.7). Iron phthalocyanine was produced as a dark blue compound.^[26]



Scheme 1.7: Synthesis of iron phthalocyanine. **16**

In 1934 Linstead was the first to use the term Phthalocyanines, deriving the name from the Greek words naphtha (rock oil) and cyanine (blue). He characterized the chemical and structural properties of iron Phthalocyanine.^[27]

1.2.2 Structure of Phthalocyanines:

The formal substitution of the four *meso*-methine bridges (=CH-) in porphyrin by nitrogen atoms (=N-) leads to *meso*-tetrazaporphyrin, which is commonly named as porphyrazine. Tetrabenzo analogues are called phthalocyanines, and structures are shown in (figure 1.16).

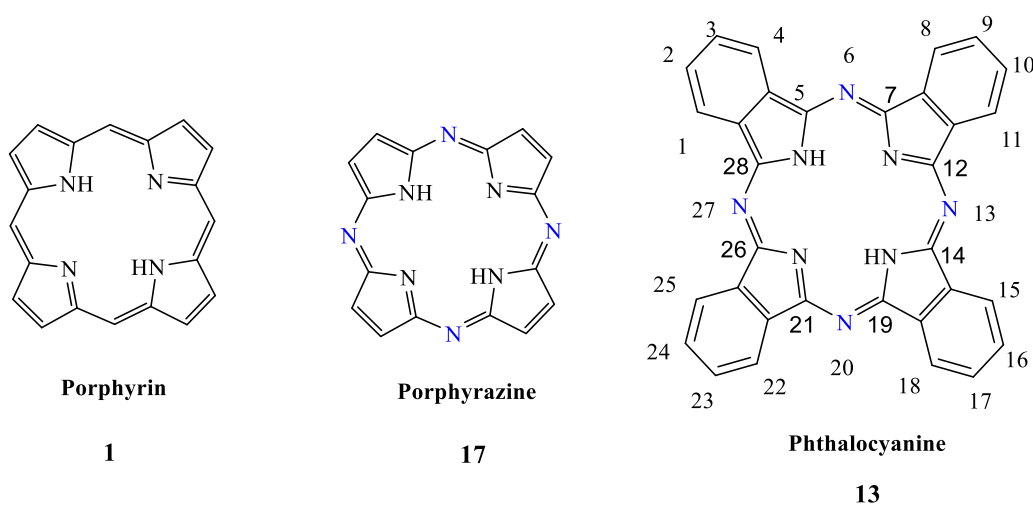


Figure 1.16: Molecular structures of tetrapyrrole macrocycles.

Phthalocyanine also has a ring system consisting of 18 π electrons which is delocalized over alternate carbon and nitrogen atoms. The delocalization of the π electrons gives the molecule unique physical and chemical properties.^{[28],[29]}

There are 16 possible sites in phthalocyanine where substituents can be placed on the benzene rings. Substituents can be incorporated on the *non-peripheral* or α -positions 1,4,8,11,15,18,22,25 and on the peripheral or β -positions 2,3,9,10,16,17,23 and 24.^[30]

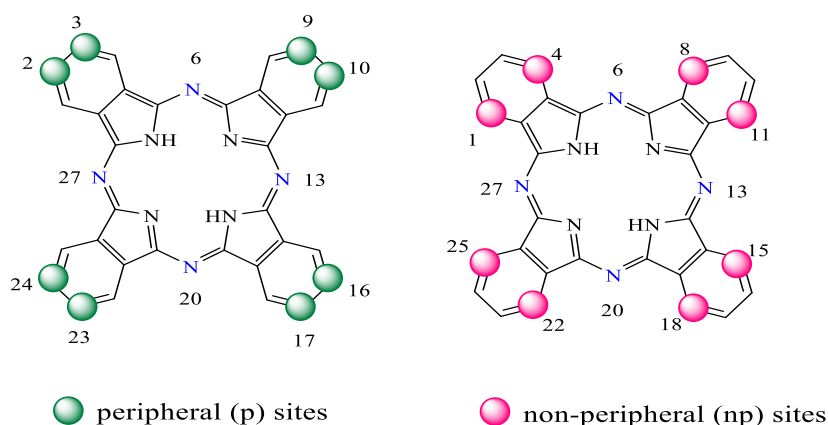


Figure 1.17: The non-peripheral and the peripheral positions of Phthalocyanine.

1.2.3 Metallated Phthalocyanine:

A Phthalocyanine (Pc) containing one or two metal ions is called metallo- Phthalocyanine. There are more than 70 different metals that can be bonded to the Phthalocyanine centre.^{[31],[10]} Some of these can fit into the central cavity of the Pc without affecting its structure, while the other metal ions can cause the macrocycle's structure to be distorted.^[32] There are two types of possible bonding between the central metal ion and the four nitrogen atoms: electrovalent and covalent.^[33] Small alkali metals that have an oxidation state of +1 such as (Li^+ , K^+ , Na^+ etc.) cannot fit into the central cavity of the Pc. This means that the surface of the Pc's planar form is distorted. This condition increases the solubility of the compounds in polar organic solvents. The four nitrogen atoms of the macrocycle form a link with the centre metal ion that is in the +1-oxidation state, which is known as an electrovalent bond because of its ionic nature and relative weakness.^[34] Transition metals, such as iron, copper, and cobalt, which have a +2-oxidation state, are able to fit into the central cavity of the Pc without affecting its structure. Formally, the two nitrogen atoms are then bonded to

the central metal atom with a +2 oxidation by covalent bonds and to the other two nitrogen atoms by coordinate covalent bonds (figure 1.18).^{[33],[34]}

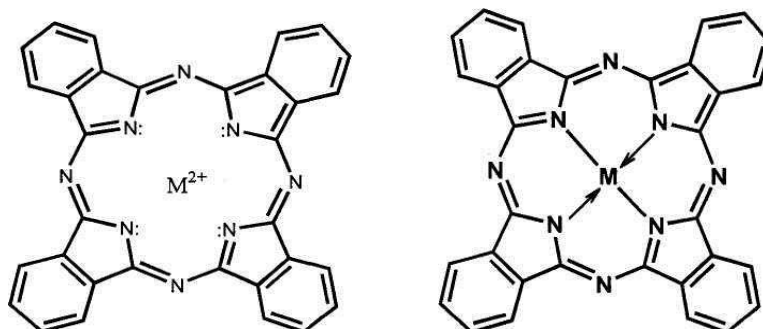


Figure 1.18: Central metal atom (M)-ligand bonding in Pc.^[33]

Some metals, such as tin and rhodium, which have oxidation state greater than +2, are known to form complexes with axial ligands to increase their solubility in organic solvents. Trivalent lanthanide ions, on the other hand, are not able to fit into the central cavity of the Pc due to their size. They prefer to form dimers or trimers, which are composed of two distorted phthalocyanine rings.^{[10],[35],[31]} Phthalocyanine derived metal complexes tend to aggregate and have low solubility, but the presence of metal ion in the Phthalocyanine central cavity allows for axial ligation which generally increases solubility and reduces molecular aggregation.^{[36],[33]}

1.2.4 Absorption spectra of Phthalocyanine:

There are various approaches used to characterise the Pcs. These methods include elemental analysis, nuclear magnetic resonance spectroscopy (NMR), infrared spectroscopy (IR), matrix-assisted laser desorption ionisation spectroscopy (MALDI), and many more. The most popular form of Pc characterisation is ultraviolet / visible spectroscopy (UV / Vis). Phthalocyanines strongly absorb light between 650-720 nm which represent the lowest energy absorption (Q band). This is responsible for the intense colour of the phthalocyanine, and its position is largely influenced by the central metal and the substituents on the Pc ring as transitions occur from $\pi - \pi^*$ orbitals.^[10] Also, a second band (Soret, B- band) appears as a broad band between 300-400 nm.^{[31],[37],[36]} Using Gouterman's four-orbital model (figure 1.19), the spectrum of phthalocyanine UV-Vis is understood; a model based on a linear combination of atomic orbitals (LCAO). The spectrum comes from transitions from

the two highest occupied molecular orbitals (HOMOs) which are the a_{1u} (π) followed by the a_{2u} (π) to the lowest unoccupied molecular orbital (LUMO) which is the doubly degenerate e_g (π^*) with b_{1u} (π^*) above it.^[10] The Q band occur from the π - π^* electronic transition that includes the a_{1u} and e_g orbitals. The B bands also occur from the π - π^* electronic transition that includes the a_{2u} or b_{2u} and e_g orbitals.^[10] Also, the Soret band was observed to split into two components, B_1 and B_2 , which occur at around the same energy and form the wide band shown in the spectra as shown in Figure 1.20.^{[10],[31],[37],[38]}

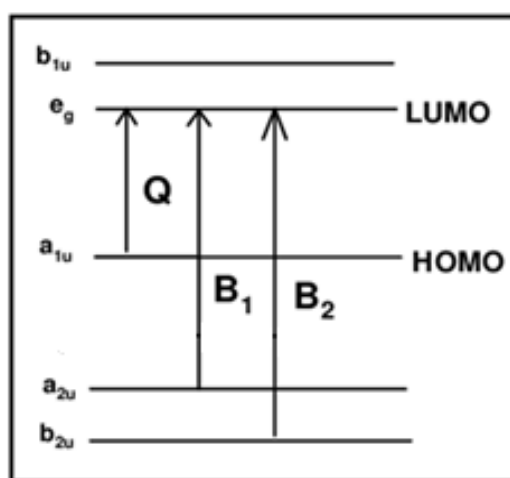


Figure 1.19: Energy level diagram of a phthalocyanine showing transitions that give rise to absorption bands.^[10]

In the case of metal phthalocyanine the symmetry of the MPc is attributed to the degenerate e_g -orbital and has one Q band. However, in the case of metal-free Phthalocyanine has a non-degenerate e_g orbital because of the loss of molecular symmetry.^{[36],[39]} The H_2Pc has two Q- bands as shown in Figure 1.20.

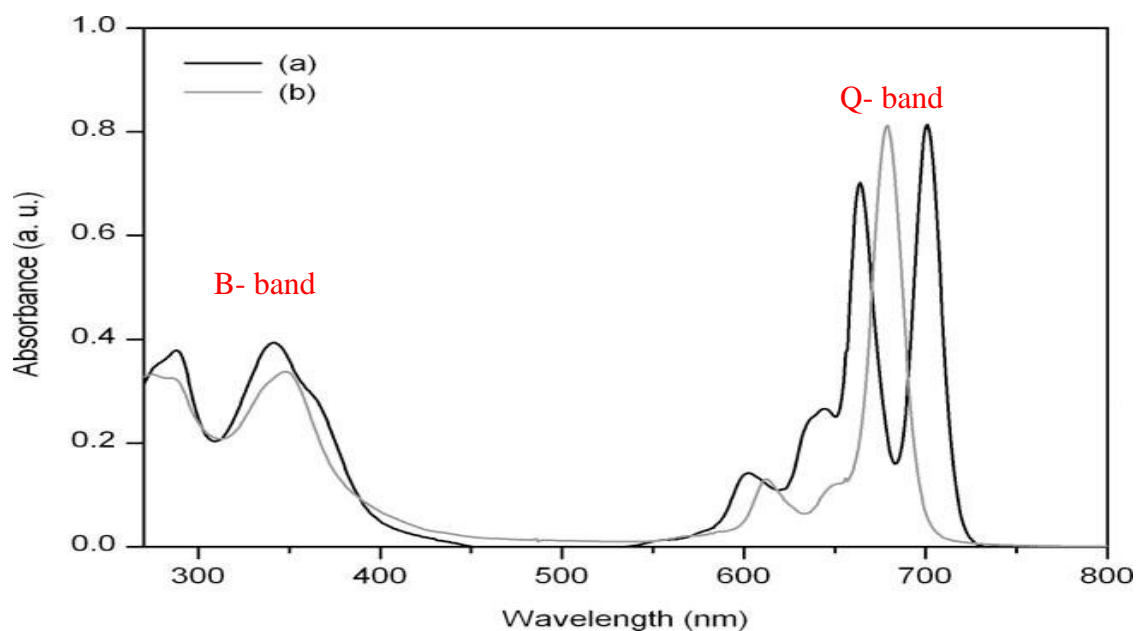
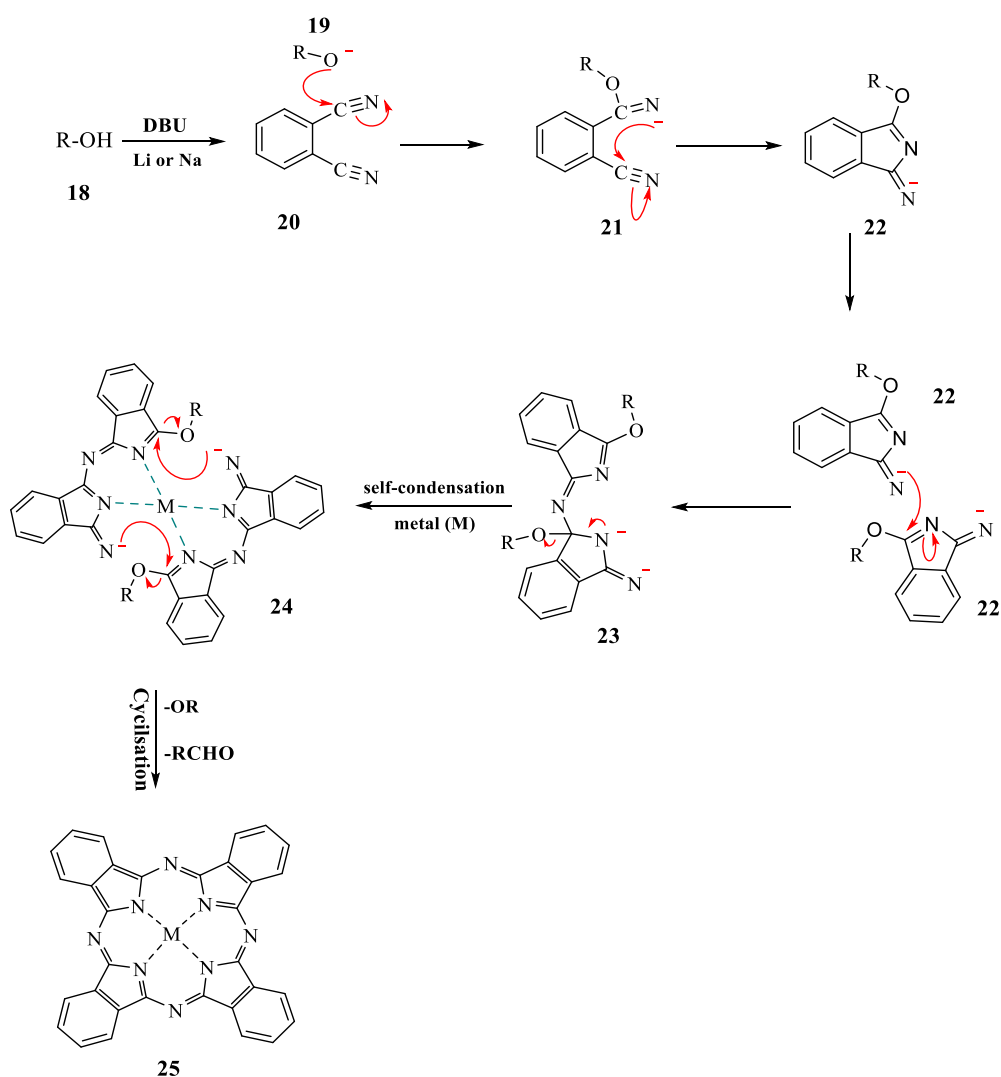


Figure 1.20 : Typical UV–vis spectra for a phthalocyanine as (a) a free-base and (b) a metal complex.^[10]

Substituted phthalocyanines show a shifted Q-band absorption relative to the unsubstituted phthalocyanine, the shift in absorption may be a blue (bathochromic) or red (hypsochromic) shift depending on the type of substituted functional groups. Substitution at the non-peripheral (α) position has been shown to cause a red shift as compared to peripheral (β) substitution shift to a blue region. This red shift is caused by the increased electron density of the ring resulting in a reduction of the phthalocyanine HOMO-LUMO energy gap. Also, electron donating groups have shown to enhance this red shift as compared to electron withdrawing substituents.^{[10],[36],[39]}

1.2.5 Chemistry of formation of phthalocyanine:

One possible mechanism suggested for the formation of metallophthalocyanine in the presence of an alcohol from the precursors phthalonitrile is shown in the scheme 1.8:

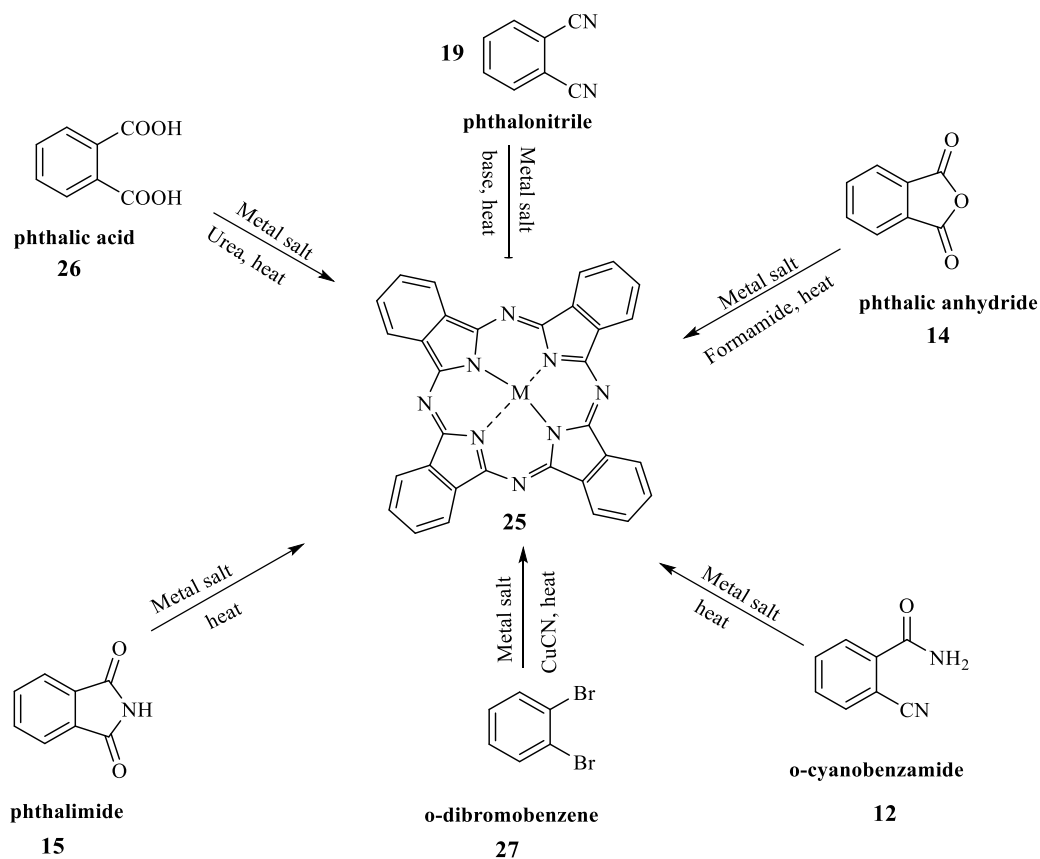


Scheme 1.8: Chemistry of formation of phthalocyanine starting from phthalonitrile.

The synthesis of phthalocyanine starts from phthalonitrile in the presence of alcohol. Firstly, deprotonation of alcohol by some base promoters such as DBU forms strong nucleophilic alkoxide species which attacks the nitrile in phthalonitrile. This leads to the intermediate **22** which can attach itself to another phthalonitrile, or as shown scheme 1.8 dimerise to give **23**. In this proposed mechanism intermediate **23** undergoes condensation to form the tetrameric intermediate **24**. Cyclisation of intermediate **24** occurs followed by the loss of an aldehyde, leading to the formation of the phthalocyanine molecule **25**.

1.2.6 Synthesis of symmetrical Phthalocyanine:

Phthalocyanine is prepared through the cyclotetramerization of different phthalic acid derivatives such as phthalimide, phthalic anhydride, phthalonitrile and diiminoisoindoline.^[40]



Scheme 1.9: Basic synthetic routes for preparing phthalocyanines.

The approach that is most popular for preparation of phthalocyanines and their complexes is based on phthalonitriles, by heating with a metal template in high boiling point solvent such as alcohols. The advantage of using phthalonitriles as precursor is that they are easy to handle and gave good yield of phthalocyanines and their complexes. Other precursors such as phthalimide and other phthalic acid derivatives often give unreliable results. This method was studied by Linstead.^[41]

Another method is the Tomoda method, which was reported in 1980, by heating phthalonitrile with catalytic amount of DBU or DBN in the presence of metal salt. This method has advantage for good yield for both product Pcs or metal Pcs, using the strong

base such as DBU or DBN favoured the formation of Pcs and gives higher yield than used weaker bases such as Piperidine and TEA.^{[42],[43]}

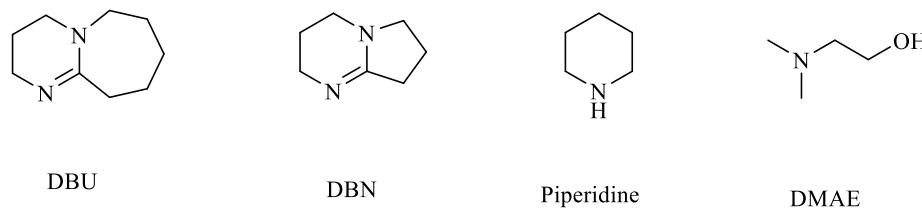
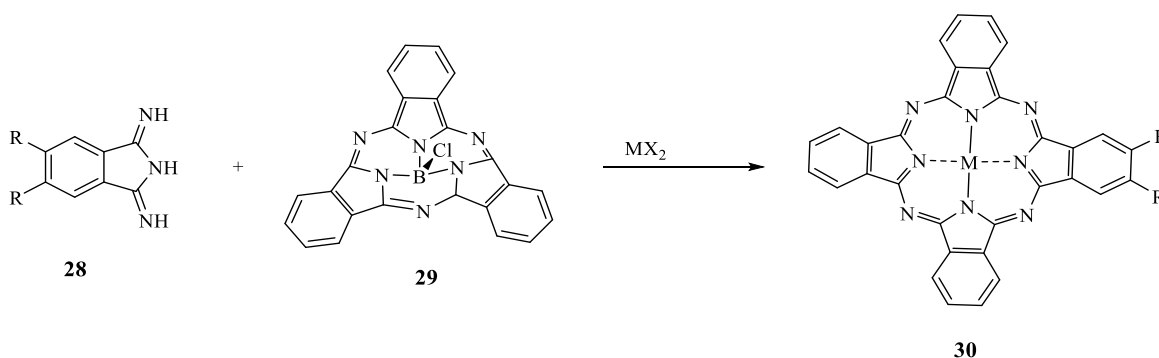


Figure 1.21: Structures of organic bases used in Pc synthesis.^[42]

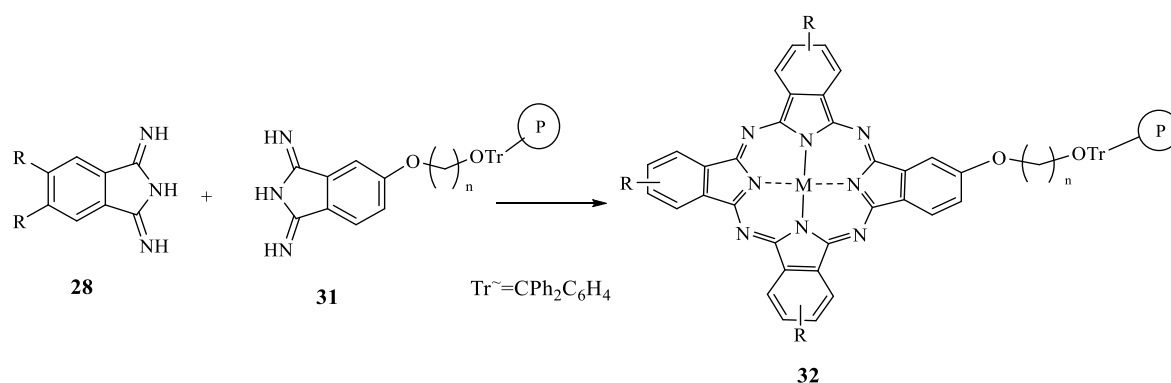
1.2.7 Synthesis of unsymmetrical Pcs (A₃B type):

Like the unsymmetrical porphyrin syntheses described earlier, unsymmetrical Pcs can be prepared by reacting a mixture of phthalonitriles. However, syntheses produce a statistical mixture of products. Few controlled methods are known. In 1980s, Kobayashi and co-workers reported a method for preparing the unsymmetrical Pcs by ring expansion of a subphthalocyanine in the presence of diiminoisoindoline derivatives or succinamide.^{[44],[45]}



Scheme 1.10: Selective synthesis of A₃B-type Pc.

In 1982 Lenzhoff^[46] and co-worker reported an alternative method to synthesise unsymmetrical Pcs by using mono- functionalized diiminoisoindoline precursor bound to solid polymer and reacting with another diiminoisoindoline derivative. Then work-up removed the symmetrical Pcs and unreacted diiminoisoindoline derivatives before cleavage of the desired Pc from the polymer support under mild conditions.^{[46],[47]}



Scheme 1.11: Synthesis of A₃B-type Pc on polymer support.^{[46],[48]}

1.3 Introduction to TBTAPs

The synthesis of a novel macrocycle, which can be defined as a hybrid of phthalocyanine and tetrabenzoporphyrin (TBP), was first reported in the mid 20 century.^{[41],[48]}

This structure; tetrabenzotriazaporphyrins (TBTAPs) **34** are phthalocyanine **13** and tetrabenzoporphyrin **33** macrocycle hybrid compounds. The only difference is that one azanitrogen of the Pc ring has been replaced by a methine group as shown in Figure 1.22.

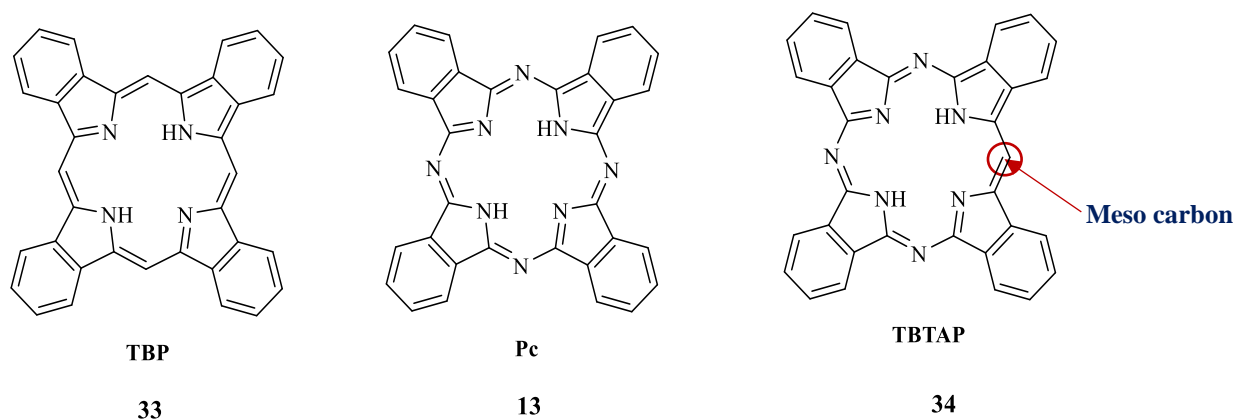


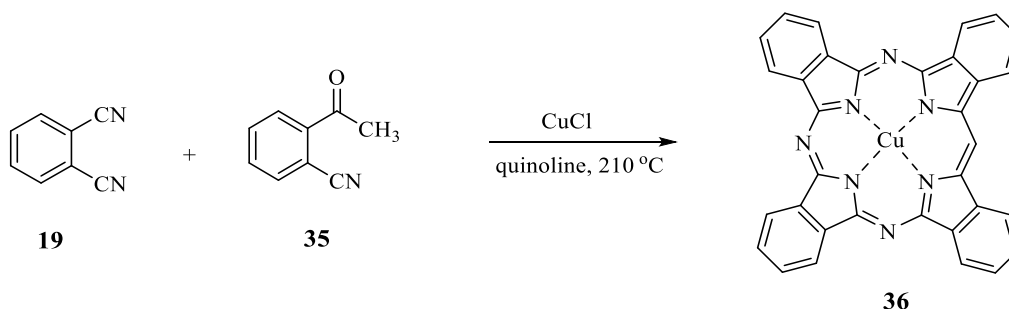
Figure 1.22: Structure of TBTAP.

TBTAP is a hybrid structure that combines the properties of both phthalocyanine and TBP. It combines the stability, robustness and intense long-wavelength electronic absorptions seen in phthalocyanines with the ability to be functionalised at a *meso*-carbon.^[49] Also, the *meso* carbon opens up a variety of possibilities that the TBTAP can undergo, including; further functionalisation or the ability to link to other moieties and surfaces.^[49]

1.3.1 Synthesis of TBTAPs:

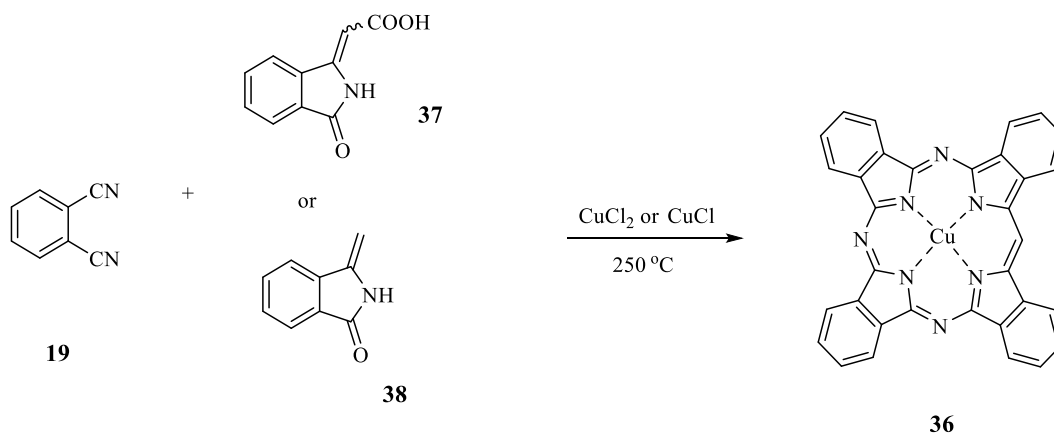
TBTAPs have recently been proposed as good semiconductors and thin films have been developed. Organic semiconductors are flexible and lightweight, making them increasingly attractive.^[50] TBTAPs have been shown to have a variety of features that can be used in a wide range of applications.

In 1936, Fischer *et al.*^[51] reported the preparation of the first macrocyclic molecules that were structurally related to phthalocyanines. In 1937, Helberger^[52] synthesised similar macrocyclic molecules containing a benzene ring fused to each of the four pyrrole rings. The author was able to prepare the copper derivatives of tetrabenzomonoazaporphyrin (**TBMAP**) and tetrabenzodiazaporphyrin (**TBDAP**) in 10 and 20 % yields, respectively. In another study carried out by Helberger and von Rebay,^[53] they found similar results were obtained using this preformed intermediate, and published the first synthesis of tetrabenzotriazaporphyrin. The authors performed the reaction of phthalonitrile (1,2-dicyanobenzene) **19** with *o*-cyanoacetophenone **35** in an equimolar ratio in the presence of copper(I)chloride (scheme 1.12).^[49]



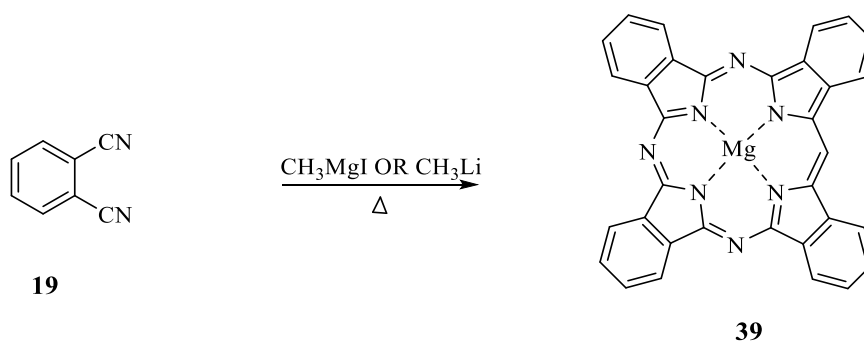
Scheme 1.12: Helberger and von Rebay's syntheses of TBTAPs.

In 1938, a better yield of the copper TBTAP was achieved by Dent.^[48] CuTBTAP **36** was made by reacting phthalonitrile **19** with either phthalimidineacetic **37** acid or methylenephthalimidine **38** in 1-chloronaphthalene at 250 °C in the presence of a copper salt to produce a green chromophore known as CuTBTAP **36**. (Scheme 1.13).^[49]



Scheme 1.13: synthesis of CuTBTAP 36.

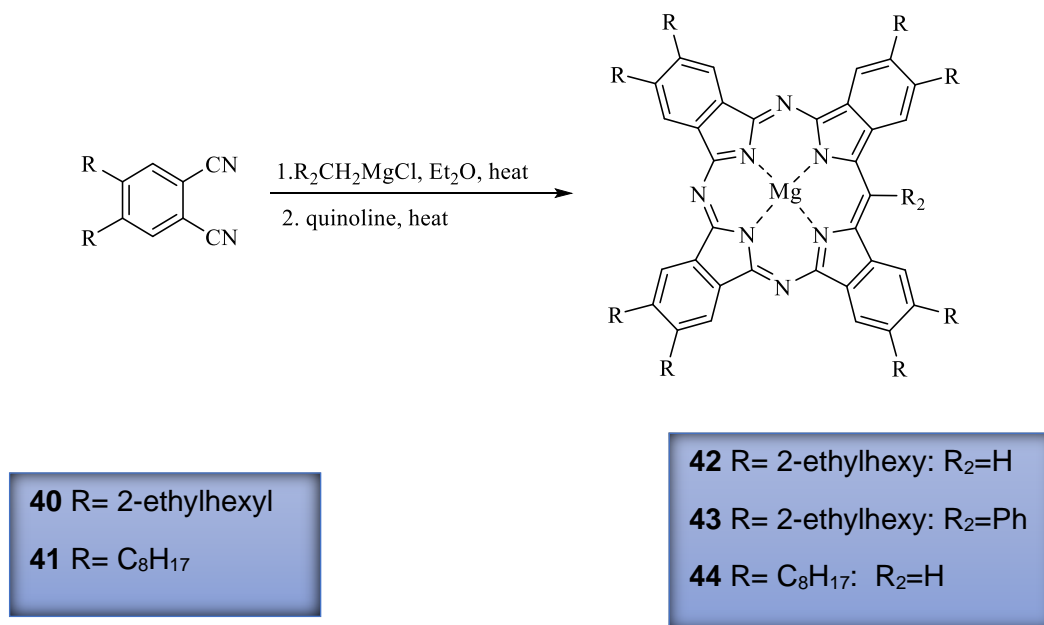
Linstead synthesised TBTAP by treating phthalonitrile **19** with methyl magnesium iodide as a Grignard reagent or methyl lithium in cold ether and then heating the intermediate in a high boiling solvent like quinoline, resulting in MgTBTAP **39** (Scheme 1.14).^[41] This method, however, has a number of drawbacks, including the formation of other hybrids combined with the TBTAP such as TBMAP, TBDAP, TBPs and phthalocyanines. Another drawback with these approaches is the ability to make a suitable Grignard reagent.^[54] Because of the difficulty in the synthesis and low yields of *meso*-functionalised TBTAPs, the reaction needed to be improved and some progress has been made.^[54]



Scheme 1.14: Linstead's syntheses of TBTAPs.

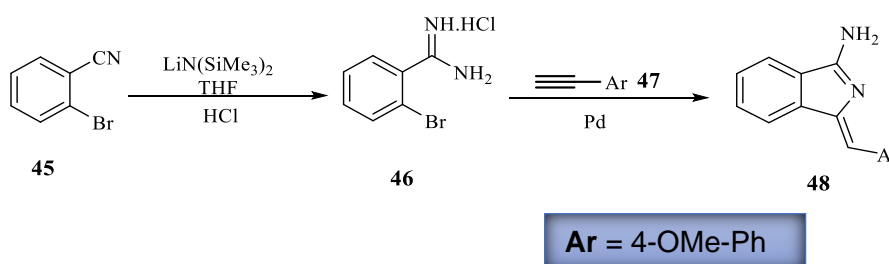
Cambridge-Cook groups^[55] also investigated using 4,5-dialkylphthalonitriles and Grignard reagent MeMgBr , the reactions gave a predominate mixture of TBTAP and Pc (scheme 1.15). Using the 4,5-dialkylphthalonitriles allows for the introduction of an alkyl or phenyl group at the *meso*-position of the TBTAP, as opposed to the 3,6-dialkylphthalonitriles. For instance, the substituted magnesium complex was generated when benzylmagnesium

chloride and 4,5-bis(2-ethylhexyl)-phthalonitrile were combined under conditions identical to those used previously. The formation of a product containing the unsubstituted methine bridge was not observed in this reaction (scheme 1.15).^[55]



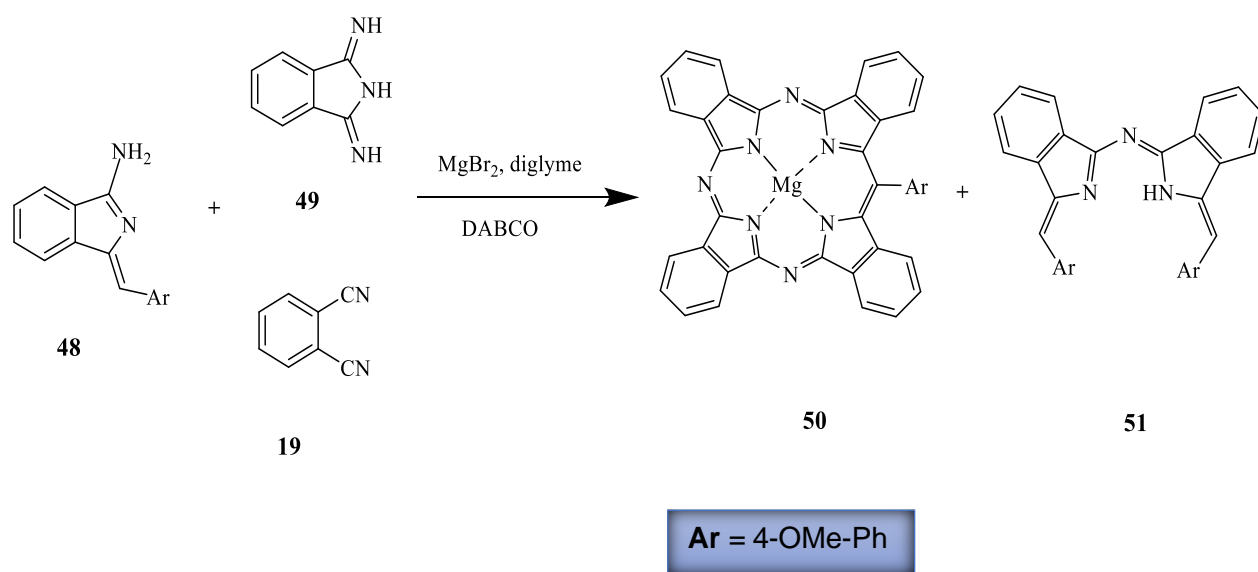
Scheme 1.15: *Meso*-Substituted MgTBTAP complexes using 4,5-dialkylphthalonitriles.

In recent years, considerable attention has been focused on the preparation of TBTAPs using more precise methods. The Cammidge group has been working on providing new and improved synthetic routes.^[56] This method proved to give a better yield of TBTAP and avoided the formation of further hybrid complexes. The synthetic strategy involves the preparation of the aminoisoindoline or its derivatives by applying the procedure developed by Hellal *et al.*^[57] The aminoisoindoline **48** was synthesised from a copper free Sonogashira coupling between terminal arylacetylenes and 2-bromo benzimidamide hydrochloride **46** under microwave irradiation (scheme 1.16).^[56]



Scheme 1.16: Synthesis of aminoisoindoline^[57]

The first attempts to synthesise TBTAP began with heating a solution of diiminoisoindoline **49** and aminoisoindoline **48** in high boiling organic solvents (starting with quinoline, DMEA, DMF, and finally diglyme) in the presence of magnesium bromide as a template agent.^[56] The reaction mixture was found to contain a trace of the desired meso-phenyl TBTAP **50** along with Pc and a self-condensation product of aminoisoindoline **51**. However, the reaction was changed to use phthalonitrile **19** as a less reactive precursor in place of diiminoisoindoline **49** due to the unsatisfactory results and the formation of side products. The group has successfully reported the synthesis of *meso*-aryl substituted TBTAP derivatives **50** in good yield. Using magnesium iodide (MgI₂)^[56] or Boron tribromide (BBr₃)^[58] the group successfully synthesised meso-phenol substituted TBTAPs from the equivalent methoxy substituted complexes. The phenol group was further functionalized by being alkylated and acylated, and the Mg in the TBTAPs' centre core was also demetallated and transmetallated (scheme 1.17).^[56]



Scheme 1.17: synthesis of *meso*-substituted magnesium TBTAP **50**.

1.4 Dyads, triads and Sandwich type complexes:

Many researchers reported porphyrin dyads that have electron acceptor and donor, in order to mimic the electron transfer and energy transfer in nature, which provides a very beneficial way to comprehend the photosynthesis process^[59] which converts light energy into chemical energy. This process involves two main steps. One is the absorption of light energy of the appropriate wavelength by antenna light harvesting molecules to the reaction centre, and the other is the photoinduced electron transfer (PET) that uses electronic excitation energy to generate charge separated entities.^[60] The antenna light harvesting system consists of chromophore arrays, which in artificial compounds is based on porphyrin chromophores, linked to one or more electron donor or acceptor molecules.^[60] For example, in porphyrin tetrathiafulvalene (TTF) **53**,^[61] the porphyrin units act as electron acceptors where electrons transfer to the porphyrin subunit. On the other hand, in porphyrin (C₆₀) **54**, the porphyrin units act as electron donor where electrons transfer from the porphyrin subunit to acceptors as show in the Figures 1.23 and 1.24.

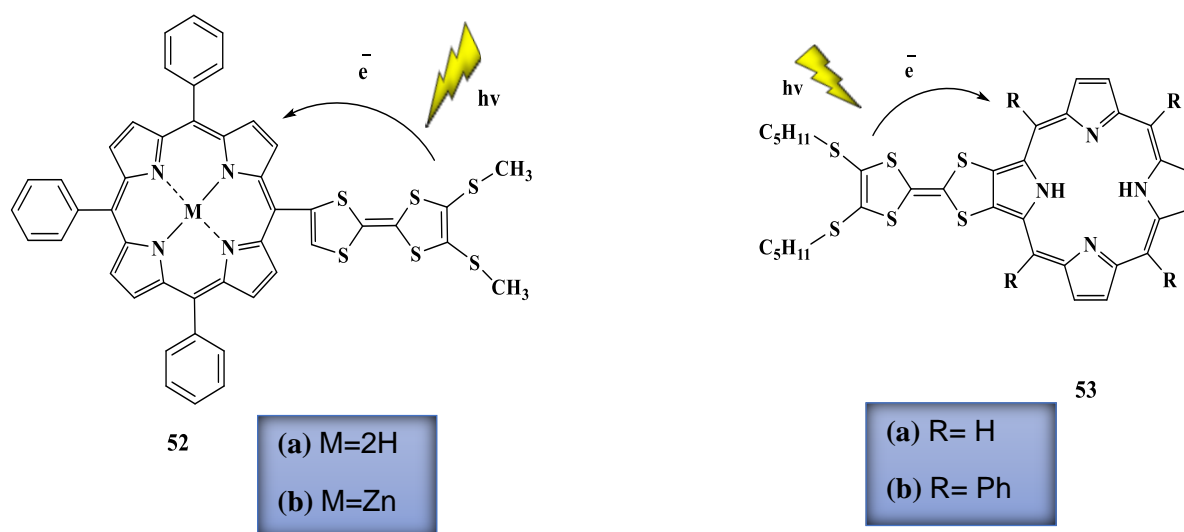


Figure 1.23: porphyrin units act as electron acceptors.^[61]

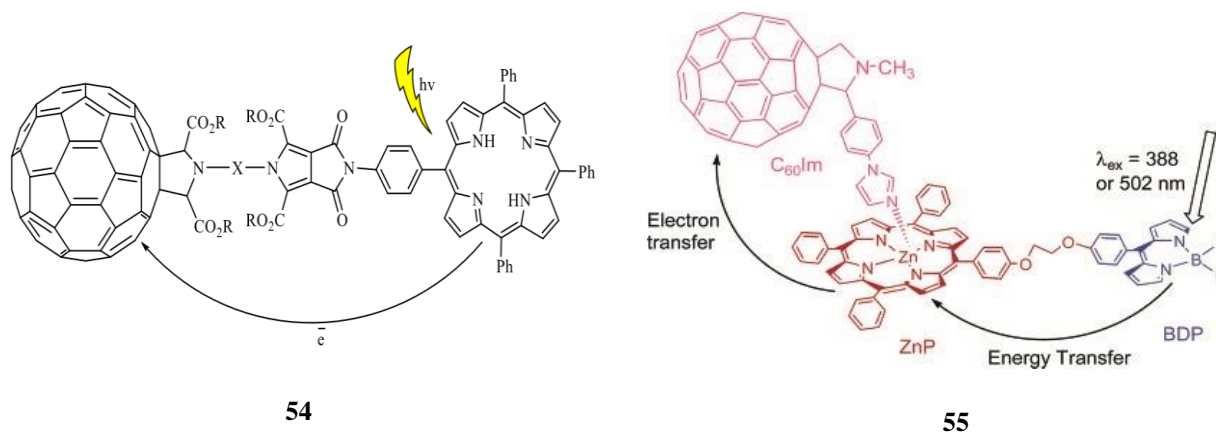


Figure 1.24: porphyrin units act as electron donor.^{[59],[60]}

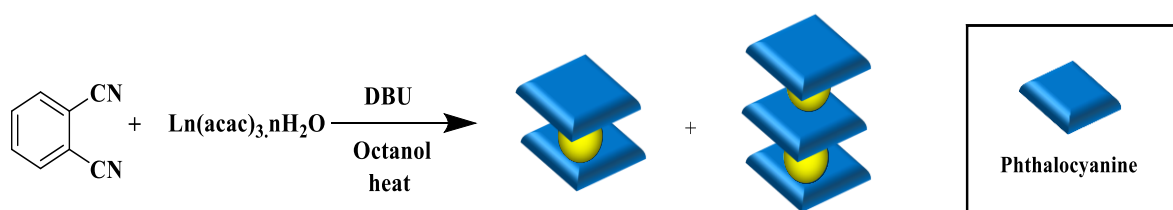
Also, the donor-acceptor system can apply in the case of symmetrical or unsymmetrical Porphyrin - Porphyrin dyads, as one of the units play role as donor molecule and the other one as acceptor.

1.5 Synthesis of (porphyrin) (phthalocyanines) triple-decker complexes (TD):

In recent decades, there has been huge research in the study of complexes of porphyrins and phthalocyanines with various metals. The mixed (porphyrinato) (phthalocyaninato) rare earth complexes can produce several homoleptic and or heteroleptic double- and triple-decker compounds. There are a range of metal ions that can be inserted in the central core of porphyrins, phthalocyanines, naphthalocyanine and other tetrapyrrole derivatives. The nature of the tetra pyrrole ligands and the size of the metal ions directly influence the outcome of the sandwich- type structures.

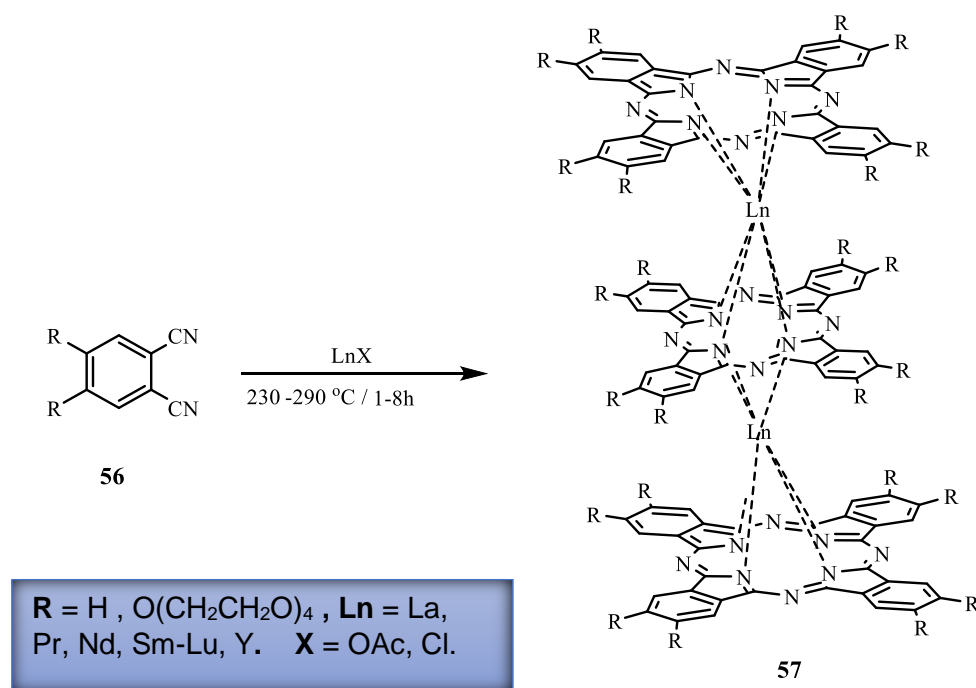
1.5.1 Synthesis of Homoleptic complexes:

Two approaches can be used to make homoleptic rare earth complexes like double- and triple-decker compounds. The cyclo-tetramerization of the phthalonitriles in the presence of rare earth metal salts and the use of an organic base like DBU were the first procedures to be used. Alternatively, metal salts can be treated with molecules like Li_2Pc or H_2Pc in a high boiling point solvent like octanol.^[62]



Scheme 1.18: Synthesis of homoleptic complexes.

In 1976, Russian scientists first reported a triple decker based on lanthanide phthalocyanine. The authors mixed phthalonitrile with lanthanide acetates at 280-290 °C for 1h and produced compounds which have the structure of bimetallic trisphthalocyanine complexes Pc_3Ln_2 ($Ln=Pr, Nd, Er, Lu$) which was proved by X-ray crystallography in 1999.^{[63], [64]}

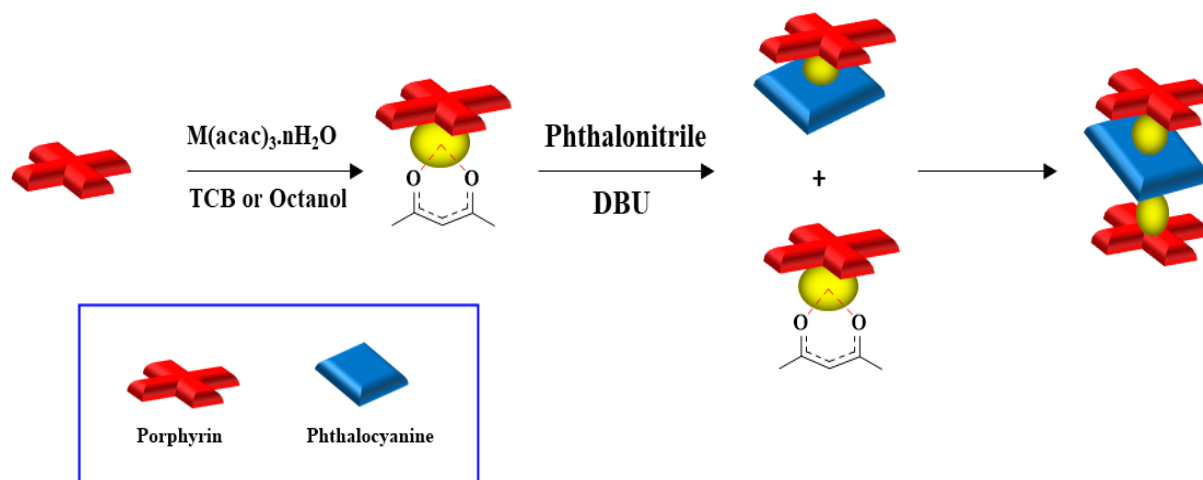


Scheme 1.19: Synthesis of homoleptic complexes **57**.^[63]

1.5.2 Synthesis of heteroleptic complexes:

Heteroleptic sandwich compounds with different porphyrinato or phthalocyaninato ligands were not reported until 1986. Since 1990 there was an increased attention to the heteroleptic tetrapyrrole rare-earth double and triple decker analogues with mixed phthalocyaninato and porphyrinato ligands.^[65] Research in this subject were published mostly in 2000-2007 where it was shown that the $\pi - \pi$ interaction between the ligands and f-f interaction of metal ion in triple decker complexes can effectively be controlled.^[63] There are several approaches to the synthesis of novel porphyrin and phthalocyanine triple decker complexes.

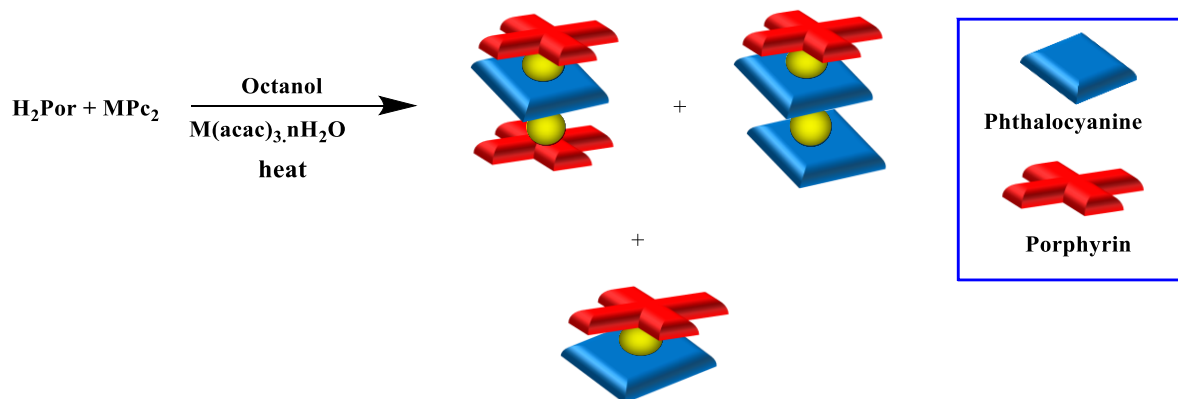
The first method called “one by one deck construction of triple decker” involves reacting the $\text{Ln}(\text{acac})_3 \cdot n\text{H}_2\text{O}$ and porphyrin into a ‘half – sandwich’ complex to give $\text{Ln}(\text{por})(\text{acac})$ which has reasonable stability. It then reacts with phthalonitrile to form the desired double decker complexes.^[65] Also, mixtures of triple-decker complexes $[\text{Por}]_2[\text{Pc}]\text{Ln}_2$ and $[\text{Por}][\text{Pc}]_2\text{Ln}_2$ were directly prepared using the corresponding double deckers and the $[\text{Por}]\text{Ln}(\text{acac})$ precursor.^[66]



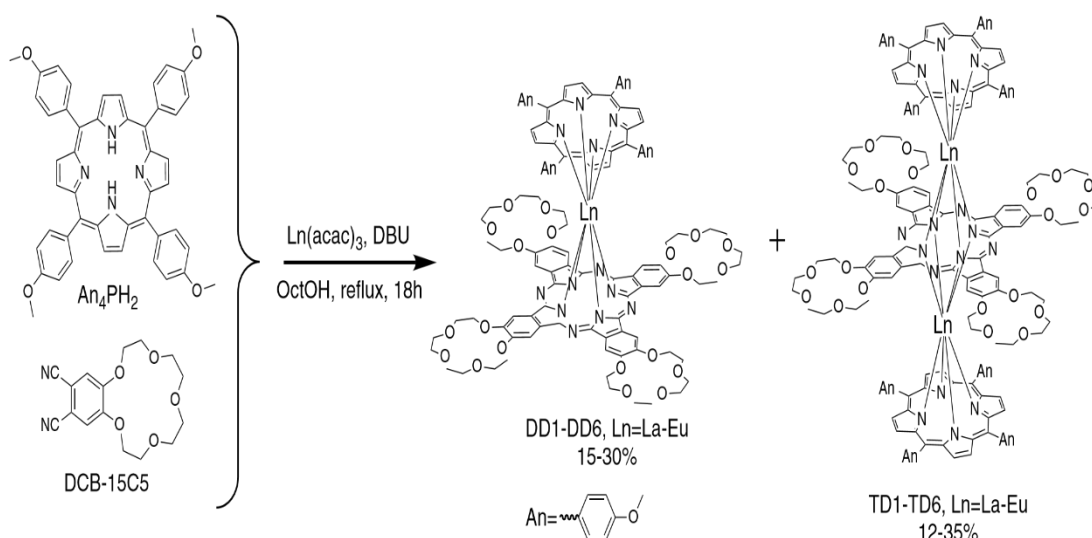
Scheme 1.20: One-by-one deck construction of triple deckers.

The second method called one-pot procedure that allows the synthesis of heteroleptic double- and triple-decker (porphyrinato)(phthalocyaninates) of various lanthanides (La, Eu, Nd) starting from porphyrin, phthalonitrile and lanthanide acetylacetonate using a high-boiling point alcohol as solvent.^{[67],[68]} The difference between the previous method and the

one-pot procedure is that the triple-decker complexes [Por]Ln[Pc]Ln[Por] can be obtained in a one-step procedure of prolonged reflux of porphyrin, phthalonitrile and $\text{Ln}(\text{acac})_3$ without any additional treatment of the reaction mixture.^{[67],[68]} This method does not need the generation of monoporphyrinates and avoids rise-by one-story formation of triple-decker complexes. However, the corresponding double-decker complexes and other triple-decker structures are also present in the reaction mixture.

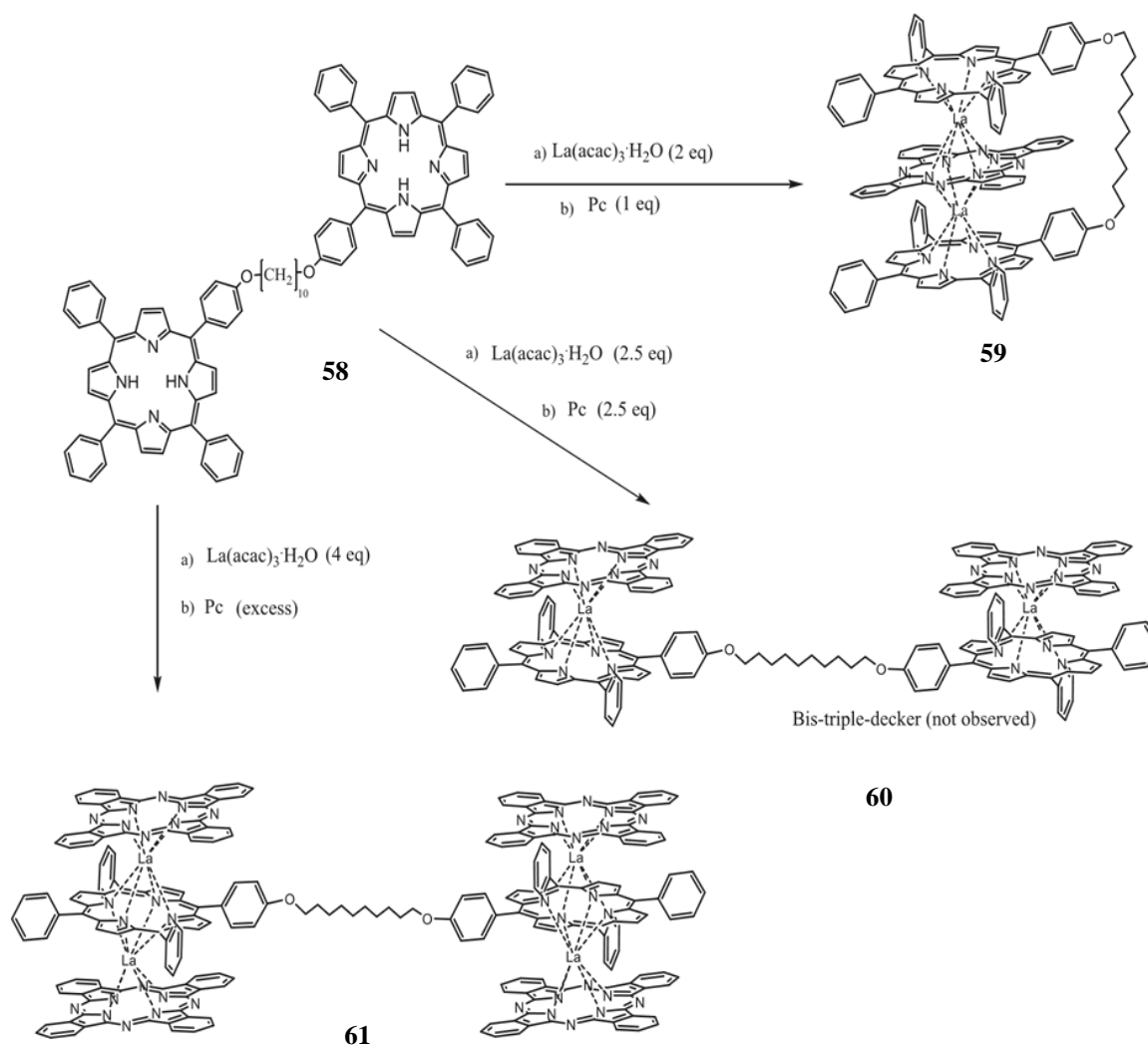


Scheme 1.21: Synthesis of heteroleptic triple-decker is by ‘one pot’ method.



Scheme 1.22: Synthesis of heteroleptic double- and triple-decker (porphyrinato)(phthalocyaninates) using one-step procedure.^[67]

Recently, Cammidge's group have prepared triple deckers from linked porphyrin units with an n-alkyl chain and discovered that n-decane works well for insertion of phthalocyanine and two lanthanide ions (scheme 1.24).^[69] Despite the fact that the porphyrin-phthalocyanine-porphyrin TD is controlled by the porphyrins bridge, an open bis-triple decker was produced by increasing the equivalent of phthalocyanine and lanthanide metal (scheme 1.23).^[69]



Scheme 1.23: General method for triple decker synthesis by Cammidge *et al.*^[69]

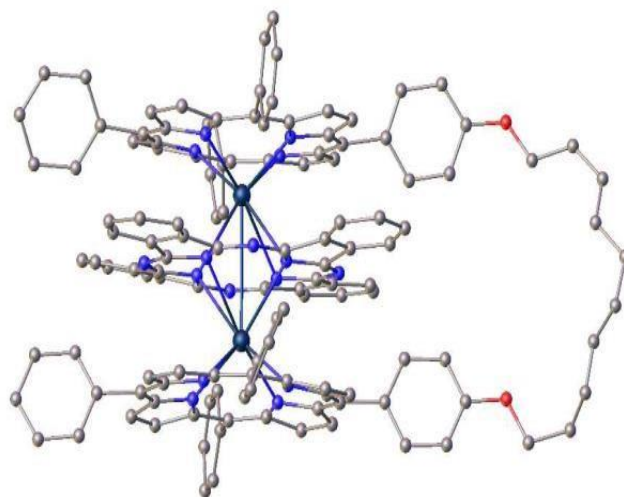


Figure 1.25: X-ray analysis obtained of triple decker model by Cammidge *et al.*^[69]

1.6 Applications of porphyrins, phthalocyanines and their triple deckers:

Porphyrins, phthalocyanine and their derivatives have been studied for a long period of time and their properties and chemistry are well known. They play important roles in a wide range of applications, such as, catalysis, molecular electronics, photonics and optical data storage (DVDs).^[70] Also, they have been used as catalysts for the oxidation in organic chemistry and in organic solar cells.^[71] The optical, physical, spectroscopic, electrical and electrochemical characteristics of such complexes are a feature of the interactions of the metal ions, and the intermolecular π - π interactions. Sandwich triple deckers, which have been synthesised by previous researchers, have demonstrated a considerable number of redox states. They also have low oxidation potentials, as well as reversible electrochemistry. Such remarkable features give these complexes great potential for their use in several applications, for example, molecular magnets, multibit molecular information storage, sensors, nonlinear optical materials, nanomaterials and field effect transistors that cannot be achieved by their mono- metallic macrocycle counterparts.^[72]

1.6.1 Photodynamic therapy:

In the medical application, porphyrins and phthalocyanines have been used as photodynamic reagents for cancer therapy (PDT).^[73] Most of the photosensitizers (PS) used in cancer therapy are based on a tetrapyrrole structure, similar to that of the protoporphyrin present in hemoglobin.^[74] Photosensitisers applied in PDT can be divided into generations. The first

PS to be clinically employed for cancer therapy was a water-soluble mixture of porphyrins called hematoporphyrin derivative (HPD), a purified form known as Photofrin. Despite the HPD is still the most widely employed PS, however, it has some disadvantages including a long-lasting skin photosensitivity and a relatively low absorbance at 630-nm. Second-generation PSs were based on benzoporphyrin derivatives, chlorins, phthalocyanines, texaphyrins and natural compounds such as hypericin.^[75] Also, A porphyrin dimer (10,15,20-tritolylporphyrin-5-(4-amidophenyl)-[5-(4-phenyl)-10,15,20-tritolylporphyrin] **62** was investigated as a potential PDT agent for the treatment of melanoma (figure1.26)^[74]. The authors pointed out that this porphyrin dimer has some distinct advantages over Photofrin for the treatment of pigmented melanoma, namely, chemical homogeneity, low aggregation.^[74]

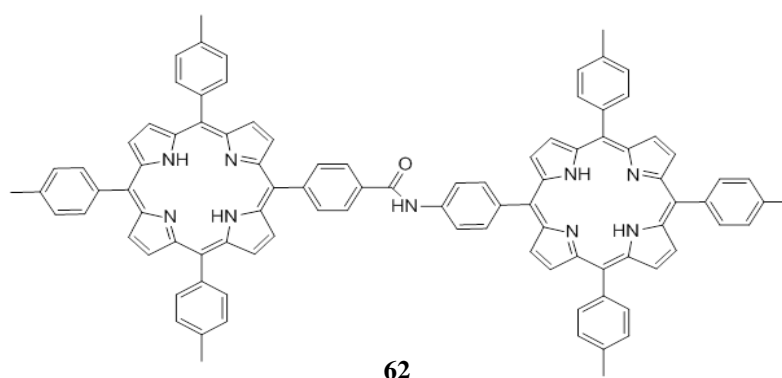


Figure 1.26: Structure of porphyrin dimer (T-D).

1.6.2 Detection of gaseous Nitric oxide:

Nitric oxide (NO) is a highly reactive toxic gas that forms as an intermediate compound during the oxidation of ammonia and is used for the manufacture of hydroxylamine in the chemical industry.^[76] Phthalocyanines, porphyrins, and their hybrid materials have been studied as active layers of chemical sensors for the detection of NO for the past ten years, with a primary focus on chemiresistive and electrochemical properties.^[76] Sensors are being developed using natural porphyrins, such as protoporphyrin IX and cytochromes to detect gaseous NO.

Knoben *et al.*^[77] investigated the sensors' properties by a Kelvin probe technique of four different protoporphyrins IX PP (Figure 1.27a). Immersing the substrate overnight of 2H-PP, Co-PP, Fe-PP, and Zn-PP solutions in dimethylformamide produced monolayers. Nitric

oxide content was found to be 100 ppb to 2 ppm in the flow cell. Figure 1.27 shows the Kelvin probe response for four protoporphyrins. Zn-PP showed the greatest and fastest reaction to Nitric oxide and allowed for ppb-level Nitric oxide detection.^[77]

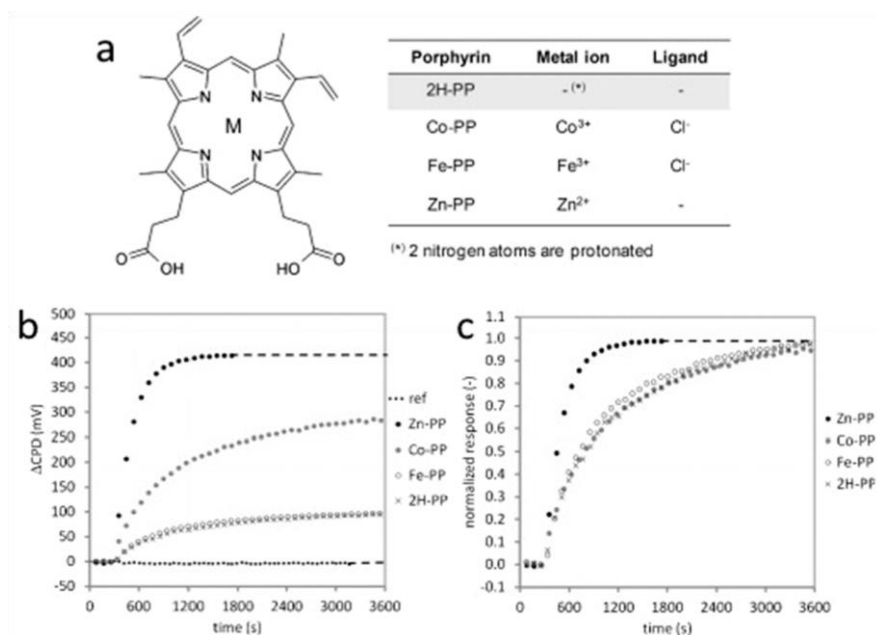


Figure 1.27: (a) Molecular structure of the used protoporphyrin IX. indicates the position of the metal ion. (b) Kelvin probe response of the different porphyrins to 2 ppm NO; (c) same as (a), normalized to the equilibrium response. (Adapted from Knoblen *et al.*^[77])^[76]

1.6.3 Single-molecule magnet (SMM):

A single-molecule magnet (SMM) is a metal-organic compound that has superparamagnetic behaviour below a certain blocking temperature at the molecular scale. SMMs exhibit magnetic hysteresis of purely molecular origin, unlike bulk magnets and molecule-based magnets.^[78] Lanthanides are metals with lots of electrons and occupied f orbitals. This provides the metals with high magnetic susceptibilities which are the origin of their behaviour. The middle-late lanthanides, dysprosium to erbium, are the Lanthanides with the highest magnetic susceptibilities.^{[72],[79]} Among the series of Ln³⁺ ions, Dy³⁺ and Tb³⁺ are arguably the ions of choice for preparing high-performance SMMs.^[80] As described by J. Jiang (figure 1.28), magnetic characteristics are the most interesting in triple decker structures made of magnetic metals like as Dy or Y. During their work, dysprosium was used as the spin carrier in three sandwiches type di-rare earth compounds, and an isostructural

triple-decker conformation was devised and synthesised. Sandwich systems with magnetic field-induced SMM, SMM, and non-SMM features revealed for the Dy–Dy, Y–Dy, and Dy–Y systems, respectively, show that the coordination geometry of the spin carrier, not the f–f interaction, is responsible for the magnetic properties.^[79]

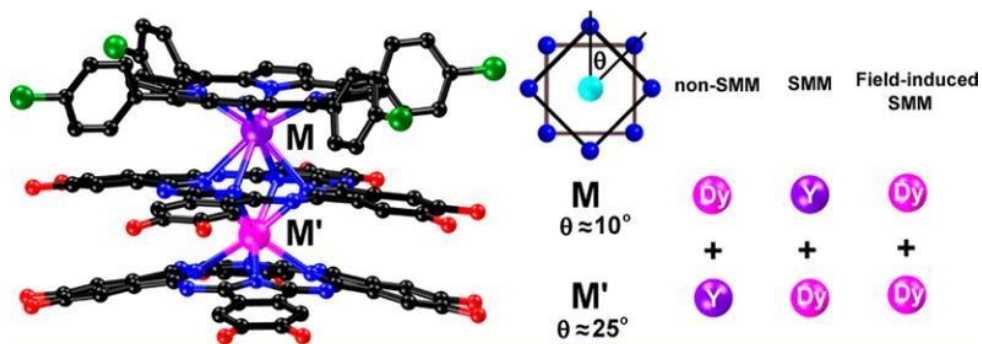


Figure 1.28: Molecular structure of magnetic triple deckers reported by J. Jiang.^[79]

References:

- [1] L. R. Milgrom, *The colours of life : an introduction to the chemistry of porphyrins and related compounds*, Oxford University Press, New York, **1997**.
- [2] A. Gelsomino, D. Tortorella, V. Cianci, B. Petrovičová, A. Sorgonà, A. Piccolo, M. R. Abenavoli, *Journal of Plant Nutrition and Soil Science* **2010**, *173*, 399-406.
- [3] M. Biesaga, K. Pyrzyńska, M. Trojanowicz, *Talanta* **2000**, *51*, 209-224.
- [4] T. D. Lash, S. A. Jones, G. M. Ferrence, *Journal of the American Chemical Society* **2010**, *132*, 12786-12787.
- [5] E. Steiner, A. Soncini, P. W. Fowler, *Organic & Biomolecular Chemistry* **2005**, *3*, 4053-4059.
- [6] P. Rothmund, *Journal of the American Chemical Society* **1936**, *58*, 625-627.
- [7] M. Schlabach, H. H. Limbach, E. Bunnenberg, A. Y. L. Shu, B. R. Tolf, C. Djerassi, *Journal of the American Chemical Society* **1993**, *115*, 4554-4565.
- [8] G. P. MOSS, *European Journal of Biochemistry* **1988**, *178*, 277-328.
- [9] A. Zhang, L. Kwan, M. J. Stillman, *Organic & Biomolecular Chemistry* **2017**, *15*, 9081-9094.
- [10] Y. Rio, M. Salomé Rodríguez-Morgade, T. Torres, *Organic & Biomolecular Chemistry* **2008**, *6*, 1877-1894.
- [11] L. B. Josefsen, R. W. Boyle, *Theranostics* **2012**, *2*, 916-966.
- [12] N. Z. Mamardashvili, O. A. Golubchikov, *Russian Chemical Reviews* **2000**, *69*, 307-323.
- [13] P. Rothmund, A. R. Menotti, *Journal of the American Chemical Society* **1941**, *63*, 267-270.
- [14] P. Rothmund, *Journal of the American Chemical Society* **1935**, *57*, 2010-2011.
- [15] J. S. Lindsey, In *Metalloporphyrins Catalyzed Oxidations*, Montanari, F., Casella, L. Eds.; Springer Netherlands, **1994**, 34,49-86.
- [16] R. W. Wagner, D. S. Lawrence, J. S. Lindsey, *Tetrahedron Letters* **1987**, *28*, 3069-3070.
- [17] J. S. Lindsey, K. A. MacCrum, J. S. Tyhonas, Y. Y. Chuang, *The Journal of Organic Chemistry* **1994**, *59*, 579-587.
- [18] M. O. Senge, *Chemical Communications* **2011**, *47*, 1943-1960.

- [19] M. O. Senge, Y. M. Shaker, M. Pinteá, C. Ryppa, S. S. Hatscher, A. Ryan, Y. Sergeeva, *European Journal of Organic Chemistry* **2010**, 2010, 207-207.
- [20] J. S. Lindsey, *Accounts of Chemical Research* **2010**, 43, 300-311.
- [21] O. Horváth, R. Huszánk, Z. Valicsek, G. Lendvay, *Coordination Chemistry Reviews* **2006**, 250, 1792-1803.
- [22] R. Giovannetti, *The Use of Spectrophotometry UV-Vis for the Study of Porphyrins, Macro to Nano Spectroscopy*, Intech, Rijeka, 87-108, **2012**.
- [23] A. Braun, J. Tcherniac, *Berichte der deutschen chemischen Gesellschaft* **1907**, 40, 2709-2714.
- [24] G. T. Byrne, R. P. Linstead, A. R. Lowe, *Journal of the Chemical Society (Resumed)* **1934**, 1017-1022.
- [25] G. W. Watt, J. W. Dawes, *Journal of Inorganic and Nuclear Chemistry* **1960**, 14, 32-34.
- [26] R. L. M. Allen, in *Colour Chemistry* (Ed.: R. L. M. Allen), Springer US, Boston, MA, **1971**, pp. 231-240.
- [27] R. P. Linstead, *Journal of the Chemical Society (Resumed)* **1934**, 1016-1017.
- [28] G. de la Torre, C. G. Claessens, T. Torres, *Chemical Communications* **2007**, 2000-2015.
- [29] G. de la Torre, P. Vázquez, F. Agulló-López, T. Torres, *Journal of Materials Chemistry* **1998**, 8, 1671-1683.
- [30] S. Arslan, I. Yilmaz, *Transition Metal Chemistry* **2007**, 32, 292.
- [31] M. N. Yaraşır, M. Kandaz, A. Koca, B. Salih, *Journal of Porphyrins and Phthalocyanines* **2006**, 10, 1022-1033.
- [32] R. P. Linstead, A. R. Lowe, *Journal of the Chemical Society (Resumed)* **1934**, 1022-1027.
- [33] S. Arslan, *Journal of Life Sciences* **2016**, 6, 2.
- [34] J. M. Robertson, *Journal of The Chemical Society (resumed)* **1936**, 1195-1209.
- [35] L. G. Tomilova, E. V. Chernykh, E. A. Luk'yanets, *Zhurnal Obshchej Khimii* **1985**, 55, 2631.
- [36] F. Ghani, J. Kristen, H. Riegler, *Journal of Chemical & Engineering Data* **2012**, 57, 439-449.
- [37] Y. Chen, D. Dini, M. Hanack, M. Fujitsuka, O. Ito, *Chemical Communications* **2004**, 340-341.

- [38] L. G. Tomilova, K. M. Dyumaev, O. P. Tkachenko, *Russian Chemical Bulletin* **1995**, *44*, 410-415.
- [39] B. R. Hollebhone, M. J. Stillman, *Chemical Physics Letters* **1974**, *29*, 284-286.
- [40] K. Sakamoto, E. Ohno-Okumura, *Materials* **2009**, *2*, 1127.
- [41] P. A. Barrett, R. P. Linstead, G. A. P. Tuey, J. M. Robertson, *Journal of the Chemical Society (Resumed)* **1939**, 1809-1820.
- [42] T. Haruhiko, S. Shojiro, O. Shojiro, S. Shinsaku, *Chemistry Letters* **1980**, *9*, 1277-1280.
- [43] T. Haruhiko, S. Shojiro, S. Shinsaku, *Chemistry Letters* **1983**, *12*, 313-316.
- [44] Á. Sastre, B. del Rey, T. Torres, *The Journal of Organic Chemistry* **1996**, *61*, 8591-8597.
- [45] A. Sastre, T. Torres, M. Hanack, *Tetrahedron Letters* **1995**, *36*, 8501-8504.
- [46] C. C. Leznoff, T. W. Hall, *Tetrahedron Letters* **1982**, *23*, 3023-3026.
- [47] A. Y. Tolbin, L. G. Tomilova, N. S. Zefirov, *Russian Chemical Reviews* **2007**, *76*, 681-692.
- [48] C. E. Dent, *Journal of the Chemical Society (Resumed)* **1938**, 1-6.
- [49] V. V. Kalashnikov, V. E. Pushkarev, L. G. Tomilova, *Russian Chemical Reviews* **2014**, *83*, 657-675.
- [50] T. Kitagawa, M. Fujisaki, S. Nagano, N. Tohnai, A. Fujii, M. Ozaki, *Applied Physics Express* **2019**, *12*, 051011.
- [51] H. Fischer, H. Haberland, A. Müller, *Justus Liebigs Annalen der Chemie* **1936**, *521*, 122-128.
- [52] J. H. v. R. Helberger, *Justus Liebigs Ann. Chem.* 1937 **1937**, *531* 279– 287.
- [53] J. H. Helberger, A. von Rebay, D. B. Hevér., *Justus Liebigs Annalen der Chemie* **1938**, *533*, 197-215.
- [54] A. N. Cammidge, I. Chambrier, M. J. Cook, E. H. G. Langner, M. Rahman, J. C. Swarts, *Journal of Porphyrins and Phthalocyanines* **2011**, *15*, 890-897.
- [55] A. N. Cammidge, I. Chambrier, M. J. Cook, D. L. Hughes, M. Rahman, L. Sosa-Vargas, *Chemistry – A European Journal* **2011**, *17*, 3136-3146.
- [56] A. Díaz-Moscoso, G. J. Tizzard, S. J. Coles, A. N. Cammidge, *Angewandte Chemie International Edition* **2013**, *52*, 10784-10787.
- [57] M. Hellal, G. D. Cuny, *Tetrahedron Letters* **2011**, *52*, 5508-5511.

- [58] N. Alharbi, A. Díaz-Moscoso, G. J. Tizzard, S. J. Coles, M. J. Cook, A. N. Cammidge, *Tetrahedron* **2014**, *70*, 7370-7379.
- [59] X. Sun, D. Li, G. Chen, J. Zhang, *Dyes and Pigments* **2006**, *71*, 118-122.
- [60] F. D'Souza, P. M. Smith, M. E. Zandler, A. L. McCarty, M. Itou, Y. Araki, O. Ito, *Journal of the American Chemical Society* **2004**, *126*, 7898-7907.
- [61] a) J. Becher, T. Brimert, J. O. Jeppesen, J. Z. Pedersen, R. Zubarev, T. Bjørnholm, N. Reitzel, T. R. Jensen, K. Kjaer, E. Levillain, *Angewandte Chemie International Edition* **2001**, *40*, 2497-2500; b) S. I. Sadaike, K. Takimiya, Y. Aso, T. Otsubo, *Tetrahedron Letters* **2003**, *44*, 161-165.
- [62] S. Bo, D. Tang, X. Liu, Z. Zhen, *Dyes and Pigments* **2008**, *76*, 35-40.
- [63] V. E. Pushkarev, L. G. Tomilova, V. T. Yu, *Russian Chemical Reviews* **2008**, *77*, 875.
- [64] S. I. Troyanov, L. A. Lapkina, V. E. Larchenko, A. Y. Tsivadze, *Doklady Chemistry* **1999**, *367*, 192-196.
- [65] H. Wang, K. Wang, Y. Bian, J. Jiang, N. Kobayashi, *Chemical Communications* **2011**, *47*, 6879-6881.
- [66] K. P. Birin, K. A. Kamarova, Y. G. Gorbunova, A. Y. Tsivadze, *Protection of Metals and Physical Chemistry of Surfaces* **2013**, *49*, 173-180.
- [67] K. P. Birin, Y. G. Gorbunova, A. Y. Tsivadze, *Magnetic Resonance in Chemistry* **2010**, *48*, 505-515.
- [68] K. P. Birin, Y. G. Gorbunova, A. Y. Tsivadze, *Dalton Transactions* **2011**, *40*, 11539-11549.
- [69] D. González-Lucas, S. C. Soobrattee, D. L. Hughes, G. J. Tizzard, S. J. Coles, A. N. Cammidge, *Chemistry – A European Journal* **2020**, *26*, 10724-10728.
- [70] M. A. Dahlen, *Industrial & Engineering Chemistry* **1939**, *31*, 839-847.
- [71] A. P. Yuen, S. M. Jovanovic, A.-M. Hor, R. A. Klenkler, G. A. Devenyi, R. O. Loutfy, J. S. Preston, *Solar Energy* **2012**, *86*, 1683-1688.
- [72] J. Jiang, D. K. P. Ng, *Accounts of Chemical Research* **2009**, *42*, 79-88.
- [73] B. W. Henderson, T. J. Dougherty, *Photochemistry and Photobiology* **1992**, *55*, 145-157.
- [74] H. Abrahamse, Michael R. Hamblin, *Biochemical Journal* **2016**, *473*, 347-364.
- [75] P. M. R. Pereira, B. Korsak, B. Sarmiento, R. J. Schneider, R. Fernandes, J. P. C. Tomé, *Organic & Biomolecular Chemistry* **2015**, *13*, 2518-2529.

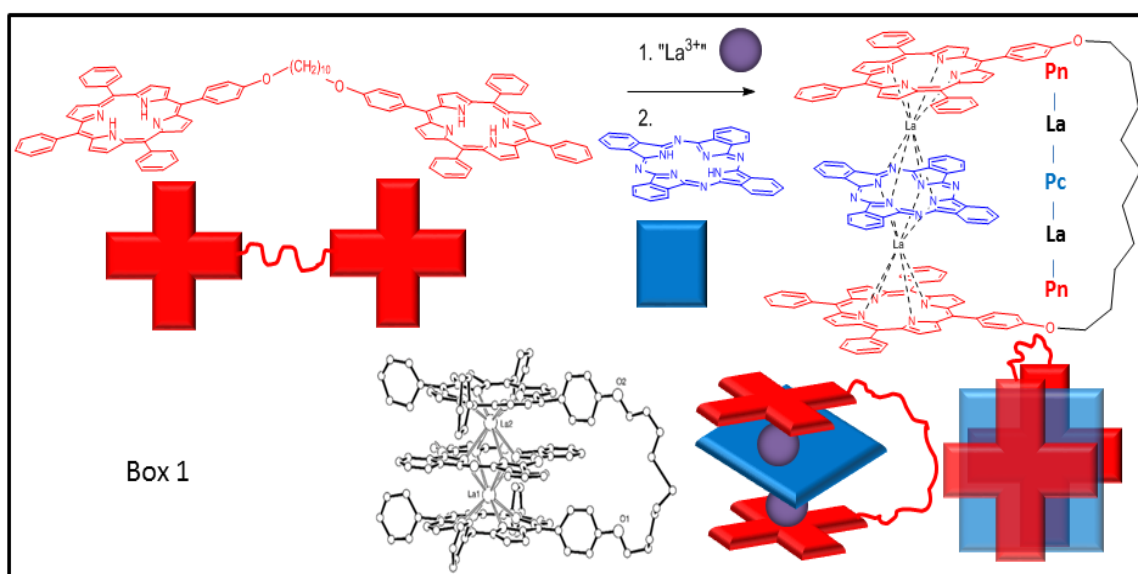
- [76] D. Klyamer, R. Shutilov, T. Basova, *Sensors (Basel)* **2022**, 22.
- [77] W. Knobon, M. Crego-Calama, S. H. Brongersma, *Sensors and Actuators B: Chemical* **2012**, 166-167, 349-356.
- [78] G. Christou, D. Gatteschi, D. N. Hendrickson, R. Sessoli, *MRS Bulletin* **2000**, 25, 66-71.
- [79] J. Kan, H. Wang, W. Sun, W. Cao, J. Tao, J. Jiang, *Inorganic Chemistry* **2013**, 52, 8505-8510.
- [80] R. Marin, G. Brunet, M. Murugesu, *Angewandte Chemie International Edition* **2021**, 60, 1728-1746.

Chapter 2: Results and discussion

2. Results and discussion

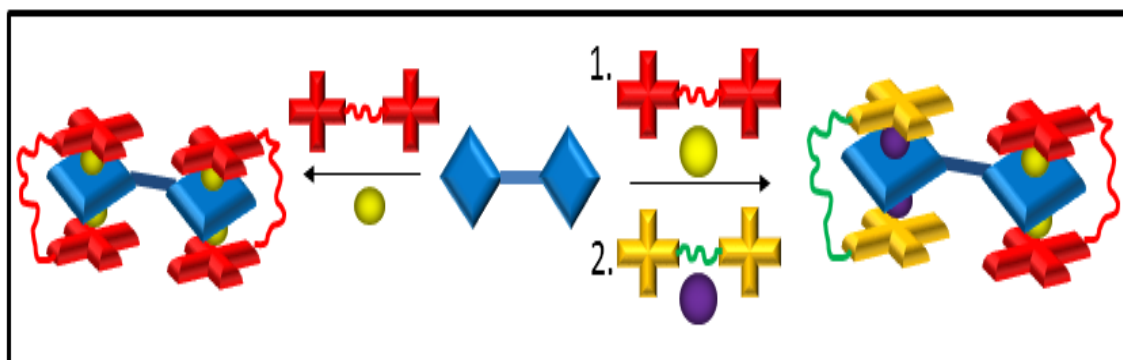
2.1 Introduction to the aims of the project:

Due to the potential applications of lanthanide-bridged triple and double deckers in molecular devices, the research on their synthesis has taken a huge steps forward recently. This project stems from a recent discovery in our laboratory that opens the way towards unique molecular architectures (scheme 2.1). Our group^[1] was able to prepare several linked multi-deckers using decyl and dodecyl linkers between (outer) porphyrins, chosen to prevent the formation of intramolecular porphyrin-porphyrin double-deckers. This process can be performed in high yields using a simple strategy and precursors.



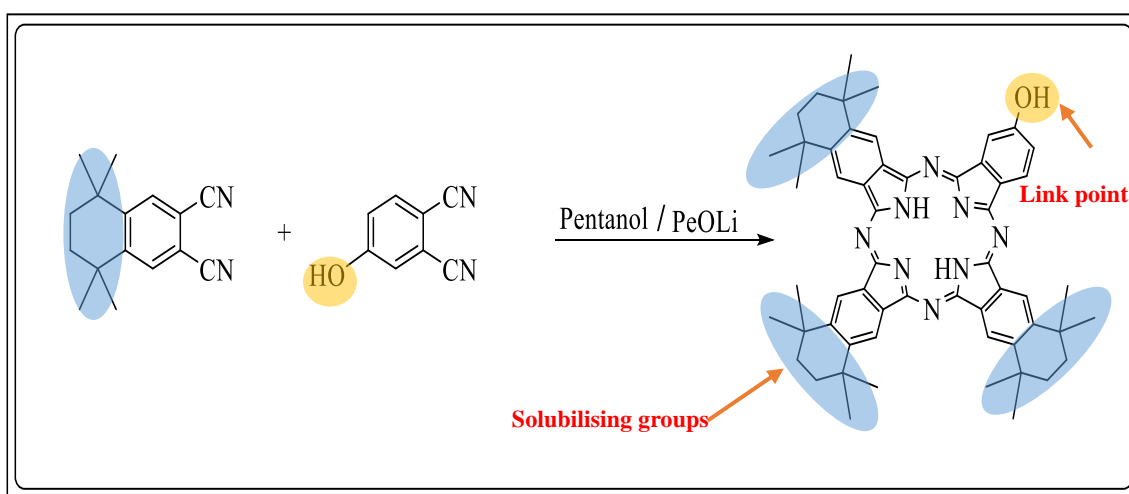
Scheme 2.1: Previous observation from our group.^[1]

The goal of this project was to develop new materials that can be used in the production of advanced electronic devices such as optoelectronics and magnetic devices. The project aimed to develop a two-dimensional lateral assembly that is composed of a pair of phthalocyanine or related macrocycles by the synthesis of unsymmetrical systems that could be inserted in a triple-deckers formed by reaction with linked porphyrins (scheme 2.2). In such structures communication is achieved or prevented by either using a rigid conjugated linker or an electronically insulated bridge.



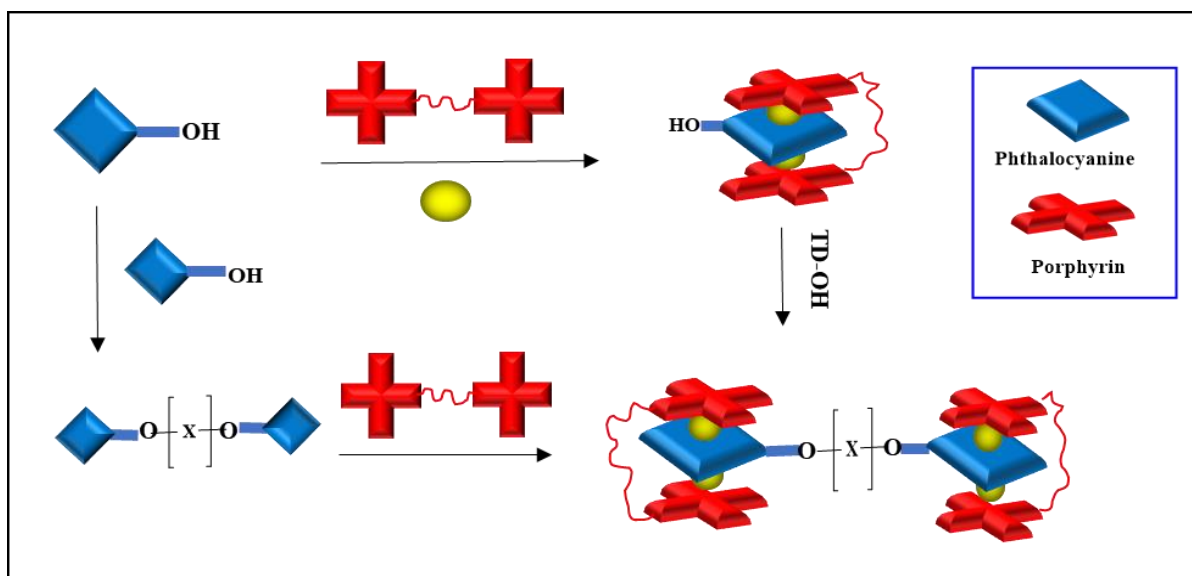
Scheme 2.2: Two most straightforward examples – single-step, homometallic (left – this project) and two-step, heterometallic (future development).

The synthesis of unsymmetrical phthalocyanines usually employs statistical reaction between two different phthalonitriles. The initially selected derivatives and the phthalonitriles required are shown below (scheme 2.3).



Scheme 2.3: Two different phthalonitriles.

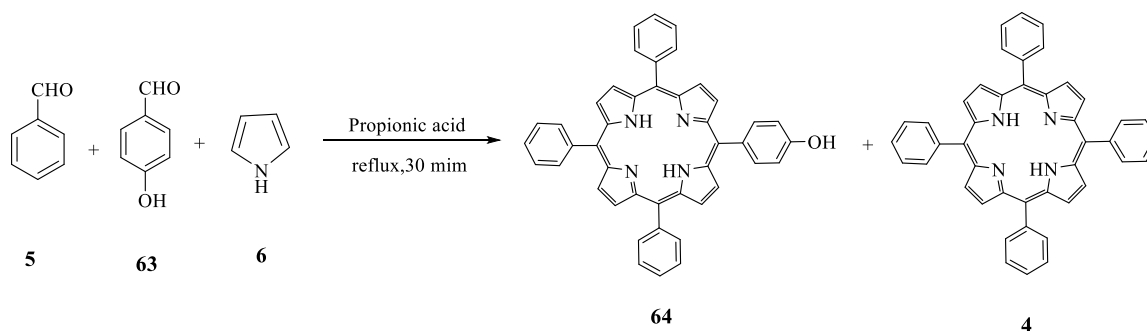
The routes to link the TDs are shown in scheme 2.4



Scheme 2.4: Initially planned routes to symmetrical linked TDs.

2.2 Synthesis of the unsymmetrical tetrasubstituted porphyrin precursor TPP-OH 64.

The first precursor for the preparation of complex structures (triple deckers) is unsymmetrical tetraphenylporphyrin (TPP-OH 64). Synthesis of TPP-OH was achieved by using Adler's ^{[2],[3]} methodology (scheme 2.5).



Scheme 2.5: Synthesis of unsymmetrically substituted porphyrin.

Small variations were performed to optimise the synthesis and isolation of precursor TPP-OH. The best procedure uses benzaldehyde (3eq), 4-hydroxybenzaldehyde (1eq) and propionic acid and heating to reflux. Then, freshly distilled pyrrole (4eq) was added dropwise to the mixture. The reaction mixture was allowed to reflux for 30 minutes then cooled to room temperature and methanol was added. The mixture was left to precipitate

overnight in the fridge. After suction filtration a purple solid was obtained that was a mixture of porphyrins plus some baseline polymeric material. The products were separated by column chromatography using a mixture of DCM and petroleum ether (1:1) as eluent to collect first fraction TPP then the solvent was changed to DCM to collect TPP-OH and after a recrystallization from DCM: MeOH, the monohydroxy porphyrin was obtained in a 6.34 % yield. In order to characterise the pure compound TPP-OH the ^1H NMR spectrum is reported. The ^1H NMR spectrum shows in figure 2.1 for TPP-OH is more complex compared to TPP in figure 2.2; the TPP-OH is no longer symmetrical it also shows a broad signal from the OH group at chemical shift of 5.2 ppm. Also, as porphyrins **4**, **64** are metal-free porphyrins, there was a signal at chemical shift of -2.77 ppm.

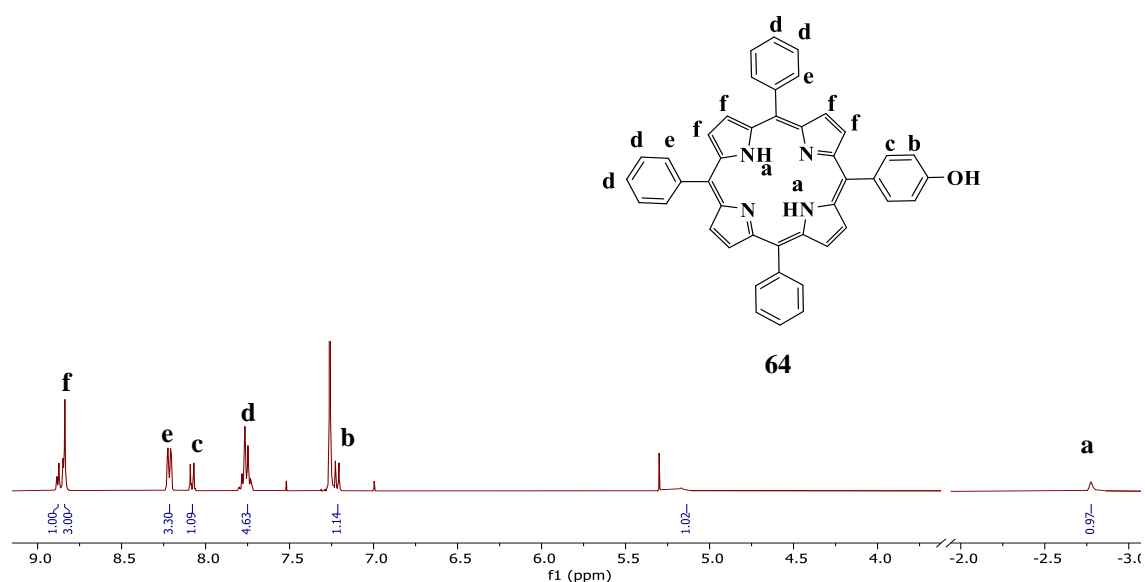


Figure 2.1: ^1H NMR spectrum of TPP-OH **64** in CDCl_3 .

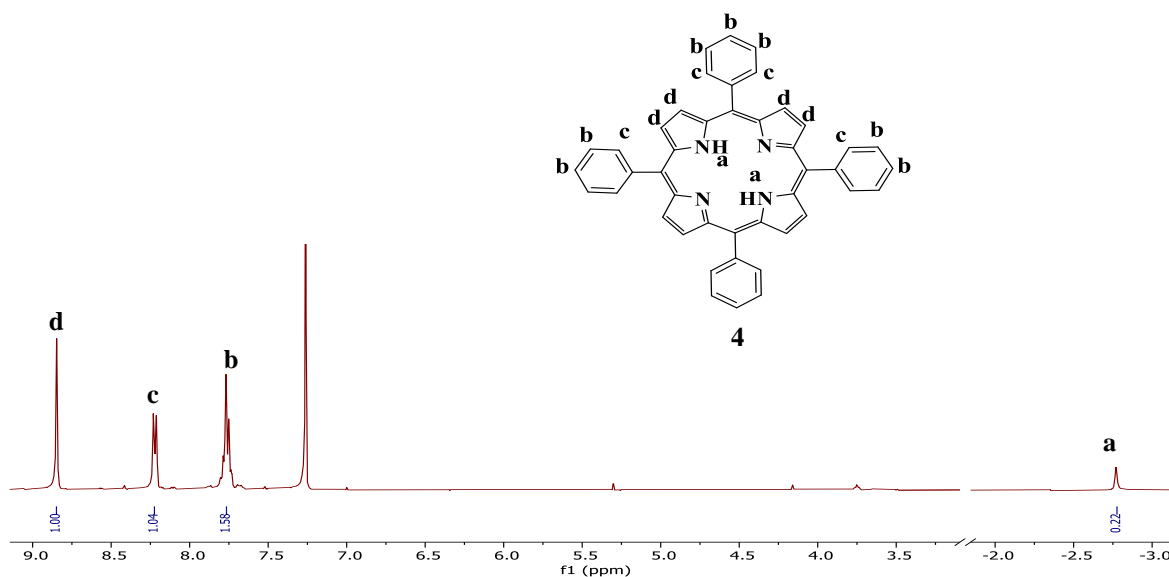
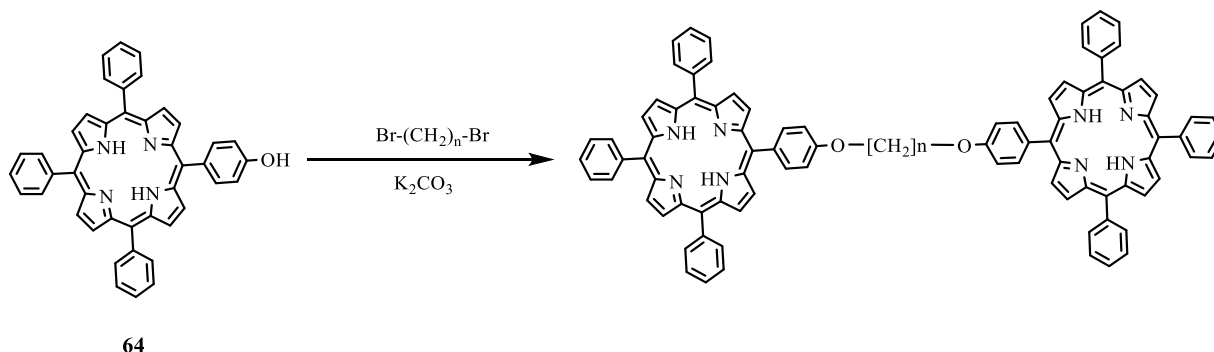


Figure 2.2: ^1H NMR spectrum of TPP **4** in CDCl_3 .

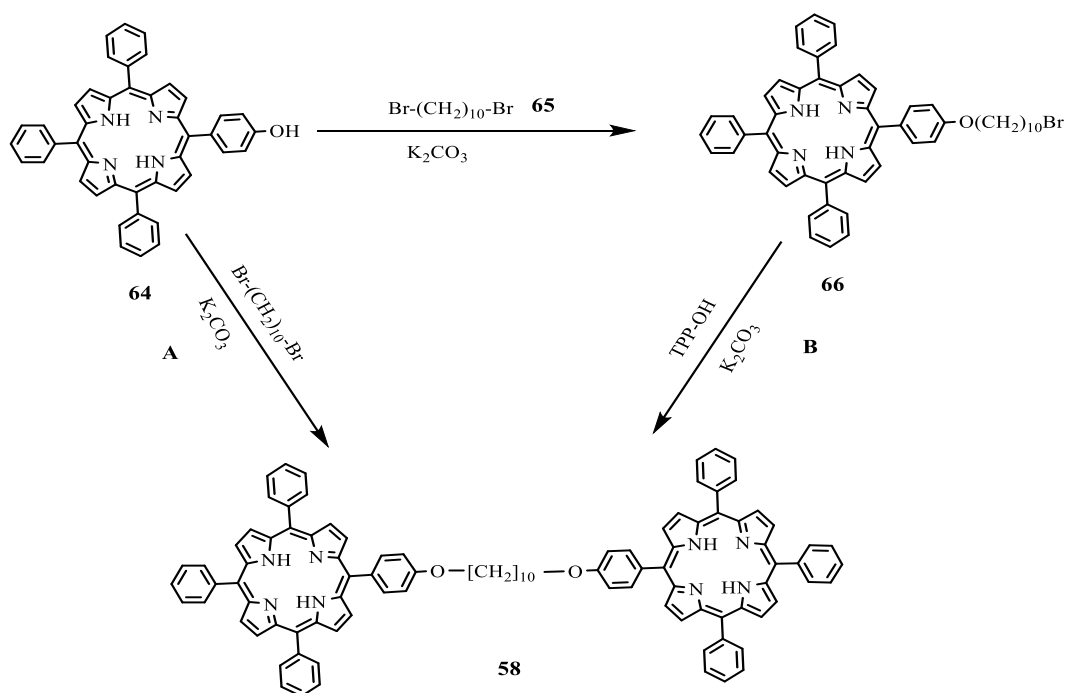
2.3 Synthesis of Porphyrin dyad **58**:

The synthesis of the triple decker requires the preparation of the pure dyad. Two porphyrin molecules are connected by an alkyl chain in our target dyad. The dyad was synthesised using 1-*n* dibromoalkane with $n = 10, 12$ (scheme 2.6).^[4]



Scheme 2.6: General synthesis of Porphyrin dyad.

As indicated in scheme 2.7 below, there are two possible approaches to prepare the dyad. Two equivalents of TPP-OH **64** and one equivalent of 1,10 dibromodecane **65** reacted in a one step in route **A**. Pathway **B**, on the other hand, produces the product in a stepwise fashion. This is accomplished by reacting one equivalent of TPP-OH with the dibromodecane to produce a monosubstituted porphyrin **66**.^[4] To make the product, the latter is reacted with another equivalent of TPP-OH **64**.



Scheme 2.7: The two pathways for synthesis of Porphyrin dyad **58**.

The porphyrin dyad was synthesised using Pathway **A**, but the process is slow. Two equivalents of TPP-OH, one equivalent of 1, 10 dibromodecane and an excess of potassium carbonate were mixed in 20 ml of acetone and refluxed for 6 days. Checking the reaction mixture by TLC revealed three spots, identified as TPP-OH, the mono-substituted product **66** and the porphyrin dyad **58**. Full consumption of starting material was not observed even after 6 days of reaction. After following the reaction by TLC for further days, it was found that the reaction completed within 10-12 days with a very low yield of 19 %.

2.3.1 Optimisation of reaction conditions for C₁₀ porphyrin dyad formation:

Even while producing a dyad appears to be a simple procedure, dealing with the undesired side-products proved to be a considerable difficulty (scheme 2.8). The type of base, solvent, temperature, all play a role in this reaction (Table 2.1).

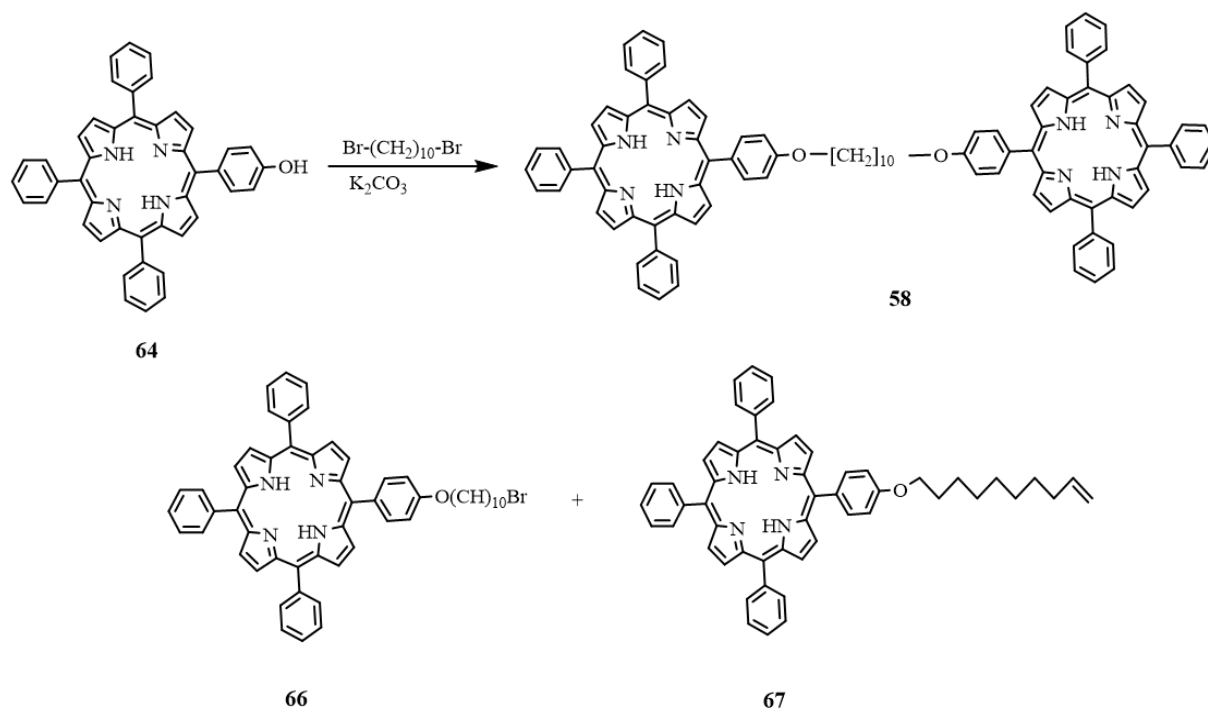
Entry	TPP-OH Eq./mg	Br (CH ₂) ₁₀ Br Eq./mg	Solvent	Base/Catalyst	Time	Temp. (°C)	Yield
1	2 / 200	1 / 47.6 mg	Acetone 20 ml	K ₂ CO ₃	10-12 d	reflux	19%
2	2 / 200	1 / 47.6 mg	acetone 5 ml	K ₂ CO ₃ 18-crown-6	6d	70 (sealed tube)	30%
3	2 / 200	1 / 47.6 mg	acetone 5 ml	K ₂ CO ₃ 18-crown-6	15d	70 (sealed tube)	45%
4	2.5 / 600	1 / 114.2	DMF	K ₂ CO ₃ (ex) KI (10%)	24h	70 (under N ₂)	20%
5	2.5 / 600	1 / 114.2	DMF	K ₂ CO ₃ (ex) KI (10%)	3h	90 (under N ₂)	59%

Table 2.1: Optimisation of dyad synthesis with different reaction conditions.

To increase the yield of the reaction, 5 ml of acetone was added to a sealed tube to prevent the solvent from evaporating due to the small volume of acetone used in presence of 18-crown-6 and the reaction was carried out at 70 °C. The porphyrin dyad was obtained in 30% yield and significant amount of side products were formed beside the product. To improve the yield, the reaction was repeated for 15 days instead of 6 days in sealed tube with the same volume of acetone. Even after 15 days of reaction, complete consumption of the starting material was not observed. The optimization with acetone solvent did not increase the overall yield more than 45% due to the formation of by-products.

The next change was to use DMF instead of acetone as reaction solvent in the presence of excess of potassium carbonate and 10% mol of KI as catalyst to try preventing the formation of side product. The reaction was carried out for 24 h at 70 °C and mostly consumption of the starting materials was achieved. However, the elimination side product was a major product of the reaction. The reaction was repeated, at temperature 90 °C for 3 hours. TLC

was used to check the reaction, and it revealed a larger consumption of TPPOH as well as the elimination product **67**, but it resulted in a higher yield of dyad (**58**) (59 %).



Scheme 2.8: Synthesis of Porphyrin dyad.

For the purification of crude reaction products, acetone was removed, and DCM was added to re-dissolve the resulting product which was then washed with distilled water to remove the base or any inorganic compounds. Then, silica gel column chromatography using 3:2 DCM: hexane as eluent removed mono substituted product and other side products. Solvent change to DCM allowed isolation of some dyad. However, the major amount of the dyad was stuck in the baseline and could not be recovered with any solvent even with THF or MeOH. Due to the low solubility of the dyad loss of the material was not avoidable although many types of solvents were used. Then purification was achieved by careful recrystallization from DCM/MeOH multiple times, yielding a purple pure product. In the practical case of using of DMF as solvent the crude reaction was filtered and washed with cold DMF then with MeOH. The solid was sonicated with water and MeOH then filtered. The product was purified by recrystallisation from DCM/MeOH multiple times, yielding a purple pure product. The behaviour of the dyad makes purification at large scale difficult. When dissolved it behaves normally on chromatography. However, when crystalline the solubility is very low.

The ^1H NMR spectrum of the porphyrin dyad is shown in figure 2.3. There is no triplet peak at around 3.5 ppm for monosubstituted porphyrin **66** ($\text{CH}_2\text{-Br}$) and an observable triplet peak at around 4.30 ppm for ($-\text{O}-\text{CH}_2$).

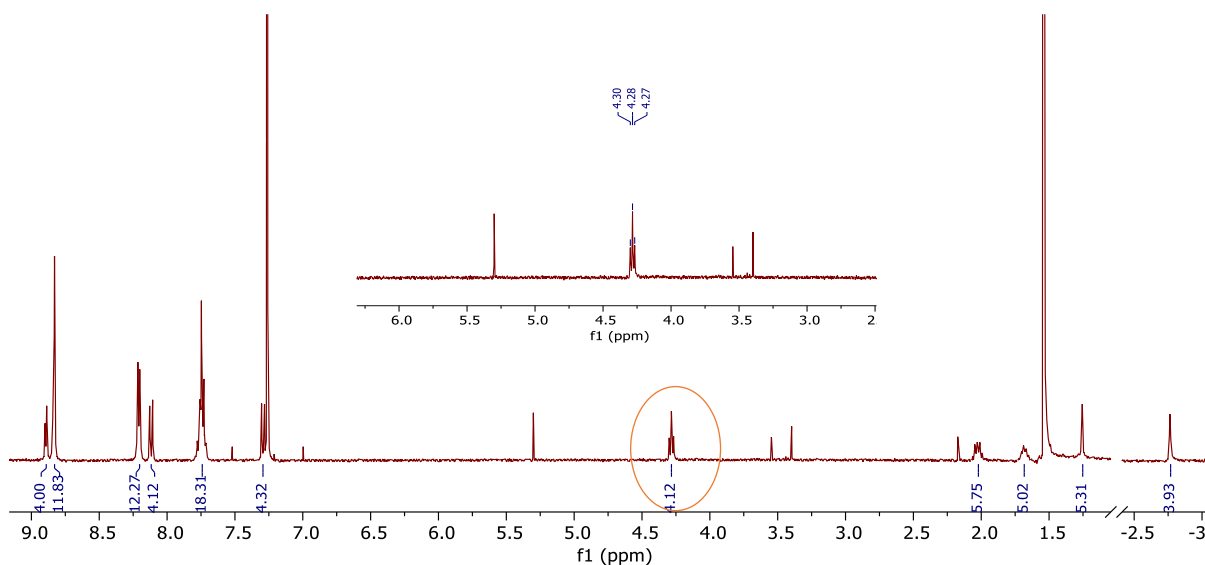
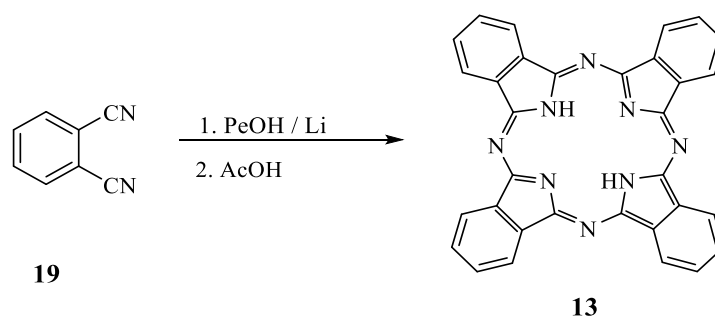


Figure 2.3: The ^1H NMR spectrum of the porphyrin dyad **58** in CDCl_3 .

At the outset of the project a repeat synthesis of TD structures was to be performed in order to understand and optimise TD reaction conditions.

2.4 Synthesis of metal-free phthalocyanine:

In the synthesis of lanthanide triple deckers, metal-free phthalocyanine is an important starting material. There are various protocols involved in the preparation of phthalocyanine. After reviewing the literature we decided to prepare the molecule following the general methodology mentioned by Galanin and Shaposhnikov because of its high yield.^[5]



Scheme 2.9: Synthesis of metal-free phthalocyanine **13**.

The preparation of metal-free phthalocyanine **13** was achieved by first dissolving phthalonitrile **19** in 1-pentanol at reflux (scheme 2.9), then excess of lithium metal was added and refluxed for another hour. Acetic acid was added to the reaction mixture and refluxed for another hour to quench the reaction by removing the excess of the metal to form metal-free phthalocyanine. The reaction was allowed to cool and MeOH was added to precipitate the desired Pc as a dark blue solid with a 52% yield. The MALDI-TOF-MS shows that metal-free phthalocyanine is formed (figure 2.4). As the Pc has very low solubility in organic solvents the ^1H NMR characterisation was not achieved.

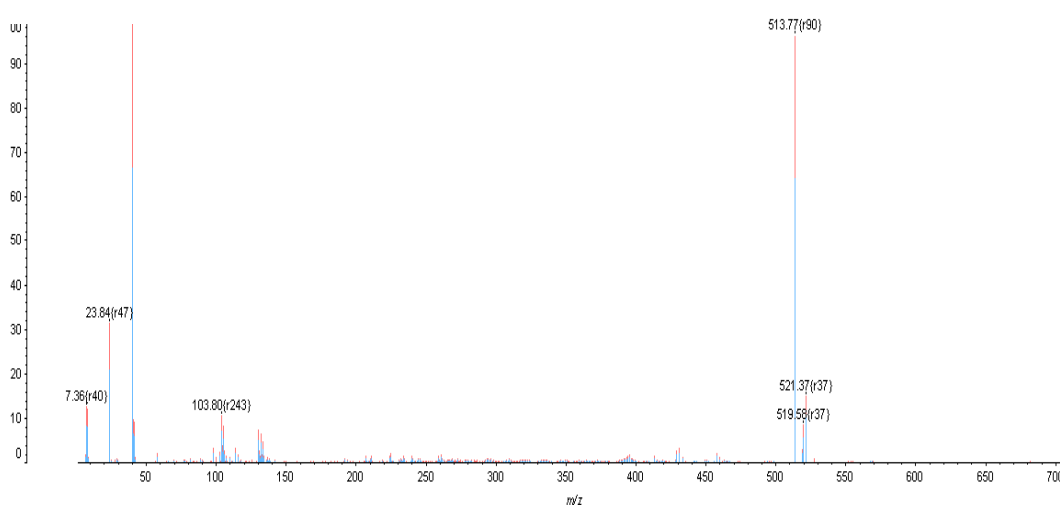
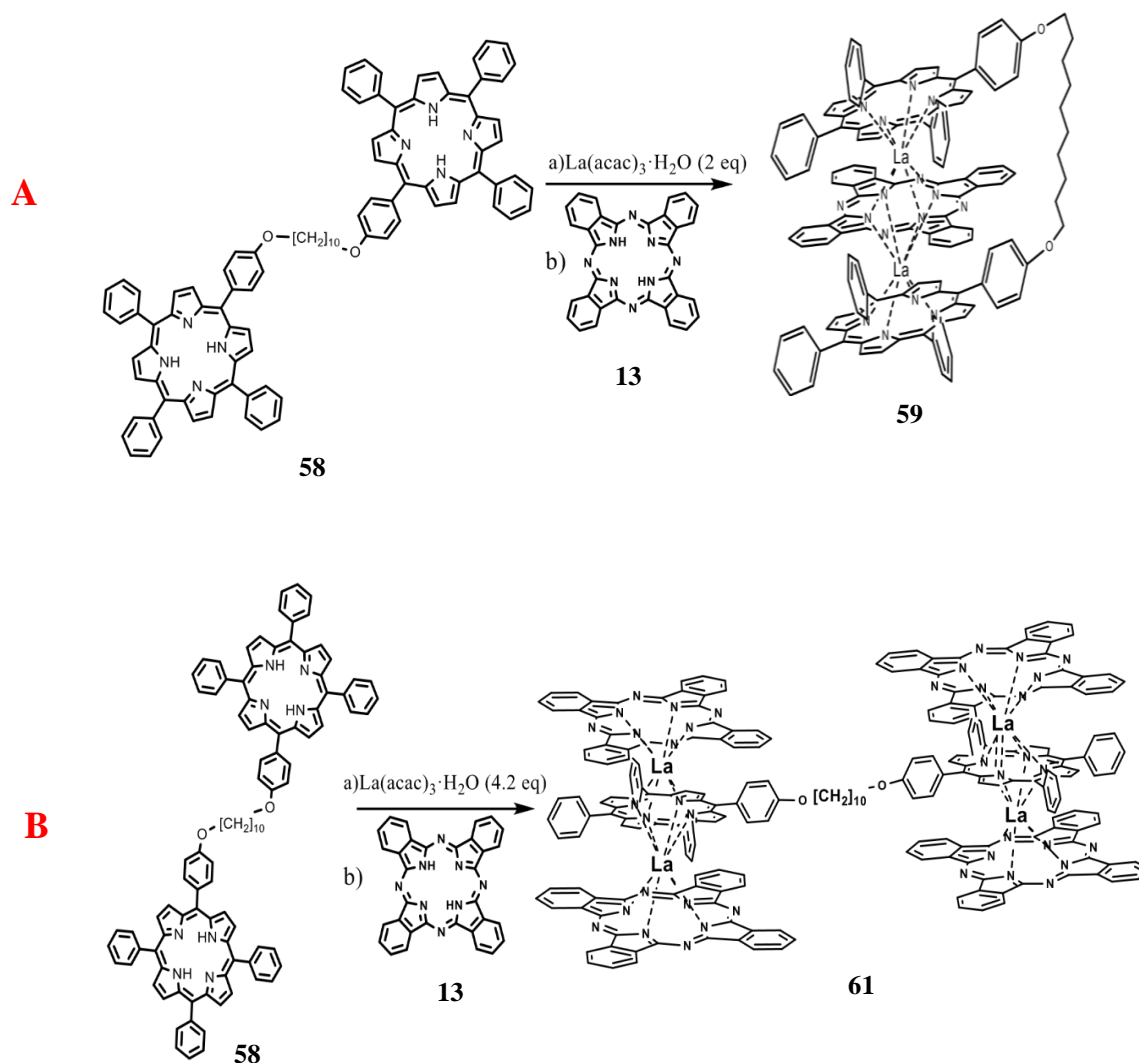


Figure 2.4: MALDI-TOF MS for metal-free phthalocyanine.

2.5 Triple decker formation using unsubstituted phthalocyanine:

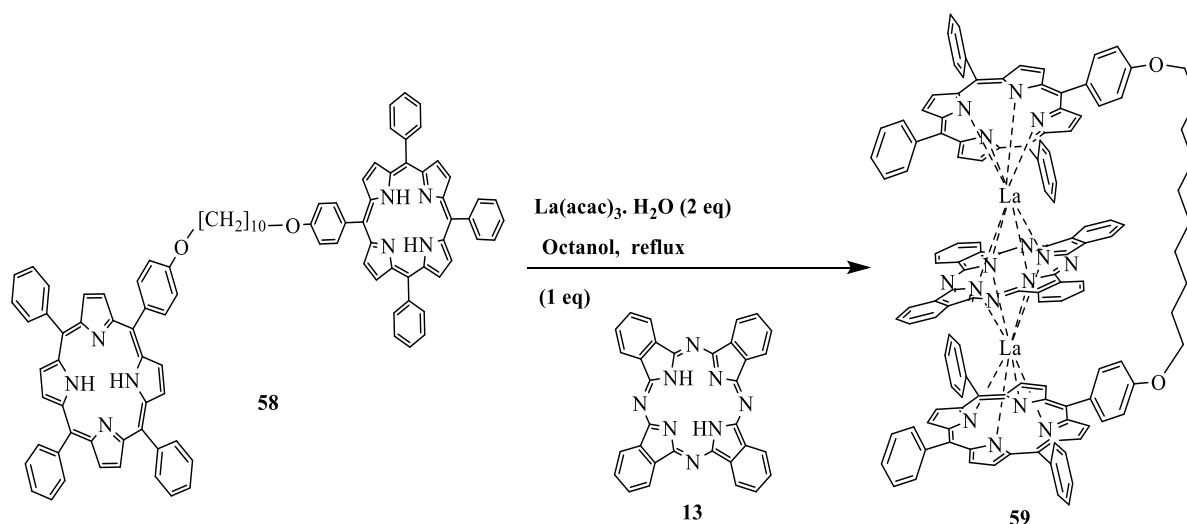
Recently, Cammidge's group has achieved the preparation of triple deckers from linked porphyrin dyads. They discovered that n-decane is the best length to use (scheme 2.10 A).^[1] Despite the fact that the porphyrin-phthalocyanine-porphyrin triple decker **59** is favoured by the bridged porphyrins, an open bis-triple decker **61** can be made by increasing the equivalents of phthalocyanine and lanthanide metal (scheme 2.10 B).^[1]



Scheme 2.10: General method for controlled triple decker synthesis by Cammidge *et al.*^[1]

2.5.1 Improvement attempts with low boiling point solvents:

To synthesise the lanthanum triple decker **59**, the general method developed by Cammidge *et al.*^[1] was followed which required one equivalent of porphyrin dyad **58**, two equivalents of lanthanum (III) acetylacetonate and one equivalent of phthalocyanine **13** refluxed in octanol as shown in (scheme 2.11).^[6]



Scheme 2.11: Synthesis of Closed triple decker **59**.

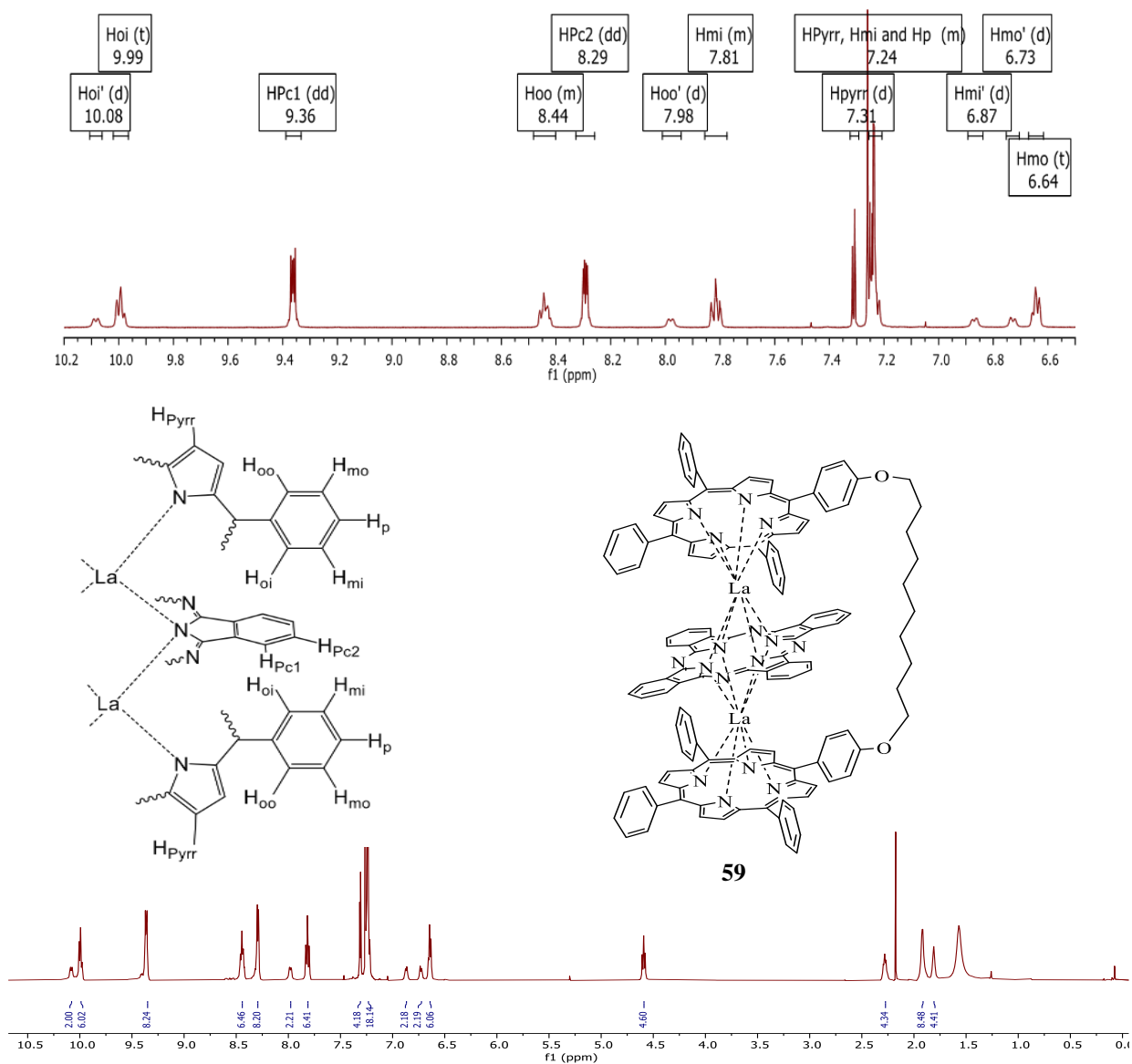
The reaction was monitored and after 24 hours, the reaction mixture was analysed by TLC and 3 spots were observed. They were the unreacted starting material, the desired triple decker and an unknown compound with a greenish blue colour. After completion of the reaction, MeOH was added. The major portion of TD remained in solution of MeOH/Octanol. Solvents were removed under reduced pressure and the residue underwent recrystallisation from DCM/MeOH, then a second recrystallization from hexane was performed taking 2 weeks. The desired TD **59** was obtained as a dark brown solid with a 48 % yield. Due to the difficulty to remove octanol, the reaction was repeated with different solvents.

1/ Pentanol was used and refluxed for 24 h. TLC analysis revealed that the desired triple decker was not achieved so the reaction mixture was transferred to a sealed tube to increase the temperature of reaction to 150 °C. Within 8 hours the reaction was checked by TLC and the triple dicker was observed as dark green spot. After 24 h, solvent was removed under reduced pressure and the triple decker was isolated in a pure state by column chromatography using DCM/Hexane (5:2) solvent system in 10 % yield.

Pentanol solvent was found suitable for formation of the lanthanum triple decker. To improve the yield, the reaction was repeated at a higher concentration in sealed tube at 150 °C. After completion of the reaction and removal of the solvent, the triple decker was isolated in a pure state by column chromatography using DCM/Hexane (5:2) solvent system, but the optimization with pentanol solvent did not increase the overall of yield.

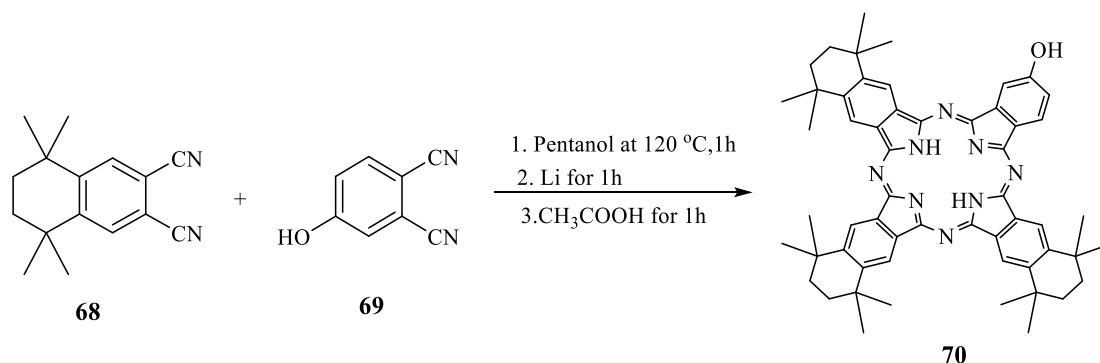
2/ Ethanol was used in sealed tube at 150-160 °C for more than 6 hours, a TLC analysis showed that the desired triple decker was not achieved and only the starting materials was present, and ethanol started to evaporate even though it was in the sealed tube.

The dark green fraction was the desired triple decker **59** confirmed by ^1H NMR and matched with literature spectra perfectly.^[1] The absence of the characteristic peak at -2.7 ppm on the spectrum indicates that there is no metal-free porphyrin and observable triplet peak at around 4.59 ppm for (-O-CH₂). Also, there are two signals at 8.29 and 9.35 ppm that is for symmetrical Pc (HPc₁ and HPc₂) as the lanthanide atoms allowed phthalocyanine units to freely spin inside the complex (figure2.5).



2.6 Synthesis of analogues with substituted phthalocyanines:

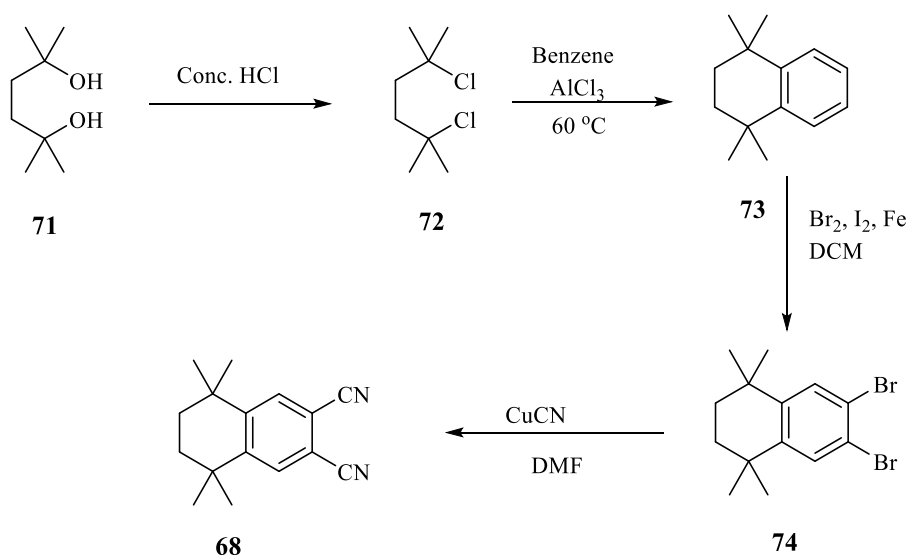
Following these refinements of TD synthesis, the first unsymmetrical phthalocyanine was targeted. As mentioned previously, the initial phthalocyanine in this series for the preparation of linked triple deckers was unsymmetrical phthalocyanine **70** as shown (scheme 2.12).



Scheme 2.12: Proposal of the synthesis of unsymmetrical phthalocyanine.

2.6.1 Synthesis of 6, 7-dicyano-1, 1, 4, 4-tetramethyltetralin:

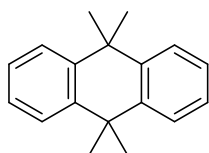
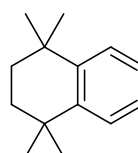
The synthesis required phthalonitrile **68** is shown in scheme 2.13.



Scheme 2.13: Synthesis of 4, 5 disubstituted phthalonitrile **68**.

The first reaction started with conversion of 2, 5- dimethyl hexane- 2, 5-diol **71** to the 2, 5- dichloro-2,5-dimethylhexane **72**.^{[7],[8]} The diol **71** was dissolved in concentrated

hydrochloric acid in an ice bath. The mixture was left to stir overnight at room temperature. The crude was filtered off and washed several times with water and extracted with DCM. Characterisation by ^1H NMR spectroscopy confirmed the identity of the product obtained. In the second step 1,1,4,4-tetramethyl-1,2,3,4-tetrahydronaphthalene **73** was prepared using Bruson's procedure via Friedel-Crafts reaction.^{[7],[9]} Dichloride **72** was dissolved in benzene in the presence of anhydrous aluminum chloride at 50 °C. We noticed that the reaction gave a liquid mono- and a crystalline di-cycloalkylation product, **73** and **75**. When we increased the reaction temperature to 60 °C the yield of desired product **73** was improved and the formation of by-product **75** decreased. After optimisation the compound was prepared by dissolving **72** in benzene and adding the anhydrous aluminium chloride in small portions at 30 °C.^[7] The mixture was left to stir at room temperature for 21 hours then refluxed for 2 hours. It was observed that the yield of desired compound increased, and by-product was decreased. The crude was worked up using petroleum ether and washed with methanol to remove the side product. Analysis by ^1H NMR spectroscopy, showed all the signals corresponding to the desired compound.

**75****73**

The next reaction is bromination of 1,1,4,4-tetramethyl-1,2,3,4-tetrahydronaphthalene **73** using Ashton's procedure.^[10] The compound **73** was dissolved in DCM followed by the addition of iron powder and iodine then treated with bromine at 0 °C over 30 minutes. The mixture was left to stir at room temperature overnight. The resulting mixture was washed by an aqueous solution of sodium metabisulfite and sodium bicarbonate to remove the excess bromine. The product was purified using column chromatography to give the desired product **74** in 55% yield. Analysis by ^1H NMR spectroscopy showed all the signals corresponding to the desired compound.

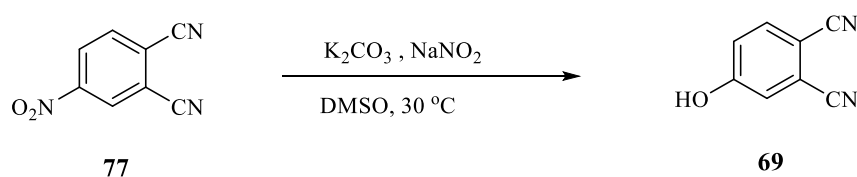
The last step to prepare desired phthalonitrile **68** was achieved following the Rosenmund von Braun cyanation reaction,^[11] in which a mixture of compound **74** and CuCN was heated

in refluxing dry DMF under an argon atmosphere for 2 hours. The reaction was checked by TLC, and it showed 2 spots; one was our product **68** and the other was compound **76**. The crude product was washed with water to remove the excess of DMF and was extracted with Et₂O. It was washed with an aqueous solution of ammonia until no blue colour from copper cyanides was obtained. Purification by column chromatography using PE: Et₂O (7:1) as eluent gave first fraction compound **76** and then the polarity of the eluent was increased to PE: Et₂O (5:1) to collect the desired product **68** as a yellow solid in 42% yield.



2.6.2 Synthesis of 4-hydroxyphthalonitrile **69**.

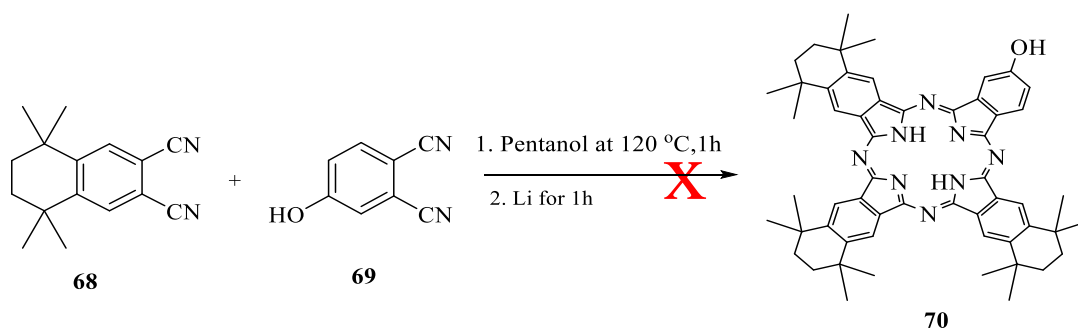
For preparation of 4-hydroxyphthalonitrile **69**, nitroththalonitrile **77** was first dissolved in DMSO. Then K₂CO₃ and NaNO₂ were added to the mixture. The mixture was heated to reflux for 30 minutes, then cooled to room temperature and added to water. The solution was acidified to pH3, and a yellow precipitate formed. The crude was recrystallized using glacial acetic acid. Characterisation by ¹H NMR spectroscopy confirmed the identity of the product obtained (Scheme 2.14).^[12]



Scheme 2.14: Synthesis of 4-hydroxyphthalonitrile **22**.

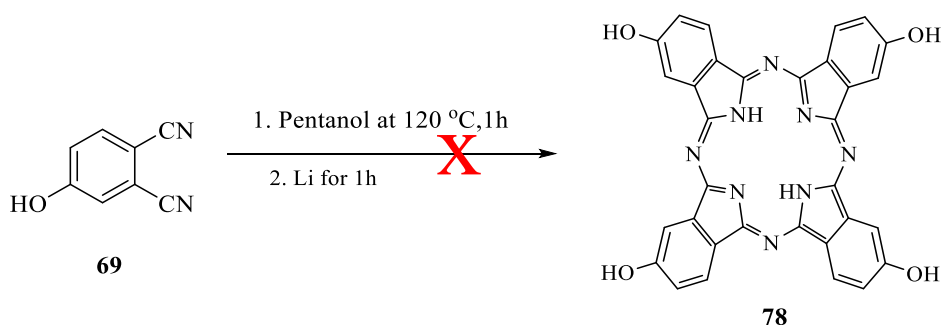
2.6.3 Attempt to synthesise unsymmetrical mono-hydroxy phthalocyanine:

At the beginning, the investigation was started by trying to prepare unsymmetrical phthalocyanine **70** by reacting 3 equivalents of phthalonitrile **68** with one equivalent of phthalonitrile **69** in 1-pentanol under reflux, then excess of lithium metal was added and refluxed for another hour. Unfortunately, there was no noticeable change observed in the reaction, the unsymmetrical Pc **70** did not form at all (scheme 2.15).^[13]



Scheme 2.15: Attempted synthesis of unsymmetrical phthalocyanine **70**.

The general problem with the strategy was confirmed by reacting the phthalonitrile **69** with 1-pentanol and heated under reflux at 150 °C,^[14] then lithium metal was added to the reaction and reflux continued. However, no phthalocyanine was formed in the reaction. This reaction was repeated by adding DBU^[15] instead of lithium, but no noticeable change was observed in the reaction (Scheme 2.16).

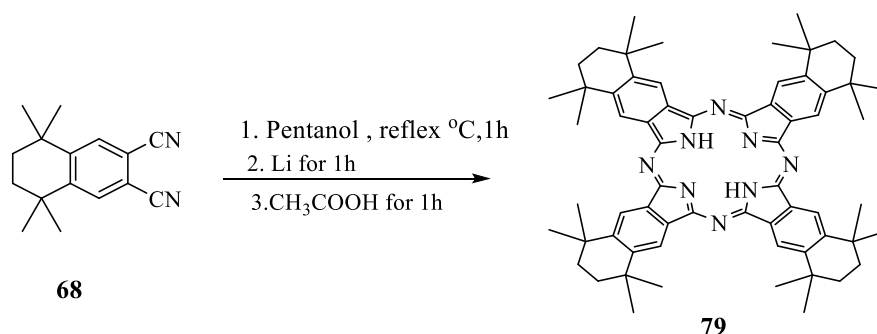


Scheme 2.16: Proposal of the synthesis of symmetrical phthalocyanine **78**.

2.6.4 Metal-free phthalocyanine **79**:

The use of phthalonitrile **68** in the synthesis of unsymmetrical phthalocyanine stemmed from our assumption that they would enhance solubility and be useful in NMR spectroscopic characterisation. Our early experiments attempting to synthesise 3:1 Pc **70** indicated that more significant synthetic effort would be required to achieve this phthalocyanine. We therefore targeted the synthesis of the symmetrical Pc from **79** alone, to establish its incorporation in TD structures before investing further synthetic effort in the unsymmetrical derivatives. Therefore the preparation of symmetrical phthalocyanine^[16] **79** was achieved by reacting phthalonitrile **68** alone in 1-pentanol under reflux. An excess of lithium metal was added and refluxed for another hour. Acetic acid was added to the reaction mixture and

refluxed for another hour. The reaction was allowed to cool and MeOH added to precipitate the desired Pc as a dark green solid (scheme 2.17). The structure, with an X-Ray analysis and ^1H NMR showed that symmetrical phthalocyanine is formed (figure 2.6).



Scheme 2.17: Synthesis of symmetrical phthalocyanine **79**.

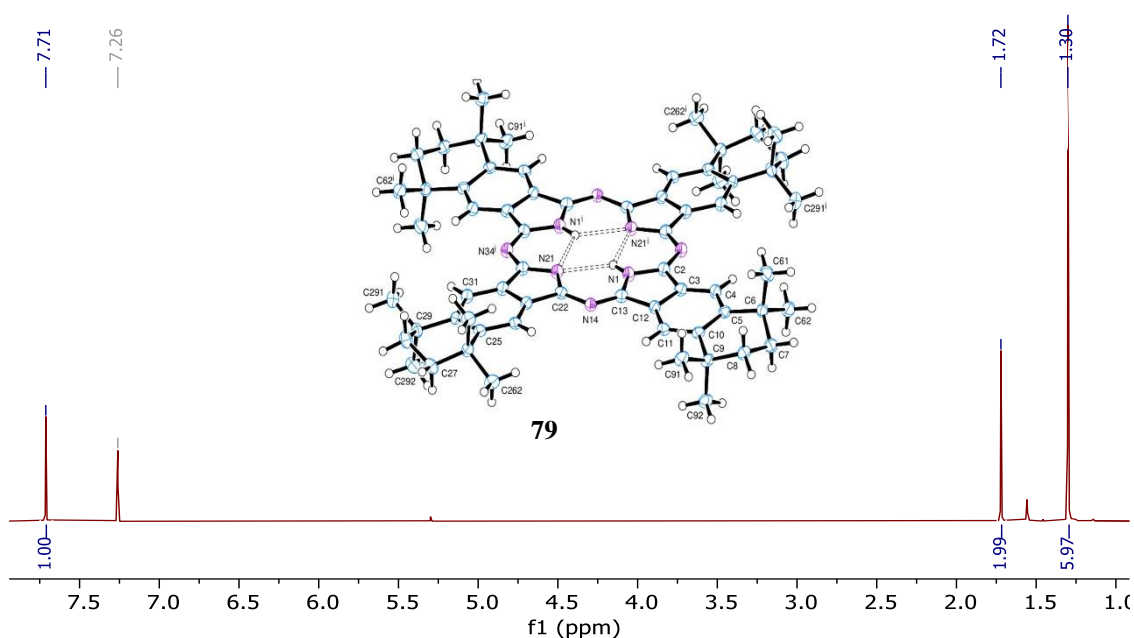
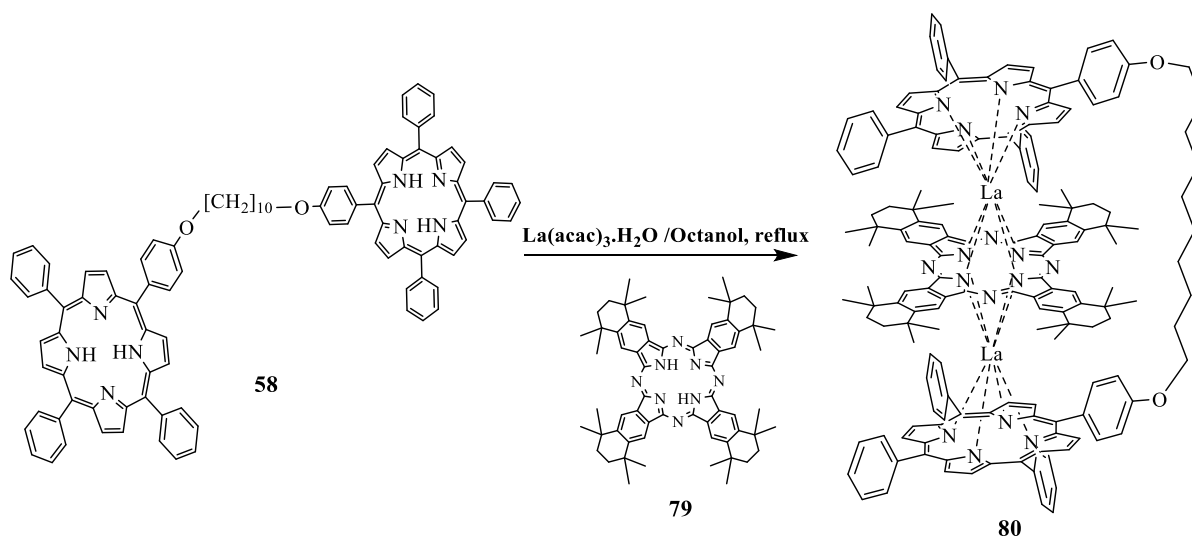


Figure 2.6: The ^1H NMR spectrum of symmetrical phthalocyanine **79** in CDCl_3 .

2.7 Synthesis of closed triple decker **80** from symmetrical Pc **79**:

Peripherally substituted Pc **79** was selected to synthesise the corresponding triple deckers using the same previously developed methodology^[1] from C_{10} porphyrin dyad **58** as shown (scheme 2.18):



Scheme 2.18: Synthesis of triple decker **80**.

The same methodology of one pot, two step reflux in octanol was followed using pre-synthesised Pc **79**. To do so, the porphyrin dyad **58** and lanthanum acetylacetonate were refluxed in octanol followed by the addition of Pc **79**. MALDI-TOF-MS was checked after the reaction and the expected peak at 2614 m/z was observed (figure 2.7).

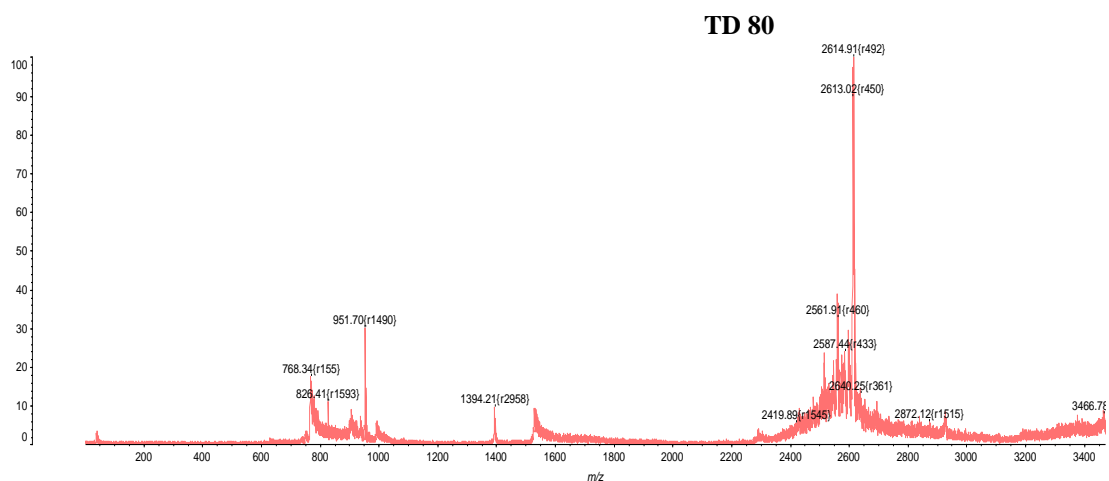


Figure 2.7: MALDI-TOF MS of triple decker **80**.

The solvent was distilled off, but it was found that the resulting black solid did not dissolve in any solvent, even THF. Several issues were discovered during these studies due to the

difficulties to dissolve the crude to obtain good ^1H NMR spectra for the first reaction attempts. Soxhlet extraction was used to dissolve the solid, but unfortunately the crude decomposed to starting materials. After several attempts to isolate this TD **80**, we decided to move our attention to simple TD formation from TPP **4** and Pc **79**. Triple decker **81** was synthesised using the same methodology of one pot procedure for the formation of other triple deckers. A mixture of metal-free tetraphenylporphyrin TPP **4**, lanthanum acetylacetonate and Pc **79** were refluxed in octanol under nitrogen (scheme 2.19). The MALDI-TOF MS was checked after the reaction and the expected peak at 2456.60 m/z was observed as shown (figure 2.8). Unfortunately, we had the same problems as previously and could not separate the largely insoluble products or obtain good NMR spectra.

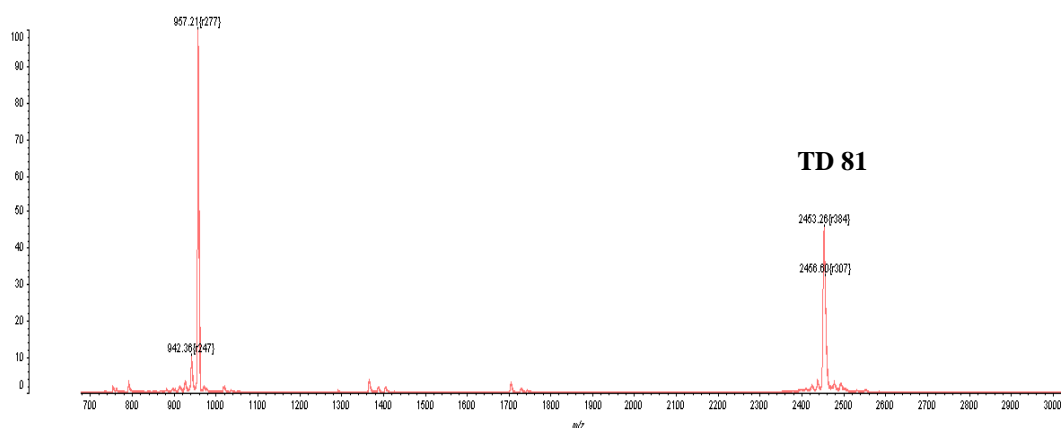
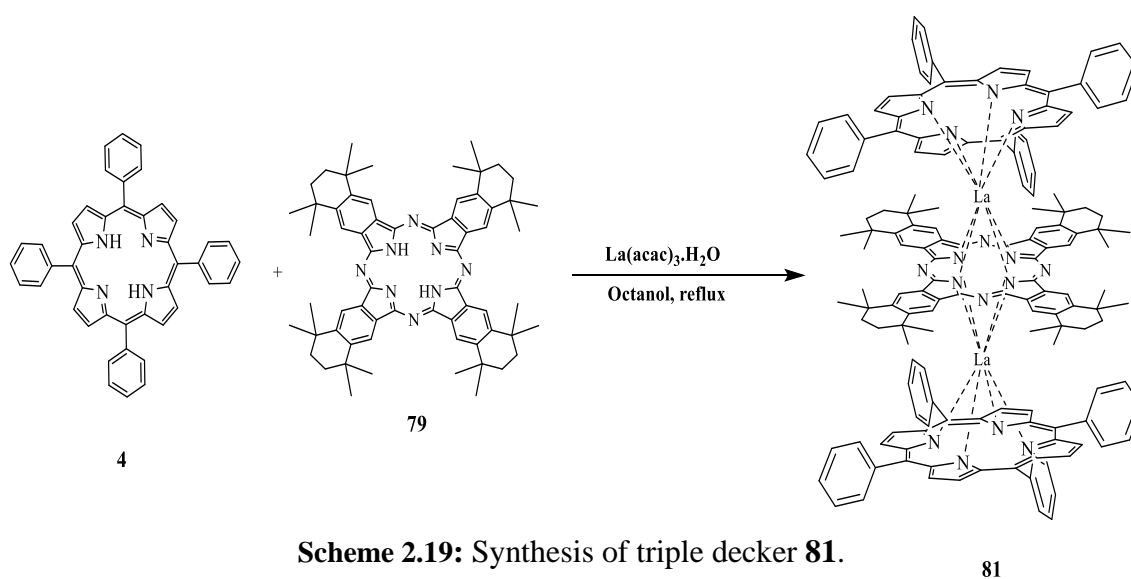
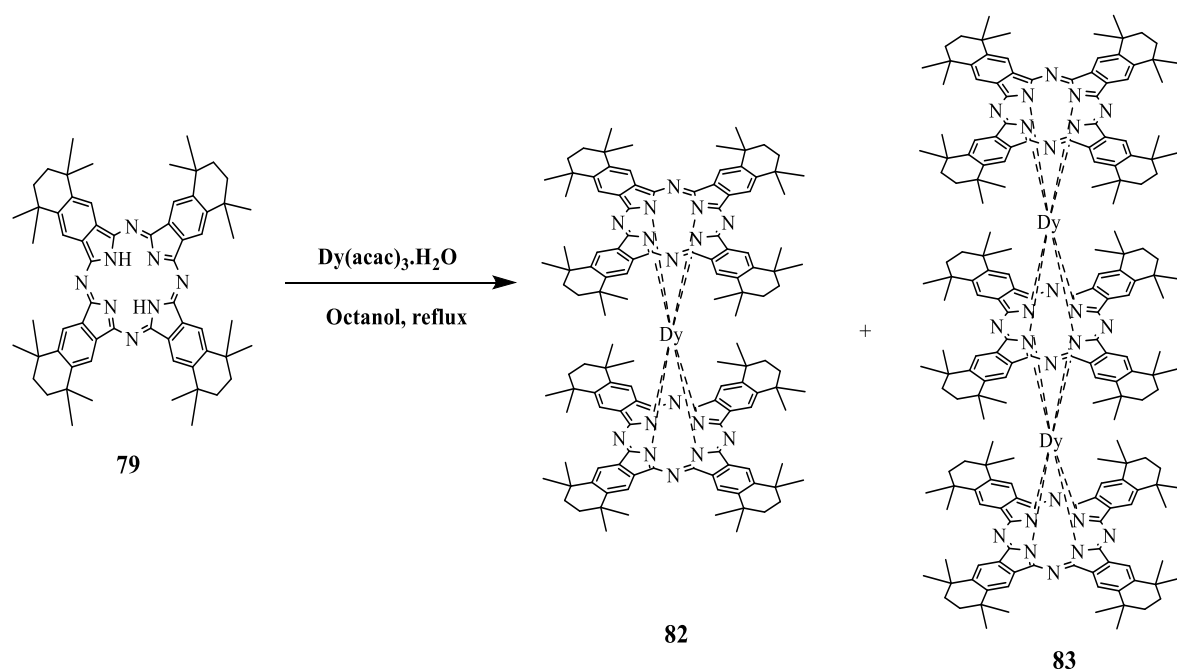


Figure 2.8: MALDI-TOF MS of triple decker **81.**

In order to see if the phthalocyanine **79** could form homoleptic rare earth complexes like double- and triple-decker compound using the same methodology of one pot procedure for the formation of triple decker, a mixture of Pc **79** and Dy(acac)₃ were refluxed in octanol under nitrogen (scheme 2.20). The MALDI-TOF-MS was checked after the reaction and the peaks found were at 2074 and 3185 m/z, corresponding to Dy double **82** and triple deckers **83** from Pc **79** as shown in figures 2.9 and 2.10. The solvent was removed under high vacuum and the residual was separated by column chromatography DCM/ Petroleum ether (1:1) then DCM. A TD **83** and DD **82** were isolated as blue and green crystals. These products also showed very low solubility.



Scheme 2.20: Synthesis of double and triple deckers **82**, **83**.

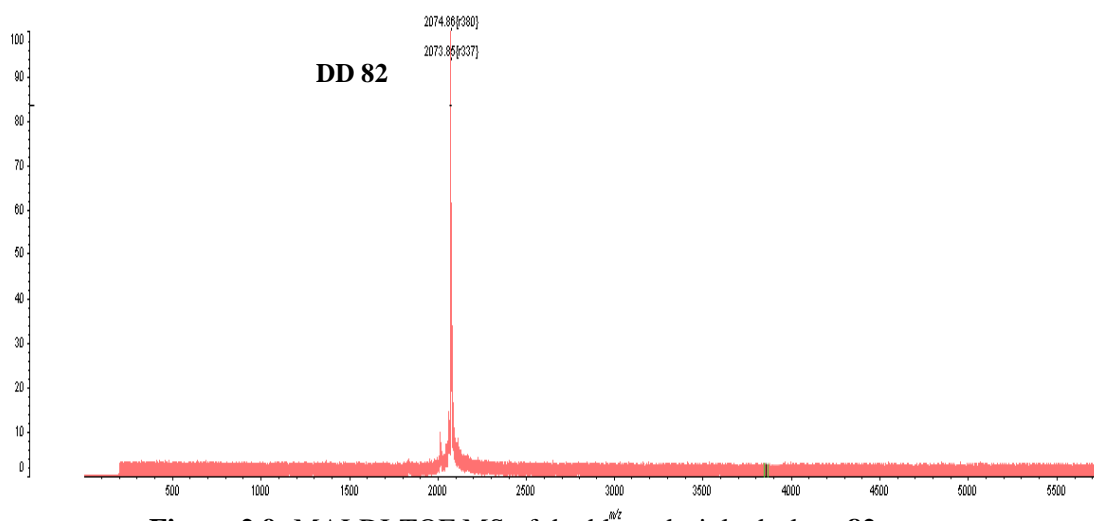


Figure 2.9: MALDI-TOF MS of double and triple deckers **82**.

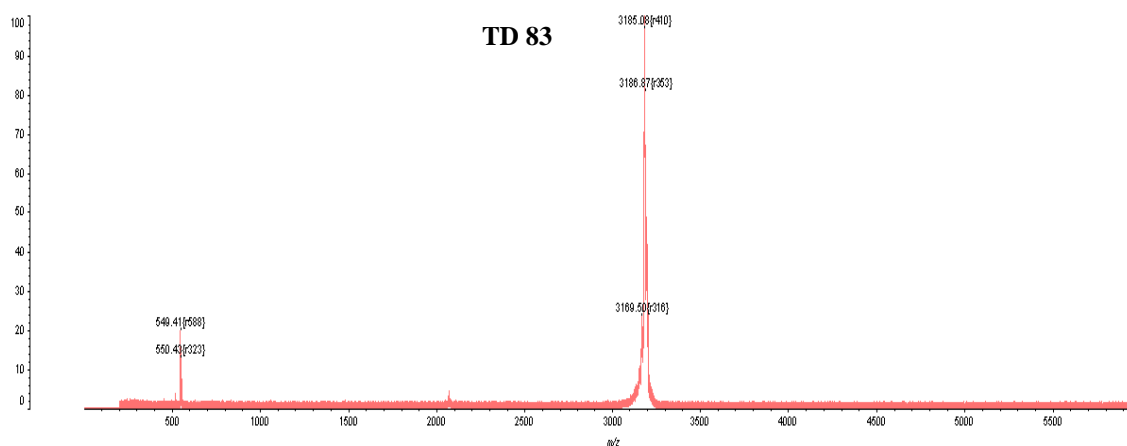
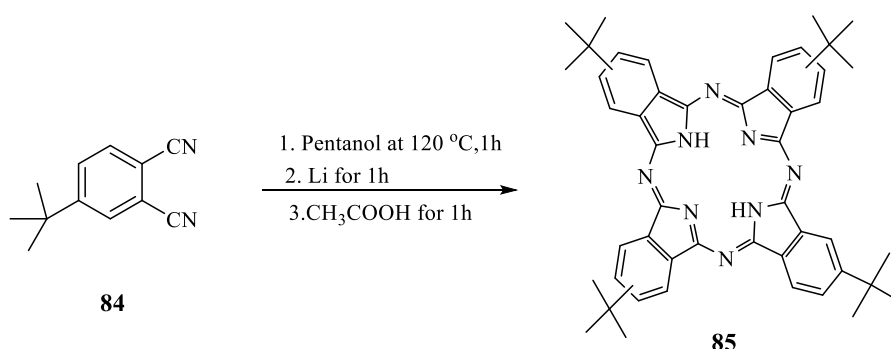


Figure 2.10: MALDI-TOF MS of double and triple deckers **83**.

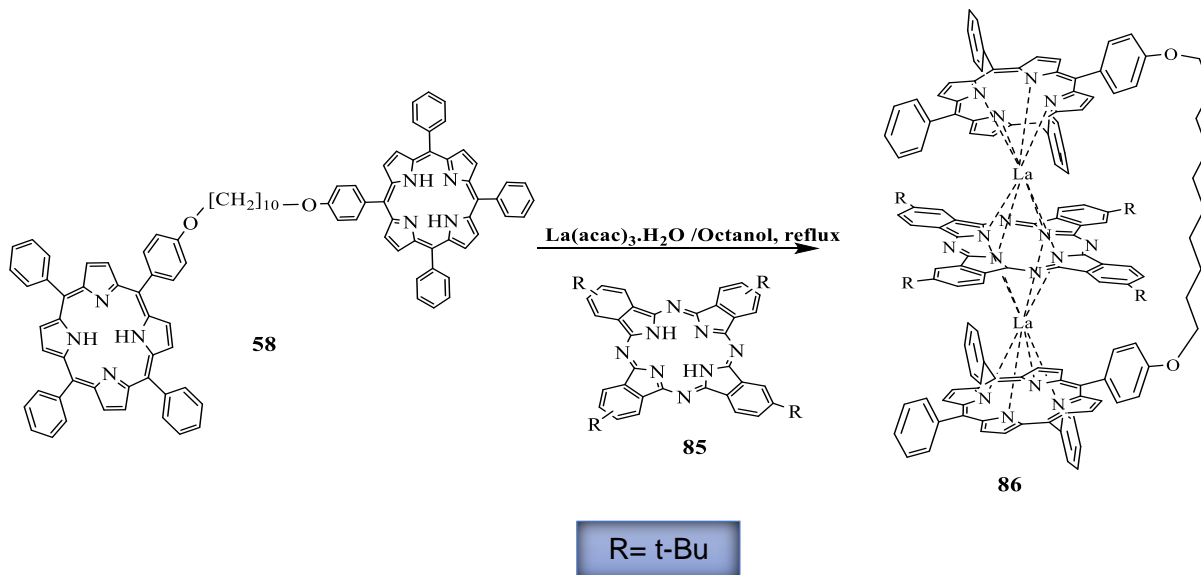
2.8 Synthesis of closed triple decker **86** from ^tbutyl phthalocyanine **85**:

The synthesis of another closed triple decker analogue was attempted in order to see if the same results could be obtained with another substituted phthalocyanine. This phthalocyanine has substituents in the peripheral positions as well. So, in part it matches the steric requirements of Pc **79**. The precursor phthalonitrile **84** is commercially available. The selected phthalocyanine was metal-free tetra-tert-butyl-phthalocyanine **85** obtained by reacting 4-(tert-butyl) phthalonitrile **84** under standard conditions. The desired Pc **85** was isolated as a dark blue solid with a 60 % yield. The MALDI-TOF-MS showed that metal-free phthalocyanine is formed (scheme 2.21). As expected, the ¹H NMR characterisation is complicated due to isomer formation. It was then used for the synthesis of the triple decker **86** as shown in the scheme 2.22.



Scheme 2.21: Synthesis of tetra-tert-butyl-phthalocyanine **85**.

The same methodology of one pot was followed using pre-synthesised Pc **85**. To do so, the porphyrin dyad, Pc and lanthanum acetylacetonate were refluxed in octanol (scheme 2.22). MALDI-TOF-MS was checked after the reaction and the expected peak at 2417 m/z was observed (Figure 2.11).



Scheme 2.22: Synthesis of triple decker **86**.

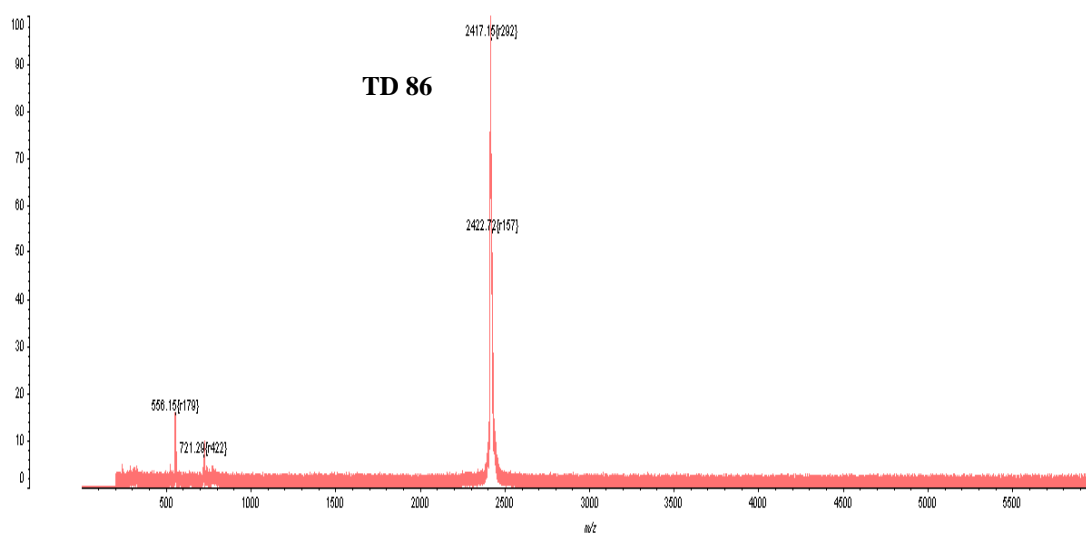


Figure 2.11: MALDI-TOF-MS for triple decker **86**.

The triple deckers **86** was isolated from the mixture in good yield using column chromatography. ^1H NMR was complicated and this can be fully understood because of a

mixture of four regioisomers,^[17] which arise due to the tert-butyl substituent on the β -position (figure 2.12).

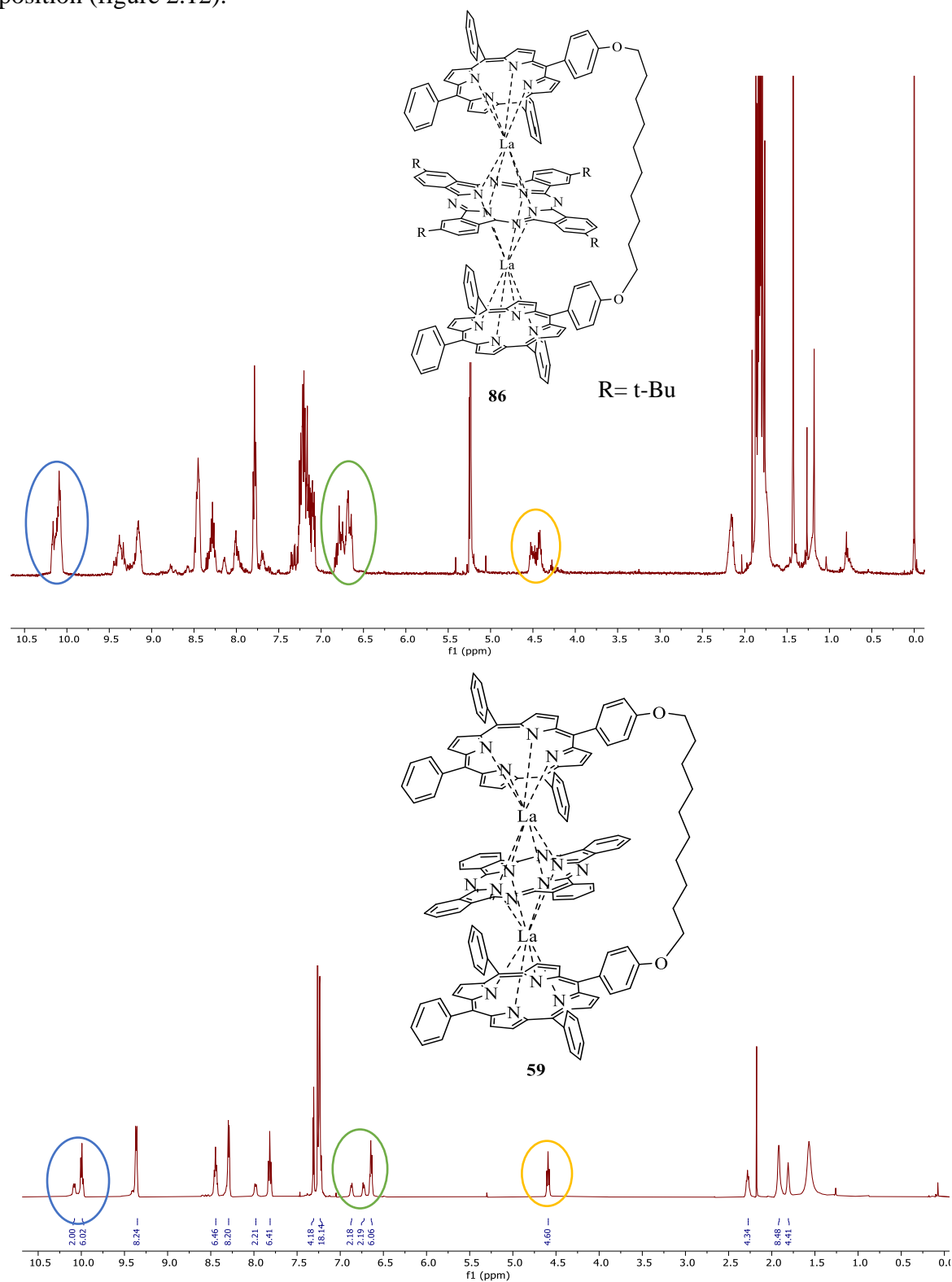


Figure 2.12: ^1H NMR spectrum of triple decker **86** (top) and previous triple decker **59** (bottom) in CDCl_3 .

As indicated in the ^1H NMR spectrum, the signals from the porphyrin peaks found in closed triple deckers **59** that were previously observed at around 10 ppm still present in this TD analogue **86**. Also, some of the other signals typical of closed triple deckers were present, such as the signals at around 4.5 ppm that corresponds to the $-\text{OCH}_2$ and the signals at around 6.5 - 7.0 ppm that corresponds to the $m\text{PhH}$ in the triple decker **59**.

The indication of TD formation can be detected by UV-Vis (figure 2.13). The TD **86** is a dark green/brown colour, which is evident by TLC analysis. This can be the indication of π overlap due to the close distance between macrocycles linked by La.

The spectra of TD **86** is consistent with TD **59** from the literature.^[1] Both closed triple deckers show a sharp absorption at the porphyrin region of 400 nm^{-1} as well as a broad absorption at 300 nm^{-1} typical of sandwich-like complexes in the UV-Vis spectroscopy and there was no absorption in the phthalocyanine region between 600 and 700 nm^{-1} . Additionally, this data was in line with the expected spectra for other structures of this type in which the Pc is sandwiched between two porphyrins ($[\text{Por}]M[\text{Pc}]M[\text{Por}]$).^[18]

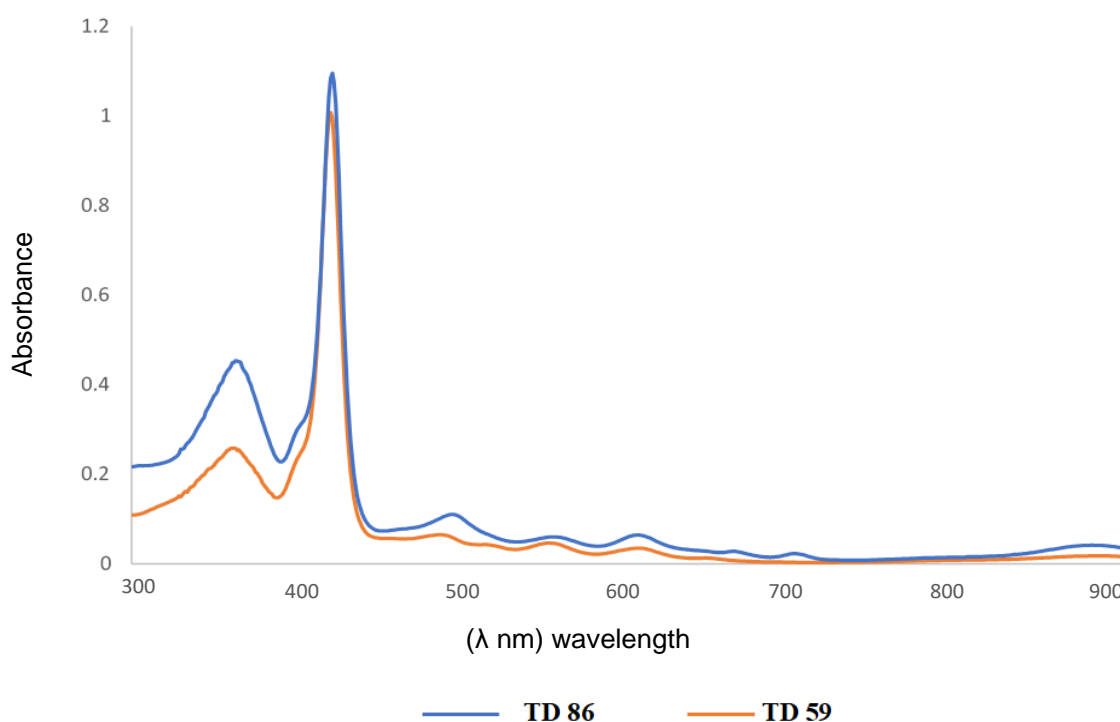
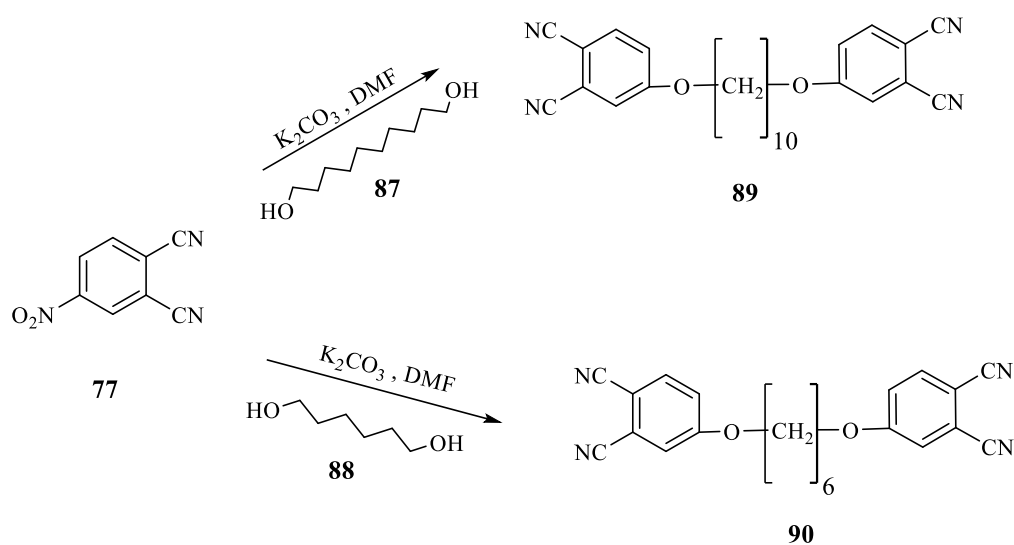


Figure 2.13: UV-Vis of triple deckers **86** and **59** in DCM.

2.9 Synthesis of phthalocyanine- phthalocyanine dimer:

2.9.1 Synthesis of Pc-Pc dimer 91:

From the model experiments it appeared that incorporation of tetramethyl tetralin fragments (from phthalonitrile **68**) caused complication during TD synthesis, whereas ^tButyl groups led to more straightforward reactions (but difficult NMR spectra due to isomers). Our new target therefore become an unsymmetrical Pc containing 3 x ^tBu substituents and one hydroxide or linking chain. From our earlier test reactions, it was known that hydroxy phthalonitrile **69** could not be reacted directly. To control this issue, we tried to make Pc-Pc dimer first then make triple decker. The first step to the synthesis of Pc-Pc dimer was to prepare bisphthalonitriles that contain a long chain as linker as shown (scheme 2.23).



Scheme 2.23: Synthesis of bisphthalonitriles **89**, **90**.

Bisphthalonitriles **89** and **90** were made through a double nucleophilic substitution of 1,10-decanediol **87** and 1,6-hexanediol **88** using 4-nitro-1,2-dicyanobenzene **77**, respectively (Scheme 2.23) in dry DMF under a nitrogen atmosphere in the presence of K₂CO₃. The mixture was stirred at room temperature for 7 days. After workup the crude products were purified by column chromatography. Both pure products (**89**, **90**) were obtained in good yield (40-42 % yield) as a pale-yellow solid. The ¹H NMR spectra (figures 2.14, 2.15) showed a triplet peak at around 4.30 ppm corresponding to the (-O-CH₂). There are characteristic signals for the methylene groups of the alkyl chain appearing 1.72 ppm and 1.50 ppm.

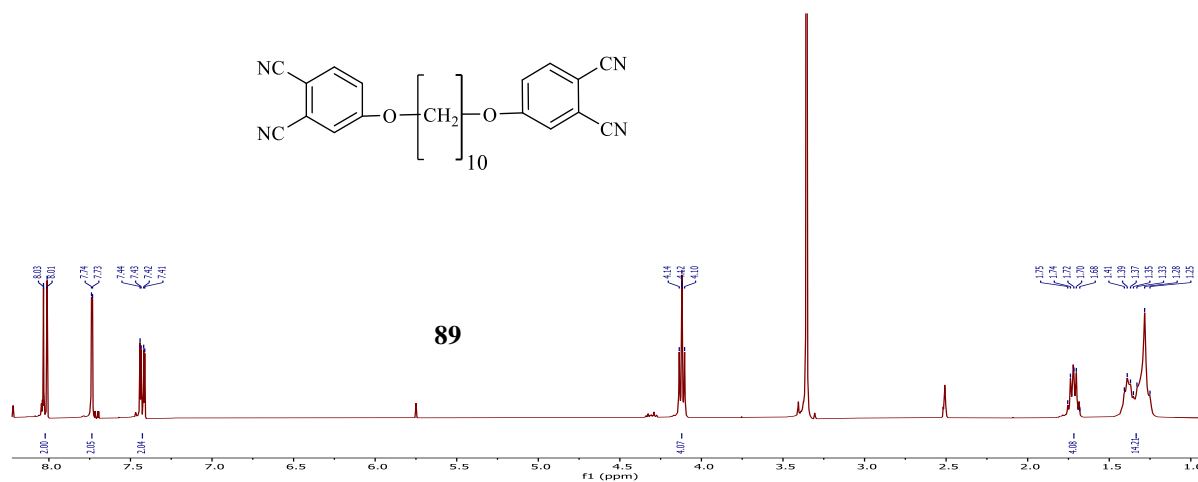


Figure 2.14: ^1H NMR spectrum of bisphthalonitrile **89** in $\text{DMSO-}d_6$.

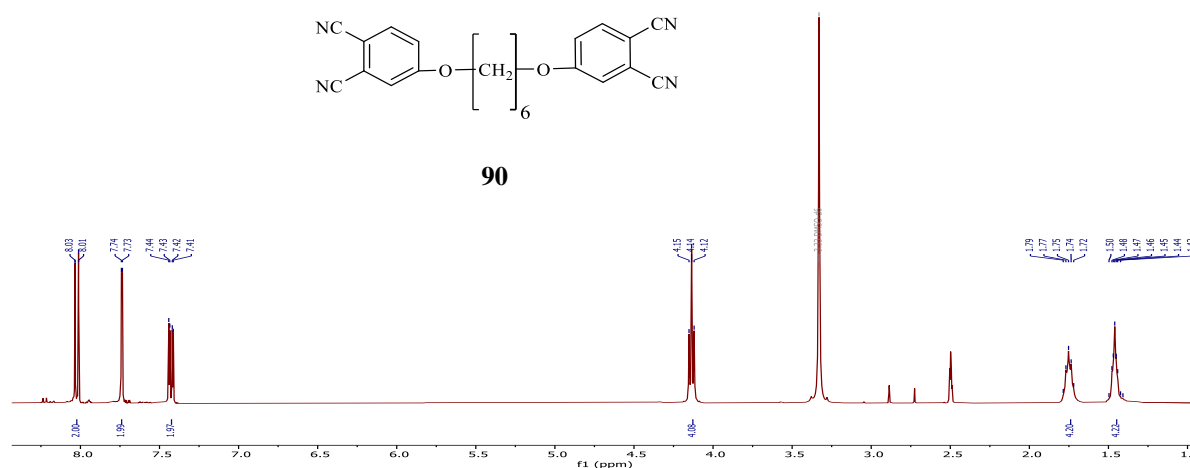
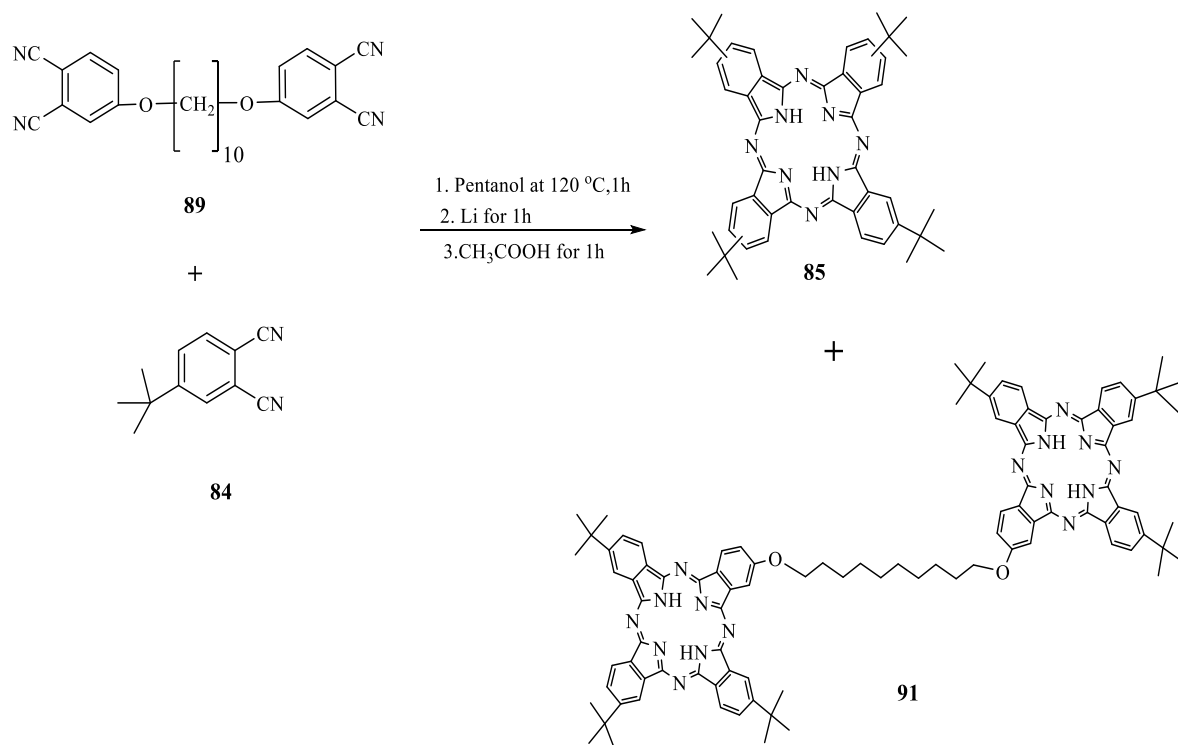


Figure 2.15: ^1H NMR spectrum of bisphthalonitrile **90** in $\text{DMSO-}d_6$.

The first attempt to prepare phthalocyanine dimers was by reacting bisphthalonitrile **89** with excess of commercially available 4-tert-butyl phthalonitrile **84** in the presence of lithium in 1-pentanol (scheme 2.24).



Scheme 2.24: Synthesis of phthalocyanine dimers **91**.

After 24 h, the crude product was precipitated by MeOH and separation of the dimer **91** from side products (a large amount of symmetrical phthalocyanine **85** due to use excess of 4-tert-Butyl phthalonitrile **84**) was attempted. Unfortunately, both of the products have similar polarity and although the mixture of the dimer **91** and symmetrical phthalocyanine **85** were confirmed by MALDI-TOF mass spectrometry (Figure 2.16), they could not be separated.

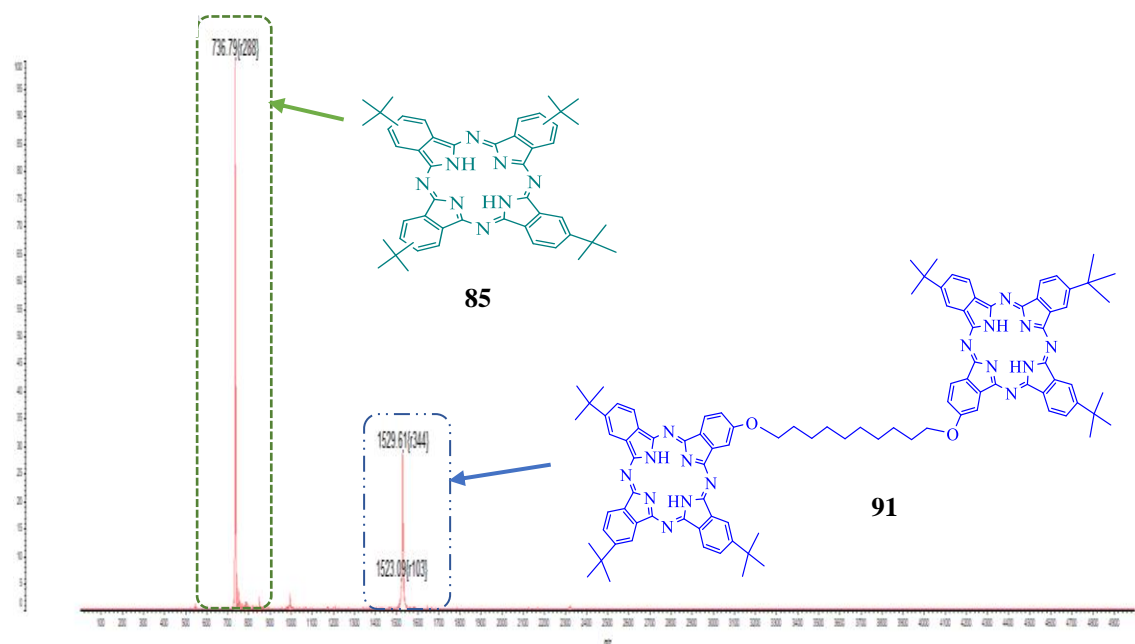
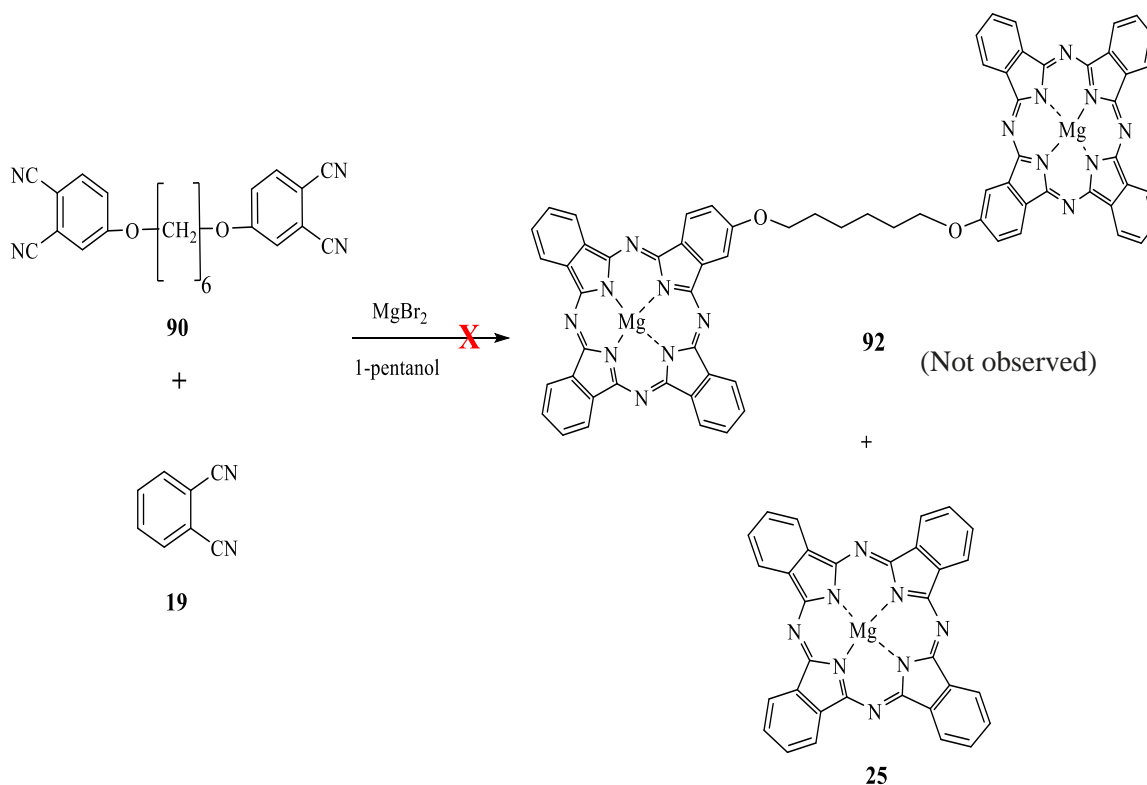


Figure 2.16: Crude MALDI-MS showing presence of compounds **85** and **91**.

2.9.2 Attempt to synthesise Pc-Pc dimer **92**:

An attempt was made to prepare Pc-Pc dimer between unsubstituted phthalocyanines, recognising that it would tend to form aggregates and be insoluble in organic solvents. In order to improve the solubility, we attempted to synthesise the phthalocyanine dimers by reacting bisphthalonitrile **90** with excess of phthalonitrile **84** in the presence of 5 equivalent of MgBr_2 (instead of lithium as shown scheme 2.25). We expected that use of MgBr_2 to form MgPc **25** and the unsymmetrical dimer of MgPc **92** that contained a link chain would make it easier separate them, Unfortunately, the unsymmetrical dimer of MgPc **92** did not form at all.



Scheme 2.25: Proposed Synthesis of phthalocyanine dimer **92**.

2.10 Conclusion:

Attempting to synthesise various analogues of the closed triple decker **59** were challenging. The main challenge was the formation of an intermediate dyad **58** that takes a long time with a low yield. Evidence suggests that the synthesis of closed triple deckers **80** and **86** were possible by the methodology for synthesising the simple triple deckers, but we could not obtain good analysis due to the low solubility of TD **80** and complicated spectra for TD **86** that had a mixture of four regioisomers. At this stage we therefore decided to switch attention to alternative macrocycles.

2.11 Porphyrin and Tetrabenzotriazaporphyrin arrays:

2.11.1 Background and aims:

The failure to link phthalocyanine derivatives with porphyrin dyad to form triple deckers was unexpected and disappointing. Despite the wide variety of structural types of sandwich metal compounds, the formation of the compounds is still mainly restricted to the phthalocyanines, porphyrins, and naphthalocyanines. Therefore, revisiting our strategy, we

decided to employ another type of macrocycle, the tetrabenzotriazaporphyrins TBTAPs as it was a hybrid of phthalocyanine **13** and tetrabenzoporphyrin (TBP) **33** (figure 2.17).

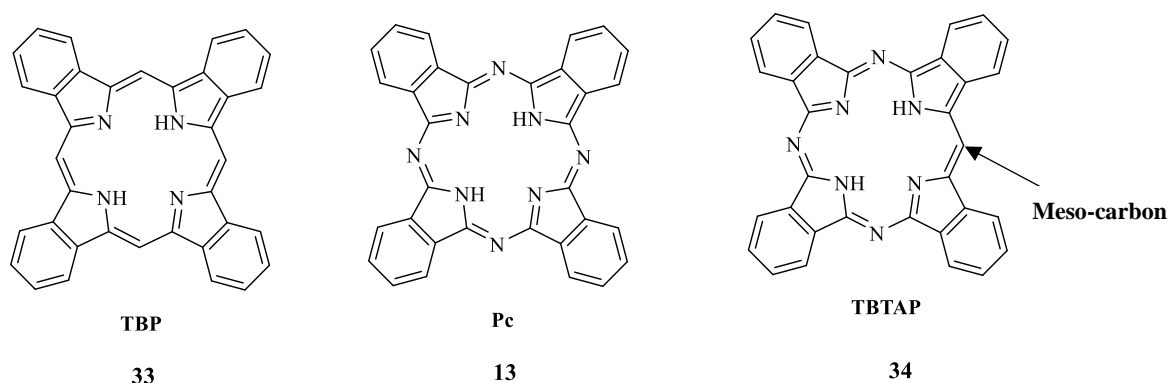
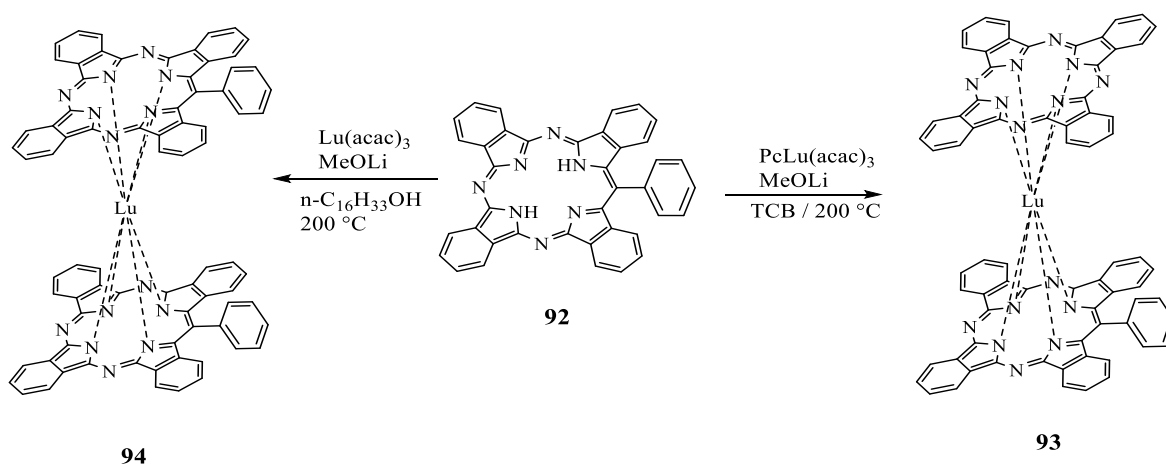


Figure 2.17: Structures of Tetrabenzoporphyrins (TBP), Phthalocyanine (Pc) and Tetrabenzotriazaporphyrins (TBTAP).

Several studies on the synthesis of tetrabenzotriazaporphrin (TBTAP) by different methods have led to the development of novel synthetic procedures that can improve the efficiency of access to the compounds. These studies have led to the synthesis of various, but limited, complexes of the TBTAPs. The first generation of sandwich-type TBTAP compounds was synthesized by Pushkarev *et al.*^[19] (scheme 2.26).



Scheme 2.26: Synthesis of symmetrical and unsymmetrical double-decker complexes^[19].

Therefore, the purpose of this part of the project was to synthesise unique chromophore triads. These triads would combine porphyrin dyad units with TBTAP using $\text{La}(\text{acac})_3 \cdot \text{H}_2\text{O}$ (scheme 2.26). These new structures could have unique features making them useful in

various fields such as materials chemistry, photochemistry, biology, and medicine as the tetrabenzotriazaporphyrin hybrids are structurally related to both phthalocyanine and porphyrin, they have similar properties and potential applications. Importantly, the meso carbon opens up a variety of possibilities in the TBTAPs, for example further functionalisation or the ability to link to other moieties and surfaces. In our case, this importantly includes simple routes to dimerization, one of the major goals in this area. A general example is shown in figure 2.18, where the linking could in theory take place before or after TD formation.

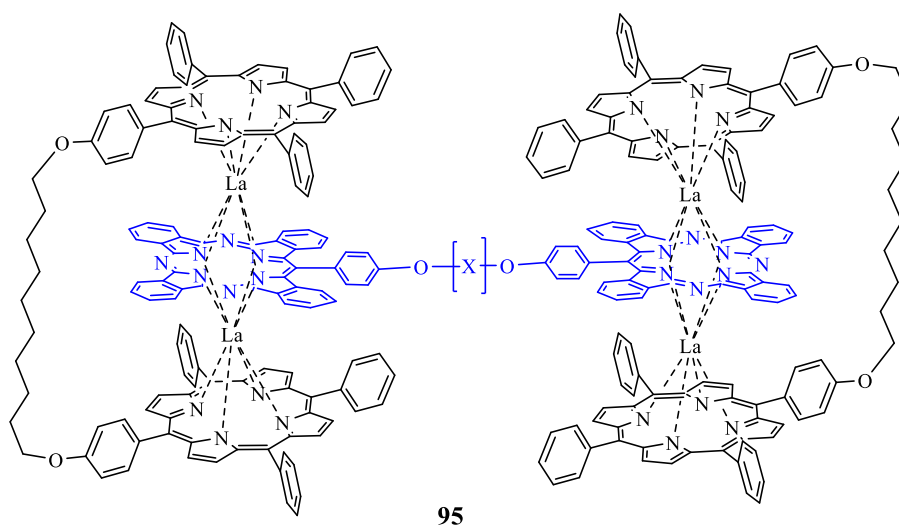


Figure 2.18: Possible linking of TDs through the meso-phenyl unit of a central TBTAP.

However, we were unsure if the twisted phenyl could be accommodated in TDs, knowing from previous work on our linked TDs that there could be a potential steric clash between this and the *meso*-phenyls of the porphyrins. Hence, we focused our investigation on TD formation with simple TBTAPs like **50** for the first series (figure 2.19).

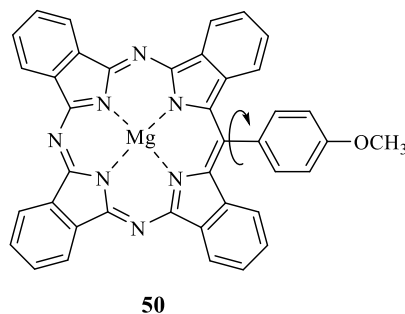
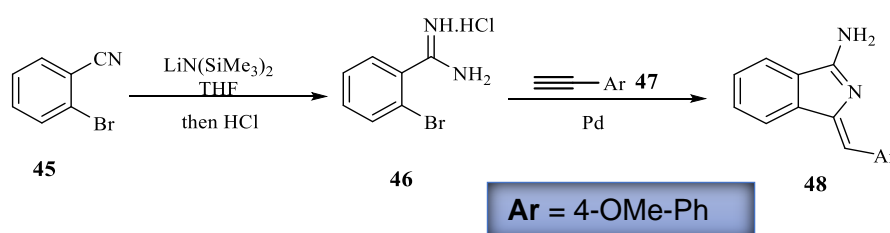


Figure 2.19: Structures of TBTAP **50**.

The difficulties and the challenges associated with TBTAPs synthesis have led to reduce the interest and there has been a lack of their investigation. However, Cammidge group has revisited and improved TBTAP synthesis using a novel approach.^[20] They started working on a modern synthetic method to produce the TBTAPs. The main advantage of this method was its ability to conveniently produce high yields of *meso*-substituted TBTAPs.

The key to the new approach of synthesis was using an aminoisoindoline **48** as an intermediate.^[20] They are easily accessed following the methodology shown scheme 2.27.

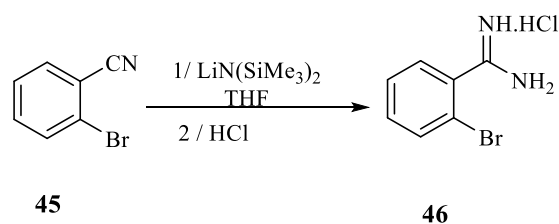


Scheme 2.27: Two-step synthetic method for the aminoisoindoline **48**.^[20]

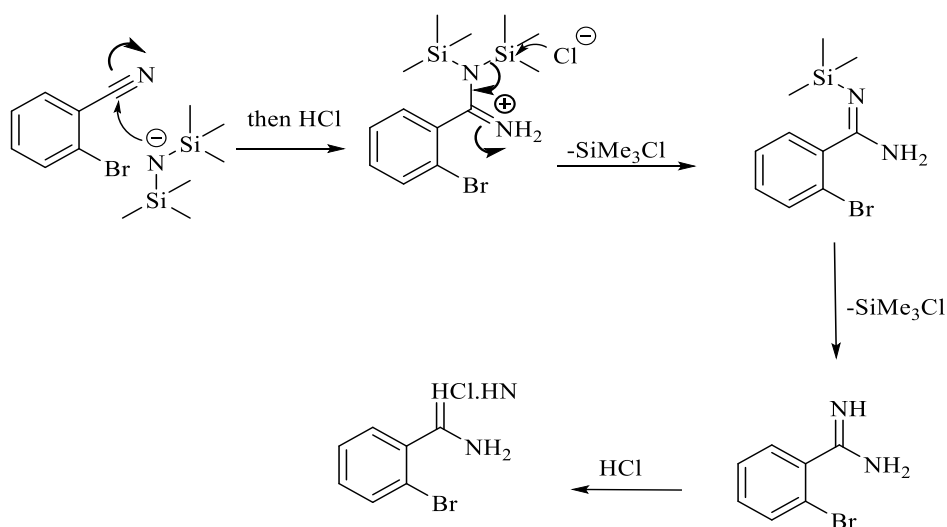
2.11.2 Synthesis of aminoisoindoline **48**:

The synthesis of aminoisoindoline required investigation before the macrocyclization could be achieved. As indicated in (scheme 2.27), Cammidge *et al.* used a two-step synthetic method for the aminoisoindoline.^[20]

The 2-bromobenzonitrile **45** was treated with LiHMDS in dry THF for the first step of the synthetic method. The LiHMDS behaves as a nucleophile, attacking the electrophilic carbon next to the nitrogen in scheme 2.29. Then the reaction mixture is treated with a solution of HCl in isopropanol to remove the silyl protecting groups. This produced a white solid, 2-bromobenzamidine hydrochloride **46**, in 71% yield (scheme 2.28).^[21] The identity of the product was confirmed by ^1H NMR spectroscopy, the spectrum was compared to literature sources,^[20] which confirmed the product was the desired amidine **46**.

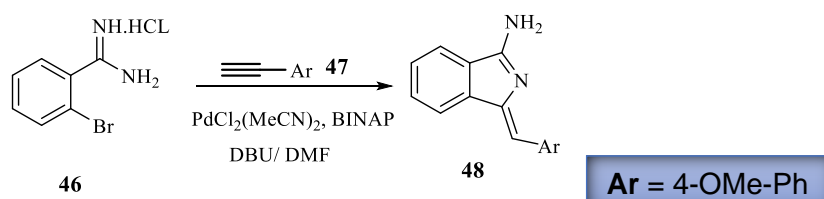


Scheme 2.28: Synthesis of amidine **46**.



Scheme 2.29: Mechanism for the formation of amidine HCl salt **46**.

The Cammidge group then prepared the aminosioindoline **48** by following the Hellal and Cuny method,^[22] (scheme 2.30), using a palladium catalysed copper-free Sonogashira cross-coupling reaction.^[23] The Hellal and Cuny method has a number of advantages in terms of synthesis. To begin with, the technique is copper-free, removing any potential copper from the macrocyclisation reaction. Instead of being copper catalysed, the Sonogashira coupling is achieved by activating the alkyne with DBU. The palladium (II) species catalyses the 5-exo-dig cycloisomerisation, creating the Z isomer, with excellent selectivity once the alkyne has been substituted onto the ring.^{[22],[23]}



Scheme 2.30: Synthesis of aminosioindoline **48**.

This is a one pot synthesis method in which amidine **46**, 4-methoxyphenyl acetylene **47**, catalytic amounts of palladium catalyst and BINAP as ligand, are placed in a microwave vial, in the presence of DBU, as a base.^[24] The solvent used for the reaction was DMF. The mixture was irradiated for 1 hour at 120 °C. The pure aminoisindoline **48** was isolated in a reasonable yield (41%), as a yellow crystal after an aqueous workup and column chromatography by using the solvent system of PE: EtOAc (1:1) then EtOAc.

The ¹H NMR spectrum of **48** (figure 2.20) matched with the literature reports.^[20] The MALDI-TOF-MS showed that we had produced the expected structure. Aminoisindolene **48** had already been synthesised successfully by our group.^[20]

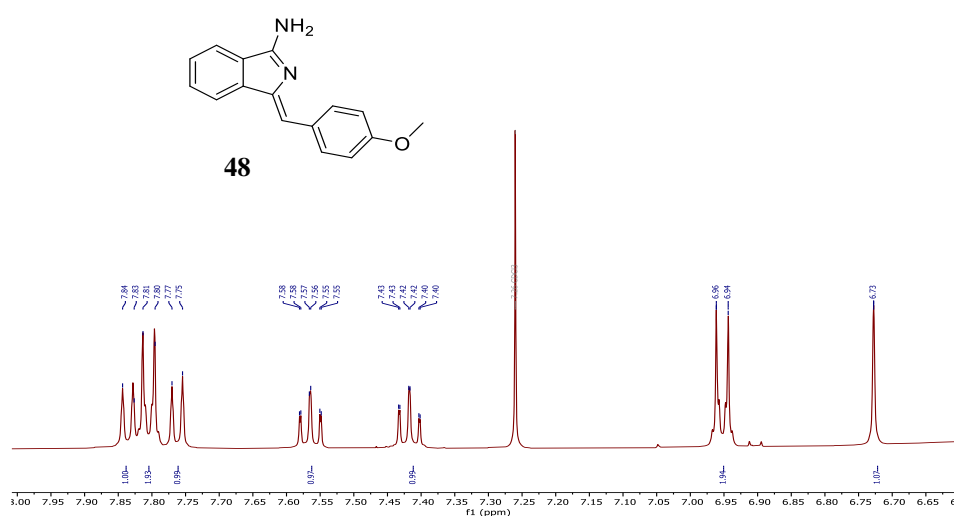
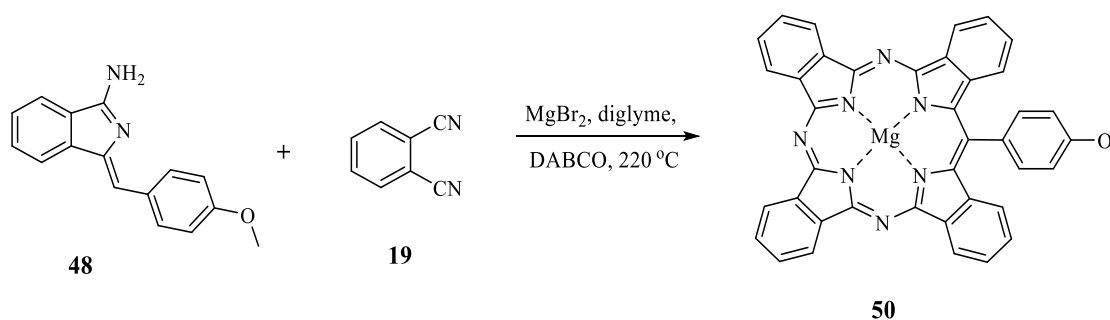


Figure 2.20: ¹H NMR of (Z)-1-(4-Methoxybenzylidene)-1H-isindol-3-amine **48** in CDCl₃.^[20]

The synthesis of the intermediate (aminoisodoline **48**) was achieved and used to prepare TBTA **50**. We initially followed Cammidge group's approach^[20] for synthesising *meso*-substituted-MgTBTA derivatives.

2.11.3 Synthesis of *meso*-substituted TBTA's:

The formation of TBTA's using the method mentioned in the introduction^[20] is achieved by reacting one subunit of the aminoisindoline **48** with three subunits of phthalonitrile **19** using a magnesium template. (Scheme 2.31).



Scheme 2.31: Macrocyclisation step to synthesise TBTAP **50**.

The synthesis of meso-substituted TBTAP **50** was carried out as described by the group (scheme 2.32). A suspension of phthalonitrile (3 equivalents) with MgBr_2 (1.5 equivalents) in dry diglyme was stirred for 10 min under a nitrogen atmosphere. A solution of aminoisoindoline **48** (1 equivalent) and phthalonitrile (1 equivalent) in dry diglyme was added dropwise over 1 hour using a syringe pump. Finally, a third solution of DABCO (1.5 eq) and phthalonitrile (1 equivalent) in dry diglyme was added dropwise over an hour. The reaction mixture was heated for 0.5 hour at 220 °C under a nitrogen atmosphere. Then, the solvent was removed under a stream of nitrogen and a 1:1 mixture of DCM: MeOH (20 ml) was added, and finally the mixture was sonicated. The solvents were concentrated in vacuum and the resulting compound was purified by two consecutive chromatography columns, which were optimized by the Cammidge group.^[20] First, using DCM: Et_3N (20:1), then solvent system changes to DCM: THF: Et_3N (10:1:3). The second column using PE: THF: MeOH (10:3:1) as eluent. A dark green fraction of the MgTBTAP -(4-OMe-Ph) was collected in an overall yield of 23.8 %.

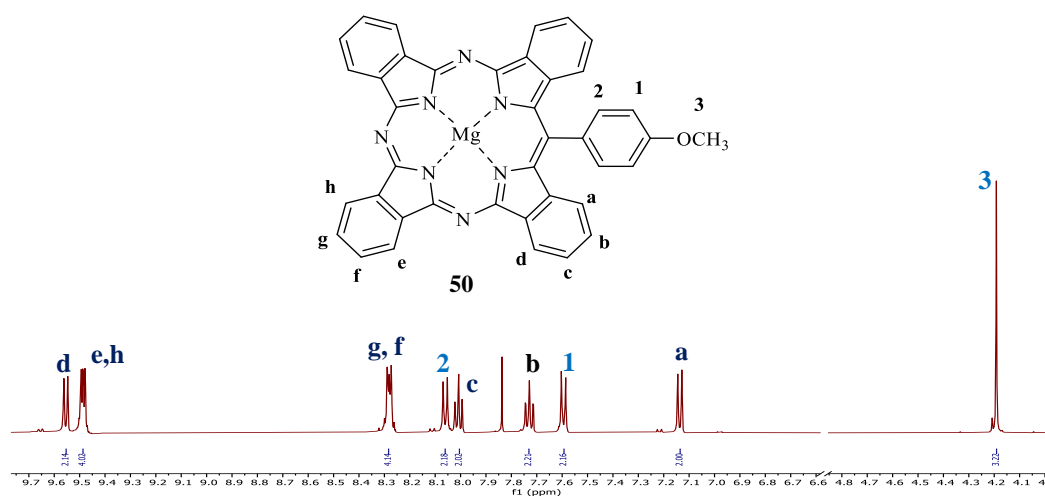
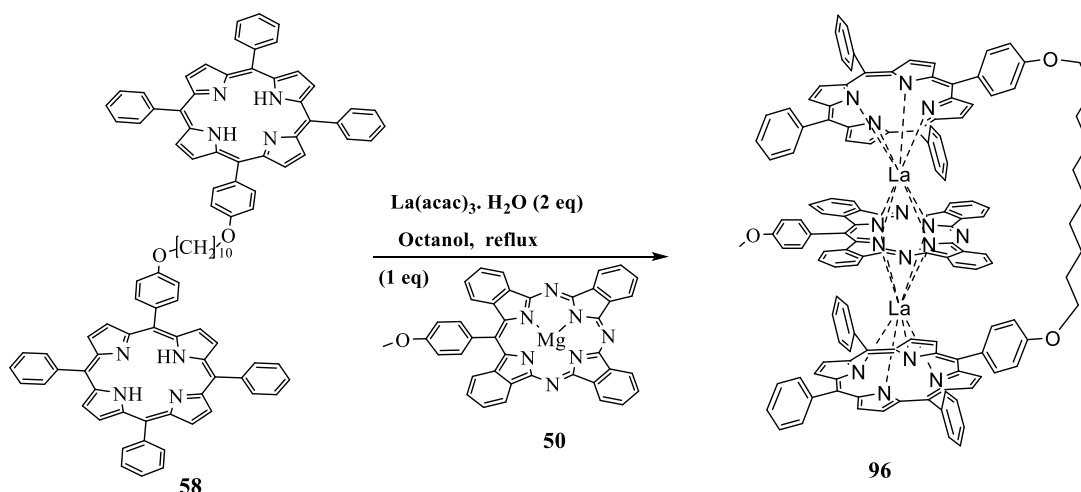


Figure 2.21: ^1H NMR spectrum of TBTAP **50** in $\text{THF}-d_8$.

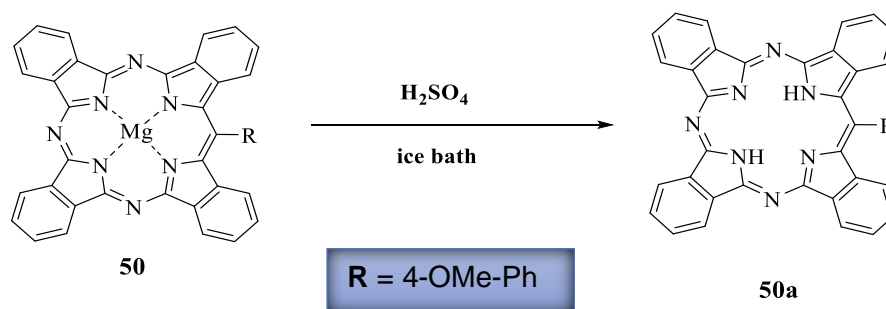
2.11.4 Attempts to synthesise triple decker with *meso*-substituted TBTAP 50:

The general method developed by Cammidge *et al.*^[1] was followed to insert *meso*-substituted TBTAP **50** to form closed triple deckers **96** as shown in scheme 2.32. The first attempts in the synthesis of the triple decker was to react C₁₀ porphyrin dyad **58**, La(acac)₃ and Mg substituted TBTAP **50**^[20]. However, no noticeable result was observed in reaction.



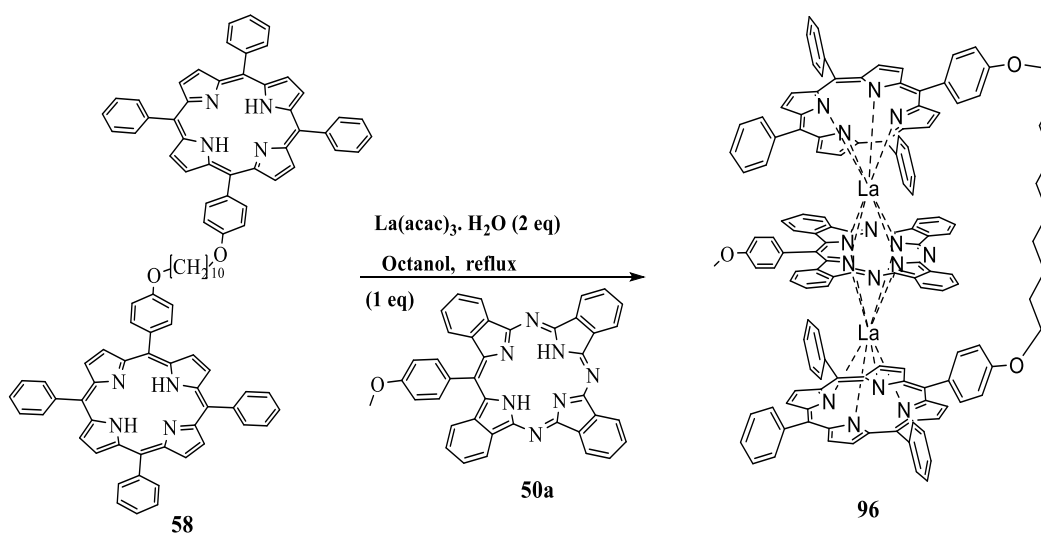
Scheme 2.32: Proposed synthesis of triple decker **96**.

We thought it would be easy to replace magnesium in the reaction, but it failed, including when the reaction was repeated with different salts of lanthanum such as Lanthanum (III) iodide and Lanthanum (III) trifluoromethanesulfonate; no noticeable difference was observed in the reaction. At this stage it was decided to remove the Mg from the TBTAPs. Metal free TBTAP **50a** was synthesised by dissolving it in concentrated sulphuric acid and then pouring onto ice. The precipitate was filtered off and washed with MeOH to give the metal-free TBTAP **50a** as a green solid (scheme 2.33) that was later used to make the triple decker derivative. MALDI-TOF MS was checked after the reaction and the peaks of the metal free MgTBTAPs were observed.



Scheme 2.33: Synthesis of metal-free TBTAP **97**.

Dyad **58**, two equivalents of lanthanum (III) acetylacetonate and one equivalent of TBTAP **50a** were refluxed in octanol and the reaction was monitored by TLC. It was found that a triple decker was formed within 24 h. The solvent was removed under high vacuum and the residue was separated by column chromatography using DCM/Hexane (3:2). The TD (formulated as **96**) was isolated as the second dark green fraction then a recrystallisation from DCM/MeOH was performed.



Scheme 2.34: Synthesis of triple decker **96**.

More analysis was conducted to confirm the formation of the compound **96** structure. MALDI-TOF MS was checked and the peak at 2287.12 m/z was observed as expected for this triple decker **96** (figure 2.22). However, the $^1\text{H-NMR}$ spectrum, run in CD_2Cl_2 , was very different from the previous triple deckers **59** and complicated (figure 2.23).^[1]

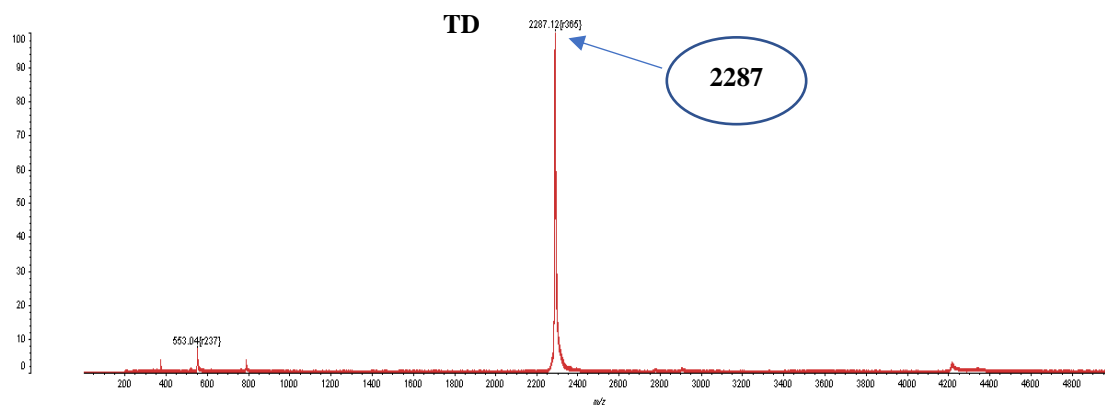


Figure 2.22: MALDI-TOF-MS shows formation of TD **96**.

As indicated in the ^1H NMR spectrum, the signals from the porphyrin peaks found in closed triple decker **59** that were previously observed at around 10 ppm were no longer present in the analogue **96** (figure 2.23).

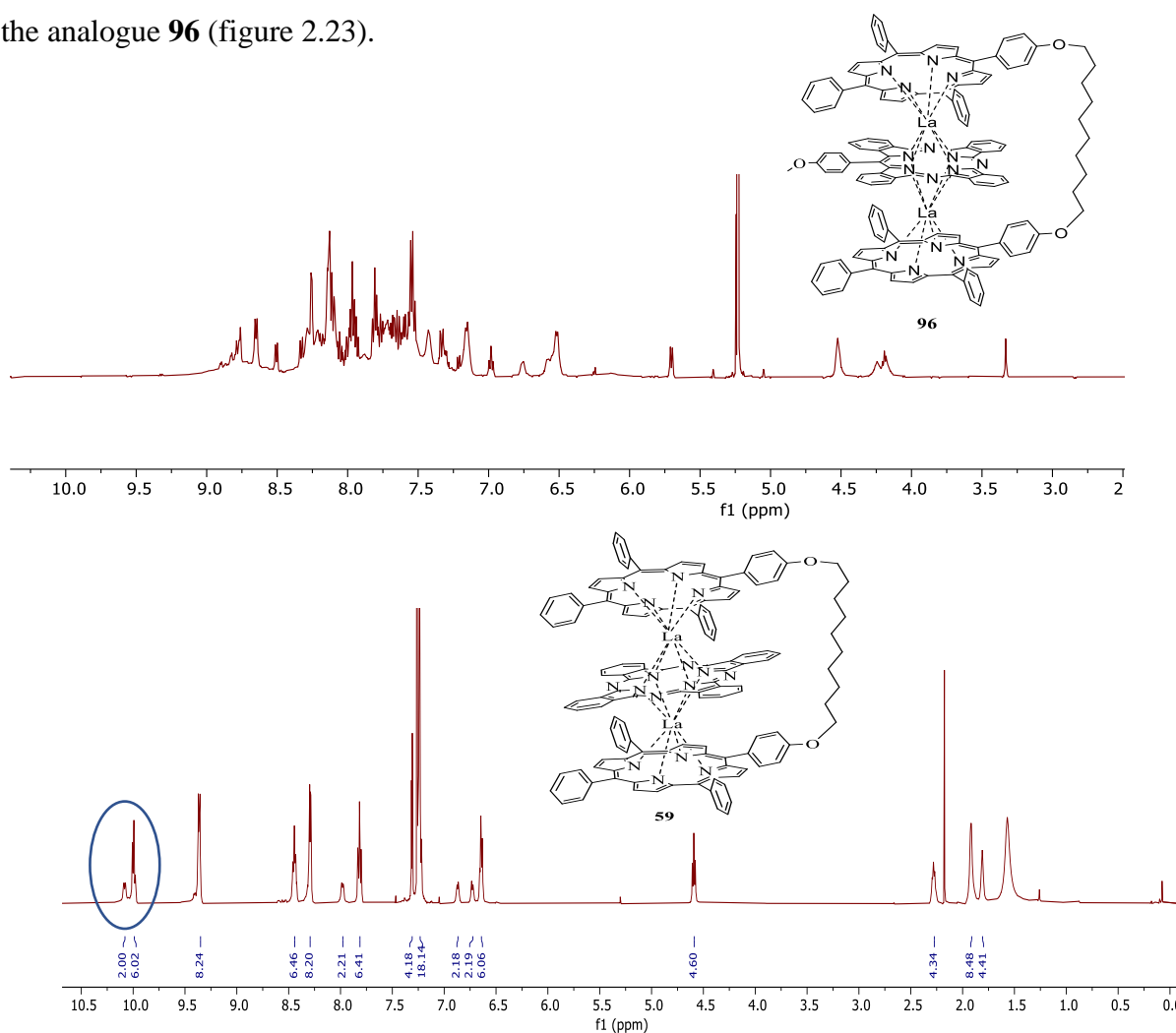


Figure 2.23: ^1H NMR spectrum of TBTAP triple decker **96** in $\text{DCM-}d_2$ and previous triple decker **59** in CDCl_3 .

By closely investigating what happened in the reaction, we recognised that a related observation had been encountered in Cammidge's group before.^[1] They compared two different types of phthalocyanines **97** and **98** (figure 2.24) to form TD, both giving a single main product, producing mass spectrometry results at $m/z=3085$ matching to the target TDs.

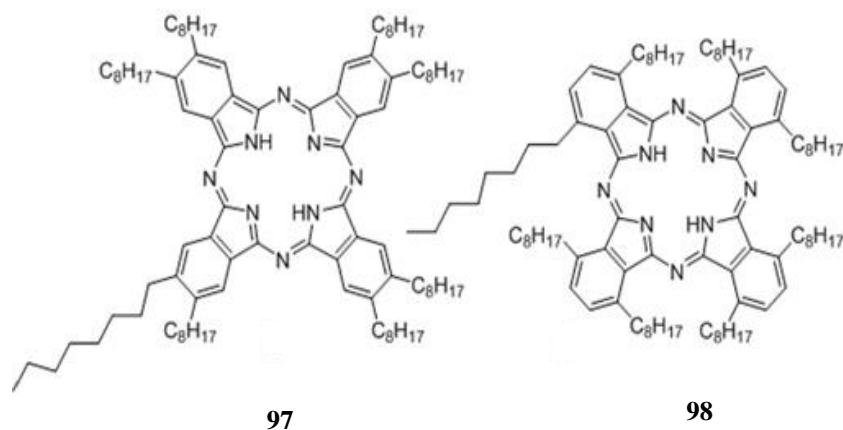


Figure 2.24: Peripherally and non-peripherally substituted phthalocyanine **97**, **98**.

In the case of the peripherally substituted phthalocyanine **97**, the closed triple decker **99** was formed. However, the long sidechains of the phthalocyanine **97** prevented the free rotation of the central unit. As a result, the aromatic protons of the central macrocycle changed from being equal to inequivalent (figure 2.25).^[1] However, the rest of the spectrum was similar to that with unsubstituted Pc, for example giving characteristic signals at 10 ppm.

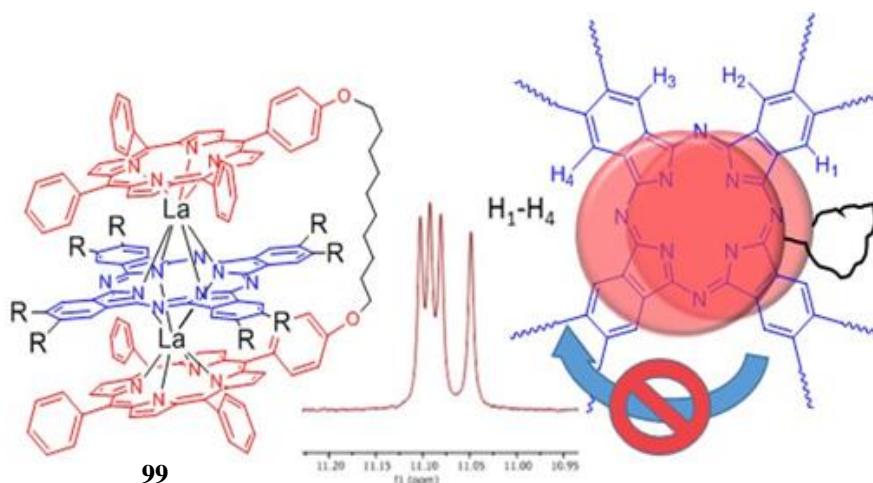
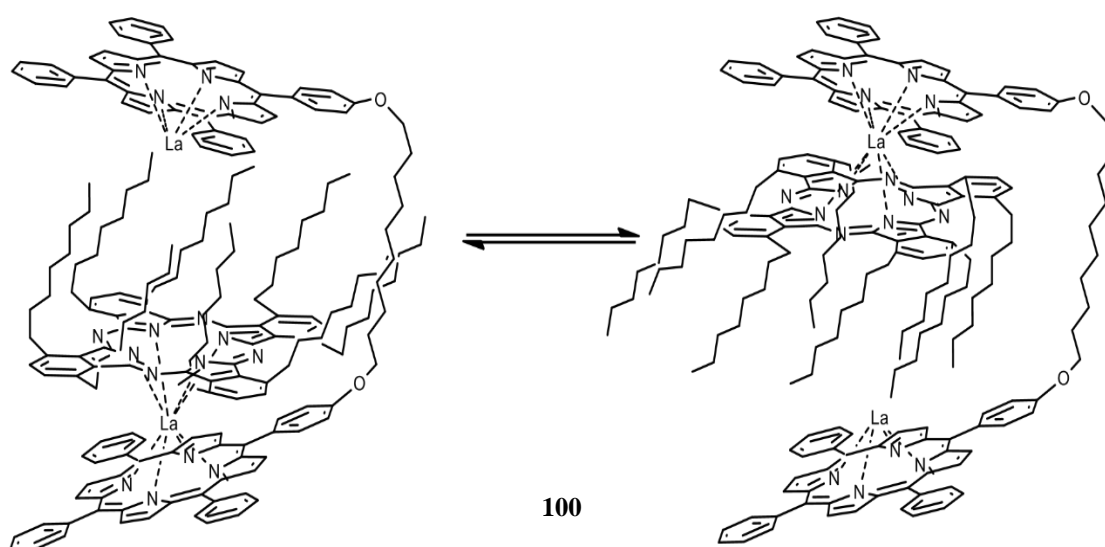


Figure 2.25: Closed triple decker **99**.

On the other hand, the non-peripherally substituted phthalocyanine **98** has greater steric hindrance. They explained that the compound had different structural arrangements, and what they saw was the average of those arrangements. If the Pc switches from one arrangement to another quickly enough in the NMR time scale, the NMR spectrum signals for closed triple decker or double decker may not be as expected. The Pc **98** switches from one porphyrin to the other to achieve an equilibrium between two distinct double deckers as shown in mechanism (scheme 2.35).^[1] Further evidence for this arrangement was provided by UV-Vis spectroscopy, with the spectrum of **100** appears similar to double-decker plus Por-La.



Scheme 2.35: Representation of the opening/closing process.^[1]

In our case, we also found that the absorption spectra of **96** does not match that of a closed triple decker **59** and is more similar to that of double decker. The absorption was around 400 cm^{-1} , which is for the porphyrins and triple decker. Also, there was the methoxyphenyl TBTAP absorption at $600\text{-}700\text{ cm}^{-1}$. (figure2.26).

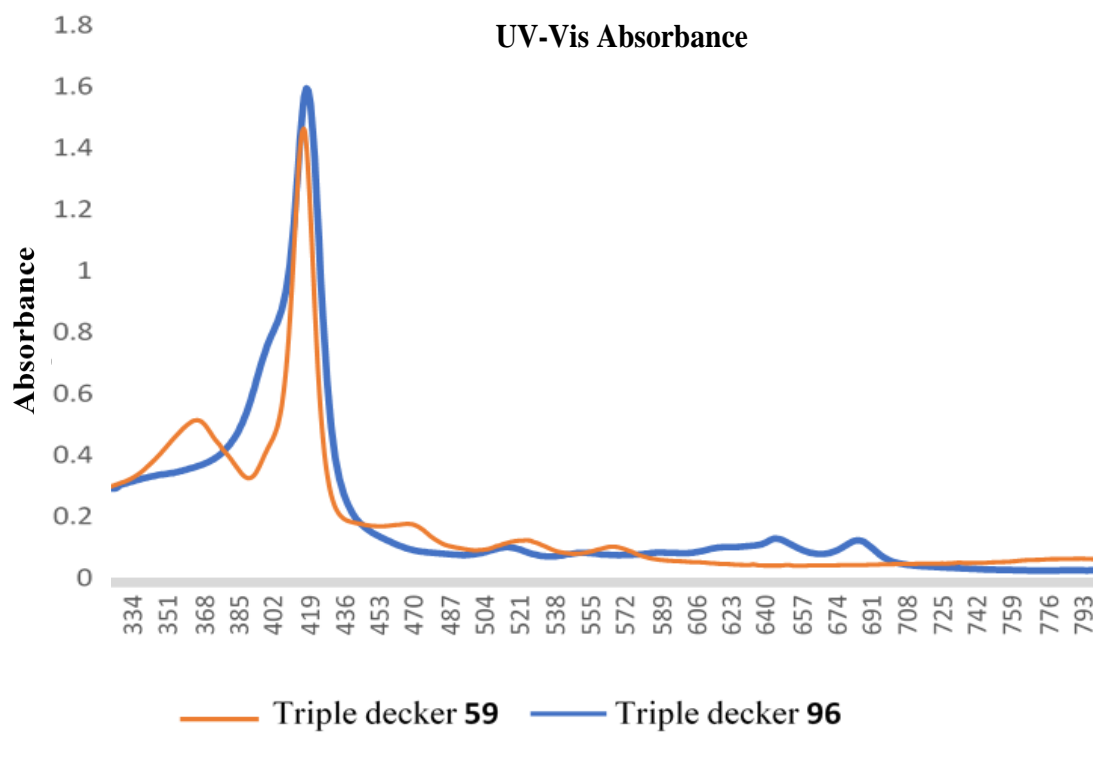
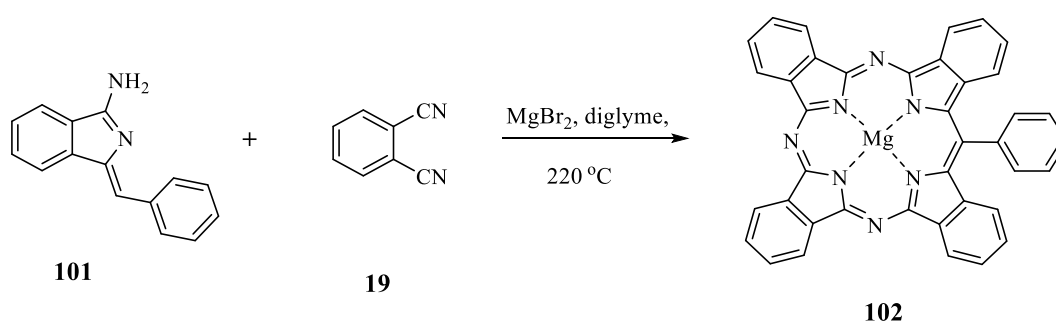


Figure 2.26: UV-Vis of triple deckers **59** and **96** in DCM.

2.11.5 Attempts to synthesise triple decker with *meso*-substituted TBTAP **102**:

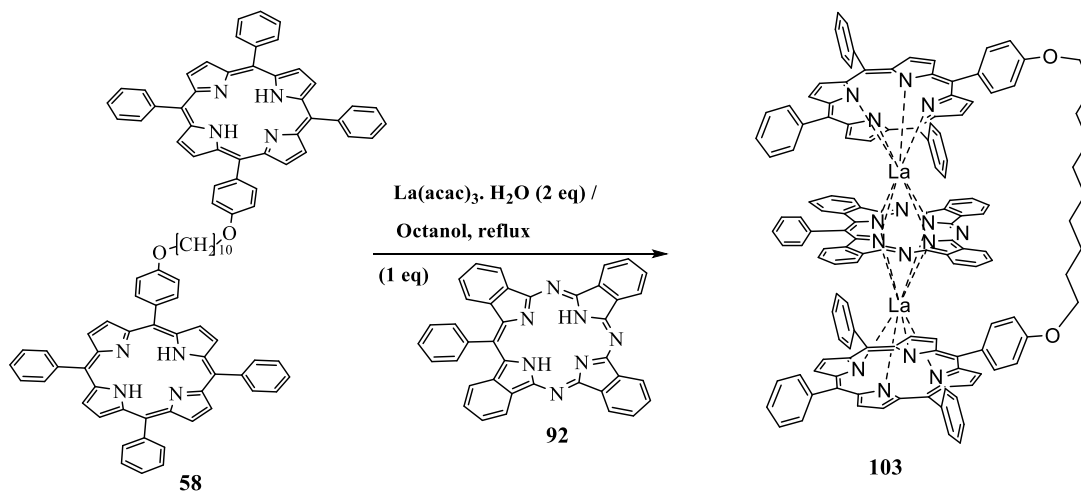
Another closed triple decker with phenyl TBTAP **102** was synthesised in order to see if the methoxy group on the twisted phenyl ring could affect the accommodation of the TBTAP in TDs.



Scheme 2.36: synthesis of metal-free TBTAP **102**.

The same method as mentioned above to prepare aminoisoindoline **48** was used to prepare aminoisoindoline **101** then TBTAP **102** was obtained by heating (3 equivalents) of aminoisoindoline **101** with phthalonitrile **19** (3 equivalents) and MgBr_2 (1.5 equivalents) in

dry diglyme at 220 °C for 6 h under a nitrogen. When the reaction was completed, the TBTAP **102** was selectively collected (scheme 2.36). It was then used for the formation of the corresponding triple decker **103** as shown in the scheme 2.37.



Scheme 2.37: Synthesis of triple decker **96**.

The same standard procedure of one pot reflux in octanol was followed and after distillation of the solvent and precipitation of the crude residue with MeOH, the solid was checked by MALDI-TOF MS and the desired peak corresponding to triple decker **103** at 2254.48 m/z was observed (figure 2.27). Then, the crude solids were separated using silica gel chromatography followed by recrystallisation to collect the green product in a 25 % yield. But the problem remained in that the ^1H NMR spectrum remained very complicated and prevented unambiguous characterisation of the isolated TD.

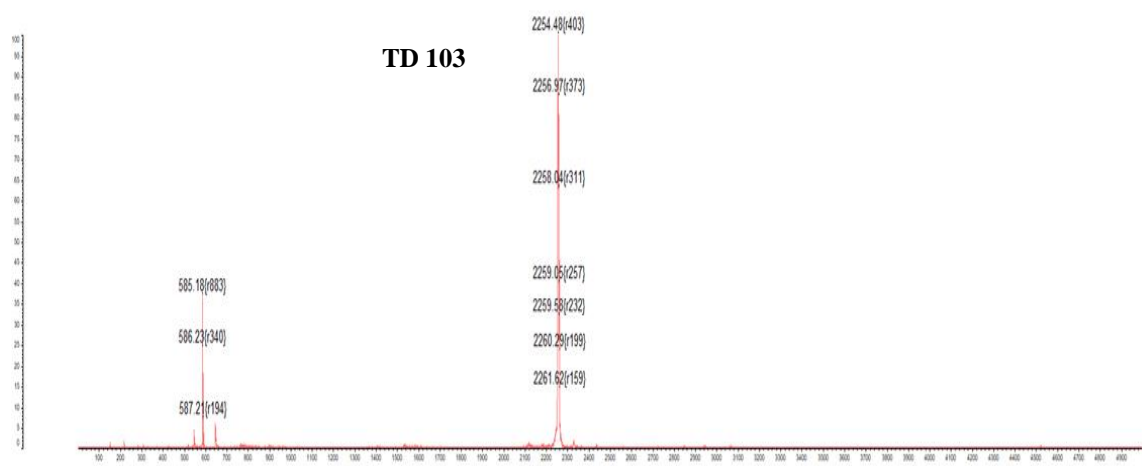
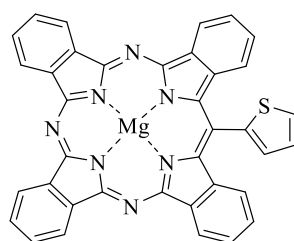


Figure 2.27: MALDI-TOF-MS shows formation of **TD 103**.

2.11.6 Attempts to synthesise triple decker with meso-substituted TBTAP 104:

The previous section on TDs formed from meso-phenyl TBTAPs summarises a large volume of work where attempts were made to synthesis and particularly to purify and characterise the TD products (initially the complicated NMR spectra were thought to be a result of impure samples). While we are now confident the TD compounds are pure, and we recognise that TDs incorporating an unsymmetrical TBTAP are expected to be complicated, their complete characterisation remains elusive and crystals suitable for X-ray crystallographic analysis have not been obtained. As briefly discussed previously, one of the possible complications in incorporation of a meso-phenyl TBTAP stems from potential steric clash. For this reason we decided to study another derivative of the TBTAPs compounds with reduced steric demand. It was *meso* thiophenyl TBTAP **104** (figure 2.28).



104

Figure 2.28: Structures of TBTAP **104**.

This derivative was chosen for a number of reasons. Thiophene might be able to planarise and have lower steric hindrance in TDs. Also, this would also give electronic communication between thiophene and TBTAP. Moreover, it is well known that thiophenes can be functionalised and directly coupled so, if successful, the route to dimeric systems is straightforward. (Figure 2.29)

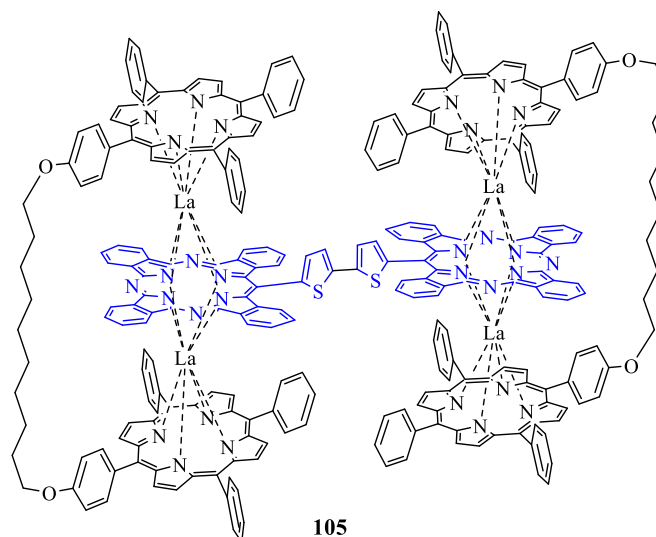
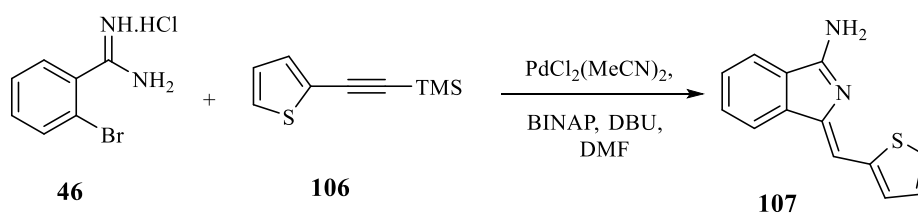


Figure 2.29: Possible linking of TDs through the *meso*-thiophenyl unit of a central TBTAP **104**.

2.11.7 Synthesis of aminoisoindoline **107**:

The same method as mentioned previously was used to prepare aminoisoindoline **107** (Scheme 2.38),^[20] by directly using the TMS protected acetylene that was commercially available. This direct use of the TMS protected acetylene was developed in conjunction with a project student (Conor Marrett-Munro). The product was fully characterised by UV-Vis, MALDI-TOF Mass and NMR spectroscopies, and full interpretation of the structure was possible after suitable crystals were grown slowly from pure DCM (figure 2.30, 2.31).



Scheme 2.38: Synthesis of aminoisoindoline **107**.

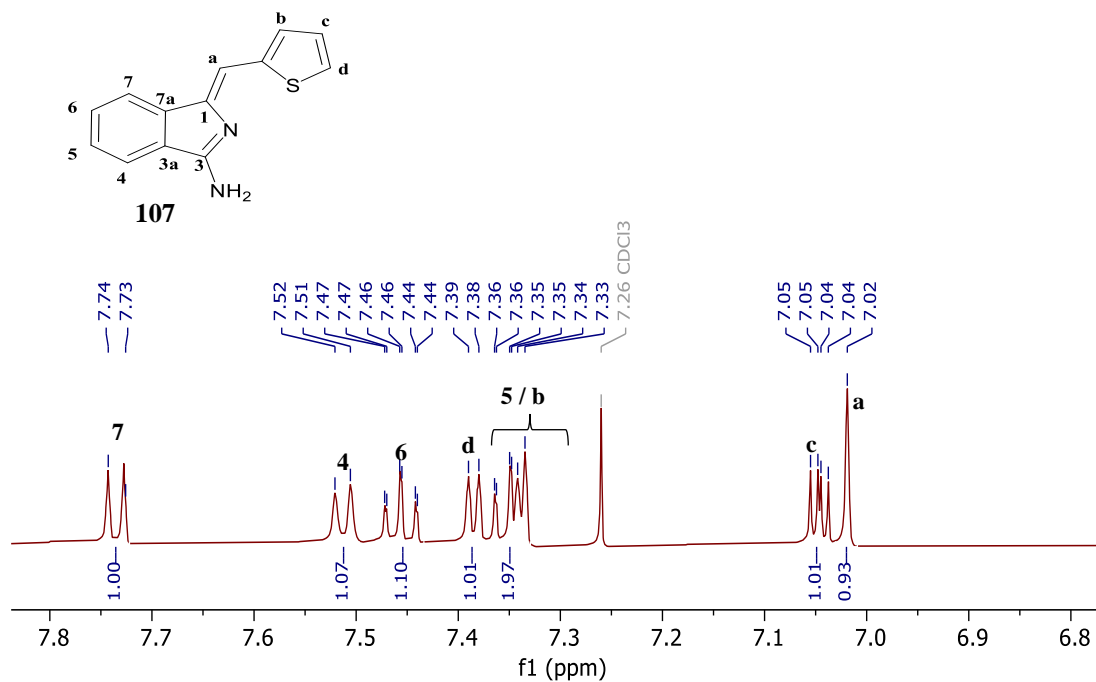


Figure 2.30: ¹H NMR spectrum of aminoisoindoline **107** in CDCl₃.

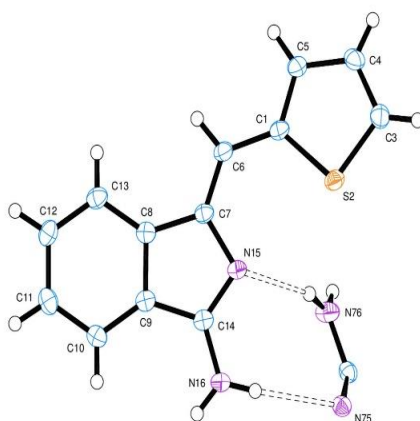


Figure 2.31: X-Ray structure of aminoisoindoline **107**.

The integration of the peaks matches with the expected number of protons, being the first indication that the product is the title compound. Also, MALDI-TOF-MS proved the formation of the aminoisoindoline **107** (figure 2.32).

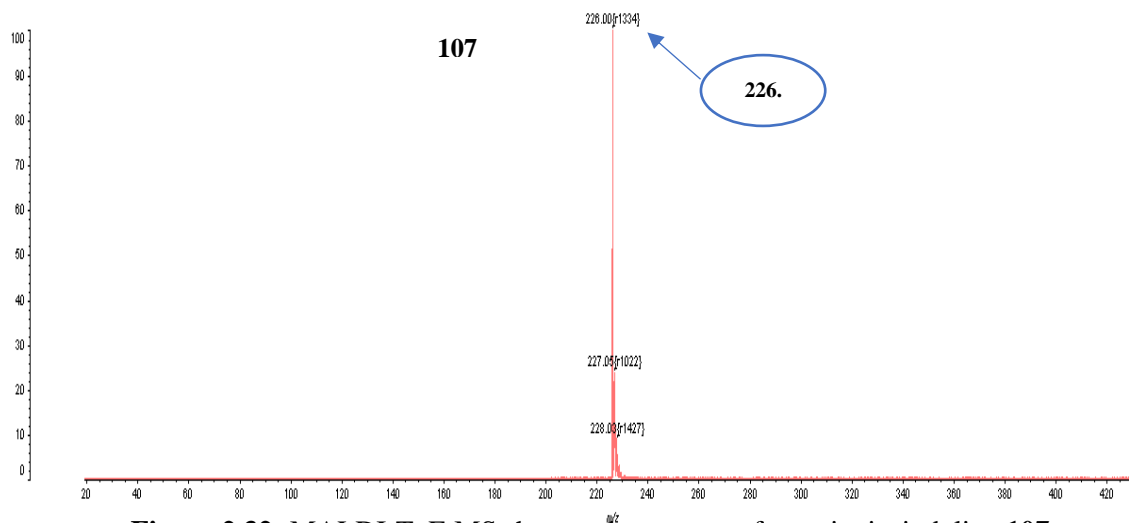
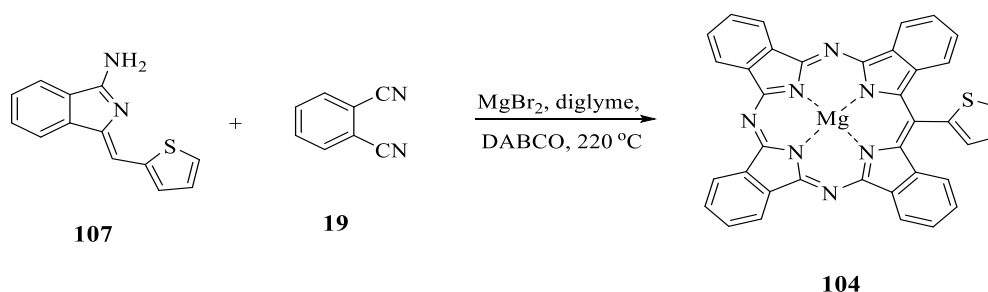


Figure 2.32: MALDI-ToF-MS shows relevant mass for aminoisodoline **107**.

2.11.8 Synthesis of meso-substituted TBTAP **104**:

The intermediate aminoisodoline **107** was prepared and used to prepare TBTAP **104** following Cammidge group's approach^[20] for synthesising meso-substituted -MgTBTAP derivatives (scheme 2.39).



Scheme 2.39: Macrocyclisation step to synthesise TBTAP **104**.

Using the optimised conditions, phthalonitrile was coupled with aminoisodoline **107** (Scheme 2.33). As before, the reaction was carried out at 220 °C with a MgBr₂ catalyst and the final addition of DABCO. The solvent was evaporated when the reaction was completed, and the crude product was eluted with DCM, DCM: Et₃N (20:1), DCM: THF: MeOH (10:4:1) on a normal phase silica column, to give 33 % of the MgTBTAP-(thiophenyl). The ¹H NMR spectrum exhibited the characteristics of a TBTAP, with the multiplet and doublet

at around 9.65 and 9.58 ppm, respectively. The peaks at 7.93 and 7.79 were suggestive of a thiophene ring (figure 2.33).

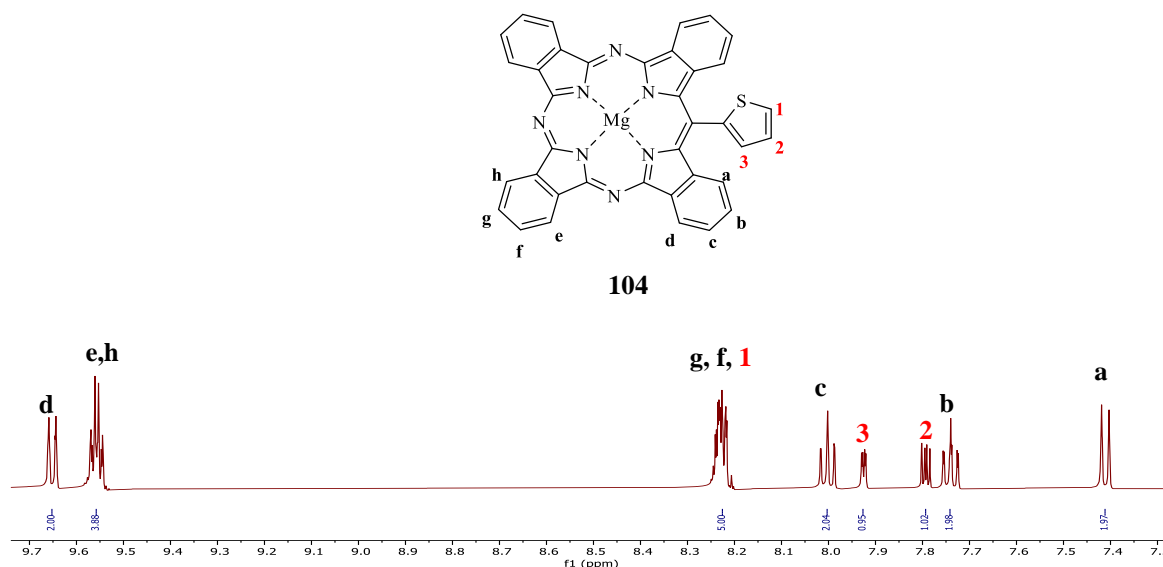
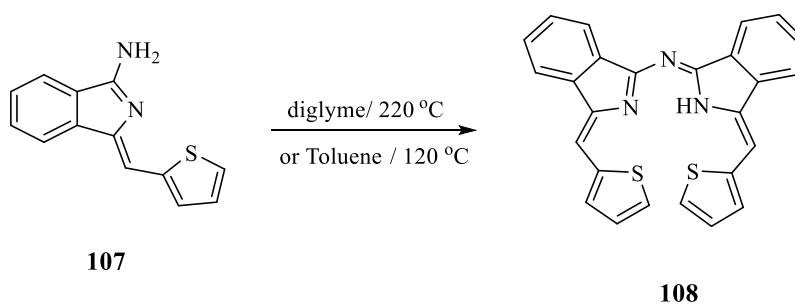


Figure 2.33: ^1H NMR spectrum of TBTAP **104** in $\text{THF-}d_8$.

The 33 % yield is comparable to the usual reaction. The reduced yield in these reactions is in part due to the condensation of aminoisoindoline in diglyme to give the dimeric product resulting from self-condensation of the aminoisoindolines (called aza-(dibenzo) dipyrromethenes **108**) (scheme 2.40), which also can be synthesised by heating a mixture of aminoisoindoline **107** in toluene to 120 °C under N_2 according to the procedure reported by Cammidge group.^[20] After work-up, purification was achieved via column chromatography, producing aza-(dibenzo) dipyrromethene **108**. The analysis was conducted to confirm the formation of the compound structure **108**. The compound gave suitable crystals for X-Ray diffraction analysis (figure 2.34). Also, the resulting peak from the MALDI-TOF MS confirm the structure with ion peak at 436 m/z. (figure 2.35).



Scheme 2.40: Synthesis of aza-(dibenzo) dipyrromethene **43**.

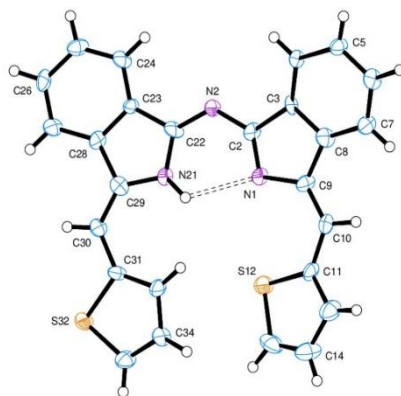


Figure 2.34: X-Ray structure of aza-(dibenzo) dipyrromethene **108**.

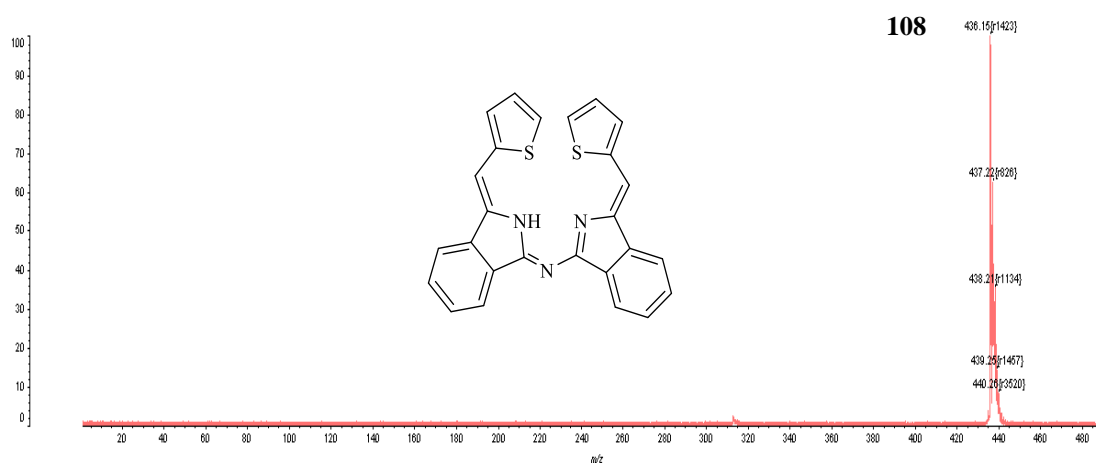


Figure 2.35: MALDI-MS spectra of aza-(dibenzo) dipyrromethene **108**.

The ^1H NMR spectrum of dimer **108** is shown in figure 2.36. The aromatic protons of the isoindoline benzene rings appeared at 8.05, 8.01, 7.6 and 7.58 ppm. Two doublet peaks at 7.40 and 7.04 ppm, with two protons each and coupling constant ($J = 5.1$ Hz), show that thiophene is present in the molecule. Vinyl proton ($\text{C}=\text{C}-\text{H}$) was at 7.30 ppm as expected.

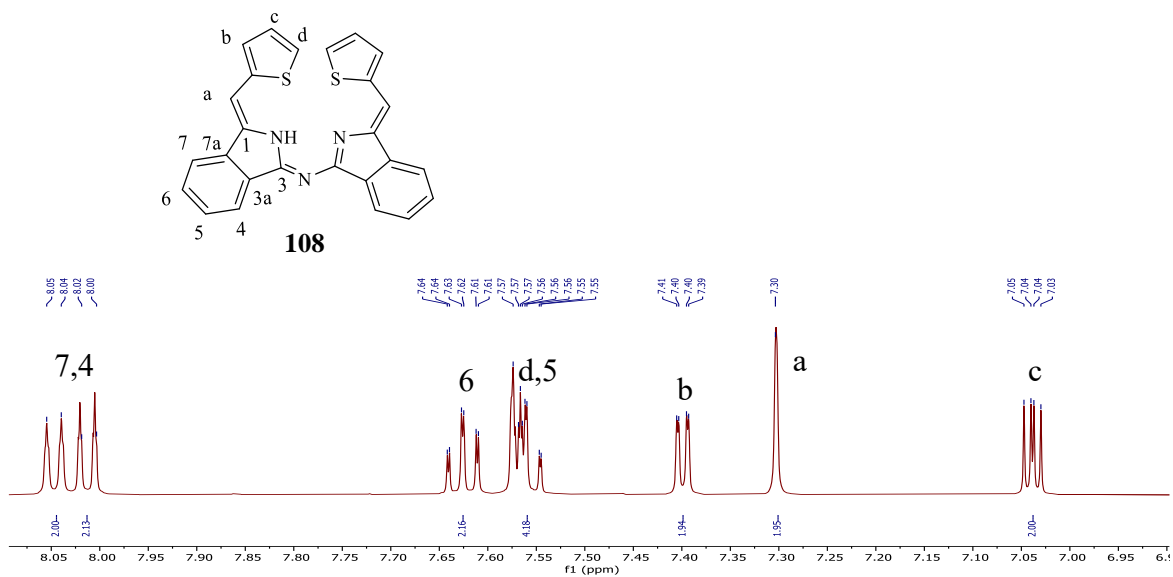


Figure 2.36: Aromatic region of $^1\text{H-NMR}$ spectrum of compound **108** in acetone- d_6 .

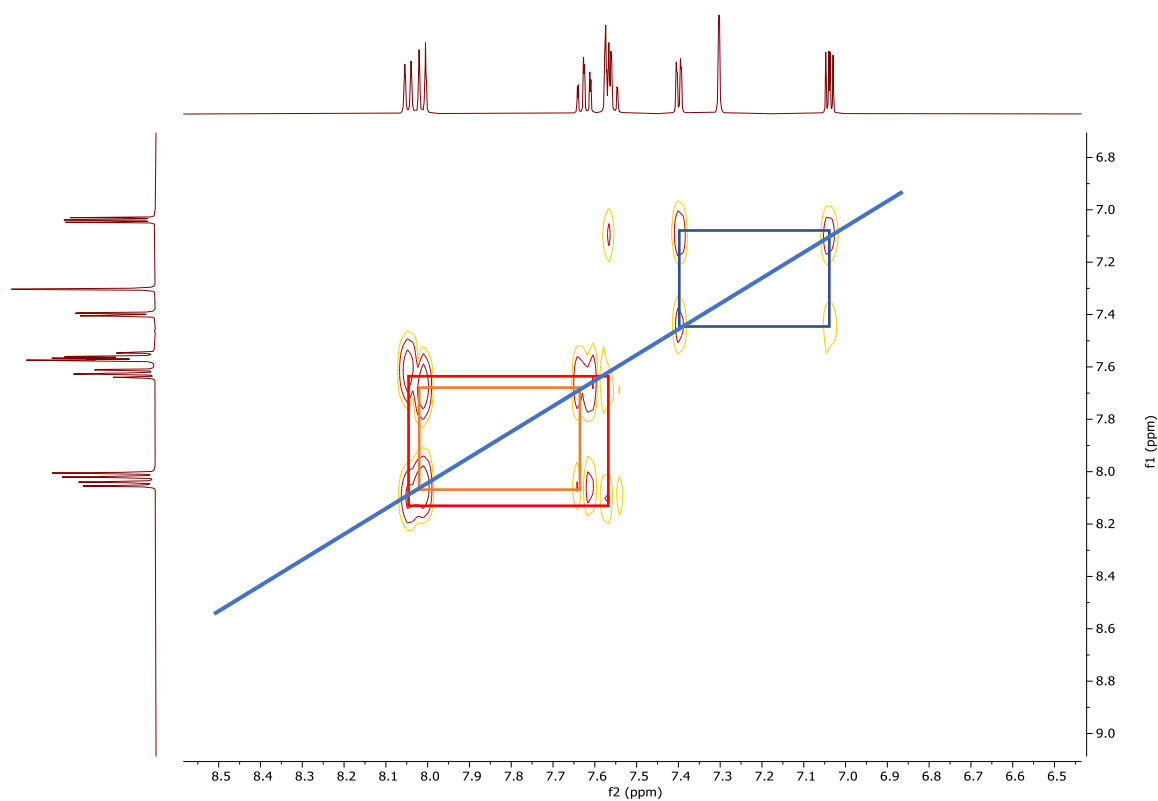
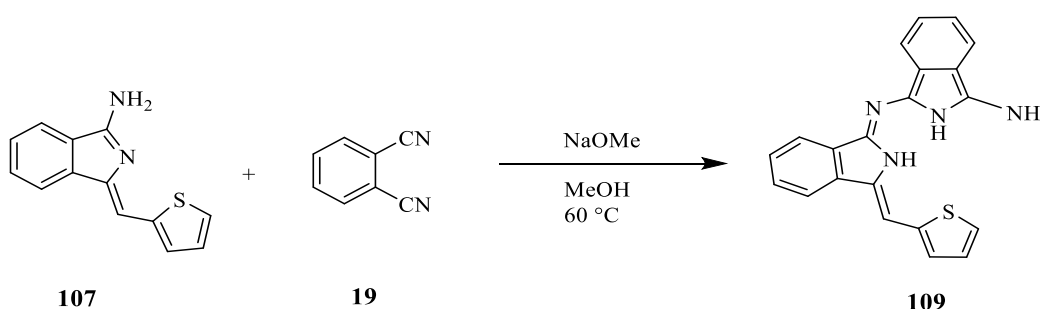


Figure 2.37: COSY experiment showing cross peaks in compound **108**.

2.11.9 Synthesis of TBTAP **104** using intermediate **109**.

To avoid formation of phthalocyanine and dimeric product, another procedure is being developed by our group to prepare thiophenyl TBTAP **104** in which a mixture of phthalonitrile (1 equivalent), aminoisoindole (1 equivalent)) and NaOMe (1.5 equivalent) was added to MeOH and was heated at 60 °C overnight. The reaction mixture was allowed to cool to room temperature and after cooling, the precipitate was filtered off and washed with a cold MeOH to give orange compound **109** (scheme 2.41).



Scheme 2.41: Synthesis of the intermediate **109**.

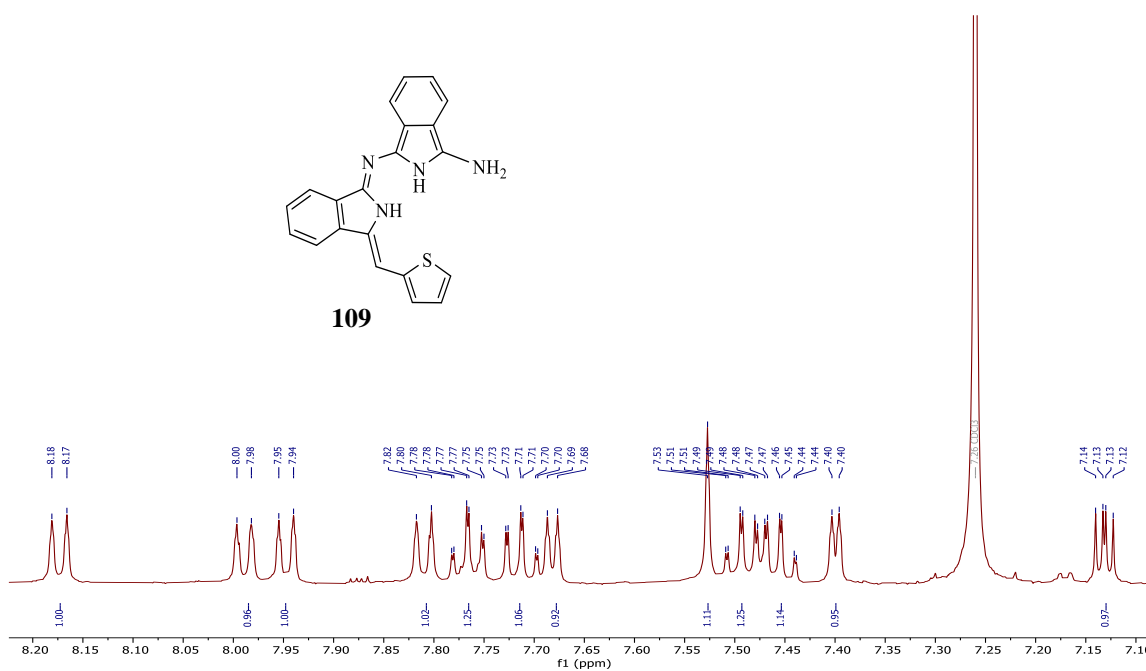
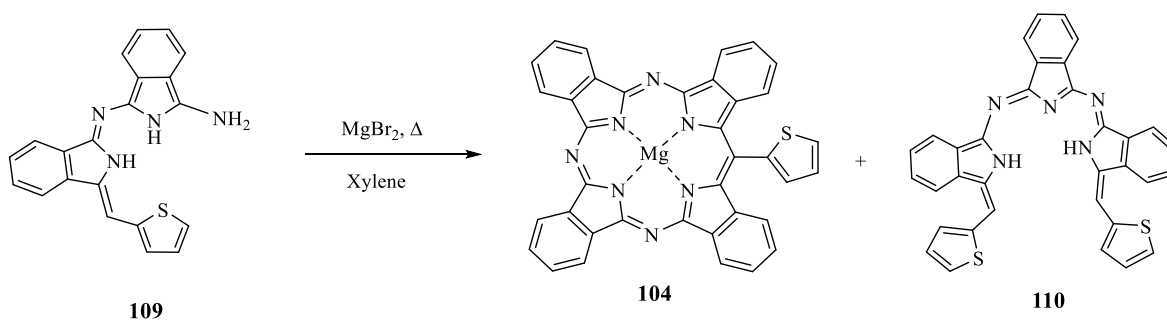


Figure 2.38: Aromatic region of ^1H NMR spectrum of compound **109** in CDCl_3 .

After the intermediate **109** was prepared, it was then used to prepare MgTBTAP-(thiophenyl) by reacting the intermediate **109** with MgBr_2 (1.5 equivalents) in xylene for 9 h

under a nitrogen atmosphere (scheme 2.42). Then, the solvent was removed and a 1:1 mixture of DCM: MeOH (20 ml) was added, and the mixture was sonicated. The solvents were concentrated in vacuum and the resulting compound was purified by chromatography columns using DCM: Et₃N (20:1), then solvent system changes to PE: THF: MeOH (10:3:1). A dark green fraction of the MgTBTAP-(thiophenyl) was collected in overall yield of 40%. Our proposal for this formation of TBTAP based on using the intermediate **109** proved time-consuming and inefficient. In terms of comparing the yield in both reactions to form TBTAP **104** the one using intermediate **109** was increased by 7%. However, the problem with this method is that the intermediate **109** decomposed and produced many side products including phthalocyanine, dimeric and trimeric products.



Scheme 2.42: Synthesis of TBTAP **104** via intermediate **109**.

The molecular ion peak of one of the side product brown fractions on the MALDI-TOF mass spectroscopy was (m/z 559). We suggested that it is for the trimer **110** but no more analyses were conducted to confirm the formation of the compound **110** structure (figure 2.39).

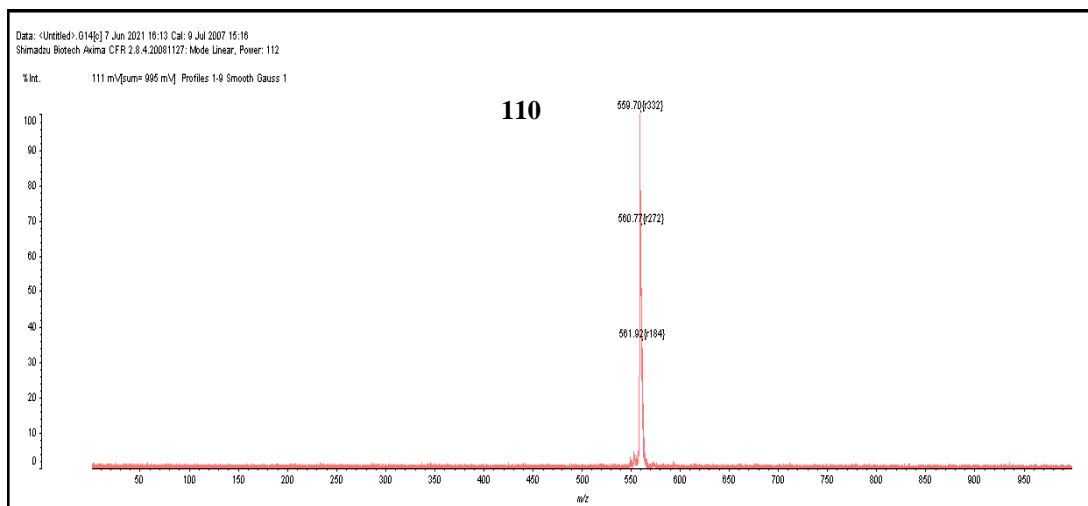
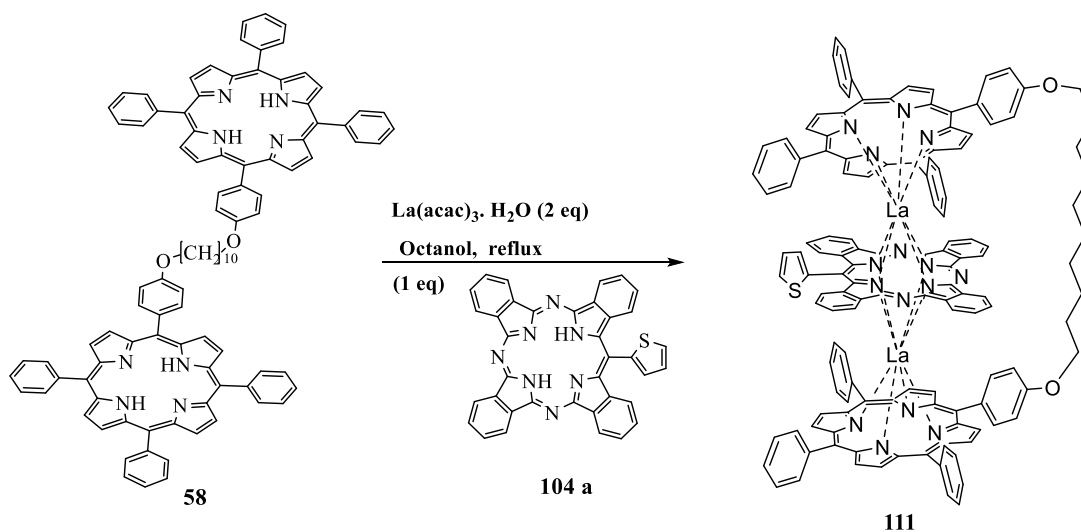


Figure 2.39: MALDI-TOF-MS shows relevant mass for **110**.

2.11.10 Attempts to synthesise triple decker with meso-substituted TBTAP **104**:

Attempts were made to synthesise the triple deckers with thiophenyl TBTAP **104**, following general method developed by Cammidge *et al.*^[1] by reacting C₁₀ porphyrin dyad **58**, La(acac)₃ and thiophenyl TBTAP **104a** (product after demetallation of magnesium with sulfuric acid) (scheme 2.43).



Scheme 2.43: synthesis of triple decker formulated as **111**.

After distillation of the solvent and precipitation of the crude residue with MeOH, the solid obtained was checked by MALDI-TOF MS (figure 2.40). The desired peak corresponding

to triple decker **111** at 2264.03 m/z was observed. Then, the crude solids were separated using silica gel chromatography followed by recrystallisation to collect the green product. However, the ^1H NMR spectrum run in CDCl_2 (figure 2.41), was complicated as well, and, while we expected the thiophene here to have reduced steric demand and easier to interpret spectra, similar results were in fact obtained.

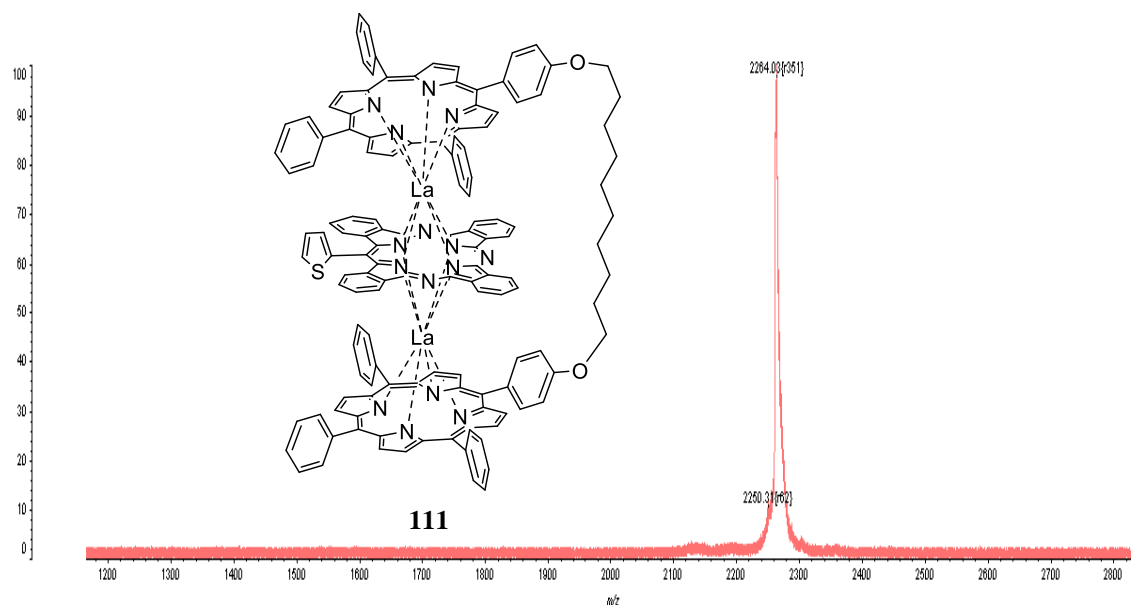


Figure 2.40: MALDI-TOF-MS shows formation of TD **111**.

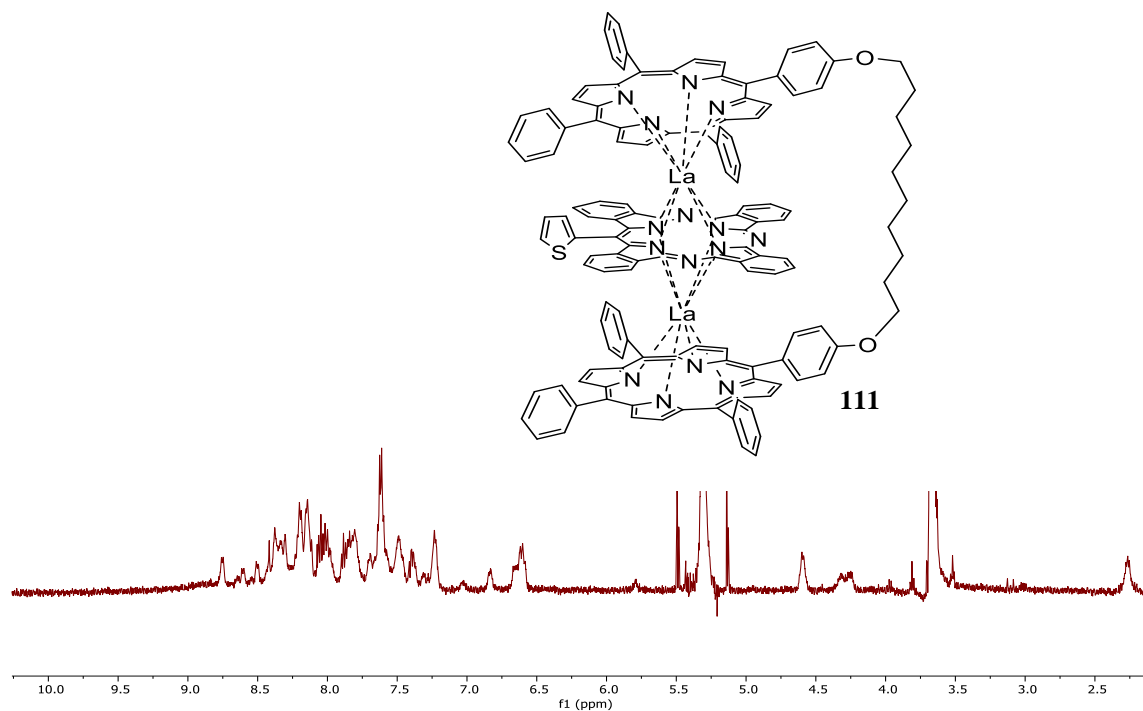
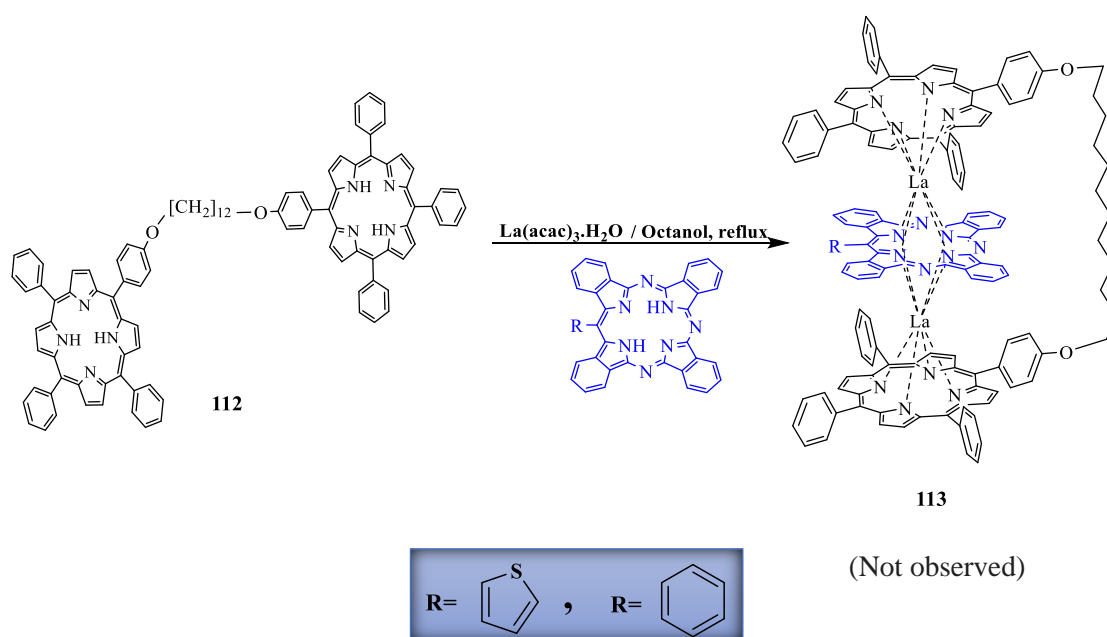


Figure 2.41: ^1H NMR spectrum obtained for the closed decker triple decker **111**.

2.11.11 Synthesis of closed triple decker with C₁₂ porphyrin dyad:

To investigate the effect of chain length on closed triple decker formation with metal free TBTAPs, we decided to consider using a longer bridging chain and in the next attempt are tried C₁₂ porphyrin dyad **112** that was synthesised from 1,12-dibromoundecane using the same conditions previously optimised for porphyrin dyad **58**. In this case, porphyrin dyad **112** was subjected to metalation with 2 eq of lanthanum acetylacetonate in refluxing octanol for 6 h. Then, metal free TBTAPs were added to the mixture and the mixture refluxed overnight as shown scheme 2.44.



Scheme 2.44: Proposed synthesis of triple deckers **113**.

During this reaction, the formation of triple decker **113** was not observed, after work-up, purification was achieved via column chromatography, producing double decker of the meso-substituted TBTAP **114**, **115** as shown in the two below figures. The resulting peak from the MALDI-TOF MS showed 1331 m/z for **114** (figure 2.42) and 1307 m/z for **115** (figure 2.43) respectively.

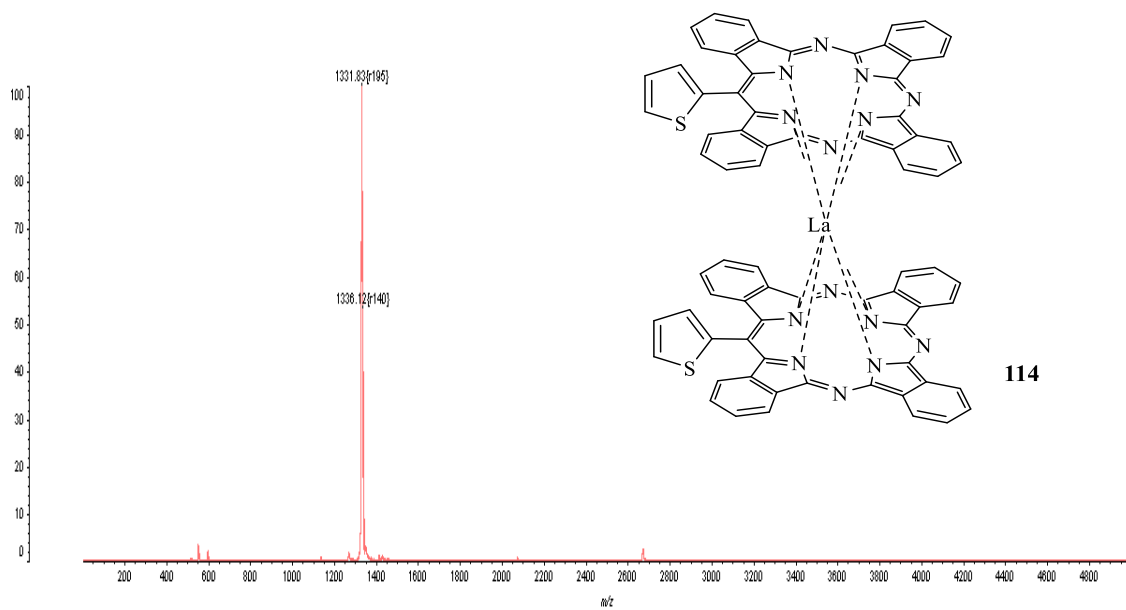


Figure 2.42: MALDI-TOF-MS confirms the formation of homoleptic double decker **114**.

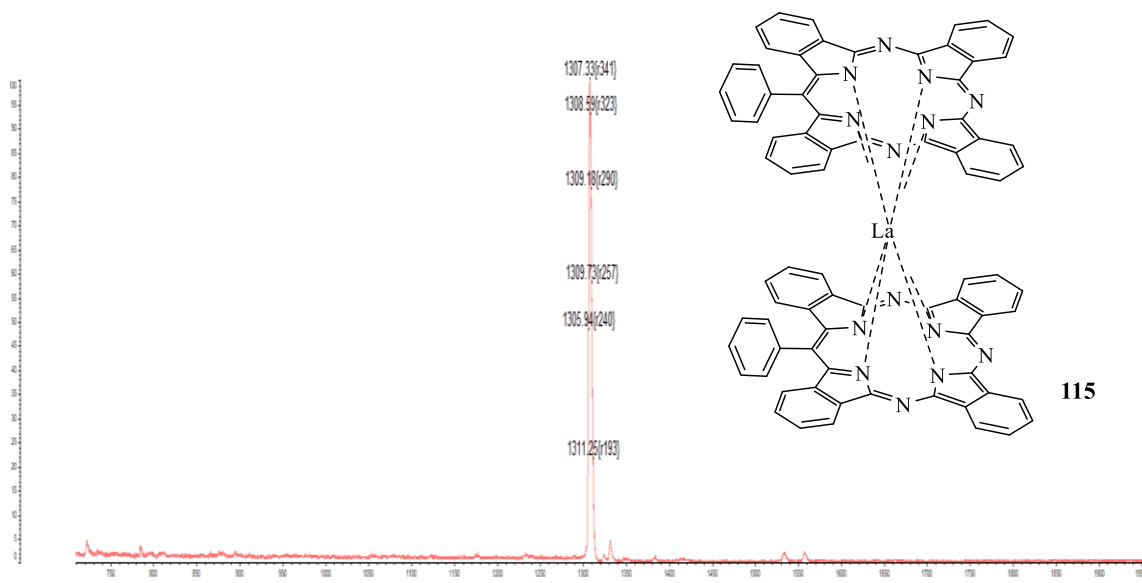


Figure 2.43: MALDI-TOF-MS confirms the formation of homoleptic double decker **115**.

The ^1H NMR spectrum was run in CD_2Cl_2 , and the spectrum proved the formation of the double decker compound **115**. Figure 2.44 shows the aromatic regions of the structure. As usual for double-deckers, hydrazine was added to the NMR tubes to achieve good spectra.

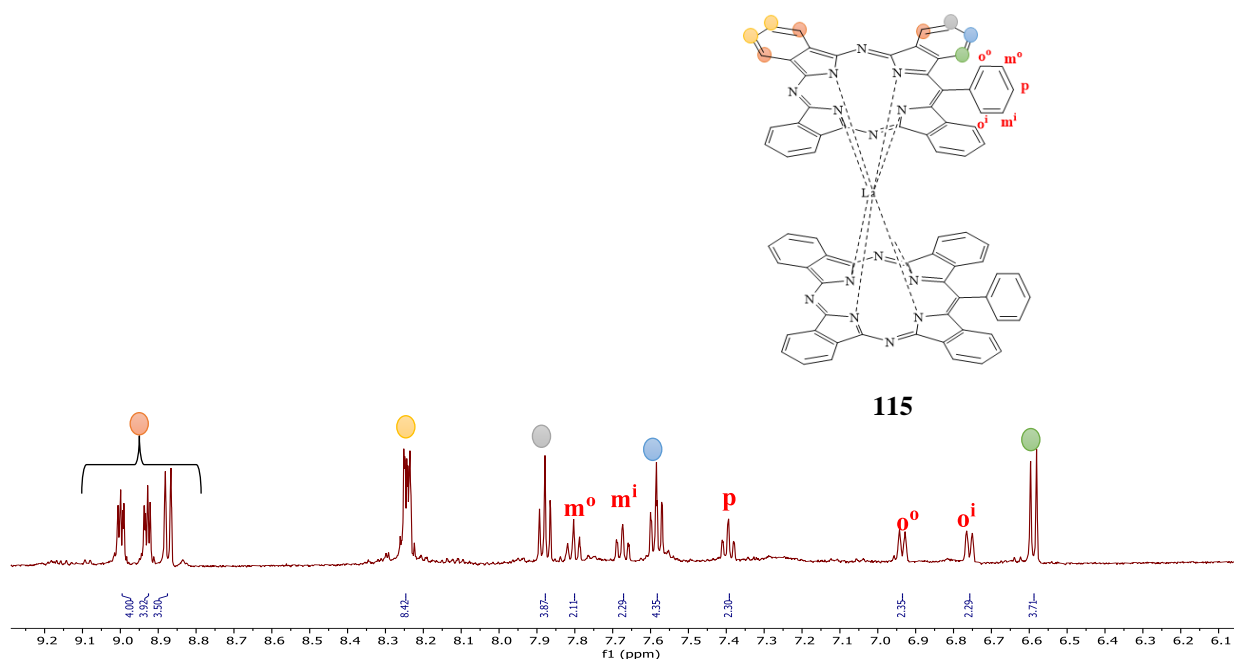


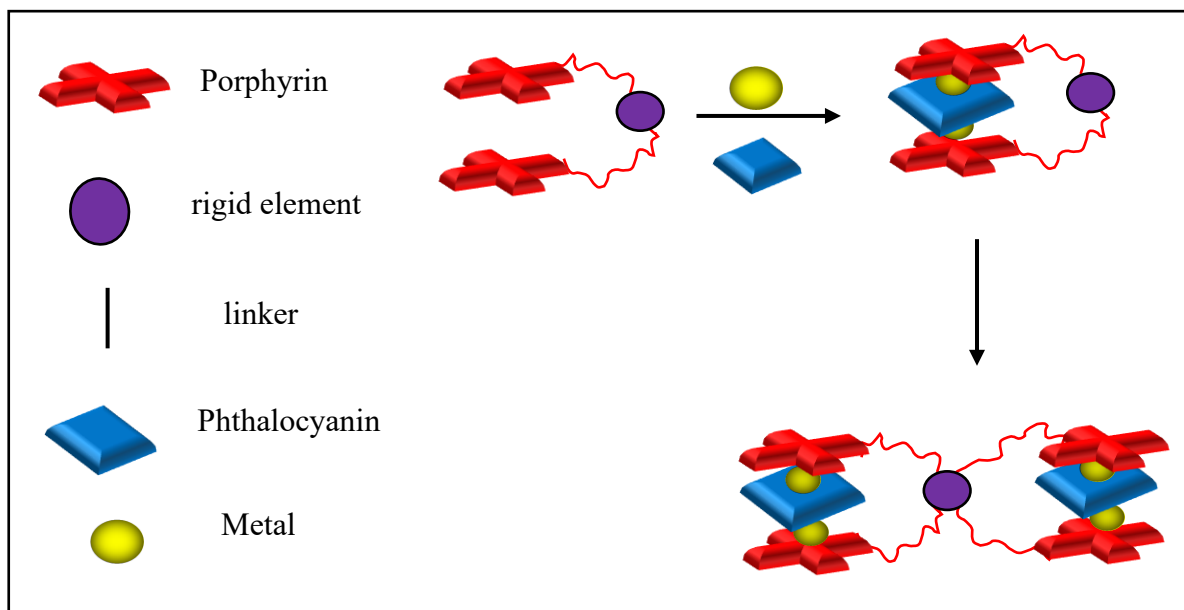
Figure 2.44: Aromatic region of $^1\text{H-NMR}$ spectrum of homoleptic double decker **115** $\text{DCM-}d_2$.

2.11.12 Conclusion:

In conclusion, the synthesis of triple deckers with different of *meso*-substituted TBTAPs has been achieved but the characterisation was much more complicated than for previous symmetric phthalocyanine derivatives. It appears that the twisted aromatic units make steric hindrance between the *meso*-phenyls of the porphyrins. We thought the thiophene might be able to planarise and have lower steric hindrance in TDs, but similar result was obtained. Further analysis (ideally by crystallography) is needed to finally prove the structure and allow (or not) subsequent elaboration into linked systems.

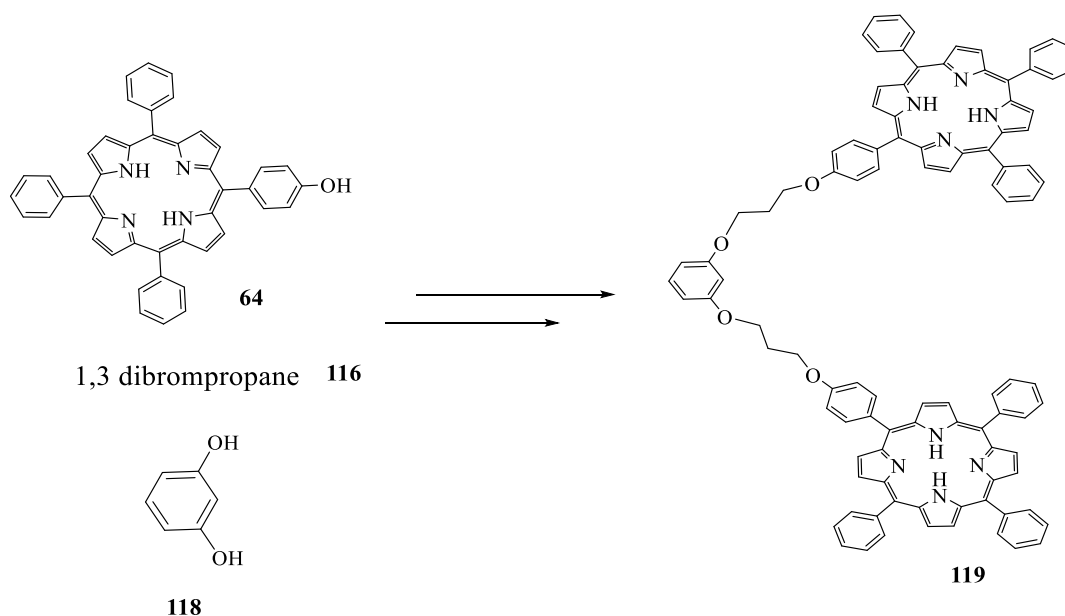
2.13 Multiple chromophores with a rigid, functionalisable element to the bridge:

The flexible $\text{C}_{10}\text{-C}_{12}$ chain work for specific Pcs which were previously reported by Cammidge group worked well but the link chain does not offer easy options for subsequent coupling or functionalisation. Incorporation of suitable (functionalised) Pcs into TDs was proving very challenging. Therefore, the decision was taken to investigate a different class of multichromophore assemblies. We aimed to synthesise a compound that bears a more rigid element to the bridge that could be further functionalised or dimerised (scheme 2.45).

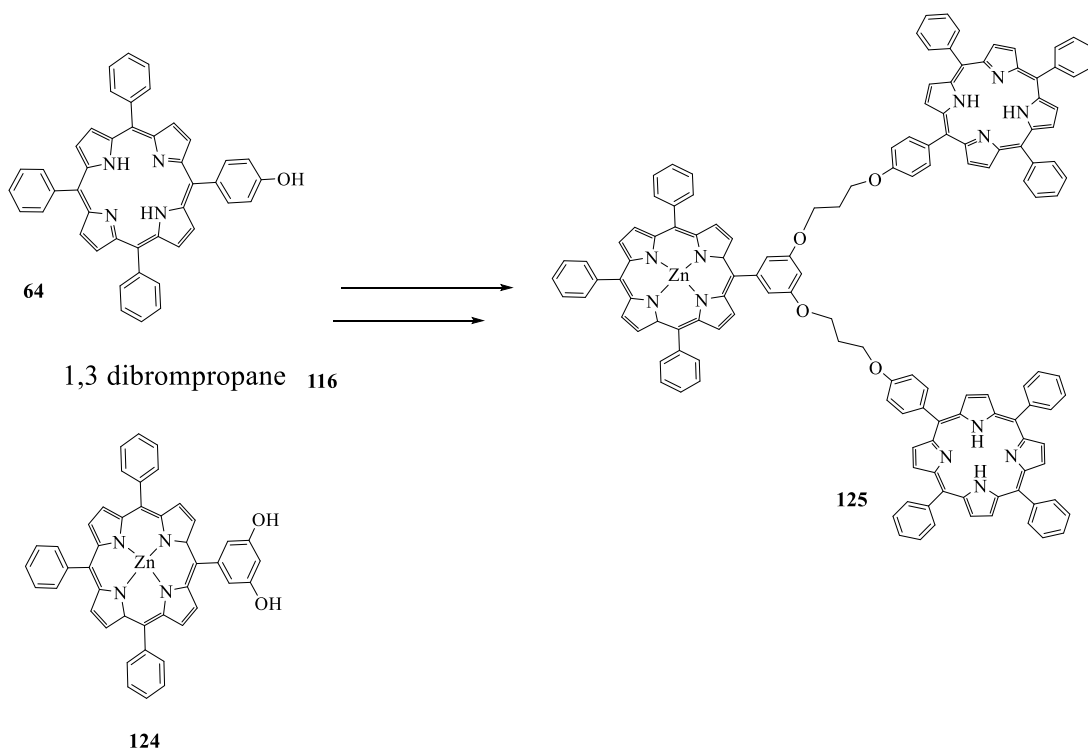


Scheme 2.45: Chromophores attached via the bridge.

A simple example is a benzene fragment with six possible substitution sites (scheme 2.46). If successful, a possible extension is to further add the bridge to another porphyrin unit (scheme 2.47).



Scheme 2.46: Systematic illustration of the synthesis of model compound 2,3-bis(porphyrin) benzene **119**.

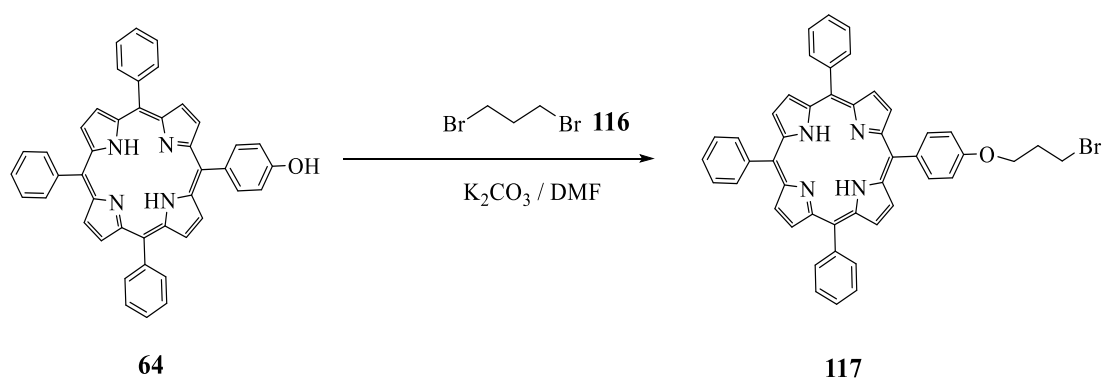


Scheme 2.47: Systematic illustration of the synthesis of model compound 2,3-bis(porphyrin) porphyrin **125**.

2.14 Synthesis of porphyrin dyad with substituted benzene in the bridge:

The intermediate to the targeted porphyrin dyad **119** were easily available as shown in the scheme:

2.14.1 Synthesis of bromoalkoxy porphyrin **117**.^[4]



Scheme 2.48: Synthesis bromoalkoxy porphyrin **117**.

The reaction between the hydroxyl groups on the porphyrin TPPOH and the alkyl bromide group on the linking chains follows a simple S_N2 substitution reaction to produce the ether.

So, TPPOH **64** in DMF, was reacted with excess 1,3-dibromopropane **116** with K_2CO_3 . The reaction was completed after 19 h and the product was purified by recrystallisation from DCM/MeOH to give the title compound **117** in an overall yield of 95% (Scheme 2.48). Spectral data corresponds to the bromoalkoxy porphyrin **117**. Figure 2.45 shows the 1H NMR spectrum and it can be observed that the methylene groups of the alkyl chain have different signals at 4.41 ppm ($-OCH_2-$), 3.79 ppm ($-CH_2Br$), and 2.52 ppm ($-CH_2$). The characteristic signal for hydrogens in the centre of the porphyrins is at -2.76 ppm.

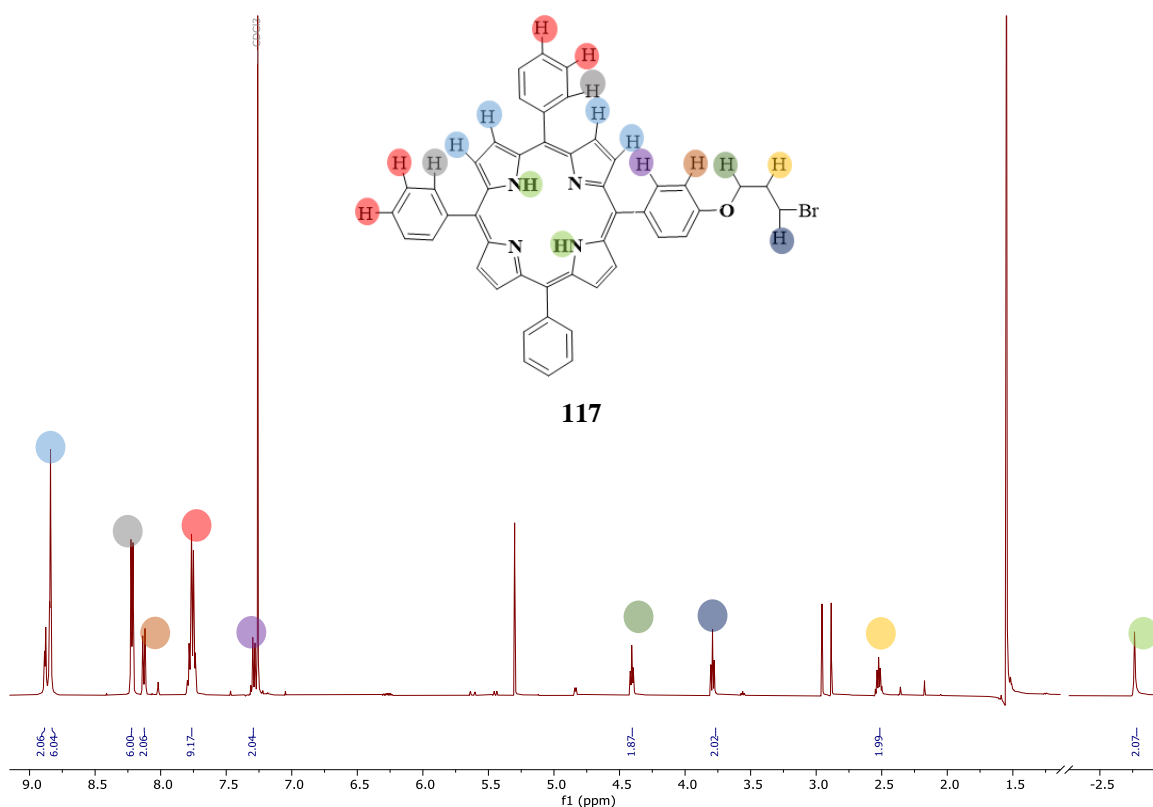


Figure 2.45: 1H NMR of bromoalkoxy porphyrin in $CDCl_3$.

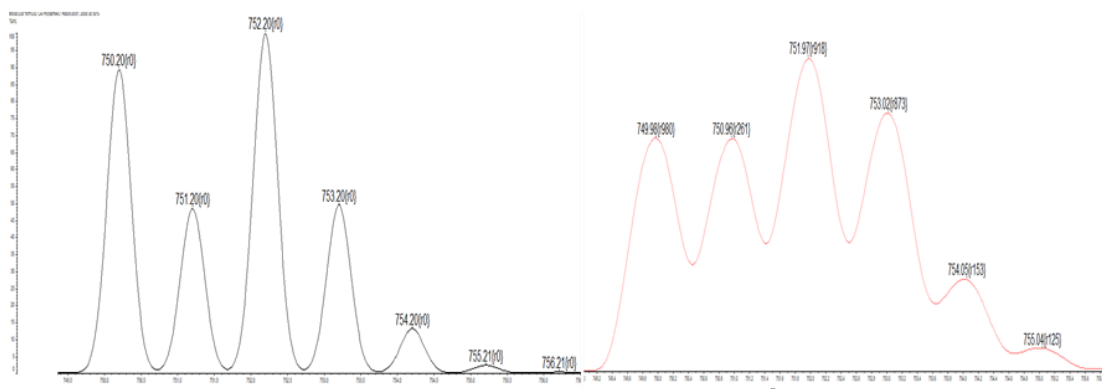
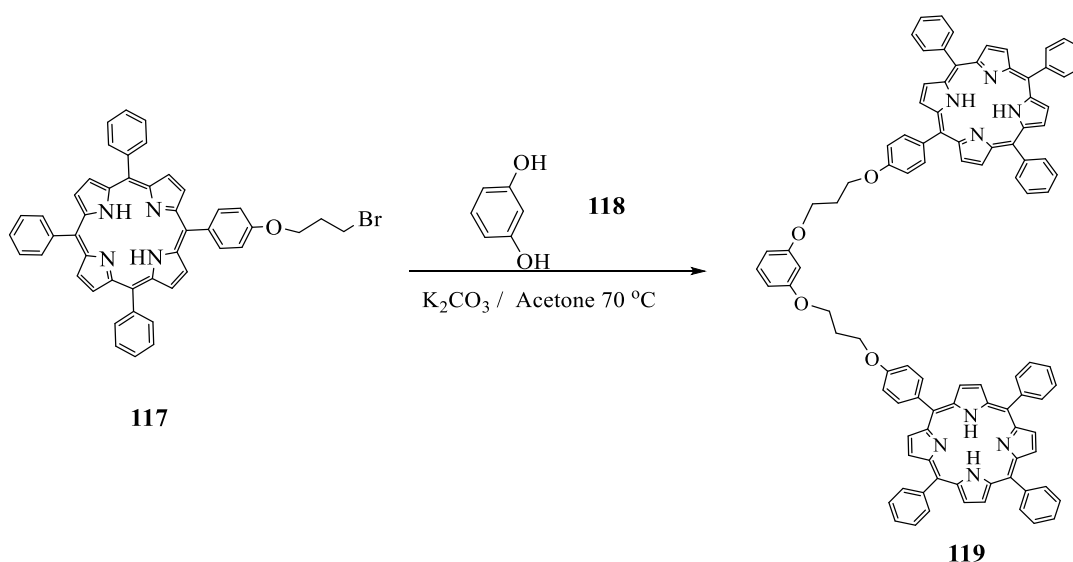


Figure 2.46: MALDI-TOF-MS of **117** (right) with its theoretical prediction.

2.14.2 Synthesis of dyad **119**:



Scheme 2.49: Synthesis of dyad **119**.

As indicated in Scheme 2.49, the target dimeric porphyrin **119** was synthesised by reacting 1,3 dihydroxybenzene **118** with bromoalkoxyporphyrin in acetone with potassium carbonate in a sealed tube and heated at 70 °C. TLC was used to monitor the reaction. The reaction was left for 7 days. The crude reaction was worked up and the crude product was purified by using column chromatography, eluting the product with DCM: PET (1:1v: v). The dyad recrystallised by methanol to gain a purple solid product in 36 % yield. The analysis was conducted to confirm the formation of the target structure **119**. The resulting peak from the MALDI-TOF MS showed 1445 m/z (figure 2.47).

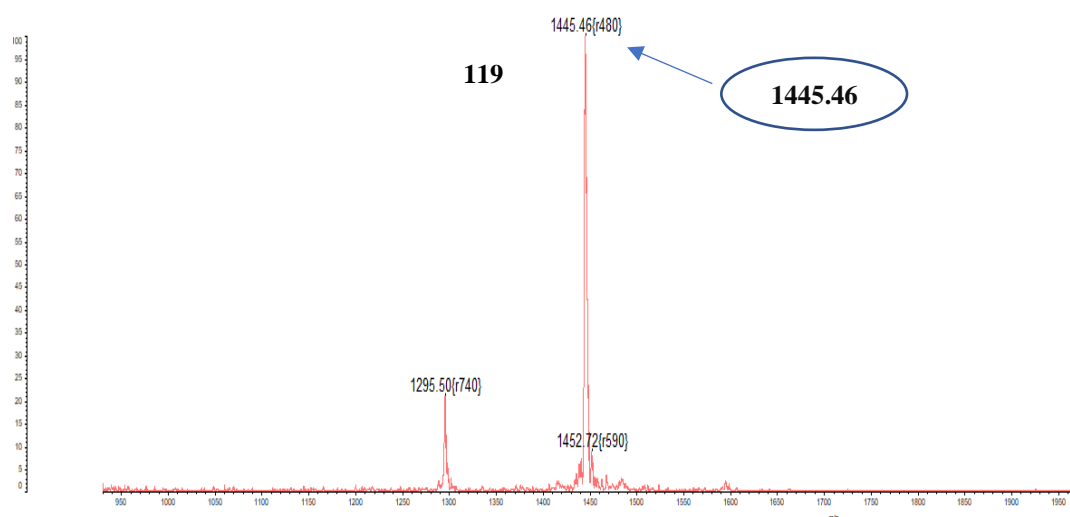


Figure 2.47: MALDI-TOF MS confirms the formation of dyad **119**.

The ^1H NMR spectroscopy data clearly matched with of the product (Figure 2.48). Because of the 1,3-substitution of the benzene in the bridge, the ^1H NMR spectrum of dyad **119** shows that there are peaks of four protons which were between 7.20-6.60 ppm. Moreover, a triplet peak for methylene group of the alkyl chain $-\text{OCH}_2$ was around 4.39 ppm (4H **1**). However, the triplet peak for $-\text{CH}_2\text{Br}$ no longer appears and instead a triplet peak of (4H **3**) is present at 4.29 ppm for $-\text{OCH}_2$ that is linked with porphyrin molecules. Finally, the methylene group of the rest of the alkyl chains of appear at 2.40ppm (4H **2**)

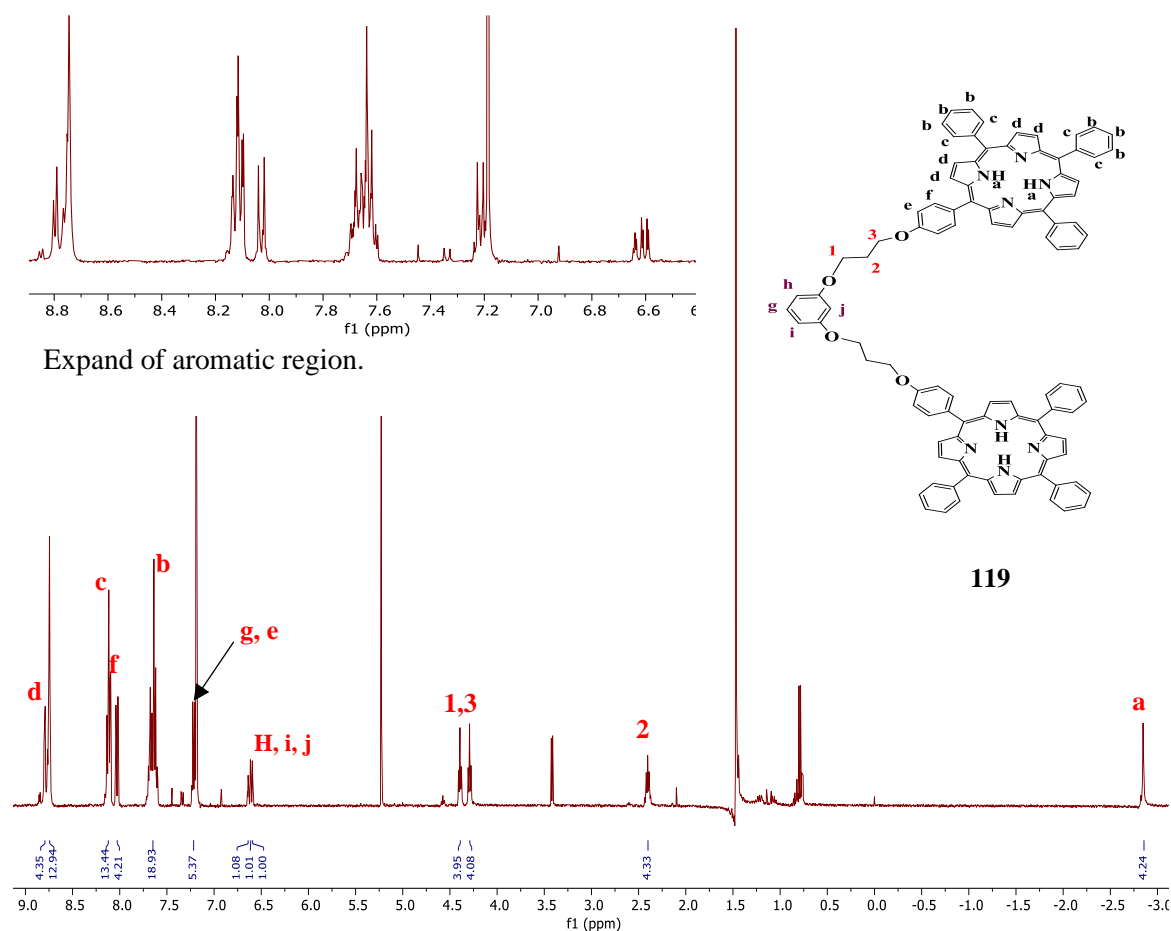
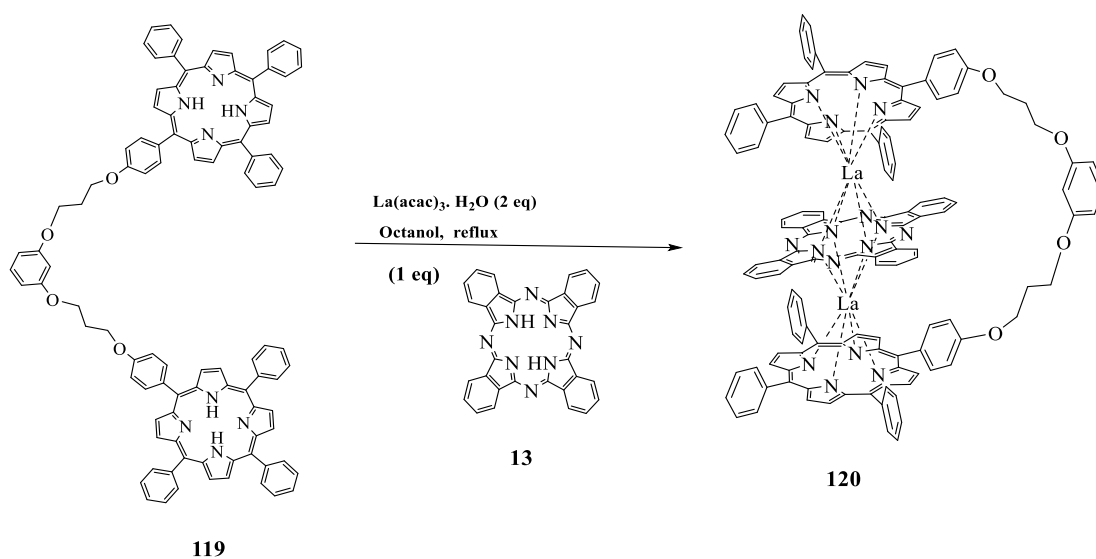


Figure 2.48: ¹H NMR characterization of 1,3-bis(porphyrin)benzene compound **119** in CDCl₃.

2.14.3 Synthesis of closed triple decker **120**:

The final stage of this model study was to create triple-deckers from dyad **119**. The general protocol which was developed by Cammidge *et al.*^[1] was followed. Two equivalents of lanthanide salt were added to porphyrin dyad **119** in hot octanol followed by Pc addition to produce TD **120** (scheme 2.50). This methodology is valid on Ln elements with large radii; therefore, we first attempted the reaction using lanthanum (La), porphyrin dyad **119** and Pc.



Scheme 2.50: Synthesis of closed TD **120**.

The reaction was done under argon and was monitored by TLC. The triple decker was observed in 24 h. After completion of the reaction solvents were removed under reduced pressure and the crude product was purified by using column chromatography, eluting the product with DCM: Hexane (3:2). The triple decker was recrystallised from DCM/MeOH to give a brown solid product in 48.6 % yield. The product was fully characterised by UV-Vis, mass spectrometry and NMR spectroscopy, and full interpretation of the structure was possible after suitable crystals were grown slowly from DCM and methanol. The ^1H -NMR spectrum obtained proved the formation of the desired compound **120**, (figure 2.49).

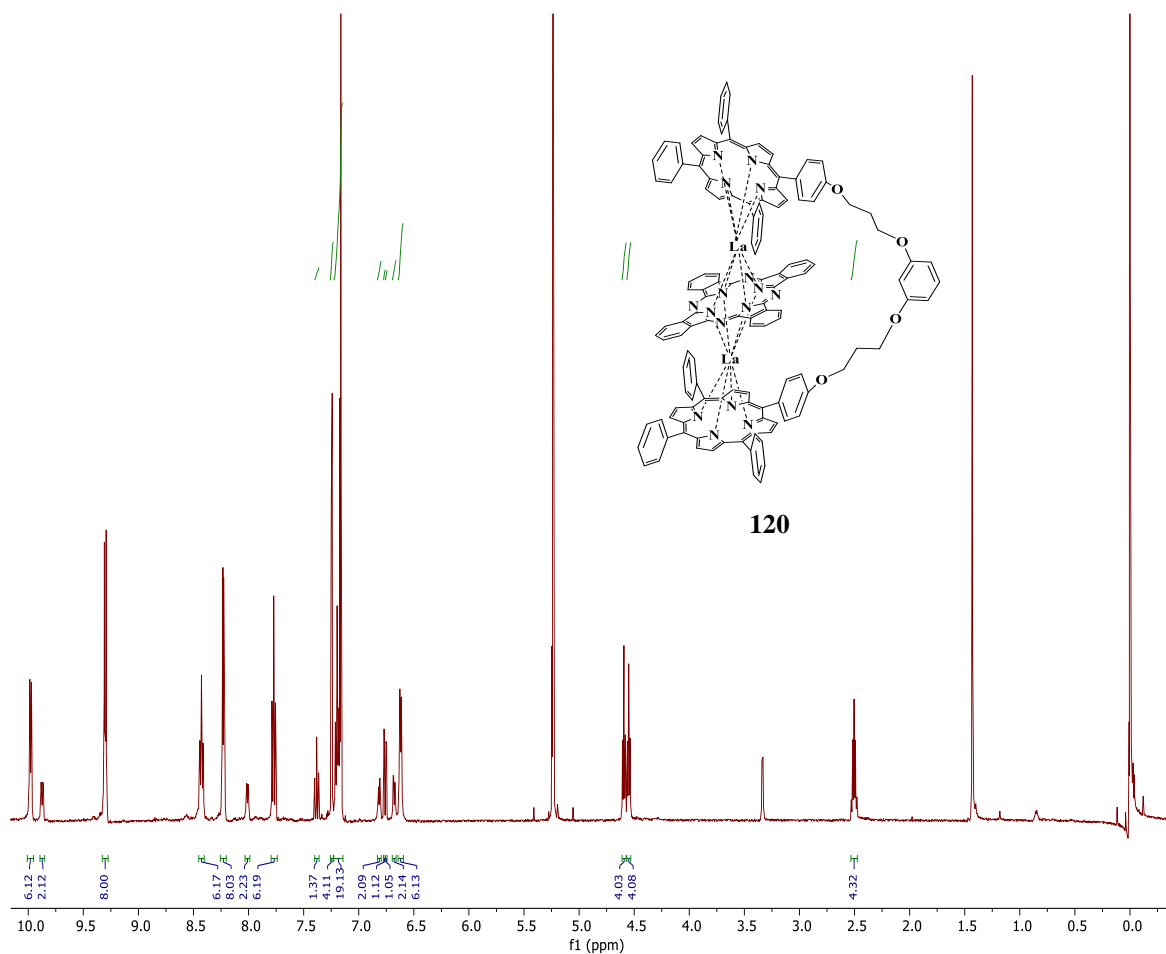


Figure 2.49: ^1H NMR spectrum obtained for triple decker **120** in DCM-d_2 .

2.13.3.1 ^1H NMR characterization of closed triple decker **120** complex:

The brown fraction was the desired triple decker as confirmed by ^1H NMR spectroscopy that closely resembled TD **59**. The absence of the characteristic peak at -2.7 ppm on the spectrum indicates that there is no metal-free porphyrin and the peaks for methylene group of the alkyl chain $-\text{OCH}_2$ was around 4.59 ppm (4H **a**), 4.55 ppm (4H **c**) and 2.50 ppm (4H **b**). Also, there are two signals at 8.30 and 9.35 ppm that is for symmetrical Pc (HPc_1 and HPc_2) as the lanthanide atoms allowed phthalocyanine units to freely spin inside molecule.^[1] The influence of electron density near lanthanum atoms resulted in the deshielding of the Pc and inner protons. On the other hand, the porphyrin β protons and outer protons, were shielded due to the opposite reason of low electrons density. Because of their geometric position, the protons of phenyl rings joined by alkyl linkers are distinguished from the rest (figure 2.50).

For more explanation the geometrical positions of protons were illustrated in (figure 2.50). The protons were assigned from studying ^1H NMR, 2D-COSY NMR, ^{13}C NMR, and HSQC NMR, which compared with the similar model **59** in the literature from Cammidge *et al.*^[1]

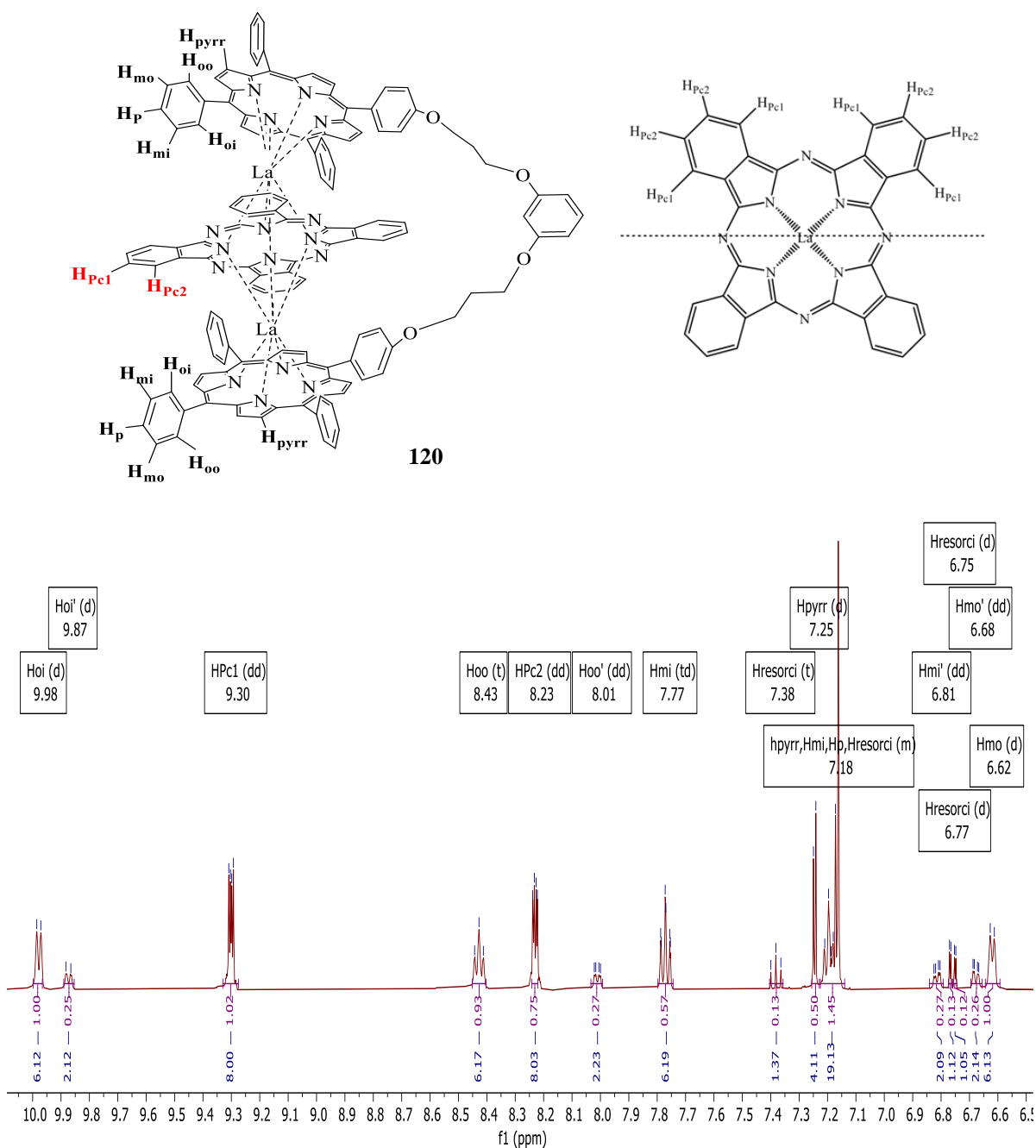


Figure 2.50: Aromatic region of ^1H NMR of triple decker **120**.

The indication of TD formation can be detected by UV-Vis (figure 2.51), as the new compound has unique absorbance peaks that are different from starting materials phthalocyanine **13** and dyad **117**.

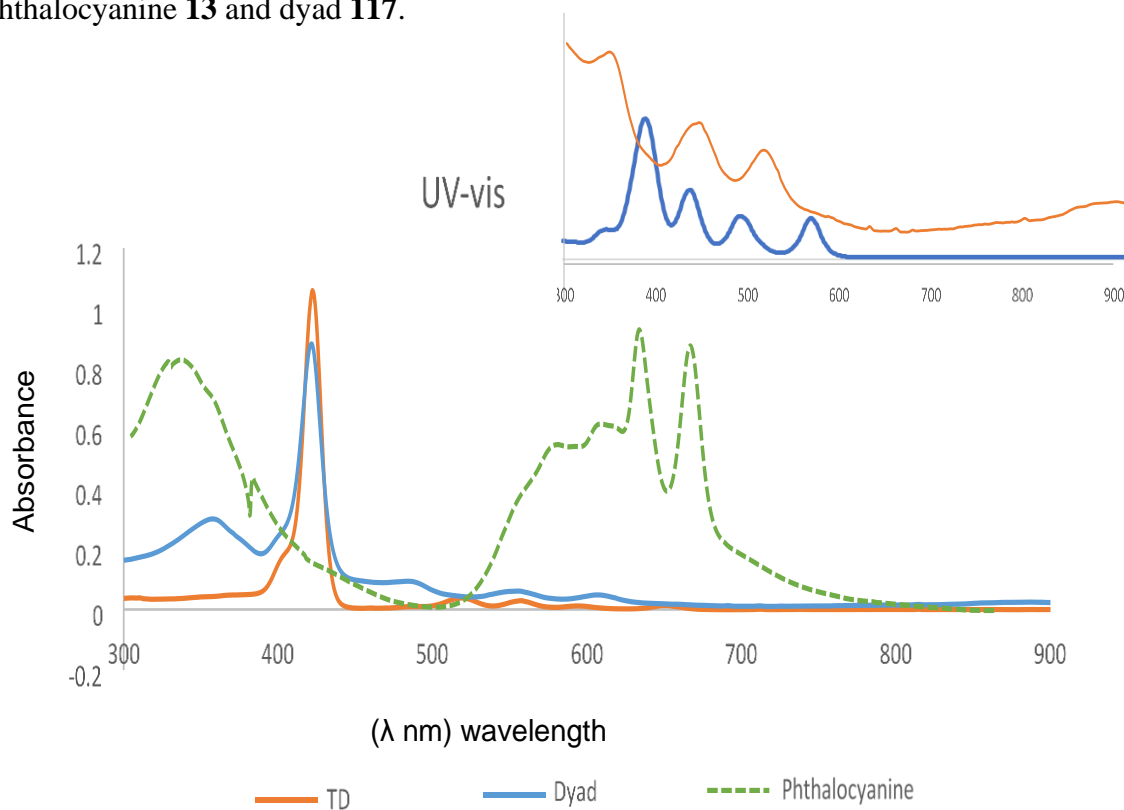


Figure 2.51: UV-Vis absorption shows the new compound TD **120** is different than the starting materials phthalocyanine **13** and trimer **117** in DCM.

The resulting dark solids were analysed by MALDI-TOF MS (figure 2.52). Formation of the pure closed triple decker **120** was observed at 2237 m/z.

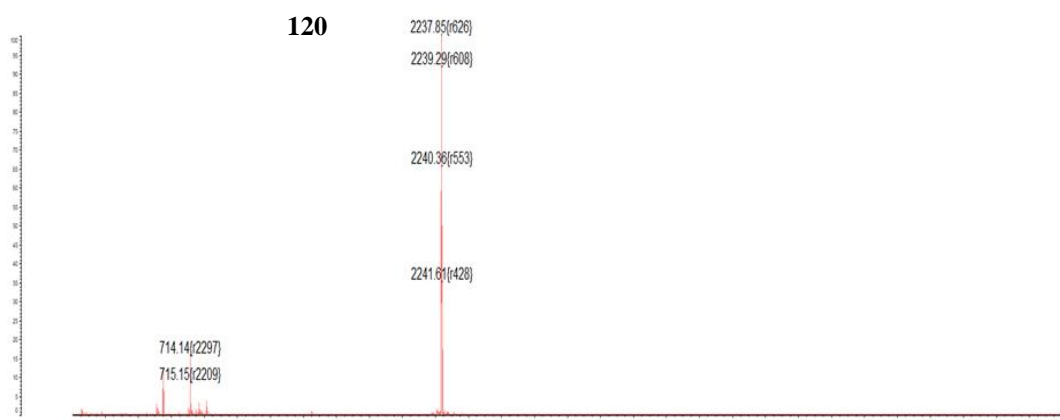
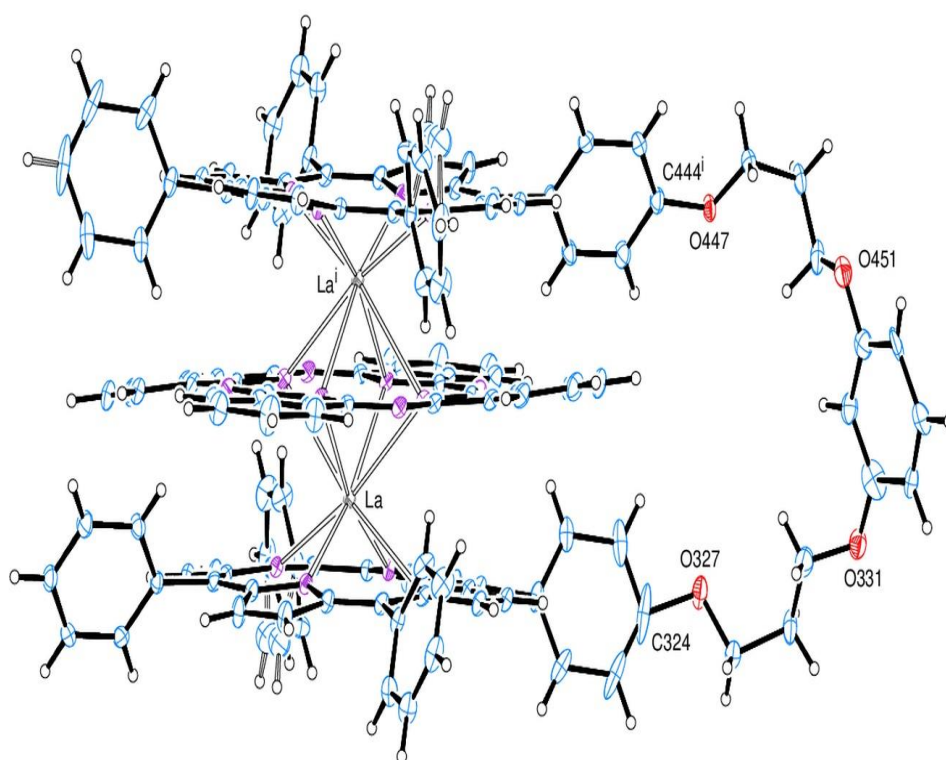


Figure 2.52: MALDI-TOF MS for TD **120**.

Crystals suitable for X-ray diffraction were obtained by slow evaporation from dichloromethane and Methanol and the structure is shown in Figure 2.53. The structure is closely related to that of the related system linked by a simple decyl chain reported earlier. In columns of the triple decker molecules the bridging chains are aligned. However, the arrangement in neighbouring columns can take the same or the opposite direction, so overall there results a centrosymmetric crystal (represented by the final picture – of course the molecule itself has just a single bridge). The three ring systems are parallel, 3.40 Å apart and almost eclipsed; it can be note that the rings are exactly eclipsed in the decyl-bridged system, and the small displacement likely arise due to the additional rigidity imparted by the 1,3-phenyl unit. The La-La distance is 3.9 Å, each lying closer to the porphyrin (1.36 Å) than the central phthalocyanine (1.95 Å). Disordered dichloromethane molecules are present in the crystal (not shown).



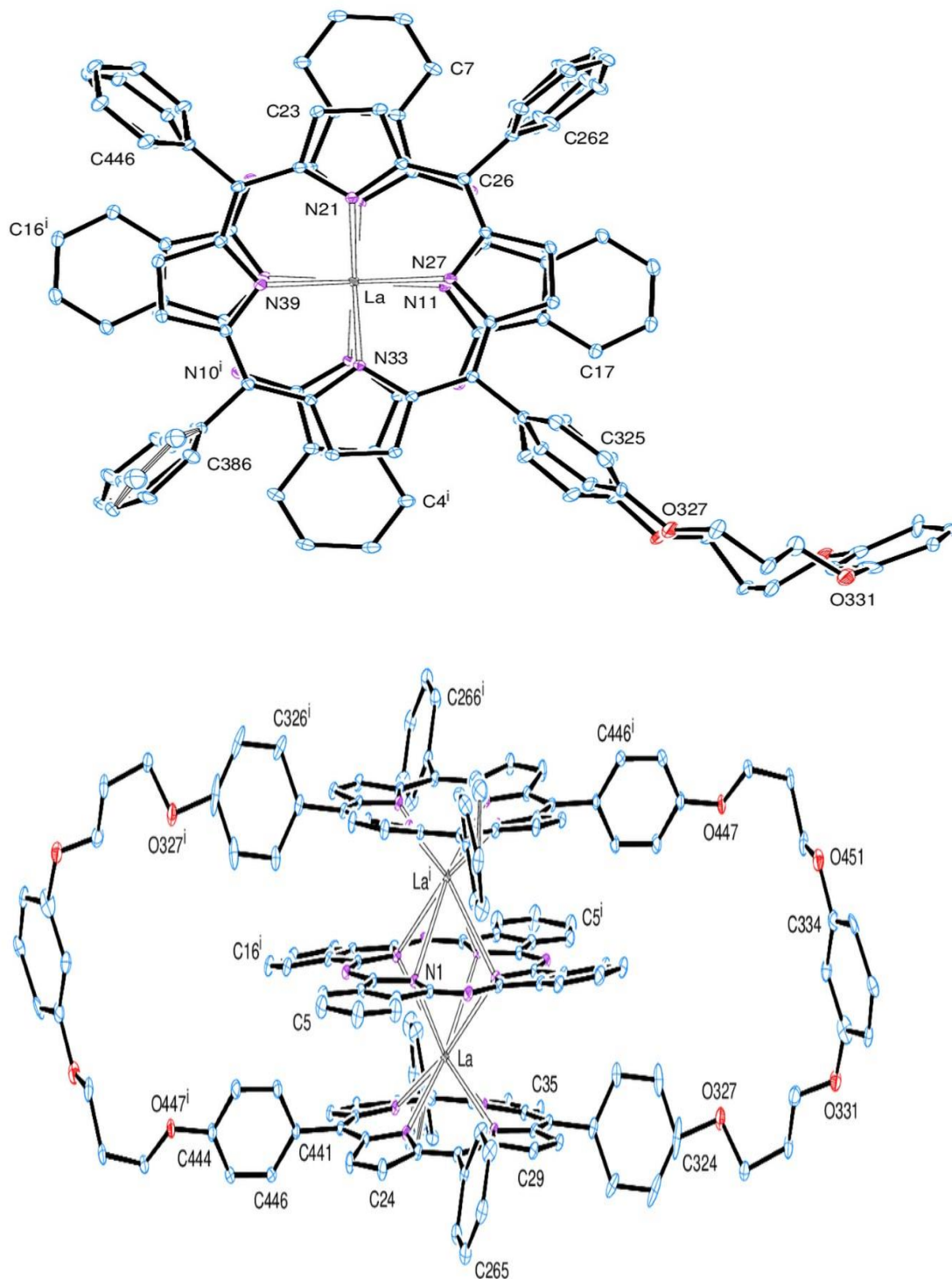
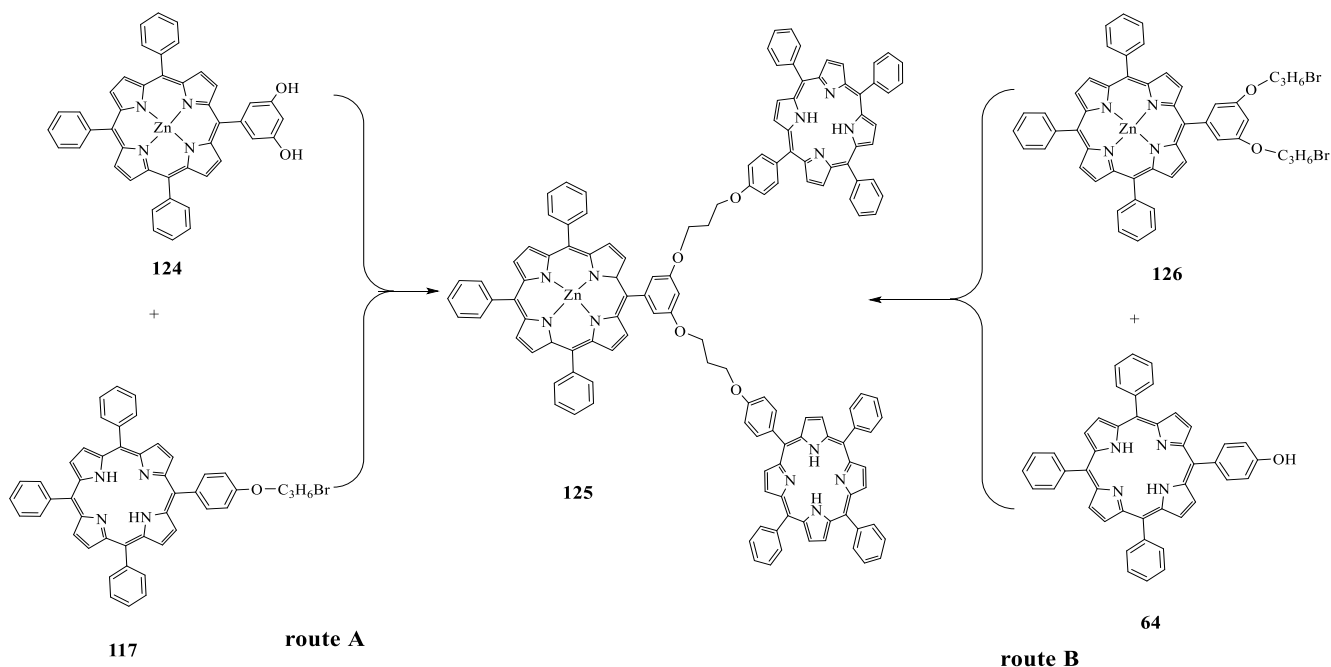


Figure 2.53: X-Ray crystal structure obtained for **120** showing side view (top), view along La-La bond (middle) and the “average” structure with equal occupancy of the bridging chains (bottom).

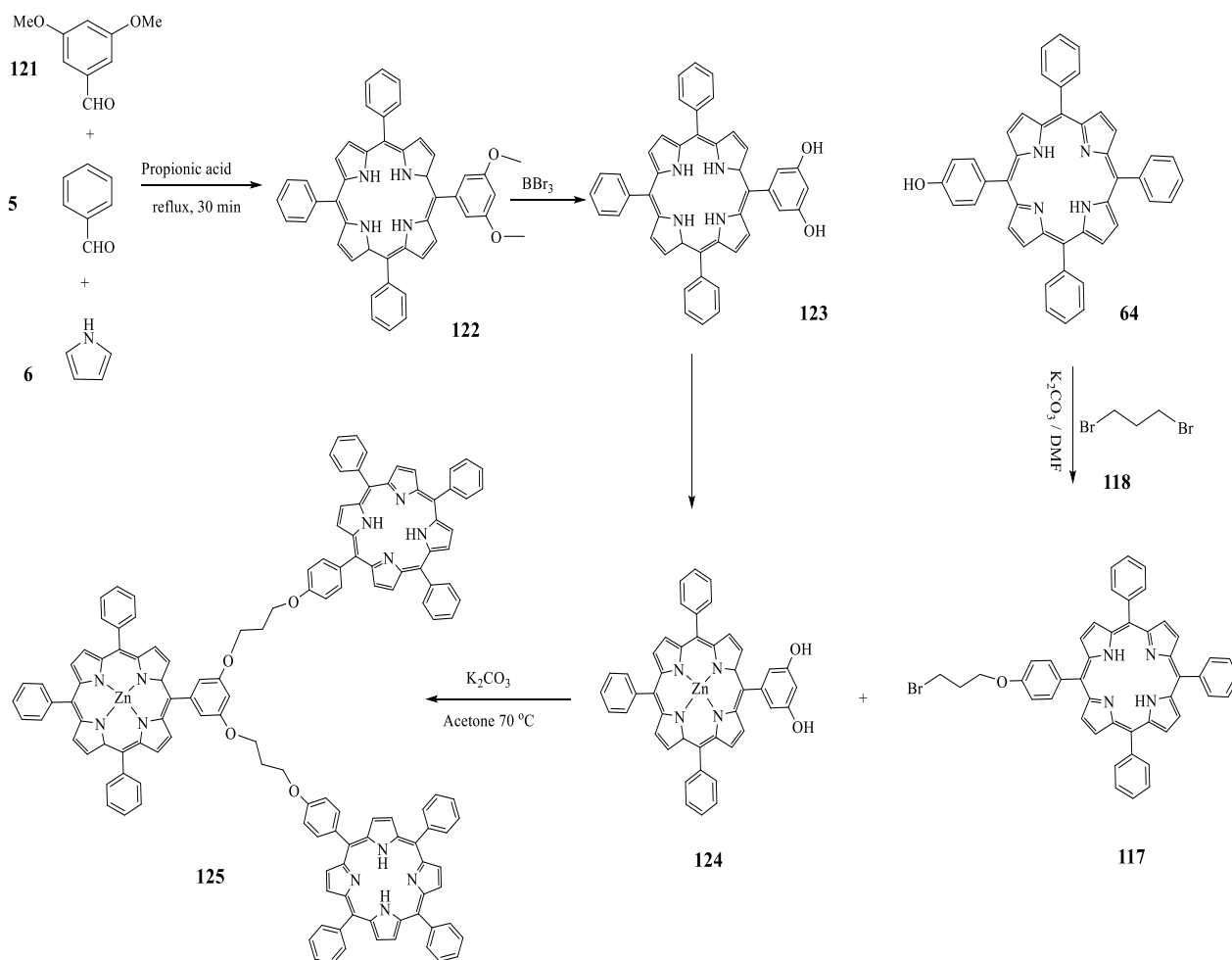
2.15 Synthesis of trimeric porphyrin with porphyrin in the bridge:

Two routes were initially considered for synthesising a trimeric porphyrin **125** (route **A** and **B**). Scheme 2.51 proposes two strategies to synthesise the porphyrin trimer using a nucleophilic substitution reaction:



Scheme 2.51: Two routes proposed synthesis of trimeric porphyrin **125**.

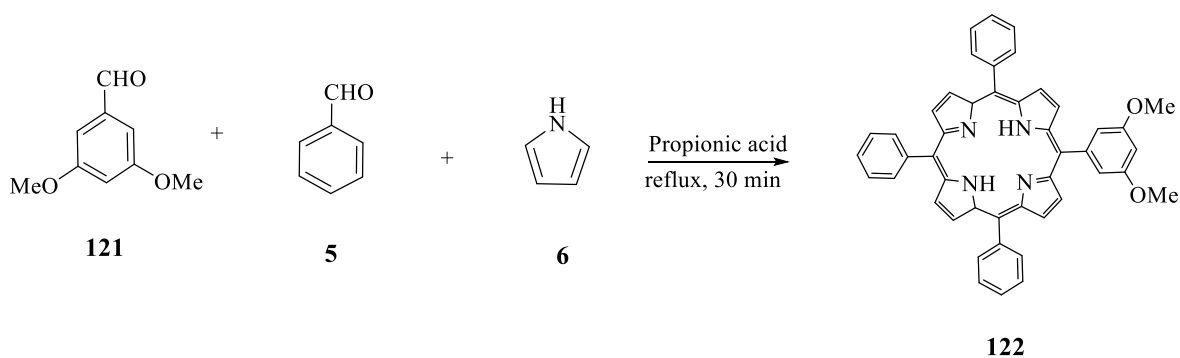
The intermediate precursors for the synthesis of the targeted trimer porphyrin were easily available, therefore the route **A** was chosen (scheme 2.52). Then route **B** was used to increase the yield of the reaction.



Scheme 2.52: Synthesis of the trimeric porphyrin **125**.

2.15.1 Synthesis of unsymmetrically substituted porphyrin:

2.15.1.1 Synthesis of 5-(3,5-dimethoxyphenyl)-10,15,20-triphenylporphyrin **122**.^{[2],[25]}



Scheme 2.53: Synthesis of 5-(3,5-methoxyphenyl)-triphenylporphyrin **122**.

Following Adler's^[2] method benzaldehyde (3eq), 3,5-dimethoxybenzaldehyde (1eq) and propionic acid were mixed and heated to reflux. Then freshly distilled pyrrole (4eq) was added dropwise to the mixture. The reaction was allowed to reflux for 30 minutes then cooled in room temperature and methanol was added. The mixture was left to precipitate overnight in the fridge. After suction filtration a purple solid was obtained. The crude products were purified by column chromatography using a mixture of DCM and petroleum ether (3:7) as eluent to collect first fraction TPP then the solvent was changed to DCM /pet ether (1:1) to collect the target compound **122** which was recrystallised from a mixture of DCM: MeOH as a purple solid (1 g, 6.16 %). In order to characterise the pure compound, the ¹H NMR spectrum is reported. The ¹H NMR spectrum for the porphyrin **122** (figure 2.54) have signals corresponding to 8H for the porphyrin-hydrogens, which are around 8.95 and 8.84 ppm. Broad signals are seen because the phenyls are not equal. The hydrogens on the three unsubstituted phenyl rings are represented by two broad signals integrating to 6H and 9H, at 8.22 ppm, 7.7 ppm respectively. At 7.4 ppm and 6.90 ppm is the signal for the hydrogens on substituted phenyl rings. The signals for the methoxy groups appear as a singlet at 3.96 ppm. Also, as porphyrins is a metal-free porphyrin, there was a signal at chemical shift of -2.78 ppm.

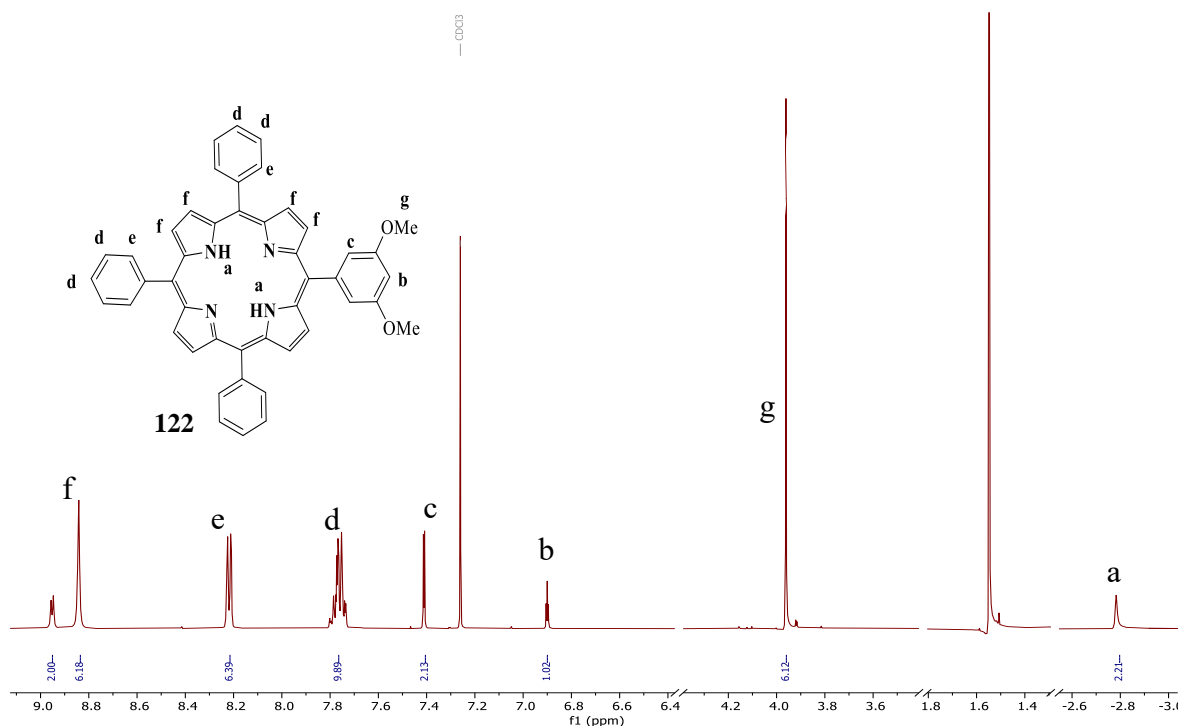
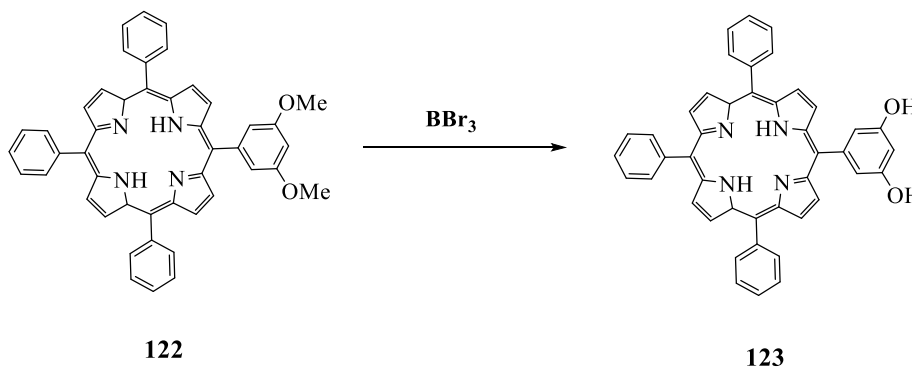


Figure 2.54: ¹H NMR of dimethoxy-TPP **122** in CDCl₃.

2.15.1.2 Synthesis of 5-(3,5-dihydroxyphenyl)-10,15,20-triphenylporphyrin **123**.^[25]

The methoxy groups can be easily removed by reacting with BBr_3 to form the corresponding hydroxy derivatives (scheme 2.54).

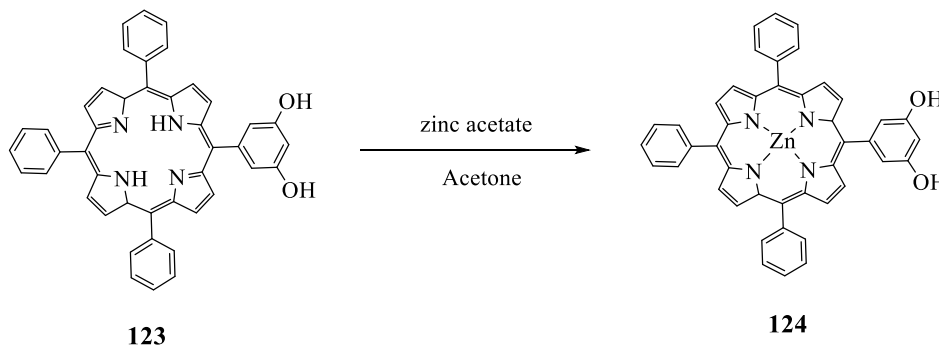


Scheme 2.54: Synthesis of 5-(3,5-dihydroxyphenyl)-10,15,20-triphenylporphyrin **123**.^[25]

The demethylation of **122** was achieved by using BBr_3 in DCM at $0\text{ }^\circ\text{C}$. After the complete addition of BBr_3 , the reaction was left to stir overnight. The reaction was monitored by TLC and confirmed by MALDI-TOF MS. The title product **123** was produced in 84.2% yield. In the ^1H NMR spectrum, the signals for the methoxy groups at 3.96 ppm disappeared. Also, the hydroxy group at 4.84 ppm appears as a broad signal.

2.15.1.3 Synthesis of Zinc 5-(3,5-dihydroxyphenyl)-10,15,20-triphenylporphyrin^[26]

The 5-(3,5-dihydroxyphenyl)-10,15,20-triphenylporphyrin was refluxed in acetone in the presence of zinc acetate for 60 minutes. After workup and recrystallisation Zn porphyrin **124** was obtained as a purple solid in 79 % yield as shown in scheme 2.55. As the porphyrin is no longer metal-free porphyrin, the signals for the two protons at -2.78 ppm disappeared (figure 2.55).



Scheme 2.55: Synthesis of Zn porphyrin **124**.

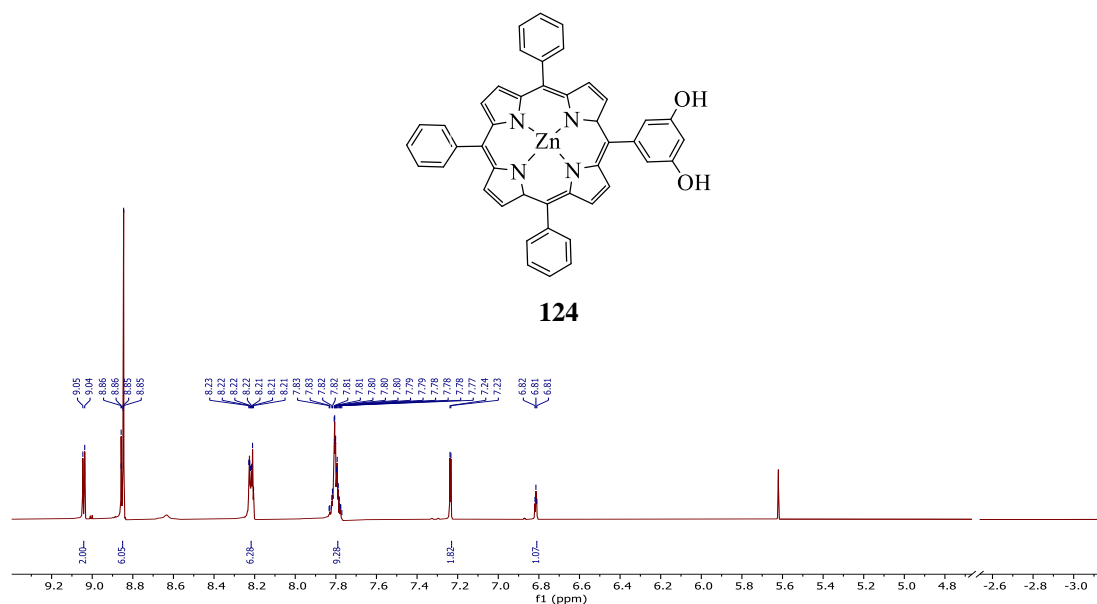
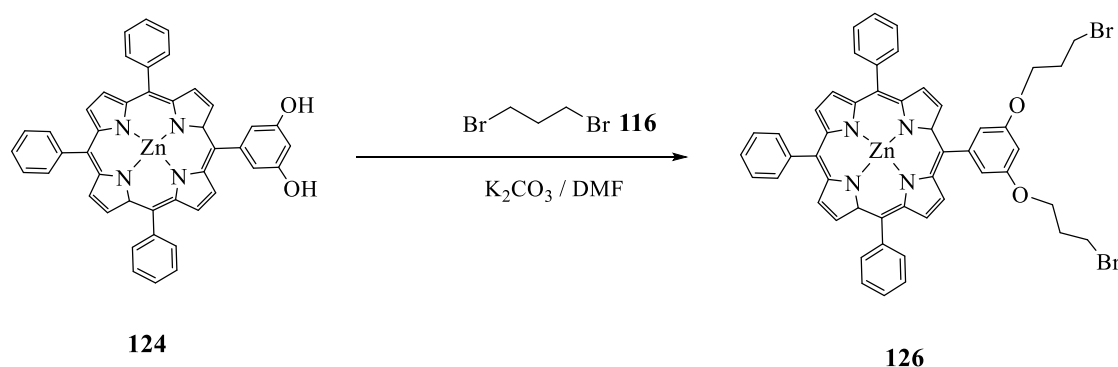


Figure 2.55: ¹H NMR of Zn porphyrin **124** in acetone-*d*₆.

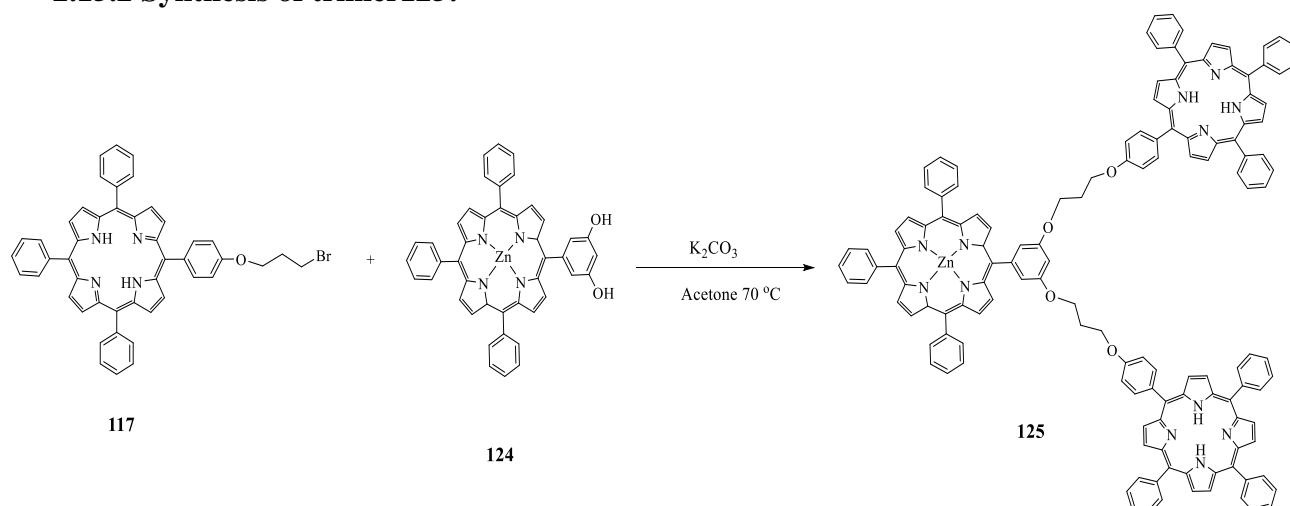
2.15.1.4 Synthesis of zinc bromoalkoxy porphyrin **126**.^[27]

The reaction between the di-hydroxyl groups on the porphyrin and the alkyl bromide follows a previous method.^[4] Zn porphyrin **124** was dissolved in DMF, followed by 1,3 dibromopropane **116** in presence of potassium carbonate. The reaction was completed after 19 h and after work up the product was purified by recrystallisation from chloroform and hexane to give porphyrin **126** as a light purple solid in 77 % yield. (Scheme 2.56).

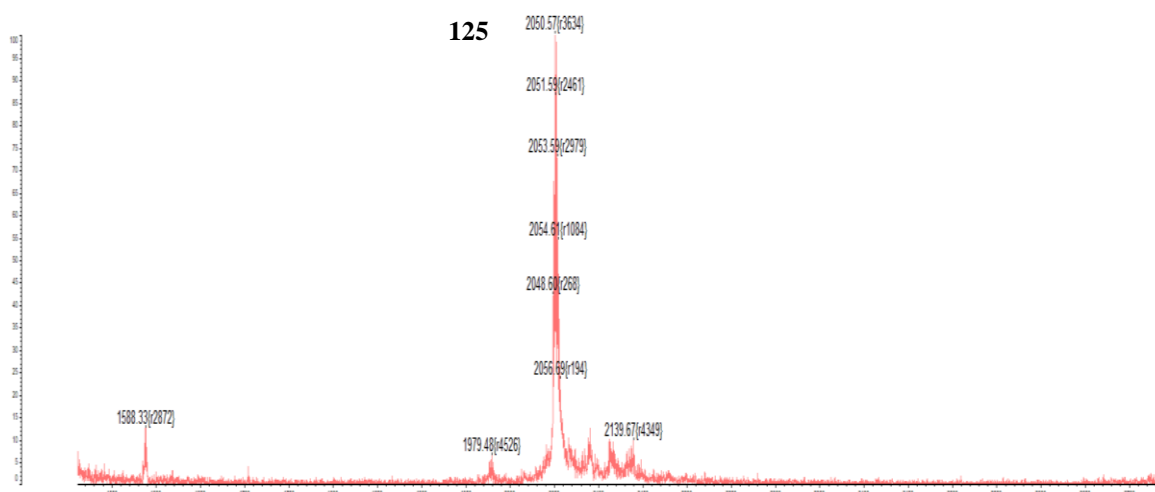


Scheme 2.56: Synthesis of bromoalkoxy porphyrin **126**.^[27]

2.15.2 Synthesis of trimer125:

Scheme 2.57: Synthesis of trimeric porphyrin **125**.

As indicated in Scheme 2.57 the target trimeric porphyrin **125** was synthesised by reacting metallated unsymmetrical porphyrin **124** with bromoalkoxyporphyrin **117** in acetone and potassium carbonate in a sealed tube and heated at 70 °C. TLC was used to monitor the reaction. The reaction was left for 7 days. The crude reaction was worked up and purified by using column chromatography, eluting the product with DCM: PET (1:1v: v). The trimer recrystallised by methanol to obtain a purple solid product **125** in 30 % yield. The MALDI-TOF MS of the trimer showed a molecular ion peak at 2050 m/z which is consistent with predicted structure (figure 2.56).

Figure 2.56: MALDI-ToF MS confirms the formation of trimeric porphyrin **125**.

As we expected the additional porphyrin in the bridge makes the ^1H NMR spectrum difficult to interpret (figure 2.57). The data clearly matched the expectation of the product. Signals corresponding to 24 H for the porphyrin-hydrogens, which are about 8.95 and 8.84 ppm. The hydrogens on the three unsubstituted phenyl rings are represented by two multiplet signals integrating to 18H and 27 H, at 8.22 ppm and 7.7 ppm respectively. A triplet peak for methylene group of the alkyl chain $-\text{OCH}_2$ was around 4.39 ppm (4H **1**). However, the triplet peak for $-\text{CH}_2\text{Br}$ no longer appears and instead a triplet peak of (4H **3**) is present at 4.29 ppm for $-\text{OCH}_2$ that is linked with porphyrin molecules. Finally, the methylene group of the rest of the alkyl chains of appear at 2.40 ppm (4H **2**).

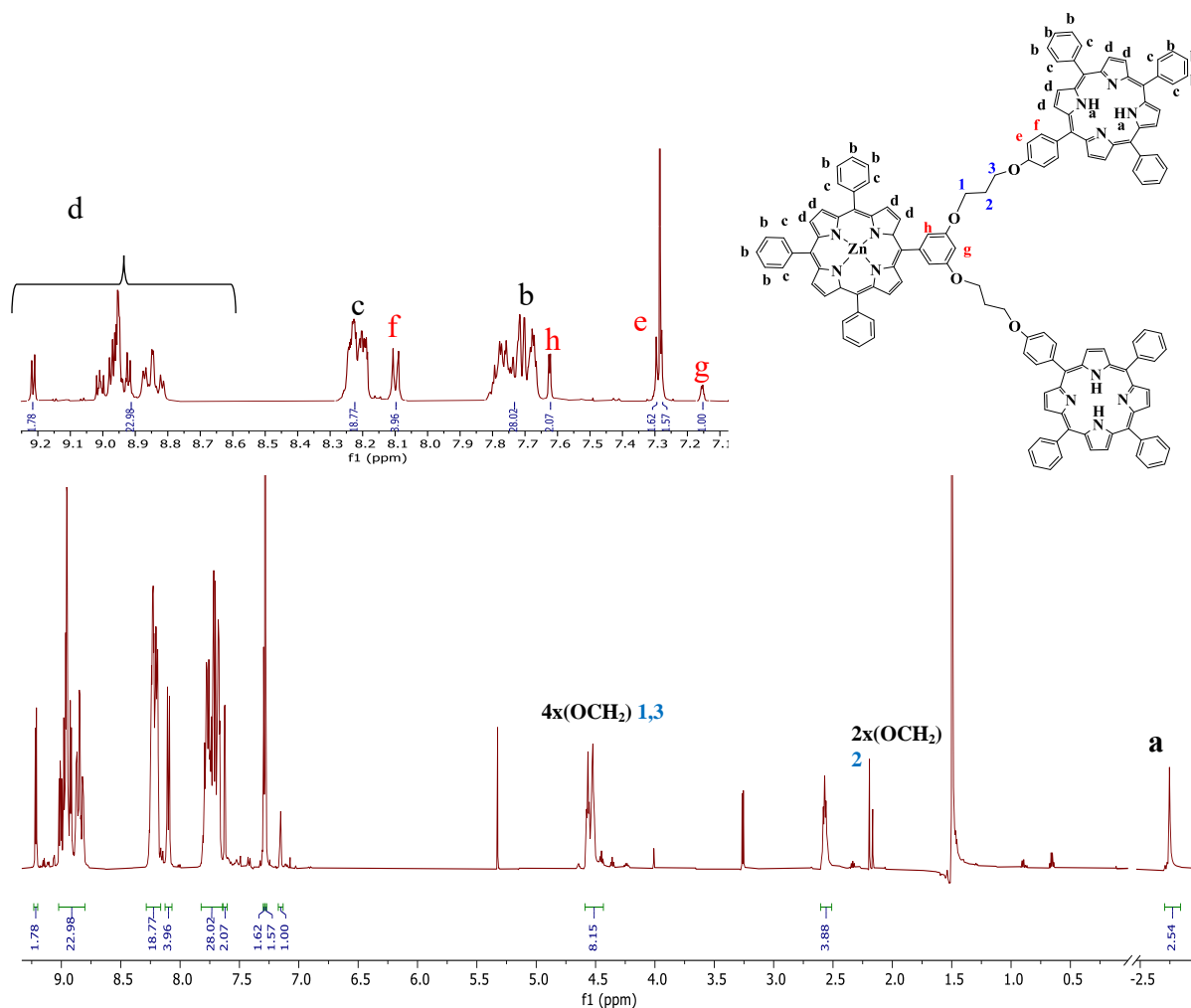
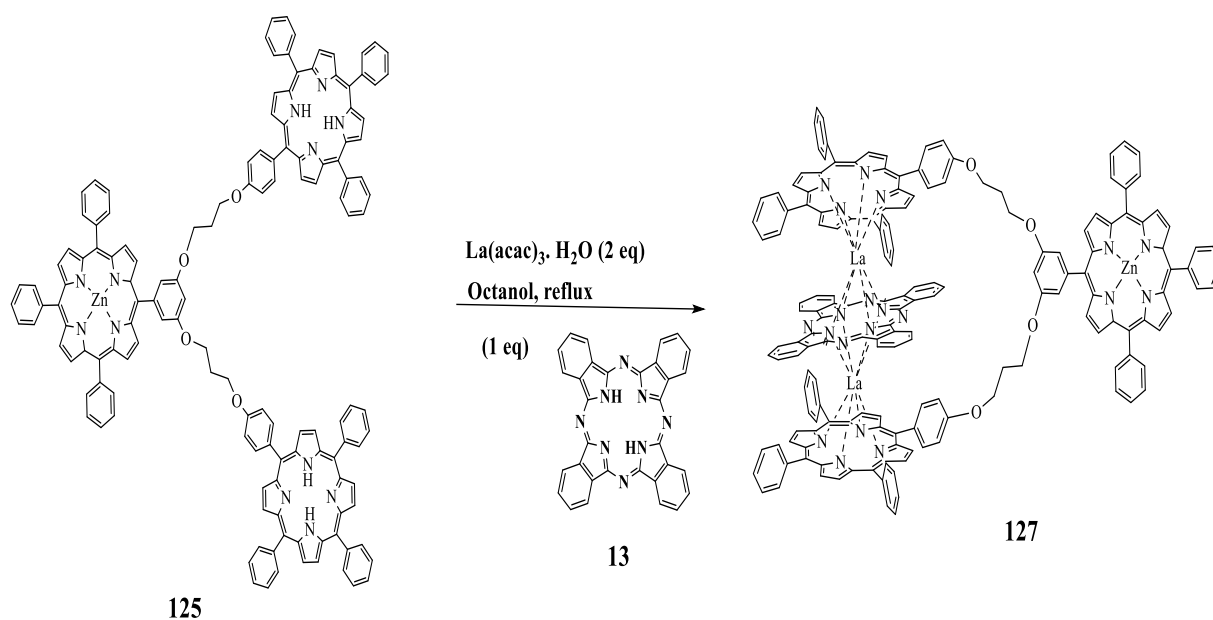


Figure 2.57: of ^1H NMR of trimeric porphyrin **125** and aromatic region.

2.15.3 Synthesis of closed triple decker **127**:

The final proof of concept experiment relied on successful synthesis of TD structures from porphyrin trimer **125** (scheme 2.58). In a test experiment trimer **125**, two equivalents of lanthanum (III) acetylacetonate and one equivalent of Pc **13** were refluxed in octanol and the reaction was followed by TLC. It was found that the triple decker was formed within 24 h. By analysing the spectrum, it could be concluded that the desired triple decker (Exact mass at 2835.42 m/z) was successfully formed (figure 2.58). Further purification attempts by column chromatography or recrystallisations were unsuccessful and a pure triple deckers could not be separated. The reaction was then tried in a bigger scale to try to separate the mixture recrystallisation or prep-TLC but attempts in the time available were not fully successful.



Scheme 2.58: Synthesis of closed triple decker **127**.

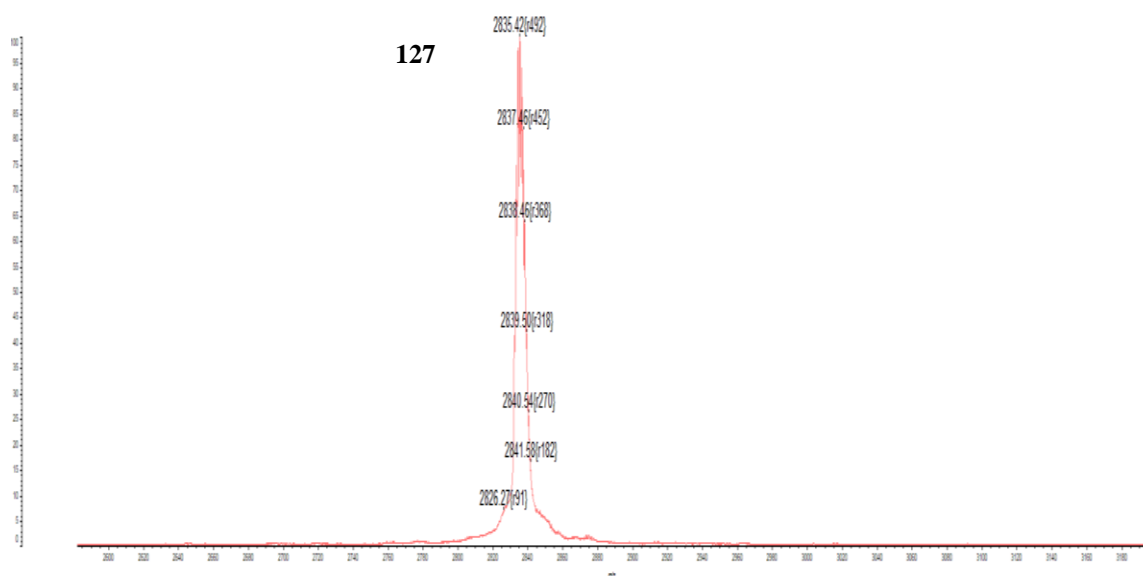


Figure 2.58: MALDI-TOF-MS confirms the formation of closed triple decker **127**.

2.16 Conclusion and future work:

Triple deckers of compounds that bear a more rigid element (such as benzene and porphyrin) to the bridge were successfully synthesised using the developed procedure for the selective formation of linked closed triple deckers, and overall, this appears to be a very promising strategy for building up more complex arrays of TDs. Starting material synthesis (where a large part of this project's time was committed) proved somewhat challenging to scale up, but the results are sufficiently conclusive to give confidence that TD formation is smooth, and that symmetrical TD are formed.

Looking to future work, firstly, a very interesting expansion to this work could be to investigate the two model compounds, **120** and **127** further as tweezer complexes. Secondly, the unique properties of lanthanides metals are always fascinating to investigate due to their magnetic behaviours and optical characteristics. Therefore, alternative paramagnetic lanthanide metals could be investigated to obtain analogous triple deckers from **120** through the series. Finally, this project's ultimate goal was to synthesise a linker between the multichromophore assemblies, and this looks promising through rigid or flexible linkers (figure 2.59 and 2.60).

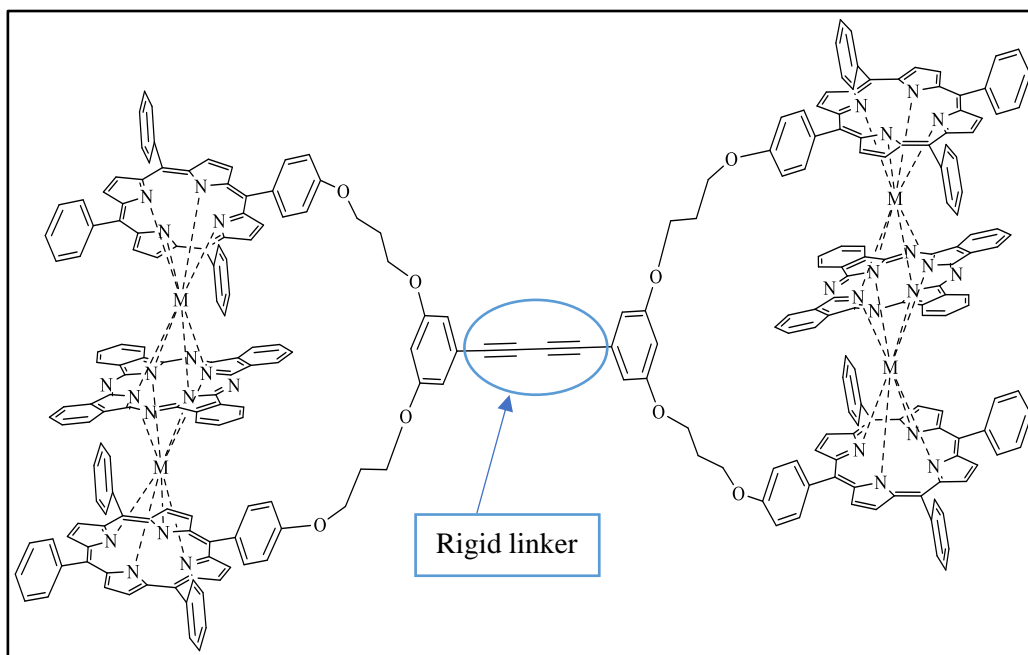


Figure 2.59: Example of rigid linker between two TD.

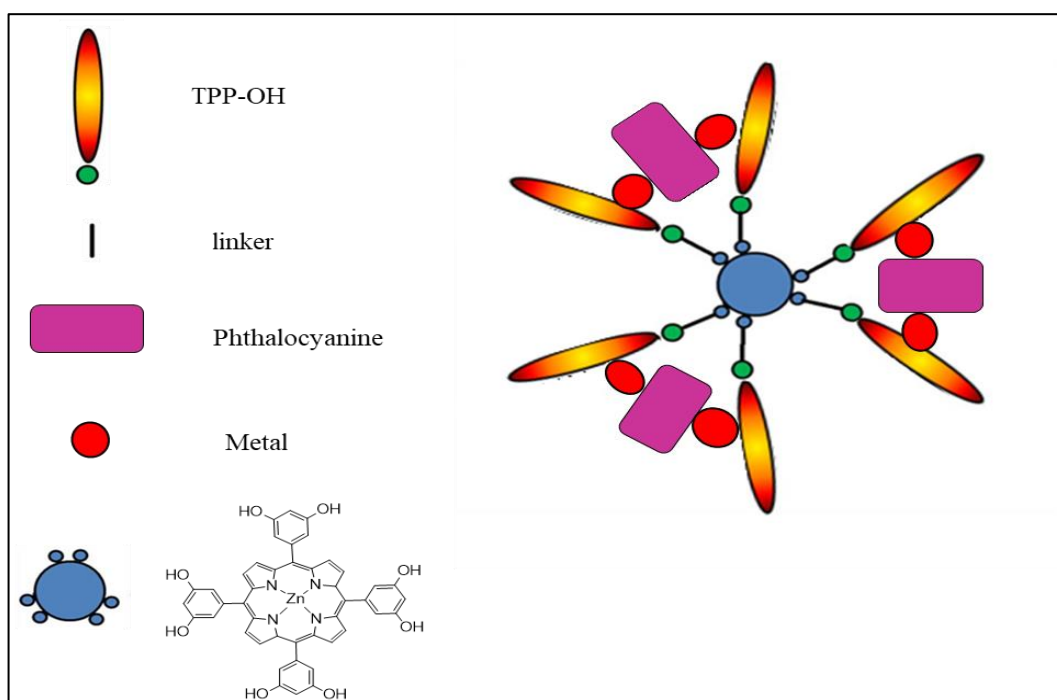


Figure 2.60: Cartoon example of another linker between multichromophore.

References:

- [1] D. González-Lucas, S. C. Soobrattee, D. L. Hughes, G. J. Tizzard, S. J. Coles and A. N. Cammidge, *Chemistry – A European Journal* **2020**, *26*, 10724-10728.
- [2] A. D. Adler, F. R. Longo, J. D. Finarelli, J. Goldmacher, J. Assour and L. Korsakoff, *The Journal of Organic Chemistry* **1967**, *32*, 476-476.
- [3] R. Yang, K. Wang, L. Long, D. Xiao, X. Yang and W. Tan, *Analytical Chemistry* **2002**, *74*, 1088-1096.
- [4] X. Sun, D. Li, G. Chen and J. Zhang, *Dyes and Pigments* **2006**, *71*, 118-122.
- [5] N. E. Galanin and G. P. Shaposhnikov, *Russian Journal of General Chemistry* **2012**, *82*, 1734-1739.
- [6] a) K. P. Birin, Y. G. Gorbunova and A. Y. Tsivadze, *Magnetic Resonance in Chemistry* **2010**, *48*, 505-515; b) K. P. Birin, Y. G. Gorbunova and A. Y. Tsivadze, *Dalton Transactions* **2011**, *40*, 11539-11549; c) K. P. Birin, K. A. Kamarova, Y. G. Gorbunova and A. Y. Tsivadze, *Protection of Metals and Physical Chemistry of Surfaces* **2013**, *49*, 173-180.
- [7] H. A. Bruson and J. W. Kroeger, *Journal of the American Chemical Society* **1940**, *62*, 36-44.
- [8] C. E. Wagner and P. A. Marshall, *Journal of Chemical Education* **2010**, *87*, 81-83.
- [9] V. N. Nemykin and E. A. Lukyanets, *ARKIVOC* **2010**, *2010*, 136-208.
- [10] P. R. Ashton, U. Girreser, D. Giuffrida, F. H. Kohnke, J. P. Mathias, F. M. Raymo, A. M. Z. Slawin, J. F. Stoddart and D. J. Williams, *Journal of the American Chemical Society* **1993**, *115*, 5422-5429.
- [11] G. P. Ellis and T. M. Romney-Alexander, *Chemical Reviews* **1987**, *87*, 779-794.
- [12] C. C. Leznoff and D. M. Drew, *Canadian Journal of Chemistry* **1996**, *74*, 307-318.
- [13] S. S. Erdem, I. V. Nesterova, S. A. Soper and R. P. Hammer, *The Journal of organic chemistry* **2008**, *73*, 5003-5007.
- [14] K. Sakamoto and E. Ohno-Okumura, *Materials* **2009**, *2*, 1127.
- [15] a) T. Haruhiko, S. Shojiro, O. Shojiro and S. Shinsaku, *Chemistry Letters* **1980**, *9*, 1277-1280; b) T. Haruhiko, S. Shojiro and S. Shinsaku, *Chemistry Letters* **1983**, *12*, 313-316.
- [16] P. A. Barrett, R. P. Linstead, G. A. P. Tuey and J. M. Robertson, *Journal of the Chemical Society (Resumed)* **1939**, 1809-1820.
- [17] N. Iida, K. Tanaka, E. Tokunaga, H. Takahashi and N. Shibata, *ChemistryOpen* **2015**, *4*, 102-106.

- [18] X. Sun, R. Li, D. Wang, J. Dou, P. Zhu, F. Lu, C. Ma, C.-F. Choi, Diana Y. Y. Cheng, Dennis K. P. Ng, N. Kobayashi and J. Jiang, *European Journal of Inorganic Chemistry* **2004**, 2004, 3806-3813.
- [19] V. E. Pushkarev, V. V. Kalashnikov, A. Y. Tolbin, S. A. Trashin, N. E. Borisova, S. V. Simonov, V. B. Rybakov, L. G. Tomilova and N. S. Zefirov, *Dalton Transactions* **2015**, 44, 16553-16564.
- [20] A. Díaz-Moscoso, G. J. Tizzard, S. J. Coles and A. N. Cammidge, *Angewandte Chemie International Edition* **2013**, 52, 10784-10787.
- [21] S. Dalai, V. N. Belov, S. Nizamov, K. Rauch, D. Finsinger and A. de Meijere, *European Journal of Organic Chemistry* **2006**, 2006, 2753-2765.
- [22] M. Hellal and G. D. Cuny, *Tetrahedron Letters* **2011**, 52, 5508-5511.
- [23] V. P. W. Böhm and W. A. Herrmann, *European Journal of Organic Chemistry* **2000**, 2000, 3679-3681.
- [24] T. Toshihiro, E. Ken and A. Yasuhiro, *Bulletin of the Chemical Society of Japan* **2001**, 74, 907-916.
- [25] L. Yu, K. Muthukumar, I. V. Sazanovich, C. Kirmaier, E. Hindin, J. R. Diers, P. D. Boyle, D. F. Bocian, D. Holten and J. S. Lindsey, *Inorganic Chemistry* **2003**, 42, 6629-6647.
- [26] F. Ogasawara, H. Kasai, Y. Nagashima, T. Kawaguchi and A. Yoshizawa, *Ferroelectrics* **2008**, 365, 48-57.

Chapter 3: Experimental

3. Experimental:

3.1 General Methods

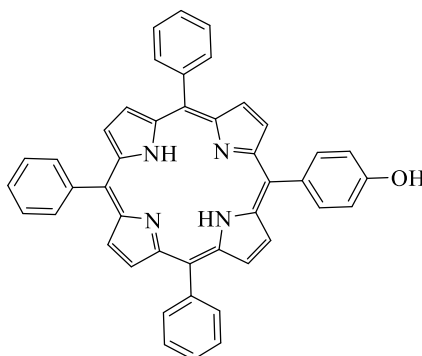
Reagents and solvents were obtained from commercial sources and used without further purification unless otherwise stated. Reactions were carried out under an inert atmosphere (argon or nitrogen gas), in most air-sensitive reactions, argon was preferred. Brine is a saturated aqueous solution of sodium chloride. Organic layers were dried using anhydrous magnesium sulphate. Evaporating of solvent was performed using a Buchi rotary evaporator at reduced pressure.

^1H NMR spectra were recorded either at 400 MHz on Ultrashield PlusTM 400 spectrometer or 500 MHz on a Bruker AscendTM 500 spectrometer in 5 mm diameter tubes. Signals are quoted in ppm as δ downfield from tetramethylsilane ($\delta=0.00$) and coupling constants J given in Hertz. ^{13}C spectra were recorded at 101 MHz or 126 MHz. NMR spectra were performed in solution using deuterated chloroform, methanol, dichloromethane or tetrahydrofuran at room temperature unless otherwise stated.

Ultraviolet-Visible absorption spectra were recorded on Hitachi U-3310 Spectrophotometer in solvent as stated. MALDI-ToF-MS mass spectra were carried out using a Shimadzu Biotech Axima instrument. Characterisation of hybrids by MALDI-ToF-MS mass spectrometry was achieved by comparison of isotopic distribution to theory. IR spectra were recorded using a Perkin-Elmer Spectrum BX FT-IR spectrometer.

Thin-layer chromatography (TLC) was performed using aluminium sheets coated with Alugram® Sil G/UV254 (Macherey-Nagel), and the compounds were visualised under shortwavelength UV-light at 254 nm or 366 nm. Column chromatography was carried out using silica gel 60Å mesh 70-230 (63-200 μm) under gravity or moderate pressure at ambient temperature. Solvent ratios are given as v: v.

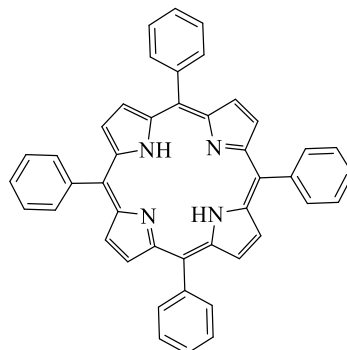
3.2 Synthesis of 5-(*p*-hydroxyphenyl)-10, 15, 20-triphenylporphyrin **64** (TPPOH).



For the synthesis of the porphyrin derivative TPP-OH, a modified version of the procedure as reported by Adler^[1] was followed:

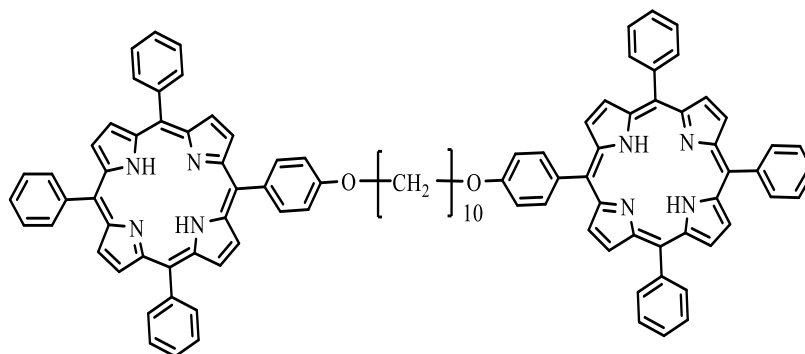
Benzaldehyde **5** (7.96 g, 75 mmol) and *p*-hydroxybenzaldehyde **63** (3.05 g, 25 mmol) were dissolved in propionic acid (200 mL) and the mixture was allowed to reflux. Freshly distilled pyrrole **5** (6.94 mL, 6.71 g, 100 mmol) was then added dropwise. Once the addition was completed, the resulting mixture was refluxed for a further 30 mins. The reaction mixture was allowed to cool to room temperature, MeOH (200 mL) was added, and the mixture was left to precipitate overnight. The resulting purple solid was collected by vacuum filtration and washed with MeOH. The crude compound was chromatographed on a silica gel column using DCM: Pet Ether (1:1 v/v) mixture as eluent. The first pink band collected was the symmetrical porphyrin TPP. The solvent was changed to DCM and TPP-OH separated out as a dark purple fraction. The title compound was recrystallised from a mixture of DCM: MeOH as a purple solid (1 g, 6 %). M.P. > 350 °C. ¹H NMR (400 MHz, CDCl₃) δ 8.88 (d, *J* = 4.5 Hz, 2H), 8.84 (d, *J* = 4.5 Hz, 6H), 8.23 – 8.19 (m, 6H), 8.08 (d, *J* = 8.5 Hz, 2H), 7.80 – 7.71 (m, 9H), 7.22 (d, *J* = 8.5 Hz, 2H), 5.18 (s, 1H), -2.77 (s, 1H). ¹³C-NMR (126 MHz, CDCl₃) δ 155.46, 142.21, 135.72, 134.71, 134.58, 127.71, 126.69, 120.11, 120.02, 119.89, 113.70. UV-Vis, (DCM)/nm: 423, 519, 552, 595, 652. MS (MALDI-TOF): *m/z* = 631.43 [M]⁺ (100%)

3.3 Synthesis of Tetraphenylporphyrin **4**^[1]



This compound was isolated from the previous reaction as side product and was obtained as a purple solid (2.21 g, 14 %). M.P. > 350 °C. ¹H NMR (400 MHz, Chloroform-*d*) δ 8.85 (s, 8H), 8.22 (d, *J* = 7.8 Hz, 8H), 7.80 – 7.72 (m, 12H), -2.77 (s, 2H). ¹³C-NMR (126 MHz, CDCl₃) δ 142.20, 134.59, 127.73, 126.71, 120.16. MS (MALDI-TOF): *m/z* = 614.22 [*M*]⁺ (100%) UV-Vis, (DCM)/nm (log ε) = 416, 515, 551, 595, 649.

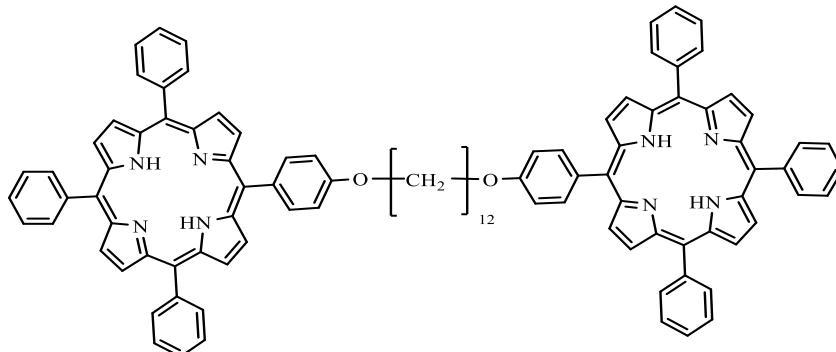
3.4 Synthesis of Porphyrin C₁₀ dyad (TPP-O-(CH₂)₁₀-O-TPP) **58**



TPP-OH **64** (200 mg, 0.32 mmol) and 1, 10- dibromodecane **65** (47.6 mg, 0.16 mmol) were dissolved in acetone (5 mL) and K₂CO₃ (220 mg, 1.5 mmol) was added in a sealed tube and heated at 70 °C for 72 h. The solvent was removed, and the residue dissolved in DCM and washed with water. The solvent was evaporated, and the product was purified by two slow and careful recrystallisations from a mixture of DCM: MeOH, to yield the pure product as a purple solid (100 mg, 45%).

As an alternative method, TPP-OH (0.6 g, 0.952 mmol), 1,10-dibromodecane (142.8 mg, 0.476 mmol) and potassium carbonate (1.5 g, 4.76 mmol) was added to dry DMF (15 mL) and the mixture stirred at 90 °C for 3 h under N₂. The reaction mixture was allowed to cool to room temperature, then the resulting purple solid was collected by vacuum filtration and washed with cold DMF then with MeOH. The solid was sonicated with a mixture of water and MeOH and then filtrated. The product was purified by recrystallisation from DCM/MeOH, (1:1) to give the titled compound as a purple solid (0.250 g, 60%). **M.P.** > 350 °C. ¹H NMR (400 MHz, CDCl₃) δ 8.89 (d, *J* = 4.5 Hz, 4H), 8.83 (m, 12H), 8.21 (dd, *J* = 7.6, 1.9 Hz, 12H), 8.12 (d, *J* = 7.6 Hz, 4H), 7.79 – 7.69 (m, 18H), 7.29 (d, *J* = 7.6 Hz, 4H), 4.28 (t, *J* = 6.5 Hz, 4H), 2.07 – 1.96 (m, 4H), 1.73 – 1.61 (m, 4H), 1.26 (s, 8H), -2.76 (s, 4H). ¹³C-NMR (126 MHz, CDCl₃) δ 159.2, 142.4, 135.8, 134.7, 134.5, 127.8, 126.8, 125.8, 120.3, 120.2, 120.1, 112.9, 31.0, 29.8, 29.7, 26.5. MS (MALDI-TOF): *m/z* = 1399.61 [M]⁺ (100%) UV-Vis, (DCM)/nm (log ε): 418, 516, 552, 592, 649.

3.5 Synthesis of Porphyrin C₁₂ dyad (TPP-O-(CH₂)₁₂-O-TPP) 112

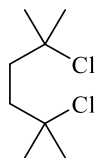


TPPOH **64** (0.6 g, 0.952 mmol), 1,12-dibromododecane (156.2 mg, 0.476 mmol) and potassium carbonate (1.5 g, 4.76 mmol) were added to dry DMF (15 mL) and the mixture stirred at 90 °C for 3 h under N₂. The reaction mixture was allowed to cool to room temperature. The resulting purple solid was collected by vacuum filtration and washed with cold DMF followed by MeOH. The solid was sonicated with water and MeOH then filtrated. The product was purified by recrystallisation from DCM/MeOH, (1:1) to give the titled compound as a purple solid (0.120 g, 18 %). **M.P.** > 350 °C ¹H NMR (500 MHz, Chloroform-d) δ 8.89 (d, *J* = 4.5 Hz, 4H), 8.84 (d, *J* = 4.5 Hz, 12H), 8.21 (dd, *J* = 8.5, 1.6

Hz, 12H), 8.11 (d, $J = 8.5$ Hz, 4H), 7.80 – 7.69 (m, 18H), 7.28 (d, $J = 8.6$ Hz, 4H), 4.25 (t, $J = 6.5$ Hz, 4H), 2.03 – 1.95 (m, 4H), 1.65 -1.63 (m, 4H), 1.45 (s, 12H), -2.76 (s, 4H). ^{13}C -NMR (126 MHz, CDCl_3) δ 159.03, 142.24, 142.21, 135.63, 134.57, 134.33, 127.69, 126.68, 120.22, 120.07, 119.94, 112.75, 77.28, 77.03, 76.77, 68.36, 29.74, 29.60, 29.55, 26.29. MS (MALDI-TOF): $m/z = 1428.65$ [M^+]. UV-Vis, (DCM)/nm ($\log \epsilon$): 418, 515, 550, 591, 647.

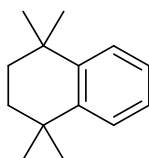
3.6 Synthesis of Substituted Phthalonitrile (68)

3.6.1 Synthesis of 2, 5-Dichloro-2, 5-dimethylhexane 72



Following a known procedure reported in R&D,^[2] a solution of 2,5-dimethylhexane-2,5-diol **71** (5.0 g, 34.24 mmol) in concentrated hydrochloric acid (50 mL) was stirred at 0 °C for 30 min. The mixture was left to warm to room temperature and stirred overnight. The light pink solid was filtered off and washed thoroughly with water. The solid was then dissolved in DCM, washed again by water and extracted with DCM (3 × 50 mL). The organic extracts were dried (MgSO_4) and the solvent removed under reduced pressure to afford the product as a white solid which was recrystallised from methanol to give title compound as colourless crystals (4.08 g, 66 %). ^1H NMR (400 MHz, CDCl_3) δ 1.96 (s, 4H), 1.60 (s, 12H).

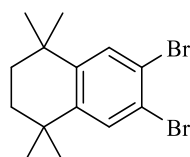
3.6.2 Synthesis of 1, 1, 4, 4-Tetramethyl-1, 2, 3, 4-tetrahydronaphthalene 73



Following Bruson's procedure via Friedel-Crafts reaction,^{[2],[3]} a solution of 2,5-dichloro-2,5-dimethylhexane **72** (2.25 g, 12.35 mmol) in benzene (50 mL, 0.56 mol) was stirred for 10 min at 30 °C. Anhydrous aluminum trichloride (1.7 g, 12.74 mmol) was added in small portions over 30 min. The thick suspension was then stirred at room temperature for 21 h

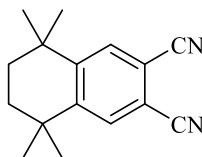
and finally refluxed for 2 h. The resulting material was cooled to room temperature, poured into dilute hydrochloric acid and extracted with petroleum ether (3×50 mL). The organic layer was washed with water, followed by dilute sodium carbonate solution, dried (Na_2SO_4), filtered and the solvent removed under reduced pressure. The resulting material was washed several times with methanol to remove the side-products. The solvent was removed under reduced pressure to give the product as yellow liquid (1.8 g, 78 %). ^1H NMR (400 MHz, CDCl_3) δ 7.36 (dd, $J = 5.9, 3.5$ Hz, 2H), 7.18 (dd, $J = 6.0, 3.4$ Hz, 2H), 1.75 (s, 4H), 1.34 (s, 12H).

3.6.3 Synthesis of 6, 7-dibromo-1,1,4,4-tetramethyl-1,2,3,4-tetrahydronaphthalene 74



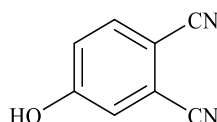
Bromination of **73** was achieved using the method described by Ashton and co-workers.^[4] 1,1,4,4-Tetramethyl-1,2,3,4-tetrahydronaphthalene **73** (1.8 g, 9.56 mmol) was dissolved in DCM (20 mL). Iron powder (61.2 mg, 1.09 mmol) and iodine (23.31 mg, 0.18 mmol) were added to the mixture and cooled to 0 °C. Bromine (0.53 mL, 1.59 g, 9.01 mmol) was added dropwise via syringe to the above mixture over 30 min. After complete addition, the reaction mixture was allowed to warm up to room temperature and stirred for 24 h. The resulting mixture was washed with an aqueous solution of sodium metabisulfite and sodium bicarbonate to remove the excess bromine. Water and brine were added, and the mixture extracted with DCM (3×50 mL). The organic extracts were dried over MgSO_4 , filtered and the solvent removed under reduced pressure to give a brownish solid. The product was purified by column chromatography over silica gel using PE/DCM (5:1) as eluents to give the title compound as a yellow solid (2.8 g, 84%). ^1H NMR (500 MHz, CDCl_3) δ 7.51 (s, 2H), 1.67 (s, 4H), 1.26 (s, 12H).

3.6.4 Synthesis of 6,7-Dicyano-1,1,4,4-tetramethyl-1,2,3,4-tetrahydronaphthalene 68



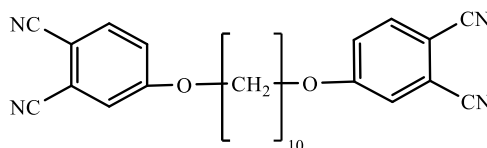
Following the procedure described by Rosenmund von Braun,^[5] a mixture of 6,7-dibromo-1,1,4,4-tetramethyl-1,2,3,4-tetrahydronaphthalene **74** (1.8 g, 5.18 mmol) and CuCN (1.97 g, 21.99 mmol) was refluxed in dry DMF (15 mL) under an argon atmosphere for 2 h. After cooling, Et₂O was added to the mixture and washed with H₂O (3 × 50 mL) and with an aqueous solution of ammonia until no blue colour was obtained in the aqueous layer, dried over MgSO₄ and filtered. The filtrate was evaporated under reduced pressure to give the crude product. The crude material was purified by column chromatography (silica: PE/ Et₂O, 7:1) to yield the product as a yellow solid (0.5 g, 40%). M.P. 205- 209 °C (lit. 206-208 °C).^[6] ¹H NMR (500 MHz, CDCl₃) δ 7.71 (s, 2H), 1.72 (s, 4H), 1.30 (s, 12H). ¹³C-NMR (126 MHz, CDCl₃) δ 151.80, 132.62, 116.05, 112.58, 35.13, 34.10, 31.45. FT-IR (NaCl), ν (cm⁻¹): 2229.9 (C≡N).

3.7 Synthesis of 4-hydroxyphthalonitrile 69



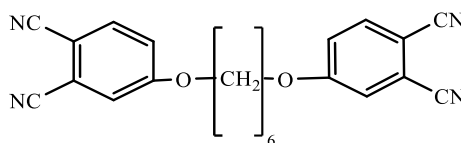
4-Nitrophthalonitrile **77** (2.0 g, 11.6 mmol) was dissolved in DMSO (30 mL). K₂CO₃ (1.8 g, 12.7 mmol) and NaNO₂ (0.8 g, 11.6 mmol) were added to this solution.^[7] The solution was heated to reflux for 30 minutes, then cooled to room temperature and water (45 mL) was added. The solution was acidified to pH3, and a yellow precipitate was formed. This was recovered by vacuum filtration and recrystallised from glacial acetic acid to yield the product as a yellow crystalline solid (0.5g, 30 %) ¹H NMR (500 MHz, Acetone-*d*₆) δ 7.88 (d, *J* = 8.5 Hz, 1H), 7.43 (d, *J* = 1.8 Hz, 1H), 7.33 (dd, *J* = 8.5, 1.8 Hz, 1H). FT-IR (NaCl), ν (cm⁻¹): 3255(OH), 2241 (C≡N).

3.8 Synthesis of bisphthalonitrile **89**^[8]



4-Nitrophthalonitrile **77** (4 g, 0.023 mol), 1,10-decanediol **87** (1 g, 0.005 mol) and potassium carbonate (8 g, 0.057 mol) were added to dry DMF (20 mL), and the mixture stirred at room temperature for 7 days. The solvent was removed, and the residue was redissolved in ethyl acetate and extracted with water. This procedure was repeated three times. The combined organic extracts were dried (MgSO_4), and the solvent removed in vacuo. The product was purified by silica gel column chromatography (DCM/Hexane, 1:1) to give the title compound as a yellow solid (1 g, 41 %). ^1H NMR (400 MHz, $\text{DMSO}-d_6$) δ 8.02 (d, $J = 8.8$ Hz, 1H), 7.74 (d, $J = 2.6$ Hz, 1H), 7.43 (dd, $J = 8.8, 2.6$ Hz, 1H), 4.12 (t, $J = 6.5$ Hz, 2H), 1.76 – 1.64 (m, 1H), 1.43 – 1.24 (m, 3H). ^{13}C NMR (126 MHz, $\text{DMSO}-d_6$) δ 162.51, 135.40, 120.69, 120.45, 116.73, 116.15, 106.18, 69.50, 29.33, 29.07, 28.65, 25.72.

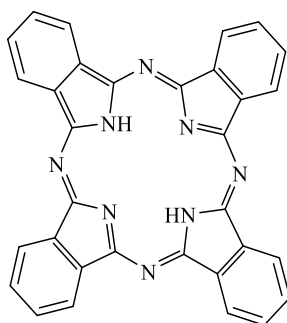
3.9 Synthesis of bisphthalonitrile **90**^[8]



4-Nitrophthalonitrile **77** (4 g, 0.023 mol), 1,6-hexanediol **88** (0.679 g, 0.0057 mol) and potassium carbonate (8 g, 0.057 mol) were added to dry DMF (20 mL) and the mixture stirred at room temperature for 7 days. The solvent was removed, and the residue was redissolved in ethyl acetate. This was washed with water and the washings extracted with ethyl acetate three times. The combined organic extracts were dried (MgSO_4) and the solvent removed in vacuo. The product was purified by silica gel column chromatography (DCM/Hexane, 1:1) to give the titled compound as a yellow solid (0.9g, 42 %). ^1H NMR (400 MHz, $\text{DMSO}-d_6$) δ 8.02 (d, $J = 8.8$ Hz, 1H), 7.74 (d, $J = 2.6$ Hz, 1H), 7.43 (dd, $J = 8.8, 2.6$ Hz, 1H), 4.14 (t, $J = 6.5$ Hz, 2H), 1.75 (t, $J = 6.6$ Hz, 1H), 1.46 (p, $J = 3.5$ Hz, 2H). ^{13}C NMR (126 MHz, $\text{DMSO}-d_6$) δ 162.49, 136.21, 120.70, 120.48, 116.74, 116.71, 116.21,

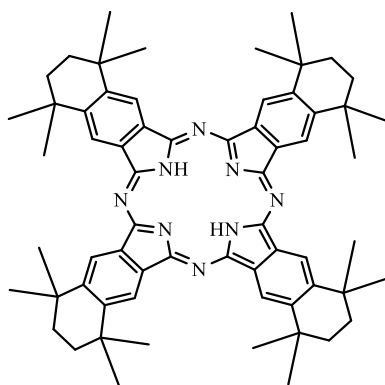
106.21, 69.41, 40.47, 40.39, 40.30, 40.22, 40.13, 40.05, 39.97, 39.80, 39.63, 39.47, 28.56, 25.38.

3.10 Synthesis Metal free phthalocyanine **13**^[9]



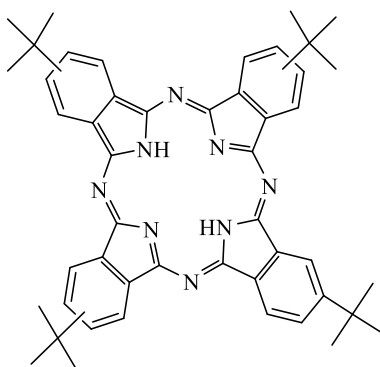
Following a general procedure using lithium as a template, a solution of phthalonitrile **19** (0.5 g, 3.9 mmol) in 1-pentanol (12 mL) was heated to reflux for 1h. Lithium (50 mg, 7.2 mmol) was washed by MeOH and added to the reaction mixture and reflux continued for another 1 h. Acetic acid was added (10 mL) and was further refluxed for 1h. The reaction mixture was cooled down to room temperature, methanol (100 mL) was added to precipitate the product and the dark blue solid of the pure phthalocyanine collected by vacuum filtration (260 mg, 52 %). MS (MALDI-tof): $m/z = 514.41$ [M+]. UV-Vis, (THF)/nm (log ϵ): 690 (0.60), 654 (0.65), 377 (0.59); Due to high insolubility in organic solvents further characterisation was not possible.

3.11 Synthesis of Metal-free phthalocyanine **79**



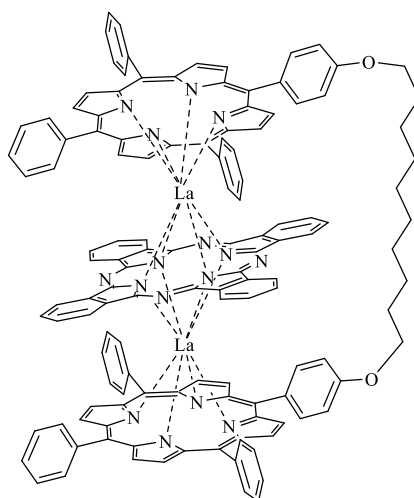
Phthalonitrile **68** (0.5 g, 2.09 mmol) was dissolved in 1-pentanol (6 mL) and heated to reflux. Lithium (50 mg, 7.2 mmol) was added to the reaction mixture and was refluxed for 1 h. Acetic acid (10 mL) was added and the mixture was further refluxed for 1 h. The resulting reaction mixture was cooled down to room temperature and methanol (100 mL) was added to precipitate the product. A dark green solid of pure phthalocyanine was collected by vacuum filtration (300 mg, 60 %). $^1\text{H NMR}$ (400 MHz, Chloroform- d) δ 7.71 (s, 8H), 1.72 (s, 16H), 1.30 (s, 48H). MS (MALDI-TOF): $m/z = 953$ [M^+]. UV-Vis, (DCM)/nm (log ϵ): 285(1.5), 399 (1.7), 660(2.2), 695(2.3).

3.12 Synthesis of tetra-tert-butyl-phthalocyanine **85**:



4-(tert-Butyl) phthalonitrile **88** (0.5 g, 2.7 mmol) was dissolved in 1-pentanol (6 mL) and heated to reflux. Lithium (50 mg, 7.2 mmol) was added to the reaction mixture and was refluxed for 1 h. Acetic acid (10 mL) was added and refluxed for 1 h. The resulting reaction mixture was cooled down to room temperature and methanol (100 ml) was added to precipitate the product, a blue solid of pure phthalocyanine was collected by vacuum filtration (300 mg, 60 %). MS (MALDI-tof): $m/z = 739$ [M^+]; UV-Vis, (DCM)/nm: 287(1.2), 341(1.5), 662(2.13), 698(2.3).

3.13 Closed triple decker **59**

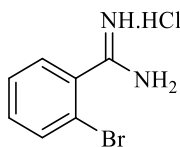


C₁₀ porphyrin dyad **58** (200 mg, 0.143 mmol) was mixed with lanthanum (III) acetylacetonate hydrate (125 mg, 0.286 mmol) in a 25 ml round bottom flask and 15 ml of octanol was added. The mixture was refluxed under Ar atmosphere for 6 h. Metal-free phthalocyanine **13** (88.17 mg, 0.171 mmol) was added and the mixture left to reflux overnight. The solvent was removed by distillation under reduced pressure and the crude recrystallised from DCM: MeOH. The resulting solids were then separated by column chromatography through silica gel using DCM/Hexane (3:2 v/v) as eluent and the first brown fraction containing the title product was collected as dark brown solid (150 mg, 48 %).

As an alternative method, in sealed tube C₁₀ porphyrin dyad **58** (20 mg, 0.0143 mmol) (1 eq), La (acac)₃.H₂O (13.7 mg, 0.03146 mmol) (2.2 eq) and metal-free phthalocyanine **13** (8.09 mg, 0.01573 mmol) (1.1 eq) were dissolved in 1-pentanol (3 mL). The mixture was heated at 150 °C for 2 h. The solvent was distilled off under reduced pressure and the resulting crude was chromatographed on a silica gel column using DCM/Hexane (5:2 v/v) mixture as eluent. The dark brown solid was obtained (3.17 mg, 10 %). MS (MALDI-TOF): *m/z* = 2187.22 ¹H NMR (500 MHz, Chloroform-*d*) δ 10.08 (d, *J* = 8.1 Hz, 2H), 9.99 (t, *J* = 7.1 Hz, 6H), 9.36 (dd, *J* = 5.3, 2.9 Hz, 8H), 8.48 – 8.40 (m, 6H), 8.32 – 8.27 (m, 8H), 7.98 (d, *J* = 6.5 Hz, 2H), 7.81 (m, 6H), 7.31 (d, *J* = 4.2 Hz, 4H), 7.27 – 7.20 (m, 18H), 6.87 (d, *J* = 7.8 Hz, 2H), 6.73 (d, *J* = 7.8 Hz, 2H), 6.65 (t, *J* = 6.4 Hz, 6H), 4.59 (t, *J* = 7.2 Hz, 4H), 2.31 – 2.25 (m, 4H), 1.92 (s, 8H), 1.81 (s, 4H). ¹³C NMR (126 MHz, CDCl₃) δ 158.60, 153.56, 148.09, 147.79, 143.00, 136.60, 133.43, 133.29, 130.06, 128.43, 128.32, 127.11,

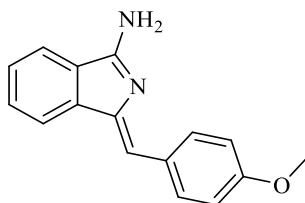
126.77, 125.82, 125.47, 123.46, 120.49, 120.08, 119.98, 29.48, 29.25, 28.61, 26.62, 16.80.
UV-Vis, (DCM)/nm: 360(4.8), 419(5.2), 485(2.7), 550(2.5), 605(2.6)

3.14 Synthesis of 2-bromobenzamidine hydrochloride **46**



Following the method reported in literature,^[10] a solution of 2-bromo-benzonitrile **45** (4.5 g, 24.72 mmol) in anhydrous THF (7 mL) was added to a solution of 1 M LiN(SiMe₃)₂ in anhydrous THF (25 mL, 25 mmol) and the reaction mixture was stirred at room temperature for 4 h. A solution of 5 N HCl in isopropanol (15 mL) was added to the reaction mixture dropwise at 0 °C. The reaction mixture was left to stir at room temperature overnight. The precipitate was filtered off then washed with Et₂O to afford 2-bromobenzamidine hydrochloride (4.1g, 71%) as colourless crystals. ¹H NMR (500 MHz, DMSO-*d*₆) δ 7.84 – 7.79 (m, 1H), 7.63 – 7.53 (m, 3H).

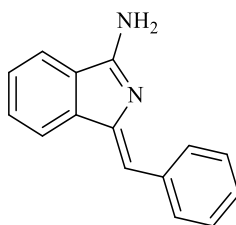
3.15 Synthesis of (Z)-1-(4-Methoxybenzylidene)-1H-indol-3-amine **48**^[11]



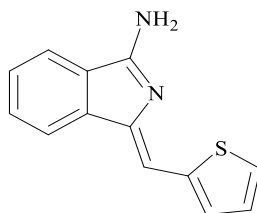
2-Bromobenzamidine hydrochloride **46** (1 g, 4.24 mmol), BINAP (0.13 g, 0.2 mmol), PdCl₂(MeCN)₂ (0.06 g, 0.2 mmol) and DMF (12 mL) were added in a sealed microwave (MW) vial. The reaction mixture was purged with argon for 5 mins then DBU (1.62g, 10.6 mmol) and 4-ethynylanisole **47** (0.67 mL, 5 mmol) were added. The resultant mixture was heated to 120 °C for 1 h by microwave irradiation. The reaction mixture was allowed to cool to room temperature. After cooling, ethyl acetate (50 ml) was added, and the mixture washed with a saturated solution of NaHCO₃ (3 × 50 mL). The organic layer was dried with MgSO₄, filtered and concentrated. The crude product was dry loaded onto silica gel and purified by normal phase chromatography using PE: EtOAc (1:1), then the solvent was changed to EtOAc, and the title compound separated out as a yellow semisolid fraction and was

recrystallized from DCM:PE (1:1) to yield the product as yellow needles (0.5 g, 47 %). **M.P.** 155 °C (lit. 156- 157 °C)^[12] ¹H-NMR (500 MHz, Chloroform) δ 7.83 (d, J = 8.6 Hz, 1H), 7.80 (d, J = 9.0 Hz, 2H), 7.76 (d, J = 7.8 Hz, 1H), 7.56 (td, J = 7.6, 1.0 Hz, 1H), 7.42 (td, J = 7.5, 0.9 Hz, 1H), 6.95 (d, J = 8.8 Hz, 2H), 6.73 (s, 1H), 3.84 (s, 3H). ¹³C-NMR (126 MHz, CDCl₃) δ 163.56, 159.77, 140.15, 136.92, 131.68, 131.48, 127.98, 127.49, 127.28, 121.64, 119.80, 114.36, 114.19, 55.34. MS (MALDI-TOF): m/z 250.1 = [M]⁺. UV-Vis (DCM) (nm): 393 (0.44), 347 (0.058).

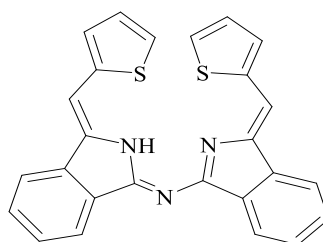
3.16 Synthesis of (Z)-1-(phenylmethylene)-1H-isoindol-3-amine **101**^[11]



A mixture of 2-bromobenzamidine hydrochloride **46** (1 g, 4.24 mmol), BINAP (0.13 g, 0.2 mmol), PdCl₂(MeCN)₂ (0.06 g, 0.2 mmol) and DMF (12 mL) were sealed in a MW vial. The reaction mixture was purged with argon for 5 mins then DBU (1.62 g, 10.6 mmol) and phenylacetylene (0.51 mL, 5 mmol) was added. The resulting mixture was heated to 120 °C for 1 hour by microwave irradiation. The reaction mixture was allowed to cool to room temperature. After cooling, ethyl acetate (50 mL) was added, and the mixture washed with a saturated solution of NaHCO₃ (3 × 50 mL). The organic layer was dried with MgSO₄, filtered and concentrated. The crude product was dry loaded onto silica gel and purified by normal phase chromatography using PE: EtOAc (1:1) then the solvent was changed to EtOAc, and the title compound separated out as a yellow semisolid fraction that was recrystallized from DCM:PE (1:1) to yield the product as yellow needles (0.60 g, 64 %). ¹H-NMR (500 MHz, Chloroform-d) δ 8.01 (d, J = 8.3 Hz, 2H), 7.71 (d, J = 8.6 Hz, 1H), 7.41 – 7.26 (m, 5H), 7.20 – 7.15 (m, 1H), 6.68 (s, 1H). ¹³C-NMR (126 MHz, CDCl₃) δ 165.35, 147.40, 142.96, 136.75, 131.10, 130.48, 129.21, 128.45, 127.27, 127.22, 119.79, 118.91, 115.02. MS (MALDI-TOF): 220 m/z = [M]⁺ UV-Vis (DCM) (nm): 400 (0.54), 379 (0.06).

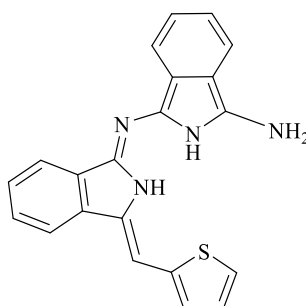
3.17 Synthesis of (Z)-1-(4-thiophenylidene)-1H-isoindol-3-amine 107^[11]

A mixture of 2-bromobenzamidinium hydrochloride **46** (1g, 4.3 mmol), BINAP (0.13g, 0.2 mmol) and PdCl₂(MeCN)₂ (0.06g, 0.2 mmol) and DMF (12 mL) were sealed in a MW vial. The reaction mixture was purged with argon for 5 mins then DBU (1.62g, 10.6 mmol) and 2-[2-(trimethylsilyl)ethynyl]-thiophene **106** (1 g, 5.55 mmol) were added. The resulting mixture was heated to 120 °C for 1 h by microwave irradiation. The mixture was allowed to cool to room temperature. After cooling, ethyl acetate (50 mL) was added, and the mixture washed with a saturated solution of NaHCO₃ (3 × 75 mL). The organic layer was dried with MgSO₄, filtered and concentrated. The crude product was dry loaded onto silica gel and purified by normal phase chromatography using PE: EtOAc (1:1) then the solvent was changed to EtOAc, and the title compound separated out as a yellow semisolid fraction that was recrystallized from DCM:PE (1:1) to yield the product as yellow needles (0.59 g, 62 %). M.P. 132.5-135°C. ¹H NMR (500 MHz, Chloroform-*d*) δ 7.73 (d, *J* = 8.5 Hz, 1H), 7.51 (d, *J* = 7.6 Hz, 1H), 7.46 (td, *J* = 7.5, 1.0 Hz, 1H), 7.38 (d, *J* = 5.1 Hz, 1H), 7.37 – 7.33 (m, 3H), 7.05 (dd, *J* = 5.1, 3.6 Hz, 1H), 7.02 (s, 1H). ¹³C NMR (126 MHz, CDCl₃) δ 164.39, 145.51, 142.32, 139.96, 131.72, 129.64, 129.38, 129.14, 127.41, 127.31, 120.02, 119.64, 110.06. MS (MALDI-TOF): *m/z* = 226 [M]⁺. UV-Vis, (DCM)/nm (log ε): 404 (0.44), 381 (0.058).

3.18 Synthesis of Aza-dipyrromethene (self-condensation dimer) 108^[13]

A solution of aminoisoindoline **107** (100 mg, 0.38 mmol) in toluene (2 mL) was heated at 120 °C for 2h under a N₂ atmosphere. The solvent was allowed to slowly evaporate during the process. After cooling, the residue was purified by column chromatography using DCM, then DCM/MeOH (50:1) as the eluent to afford a red compound that was recrystallized from DCM and washed with MeOH to yield the product as red crystals, (80 mg, 42%). M.P. 183-185°C. ¹H NMR (500 MHz, Acetone-*d*₆) δ 8.05 (d, *J* = 7.5 Hz, 2H), 8.01 (d, *J* = 7.5 Hz, 2H), 7.63 (td, *J* = 7.5, 1.2 Hz, 2H), 7.58 – 7.54 (m, 4H), 7.40 (dd, *J* = 5.1, 1.1 Hz, 2H), 7.30 (s, 2H), 7.04 (dd, *J* = 5.1, 3.6 Hz, 2H). ¹³C NMR (126 MHz, Acetone-*d*₆) δ 205.23, 140.51, 139.10, 138.71, 135.04, 130.42, 129.41, 129.05, 128.29, 127.99, 122.11, 119.77, 108.17. MS (MALDI-TOF): *m/z* = 436 [M]⁺ UV-Vis, (DCM)/nm (log ε): 364(1.05), 512(0.17).

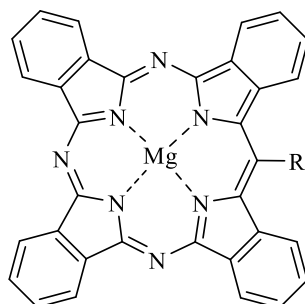
3.19 Synthesis of (Z)-1-(((Z)-1-(4-thiophenylidene))-1H-isoindol-3-yl) imino)-1H-isoindol-3-amine **109**



Aminoisoindoline **107** (0.26 g, 1.15 mmol), phthalonitrile **13** (0.22 g, 1.72 mmol) and NaOMe (0.09 g, 1.72mmol) were dissolved in MeOH (15 mL). The reaction mixture was heated at 60 °C overnight. The mixture was allowed to cool to room temperature. After cooling, the formed precipitate was filtered off and washed with a cold MeOH to give the title compound as an orange solid (0.211 g, 53%). M.P. 218-220°C. ¹H NMR (500 MHz, Chloroform-*d*) δ 8.10 (d, *J* = 7.5 Hz, 1H), 7.92 (d, *J* = 7.5 Hz, 1H), 7.88 (d, *J* = 7.5 Hz, 1H), 7.74 (d, *J* = 7.5 Hz, 1H), 7.70 (td, *J* = 7.5, 1.2 Hz, 1H), 7.64 (td, *J* = 7.5, 1.1 Hz, 1H), 7.61 (d, *J* = 5.1 Hz, 1H), 7.46 (s, 1H), 7.44 – 7.37 (m, 2H), 7.33 (d, *J* = 3.6 Hz, 1H), 7.06 (dd, *J* = 5.1, 3.7 Hz, 1H). ¹³C NMR (126 MHz, Chloroform-*d*) δ 169.30, 168.80, 157.01, 145.39, 140.83, 139.53, 137.59, 137.12, 134.03, 133.28, 133.26, 132.91, 131.22, 129.64, 128.10,

127.61, 124.38, 123.58, 122.19, 119.72, 119.62, 77.67, 77.41, 77.16. MS (MALDI-TOF): $m/z = 354 [M]^+$. UV-Vis, (DCM)/nm ($\log\epsilon$): 481(0.60), 450(0.62), 325(0.91), 273(1.015).

3.20 Synthesis of MgTBTAPs^{[13], [12]}:



General procedure A

A suspension of phthalonitrile (3 equivalents) and $MgBr_2$ (1.5 equivalents) in dry diglyme (0.5 mL) was stirred at 220 °C for 10 min under a nitrogen atmosphere. A solution of aminoisoindoline (1 equivalent) and phthalonitrile (1 equivalent) in dry diglyme (1 mL) was added dropwise over 1 hour using a syringe pump. Finally, a third solution of DABCO (1.5 equivalents) and phthalonitrile (1 equivalent) in dry diglyme (0.5 mL) was added dropwise over an hour. The reaction mixture was heated further at 220 °C for 0.5 hours under a nitrogen atmosphere.

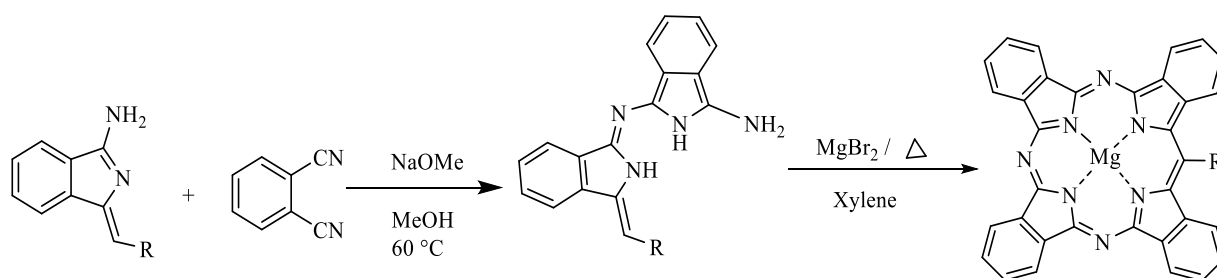
Then, the solvent was removed under a stream of nitrogen and a 1:1 mixture of DCM: MeOH (20 ml) was added, and the mixture was sonicated. The solvent was concentrated in vacuum and the resulting compound was purified by two consecutive chromatography columns. First, using DCM: Et_3N (20:1), then solvent system changes to DCM: THF: Et_3N (10:1:3). The second column using PE: THF: MeOH (10:3:1) as eluent. A dark green fraction containing the desired compound was collected.

General procedure B

A suspension of phthalonitrile (3 equivalents), aminoisoindoline (1 equivalent) and $MgBr_2$ (1.5 equivalents) in dry diglyme (3 mL) was stirred at 220 °C for 6 h under a nitrogen atmosphere.

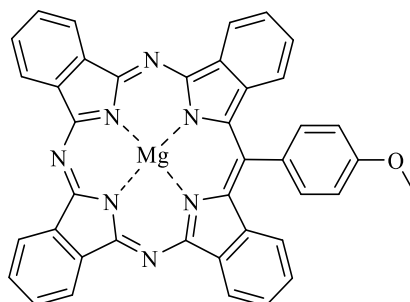
Then, the solvent was removed under a stream of nitrogen and a 1:1 mixture of DCM: MeOH (20 ml) was added, and the mixture sonicated. The solvent was removed under vacuum and the resulting compound was purified by two consecutive chromatography columns. First, using DCM: Et₃N (20:1), then solvent system changes to DCM: THF: Et₃N (10:1:3). The second column using PE: THF: MeOH (10:3:1) as eluent. A dark green fraction containing the desired compound was collected.

General procedure C



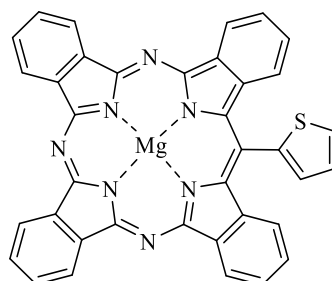
To a mixture of, phthalonitrile (1 equivalent), aminoisindoline (1 equivalent)) and NaOMe (1.5 equivalent) was added MeOH (15 mL) The reaction mixture was heated at 60 °C overnight. The reaction mixture was allowed to cool to room temperature and After cooling, the precipitate was filtered off and washed with a cold MeOH to give orange compound as it is a dimer from phthalonitrile and aminoisindoline, then reacted this compound with MgBr₂ (1.5 equivalents) in xylene for 9 h under a nitrogen atmosphere. Then, the solvent was removed and a 1:1 mixture of DCM: MeOH (20 ml) was added, and the mixture sonicated. The solvent was removed under vacuum and the resulting compound was purified by chromatography column using DCM: Et₃N (20:1), then solvent system changes to PE: THF: MeOH (10:3:1). A dark green fraction containing the desired compound was collected.

3.20.1 Synthesis of MgTBTAP-(4-OMe-Ph) 50



Prepared using procedure A using of phthalonitrile **19** (154 mg, 1.2 mmol) and MgBr_2 (110 mg, 0.6 mmol) in dry diglyme (0.5 mL) was stirred at 220 °C of for 10 min under an argon atmosphere. A solution of aminoisoindoline **48** (100 mg, 0.4 mmol, 1eq) and phthalonitrile (51 mg, 0.4 mmol, 1eq) in dry diglyme (1 mL) was added dropwise over 1 hour using a syringe pump. Finally, a third solution of DABCO (67.5 mg, 0.6 mmol, 1.5eq) and phthalonitrile (51 mg, 0.4 mmol, 1eq) in dry diglyme (0.5 ml) to give MgTBTAP-(4-OMe-Ph) (60 mg, 24 %). $^1\text{H-NMR}$ (500 MHz, THF-d_8) δ 9.60 (d, $J = 7.3$ Hz, 2H), 9.53-9.50 (m, 4H), 8.22 – 8.13 (m, 4H), 8.05 (d, $J = 8.5$ Hz), 7.92 (t, $J = 7.2$ Hz, 2H), 7.62 (t, $J = 7.4$, 2H), 7.52 (d, $J = 8.5$ Hz, 2H), 7.25 (d, $J = 8.3$ Hz, 2H), 4.20 (s, 3H, OCH_3). $^{13}\text{C-NMR}$ (126 MHz, THF-d_8) δ 162.01, 156.56, 153.51, 152.60, 143.53, 141.32, 141.21, 140.99, 140.24, 135.98, 134.16, 130.08, 129.79, 128.24, 127.39, 126.76, 125.89, 123.91, 123.70, 123.63, 115.30, 56.14. MS (MALDI-TOF): $m/z = 641.72$ $[\text{M}]^+$. UV-Vis, (THF)/nm ($\log \epsilon$) = 398(0.34), 449(0.10), 594(0.16), 648(0.7), 670(0.95).

3.20.2 Synthesis of MgTBTAP-(thiophenyl) 104

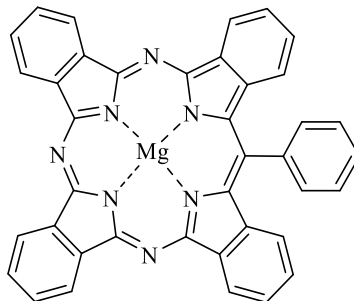


Prepared using procedure A using of phthalonitrile **19** (170 mg, 1.3 mmol) and MgBr_2 (122 mg, 0.66 mmol) in dry diglyme (0.5 mL) was stirred at 220 °C of for 10 min under an

argon atmosphere. A solution of aminoisoindoline **107** (100 mg, 0.44 mmol, 1eq) and phthalonitrile (51 mg, 0.4 mmol, 1eq) in dry diglyme (1 mL) was added dropwise over 1 hour using a syringe pump. Finally, a third solution of DABCO (67.5 mg, 0.6 mmol, 1.5eq) and phthalonitrile (51 mg, 0.4 mmol, 1eq) in dry diglyme (0.5 ml) to give MgTBTAP-(thiophenyl) (150 mg, 55 %).

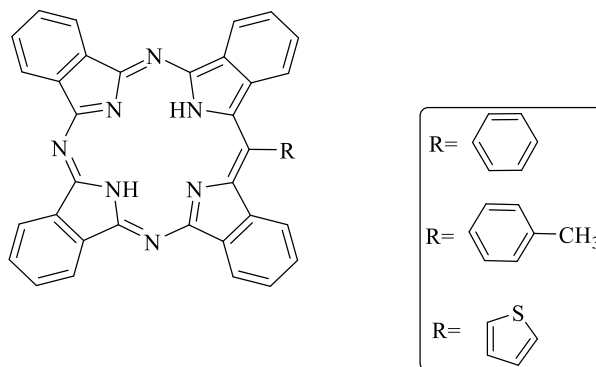
Prepared using procedure C A solution of compound **109** (200 mg, 0.56 mmol, 2 eq.) and MgBr₂ (78 mg, 0.42 mmol, 1.5 eq.) xylene for 9 hs under a nitrogen atmosphere, to give MgTBTAP-(thiophenyl) (50 mg, 29 %). M.P. 188-190 °C. ¹H NMR (500 MHz, THF-*d*₈) δ 9.65 (dt, *J* = 8.1, 1.0 Hz, 2H), 9.58 – 9.54 (m, 4H), 8.25 – 8.20 (m, 5H), 8.02 – 7.99 (m, 2H), 7.93 (dd, *J* = 3.3, 1.2 Hz, 1H), 7.79 (dd, *J* = 5.5, 3.3 Hz, 1H), 7.74 (ddd, *J* = 8.1, 8.1, 1.2 Hz, 2H), 7.41 (d, *J* = 8.0 Hz, 2H). ¹³C NMR (126 MHz, THF-*d*₈) δ 140.01, 139.83, 139.70, 139.08, 137.15, 128.75, 127.81, 127.41, 126.60, 124.92, 124.50, 122.77, 122.59, 122.55, 115.92. MS (MALDI-TOF): *m/z* = 621.01 [M]⁺. UV-Vis, (THF)/nm (log ε) = 393(0.36), 403(0.10), 595(0.16), 651(0.68), 670(0.94).

3.20.3 Synthesis of MgTBTAP-(phenyl) **102**



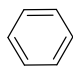
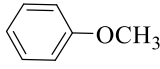
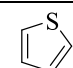
Prepared using procedure B A mixture of phthalonitrile **19** (174.5 mg, 1.36 mmol), aminoisoindoline **101** (100 mg, 0.454mmol) and MgBr₂ (125 mg, 0.68 mmol) in dry diglyme (6 mL) was stirred at 220 °C for 6 h under a nitrogen atmosphere. to give MgTBTAP-(phenyl) (70 mg, 25%). ¹H NMR (500 MHz, THF-*d*₈): δ = 9.59 (d, *J* = 7.5 Hz, 2H), 9.55 – 9.48 (m, 4H), 8.21 – 8.14 (m, 6H), 8.06 (t, *J* = 7.7 Hz, 1H), 7.96 (t, *J* = 7.6 Hz, 2H), 7.91 (t, *J* = 7.5 Hz, 2H), 7.56 (t, *J* = 8.0 Hz, 2H), 7.10 (d, *J* = 8.1 Hz, 2H). ¹³C NMR (126 MHz, THF-*d*₈) δ 155.58, 152.91, 141.81, 139.86, 139.10, 132.16, 128.97, 128.18, 127.02, 126.24, 124.57, 122.77, 122.51, 66.25, 66.07, 49.76, 24.18, 24.02. MS (MALDI-TOF): *m/z* = 613.17 [M]⁺. UV-Vis, (THF)/nm (log ε) = 393 (0.36), 449 (0.10), 590 (0.16), 651(0.7), 669 (0.95).

3.21 Synthesis of Mg-free TBTAPs^[14]:



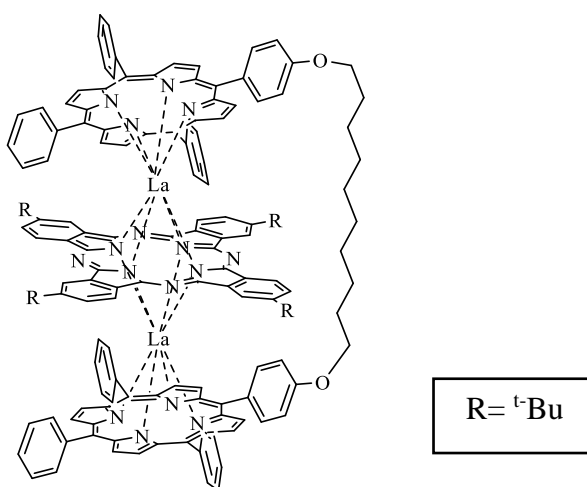
General procedure

The demetallation was performed on a 100 mg scale. The metalated compound was dissolved in concentrated sulphuric acid (10 mL). The solution turned to brown colour, then sonicated in ultrasonic bath for 2 min and poured into ice. A green precipitate formed immediately. The precipitate was filtered off and washed with MeOH to give the title compound as green solid.

Compound	MS (MALDI-TOF): m/z	Yield
R= 	=587.14 [M] ⁺	(81 mg, 84 %)
R= 	= 619.21 [M] ⁺	(45 mg, 47 %)
R= 	= 595.69 [M] ⁺	(70 mg, 74 %)

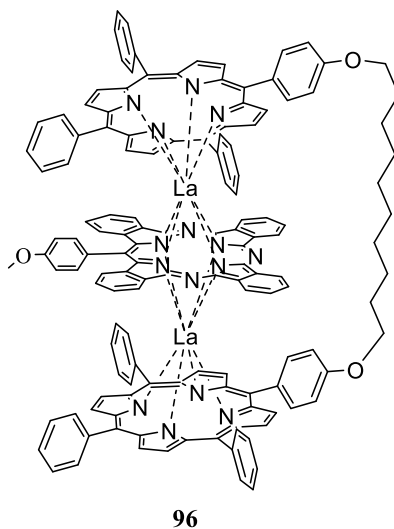
3.22 Closed triple deckers

3.22.1 Closed triple decker **86**

**86**

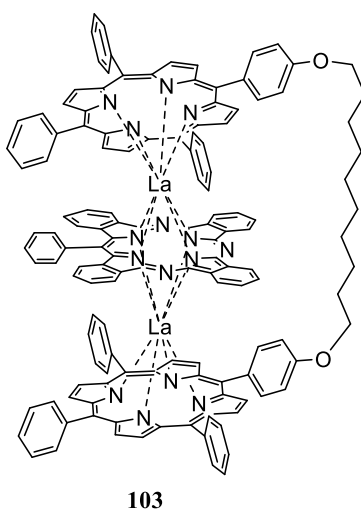
Following a modified version of Cammidge methodology^[15], a mixture of dyad **58** (100 mg, 0.071 mmol) was mixed with lanthanum (III) acetylacetonate hydrate (62 mg, 0.142 mmol) and metal-free phthalocyanine **85** (53 mg, 0.071 mmol) in a 25 mL round bottom flask and dissolved in 10 mL of octanol. The mixture was left to reflux overnight under inert atmosphere. The solvent was removed by distillation under reduced pressure. The resulting solids were then separated by column chromatography through silica gel using DCM/Hexane (3:2 v/v) as eluent and the second fraction containing the title product was collected as dark brown solid (100 mg, 58 %). MS (MALDI-TOF): $m/z = 2417$. ¹H NMR was complicated because of a mixture of four regioisomers,^[16] which arise due to the tert-butyl substituent on the β -position.

3.22.2 Closed triple decker formulated as 96



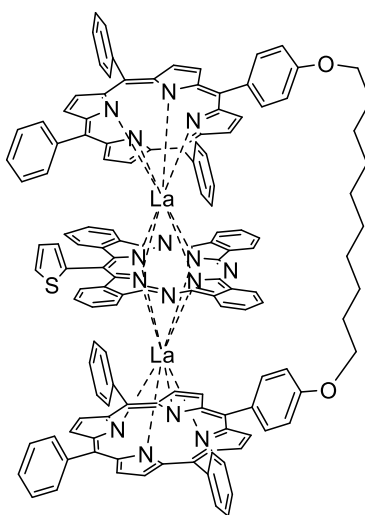
Following a modified version of Cambridge methodology^[15], C₁₀ porphyrin dyad **58** (160 mg, 0.114 mmol), lanthanum(III) acetylacetonate hydrate (100 mg, 0.228 mmol) and Mg-free TBTAP-(4-OMe-Ph) (71 mg, 0.114 mmol) were refluxed in 10 ml of octanol for 24h at 200 °C under Ar. Solvent was removed and the residual separated by column chromatography using DCM/hexane (3:2) and the second fraction as green solid was collected (50 mg, 19 %). MS (MALDI-TOF): m/z = 2287. ¹H NMR was complicated as mentioned in R&D.

3.22.3 Closed triple decker formulated as 103



C₁₀ porphyrin dyad **58** (100 mg, 0.0714 mmol) was mixed with lanthanum (III) acetylacetonate hydrate (62 mg, 0.142 mmol) and Mg-free TBTAP-(phenyl) (42 mg, 0.071 mmol) in a 25 mL round bottom flask and dissolved in 10 mL of octanol. The mixture was left to reflux overnight under inert atmosphere. The solvent was removed by distillation under reduced pressure. The resulting solids were then separated by column chromatography through silica gel using DCM/Hexane (3:2 v/v) as eluent and the second fraction as green solid was collected (25 mg, 16 %). MS (MALDI-TOF): $m/z = 2256$. ¹H NMR was complicated as mentioned in R&D.

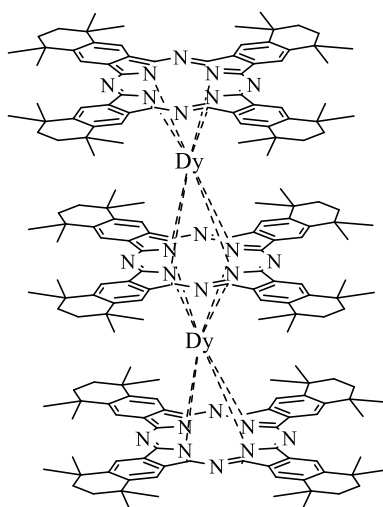
3.22.4 Closed triple decker formulated as 111



111

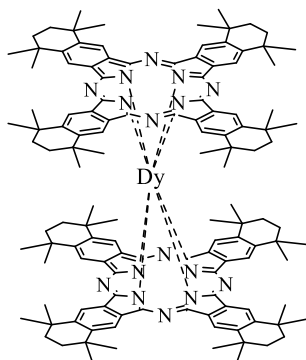
C₁₀ porphyrin dyad **58** (240 mg, 0.172 mmol) was mixed with lanthanum (III) acetylacetonate hydrate (150 mg, 0.343 mmol) and Mg-free TBTAP-(thiophenyl) (102.7 mg, 0.172 mmol) in a 25 mL round bottom flask and dissolved in 15 mL of octanol. The mixture was left to reflux overnight under inert atmosphere. The solvent was removed by distillation under reduced pressure. The resulting solids were then separated by column chromatography through silica gel using DCM/Hexane (3:2 v/v) and the second fraction as dark green solid was collected (100 mg, 26 %). MS (MALDI-TOF): $m/z = 2264$. ¹H NMR was complicated as mentioned in R&D.

3.23 Synthesis of homoleptic triple decker **83** from symmetrical Pc **79**.



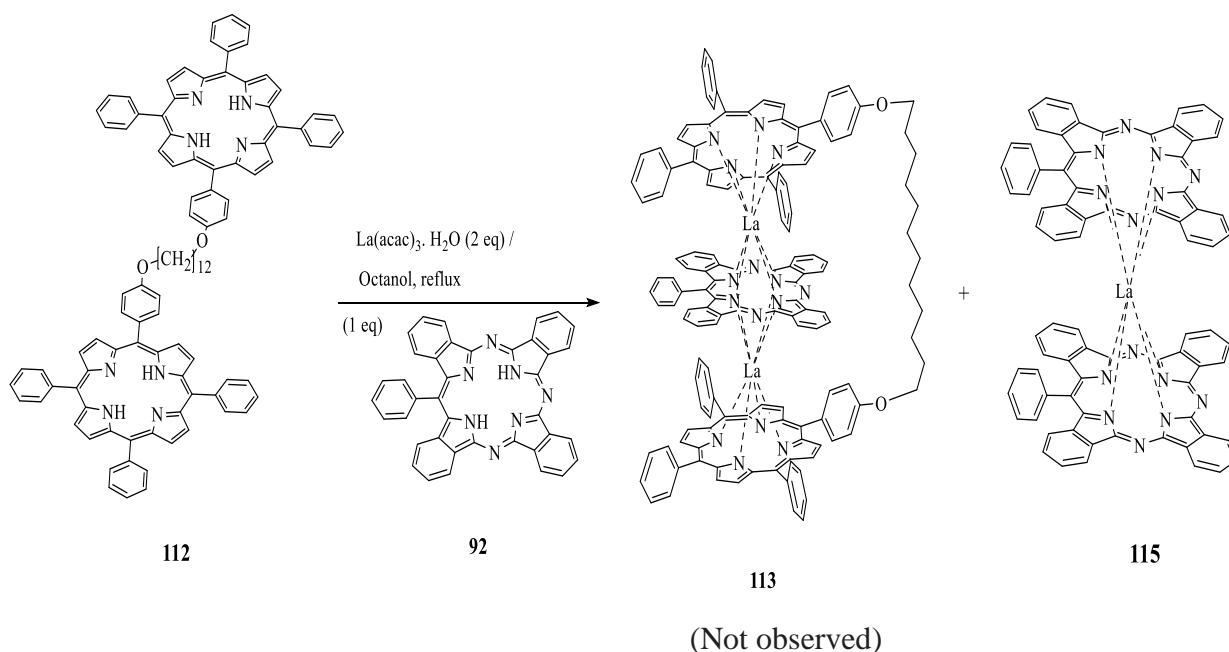
Symmetrical phthalocyanine **79** (100 mg, 0.105 mmol) and dysprosium (III) acetylacetonate hydrate (32.2 mg, 0.070 mmol) were added to octanol (10 mL) and the mixture was left to reflux overnight under inert atmosphere. The solvent was removed under high vacuum and the residual was separated by column chromatography DCM/ Petroleum ether (1:1) then DCM. A title compound was isolated in second fraction as blue crystals (50 mg, 45%); ^1H NMR & ^{13}C NMR are not achieved due to low solubility of the compound; MS (MALDI-TOF): $m/z = 3185.03$ $[\text{M}]^+$.

3.24 Synthesis of homoleptic double decker **82** from symmetrical Pc **79**.

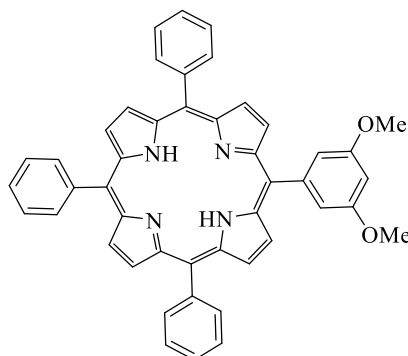


This compound was isolated from the previous reaction as side product and was obtained as a green solid (15 mg, 21 %); ^1H NMR & ^{13}C NMR are not achieved due to low solubility of the compound; MS (MALDI-TOF): $m/z = 2074.86$ $[\text{M}]^+$

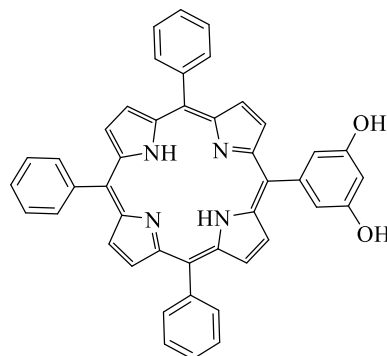
3.25 Synthesis of lanthanum *meso*-phenyltetrabenzotriazaporophyrin double decker **115** [17], [18]



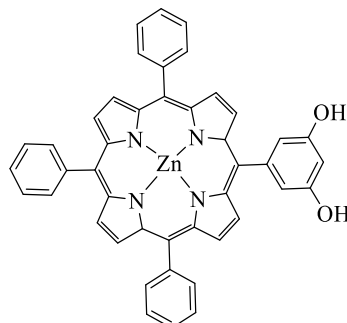
The DD **115** was isolated from the attempt to synthesise triple decker **113**. C₁₂ porphyrin dyad **112** (40 mg, 0.0280 mmol, 1 eq), La(acac)₃·H₂O (26.8 mg, 0.061 mmol, 2.2 eq) and metal-free TBTAP **92** (17 mg, 0.0280 mmol, 1 eq) were dissolved in octanol (5 mL). The mixture was left to reflux overnight under inert atmosphere. The solvent was distilled off under reduced pressure and the resulting crude was chromatographed on a silica gel column using DCM/Hexane (3:2 v/v). The DD **115** was obtained as a green solid (10 mg, 27.7 %). M.p. 148-150 °C. ^1H NMR (500 MHz, DCM-*d*₂) δ 9.00 (d, $J = 7.7$ Hz, 4H), 8.95 – 8.90 (m, 4H), 8.87 (d, $J = 7.4$ Hz, 4H), 8.24 (d, $J = 7.7$ Hz, 8H), 7.88 (t, $J = 7.0$ Hz, 4H), 7.80 (t, $J = 8.0$ Hz, 3H), 7.67 (t, $J = 7.7$ Hz, 3H), 7.58 (t, $J = 7.2$ Hz, 5H), 7.39 (t, $J = 7.3$ Hz, 3H), 6.94 (d, $J = 7.3$ Hz, 2H), 6.76 (d, $J = 7.3$ Hz, 2H), 6.59 (d, $J = 7.9$ Hz, 4H). MS (MALDI-TOF): $m/z = 1307.33$ $[\text{M}]^+$. UV-Vis, (DCM)/nm (log ϵ): 352 (0.22), 417 (0.20), 654 (0.15), 676 (0.14).

3.26 Synthesis of 5-(3,5-dimethoxyphenyl)-10,15,20-triphenylporphyrin 122^[19]

3,5-Dimethoxybenzaldehyde **121** (4.0 g, 24mmol) and benzaldehyde **5** (7.69 mL, 72 mmol) were dissolved in propionic acid (200 mL) and the mixture was refluxed. Freshly distilled pyrrole **6** (6.44 mL, 96 mmol) was then added dropwise. Once the addition was completed, the resulting mixture was further refluxed for 30 min. The reaction mixture was allowed to cool to room temperature, MeOH (200 mL) was added, and the mixture was left to precipitate overnight. The resulting purple solid was collected by vacuum filtration and washed with MeOH. The crude compound was chromatographed on a silica gel column using DCM: Pet Ether (3:7 v/v) mixture as eluent. The first pink band collected was the symmetrical porphyrin TPP. The solvent was changed to DCM /pet ether (1:1) and a dark purple fraction was collected. The title compound was recrystallised from a mixture of DCM: MeOH as a purple solid (1 g, 6 %). M.P. 290°C. ¹H NMR (500 MHz, Chloroform-*d*) δ 8.95 (d, *J* = 4.7 Hz, 2H), 8.84 (s, 6H), 8.22 (dd, *J* = 8.8, 1.6 Hz, 6H), 7.80 – 7.73 (m, 9H), 7.41 (d, *J* = 2.4 Hz, 2H), 6.90 (t, *J* = 2.3 Hz, 1H), 3.96 (s, 6H), -2.78 (s, 2H). MS (MALDI-TOF): *m/z* = 675 [M]⁺ (100%). UV-Vis, (DCM)/nm (log ε): 422 (2.86), 517 (0.31), 546 (0.16), 596 (0.12), 652 (0.09).

3.27 Synthesis of 5-(3,5-dihydroxyphenyl)-10,15,20-triphenylporphyrin **123**^[19]

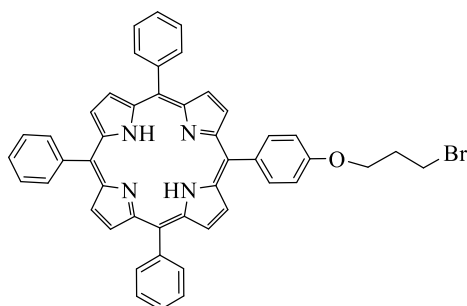
5-(3,5-Dimethoxyphenyl)-10,15,20-triphenylporphyrin **122** (0.1 g, 0.148 mmol) was dissolved in DCM (5 mL) and stirred. Then, BBr₃ (0.22 mL of 1 M solution in DCM, 0.89 mmol) was added dropwise and the reaction was left to stir overnight. After quenching the reaction with MeOH and neutralising it with Ammonia solution the colour turned back to the desired purple. The mixture was poured into water and was extracted several times with ethyl acetate, dried with MgSO₄, filtered and concentrated to obtain the title product (0.8 g, 84 %). M.P. 300°C. ¹H NMR (500 MHz, Acetone-*d*₆) δ 8.29 (d, *J* = 4.8 Hz, 2H), 8.02 (d, *J* = 4.7 Hz, 6H), 7.47 (td, *J* = 7.8, 6.1, 1.8 Hz, 6H), 7.09 – 7.02 (m, 9H), 6.50 (d, *J* = 2.2 Hz, 2H), 6.08 (t, *J* = 2.2 Hz, 1H), -3.52 (s, 2H). MS (MALDI-TOF): *m/z* = 642.90[M]⁺. UV-Vis, (DCM)/nm (log ε): 422 (2.8), 517 (0.27), 553 (0.09), 596 (0.07), 649 (0.05).

3.28 Synthesis of Zinc 5-(3,5-dihydroxyphenyl)-10,15,20-triphenylporphyrin **124**^[20]

5-(3,5-Dihydroxyphenyl)-10,15,20-triphenylporphyrin **123** (0.7 g, 1.08 mmol) and zinc acetate (0.2 g, 0.119 mmol) were dissolved in 200 ml of acetone. The mixture was stirred and refluxed for 2 h protected from light, then concentrated, redissolved in ethyl acetate (10 ml) and extracted with water and brine to recover the product as a light purple solid (0.6 g, 79 %). ^1H NMR (500 MHz, Acetone- d_6) δ 9.04 (d, J = 4.6 Hz, 2H), 8.86 – 8.84 (m, 6H), 8.24 – 8.20 (m, 6H), 7.84 – 7.76 (m, 9H), 7.24 (d, J = 2.2 Hz, 2H), 6.81 (t, J = 2.2 Hz, 1H). ^{13}C NMR (126 MHz, Acetone- d_6) δ 156.47, 150.03, 149.91, 149.87, 145.10, 143.33, 134.32, 134.30, 131.80, 131.71, 131.61, 131.42, 131.37, 131.26, 131.08, 127.39, 126.49, 120.80, 120.57, 120.51, 114.58, 101.85. MS (MALDI-TOF): m/z = 705.76[M] $^+$. UV-Vis, (DCM)/nm (log ϵ): 422 (2.64), 546 (0.40), 590 (0.004).

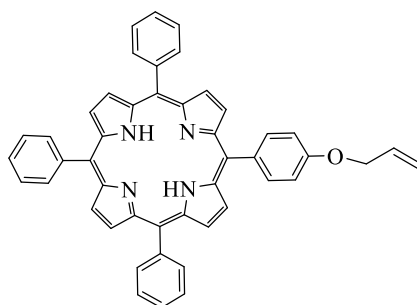
3.29 Synthesis of bromoalkoxyporphyrin:

3.29.1 Synthesis of 5-((*p*-bromopropyl) oxy)phenyl)-10,15,20 triphenylporphyrin **117**^[21]



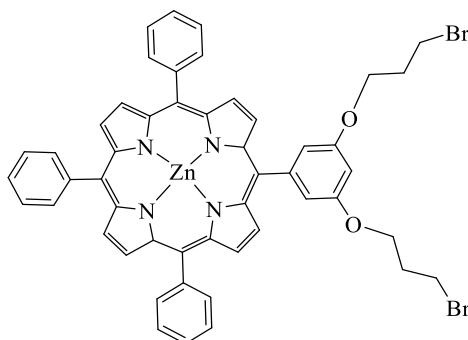
TPP-OH **64** (0.89 g, 1.41 mmol), 1,3-dibromopropane **116** (1.4 mL, 7.05 mmol) and potassium carbonate (1.94 g, 14.1 mmol) were added to dry DMF (20 mL), and the mixture stirred at room temperature for 19 h. The solvent was removed, and the residue redissolved in DCM. This was washed with water and extracted with DCM three times. The combined organic extracts were dried (MgSO_4), and the solvent removed in vacuo. The product was purified by recrystallisation from DCM/MeOH, (1:1) to give the title compound as a purple solid (1 g, 95 %). ^1H NMR (500 MHz, Chloroform- d) δ 8.88 (d, J = 4.7 Hz, 2H), 8.84 (d, J = 4.7 Hz, 6H), 8.22 (d, J = 8.0 Hz, 6H), 8.13 (d, J = 8.5 Hz, 2H), 7.81 – 7.71 (m, 9H), 7.29 (d, J = 8.5 Hz, 2H), 4.41 (t, J = 5.7 Hz, 2H), 3.79 (t, J = 6.4 Hz, 2H), 2.55 – 2.50 (m, 2H), -2.76 (s, 2H). ^{13}C -NMR (126 MHz, CDCl_3) δ 142.22, 135.64, 134.57, 127.70, 126.68, 120.09, 112.78, 65.62, 53.44, 32.63, 30.96, 30.20. MS (MALDI-TOF): m/z = 752.37 [M] $^+$. UV-Vis, (DCM)/nm (log ϵ): 420 (2.25), 512 (0.12), 550 (0.06), 593 (0.04), 648 (0.03).

3.29.2 Synthesis of 5-((*p*-bromopropyl) propenyl) oxy) phenyl)-10,15,20triphenylporphyrin **128**



This compound was isolated from the previous reaction as side product and was obtained as a purple solid (50 mg, 5 %). ^1H NMR (500 MHz, Chloroform-*d*) δ 8.81 (d, $J = 4.7$ Hz, 2H), 8.77 (d, $J = 4.7$ Hz, 6H), 8.14 (dd, $J = 8.5, 2.4$ Hz, 6H), 8.05 (d, $J = 8.5$ Hz, 2H), 7.68 (q, $J = 8.2, 7.5$ Hz, 9H), 7.23 (d, $J = 8.6$ Hz, 2H), 6.24 – 6.15 (m, 1H), 5.55 (dq, $J = 17.3, 1.6$ Hz, 1H), 5.37 (dq, $J = 10.6, 1.4$ Hz, 1H), 4.76 (dt, $J = 5.3, 1.6$ Hz, 2H), -2.84 (s, 2H). ^{13}C -NMR (500 MHz, CDCl_3) δ 142.23, 135.60, 134.57, 133.38, 127.70, 126.68, 120.08, 118.04, 112.99, 69.17. δ . MS (MALDI-TOF): $m/z = 664.85[\text{M}]^+$. UV-Vis, (DCM)/nm ($\log \epsilon$) : 422 (3.02), 514 (0.88), 552 (0.43), 592 (0.26), 650 (0.20).

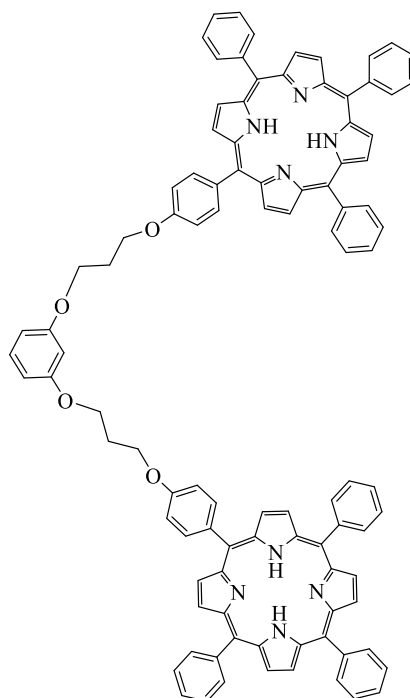
3.29.3 Synthesis of 5-((3,5-bis((3-bromopropyl)oxy)phenyl)-10,15,20-triphenylporphyrin **126**^[21]:



Zinc porphyrin **124** (0.200 g, 0.281 mmol), 1,3-dibromopropane **116** (0.11 mL, 0.843 mmol) and potassium carbonate (0.38 g, 2.81 mmol) were added to dry DMF (6 mL) and the mixture stirred at rt for 19 h. The solvent was removed, and the residue redissolved in ethyl acetate. This was washed with water and extracted with ethyl acetate three times. The combined organic extracts were dried (MgSO_4) and the

solvent removed in vacuo. The product was purified by recrystallisation from chloroform and hexane to give the title compound as a light purple solid (0.2 g, 77 %). ^1H NMR (500 MHz, Acetone- d_6) δ 8.86 (d, $J = 4.6$ Hz, 2H), 8.75 – 8.69 (m, 6H), 8.08 (dd, $J = 7.5, 1.8$ Hz, 6H), 7.72 – 7.62 (m, 9H), 7.30 (d, $J = 2.2$ Hz, 2H), 6.89 (t, $J = 2.3$ Hz, 1H), 4.24 (t, $J = 5.9$ Hz, 4H), 3.61 (t, $J = 6.6$ Hz, 4H), 2.27 (q, $J = 6.2$ Hz, 4H). ^{13}C NMR (500 MHz, CDCl_3) δ 157.83, 150.29, 150.27, 150.20, 149.93, 142.79, 134.42, 132.08, 132.03, 131.99, 131.91, 127.53, 126.57, 121.18, 114.53, 101.12, 65.71, 32.48, 30.02. MS (MALDI-TOF): $m/z = 954.14[\text{M}]^+$. (100%) UV-Vis, (DCM)/nm (log ϵ): 422 (2.77), 546 (0.86), 594 (0.05).

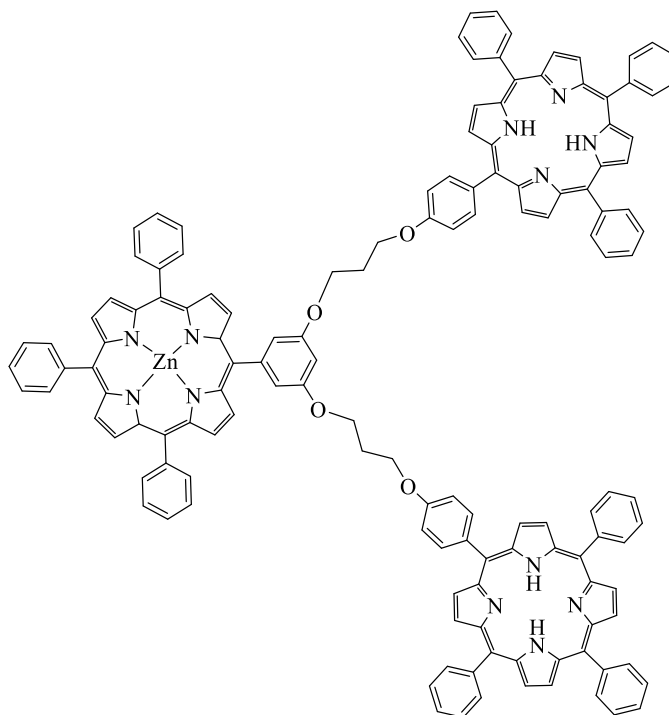
3.30 Synthesis of porphyrin dimer 119:



Bromoalkoxyporphyrin **117** (0.5 g, 0.66 mmol), 1,3-dihydroxy benzene **118** (0.49 g, 0.26 mmol) and K_2CO_3 (0.18 g, 1.3 mmol) were added to 10 mL acetone in a sealed tube and heated at 70 °C for 7 days. The solvent was removed, and the residue dissolved in DCM and washed with water and extracted with DCM three times. The combined organic extracts were dried (MgSO_4), and the solvent removed in vacuo. The crude product was purified by using column chromatography, eluting the product with DCM: PE (1:1). The product was recrystallised from methanol to yield

a purple solid product (0.137 g, 36 %); M.P. 331- 335 °C. ^1H NMR (400 MHz, Chloroform- d) δ 8.80 (d, $J = 4.8$ Hz, 4H), 8.75 (d, $J = 2.9$ Hz, 12H), 8.15 – 8.08 (m, 12H), 8.03 (d, $J = 8.6$ Hz, 4H), 7.72 – 7.59 (m, 18H), 7.24 – 7.19 (m, 5H), 6.64 (t, $J = 2.3$ Hz, 1H), 6.61 (d, $J = 2.3$ Hz, 1H), 6.59 (d, $J = 2.3$ Hz, 1H), 4.39 (t, $J = 6.0$ Hz, 4H), 4.29 (t, $J = 6.0$ Hz, 4H), 2.40 (p, $J = 6.0$ Hz, 4H), -2.85 (s, 2H). ^{13}C NMR (126 MHz, CDCl_3) δ 160.30, 158.75, 142.20, 135.62, 134.56, 134.54, 127.66, 126.68, 126.65, 120.07, 119.96, 112.77, 107.06, 77.28, 77.03, 76.77, 64.74, 64.60, 29.57. MS (MALDI-TOF): $m/z = 1445.46$ $[\text{M}]^+$. UV-Vis, (DCM)/nm ($\log \epsilon$): 421, 486, 556, 605, 687.

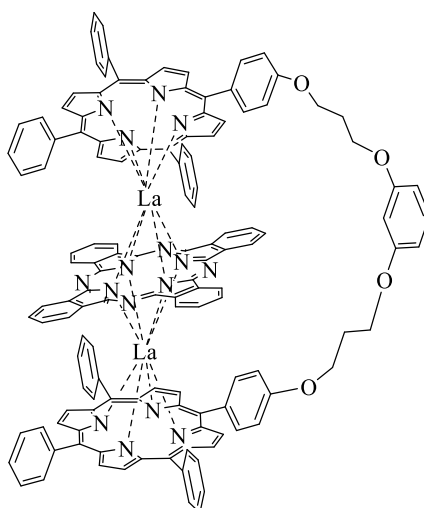
3.31 Synthesis of trimeric porphyrin 125:



Zinc porphyrin **124** (0.227 g, 0.32 mmol), bromoalkoxyporphyrin **117** (0.6 g, 0.80 mmol), K_2CO_3 (0.44 g, 3.2 mmol) were all added to 10 mL acetone in a sealed tube and heated at 70 °C for 7 days. The solvent was removed, and the residue dissolved in DCM and washed with water and the washings extracted with DCM three times. The combined organic extracts were dried (MgSO_4), and the solvent removed in vacuo. The crude product was purified by using column chromatography, eluting the product with DCM: PE (1:1). The trimer was recrystallised from methanol to gain a purple solid product (0.2 g, 30 %); ^1H

NMR (500 MHz, Chloroform-*d*) δ 9.21 (d, $J = 4.6$ Hz, 2H), 9.04 – 8.74 (m, 22H), 8.27 – 8.16 (m, 18H), 8.10 (d, $J = 8.3$ Hz, 4H), 7.82 – 7.64 (m, 27H), 7.62 (d, $J = 2.2$ Hz, 2H), 7.29 (d, $J = 8.5$ Hz, 2H), 7.15 (d, $J = 2.3$ Hz, 1H), 4.59 – 4.48 (m, 8H), 2.57 (t, $J = 6.1$ Hz, 4H), -2.75 (s, 4H). ^{13}C NMR (126 MHz, CDCl_3) δ 150.58, 150.16, 142.83, 142.16, 135.35, 134.95, 134.47, 132, 127.68, 127.46, 126.59, 121.05, 120.11, 112.56, 68.28, 68.12, 67.81, 29.38, 26.06. MS (MALDI-TOF): $m/z = 2052.47$ $[\text{M}]^+$ UV-vis, (DCM)/nm ($\log \epsilon$): 422, 455, 519, 557, 593, 651.

3.32 Synthesis of closed triple decker **120**:



Porphyrin dyad **119** (100 mg, 0.069 mmol) was mixed with lanthanum (III) acetylacetonate hydrate (60.19 mg, 0.138 mmol) and metal-free phthalocyanine **19** (42.6mg, 0.082mmol) in a 25 mL round bottom flask and dissolved in 10 mL of octanol. The mixture was left to reflux overnight under inert atmosphere. The solvent was removed under reduced pressure. The resulting solids were then separated by column chromatography through silica gel using DCM/Hexane (3:2 v/v) as eluent and the first brown fraction containing the title product was collected as dark brown solid that was recrystallised from DCM: MeOH to give the product as brown needles (75 mg, 49 %). M.P. > 380 °C. ^1H NMR (500 MHz, $\text{DCM-}d_2$) δ 9.98 (d, $J = 7.1$ Hz, 6H), 9.87 (d, $J = 8.8$ Hz, 2H), 9.30 (dd, $J = 5.3, 2.9$ Hz, 8H), 8.43 (t, $J = 7.7$ Hz, 6H), 8.24 – 8.22 (m, 8H), 8.01 (dd, $J = 8.1, 2.8$ Hz, 2H), 7.77 (td, $J = 8.0, 1.2$ Hz, 6H), 7.38 (t, $J = 8.8$ Hz, 1H), 7.25 (d, $J = 4.2$ Hz, 4H), 7.23 – 7.14 (m, 19H), 6.81 (dd, $J = 8.0, 2.8$ Hz, 2H), 6.77 (d, $J = 2.3$ Hz, 1H), 6.75 (d, $J = 2.3$ Hz, 1H), 6.68 (dd, $J = 7.9, 2.3$ Hz, 2H), 6.62

(d, $J = 7.3$ Hz, 6H), 4.59 (t, $J = 6.4$ Hz, 4H), 4.55 (t, $J = 6.1$ Hz, 4H), 2.50 (p, $J = 6.4$ Hz, 4H). ^{13}C NMR (126 MHz, DCM- d_2) δ 160.64, 158.49, 153.57, 147.83, 147.57, 142.79, 142.06, 136.59, 135.15, 134.48, 133.55, 133.33, 130.10, 128.46, 128.40, 128.33, 127.65, 127.19, 126.65, 126.02, 125.87, 123.53, 120.08, 107.35, 65.91, 65.79, 29.68, 29.36. MS (MALDI-TOF): $m/z = 2237.85$ $[\text{M}]^+$. UV-Vis, (DCM)/nm ($\log \epsilon$) = 359 (0.096), 422 (0.229), 486 (0.024), 556 (0.0146), 606 (0.0143), 687 (0.100).

References:

- [1] A. D. Adler, F. R. Longo, J. D. Finarelli, J. E. Goldmacher, J. M. Assour and L. Korsakoff, *Journal of Organic Chemistry* **1967**, 32, 476-476.
- [2] H. A. Bruson and J. W. Kroeger, *Journal of the American Chemical Society* **1940**, 62, 36-44.
- [3] V. N. Nemykin and E. A. Lukyanets, *ARKIVOC* **2010**, 2010, 136-208.
- [4] P. R. Ashton, U. Girreser, D. Giuffrida, F. H. Kohnke, J. P. Mathias, F. M. Raymo, A. M. Z. Slawin, J. F. Stoddart and D. J. Williams, *Journal of the American Chemical Society* **1993**, 115, 5422-5429.
- [5] G. P. Ellis and T. M. Romney-Alexander, *Chemical Reviews* **1987**, 87, 779-794.
- [6] S. A. Mikhalenko, L. I. Solov'Eva and E. A. Luk'Yanets, *J. Gen. Chem. USSR* **1988**, 58, 2618-2619.
- [7] C. C. Leznoff and D. M. Drew, *Canadian Journal of Chemistry* **1996**, 74, 307-318.
- [8] S. Alpugan, G. Ekiner, V. Ahsen, S. Berber, E. Önal and F. Dumoulin, *Crystals* **2016**, 6, 89.
- [9] M. J. Cook, A. J. Dunn, S. D. Howe, A. J. Thomson and K. J. Harrison, *Journal of the Chemical Society, Perkin Transactions 1* **1988**, 2453-2458.
- [10] S. Dalai, V. N. Belov, S. Nizamov, K. Rauch, D. Finsinger and A. de Meijere, *European Journal of Organic Chemistry* **2006**, 2006, 2753-2765.
- [11] M. Hellal and G. D. Cuny, *Tetrahedron Letters* **2011**, 52, 5508-5511.
- [12] A. Díaz-Moscoso, G. J. Tizzard, S. J. Coles and A. N. Cammidge, *Angewandte Chemie International Edition* **2013**, 52, 10784-10787.
- [13] A. Díaz-Moscoso, E. Emond, D. L. Hughes, G. J. Tizzard, S. J. Coles and A. N. Cammidge, *The Journal of Organic Chemistry* **2014**, 79, 8932-8936.
- [14] T. V. Dubinina, K. V. Paramonova, S. A. Trashin, N. E. Borisova, L. G. Tomilova and N. S. Zefirov, *Dalton Transactions* **2014**, 43, 2799-2809.
- [15] D. González-Lucas, S. C. Soobrattee, D. L. Hughes, G. J. Tizzard, S. J. Coles and A. N. Cammidge, *Chemistry – A European Journal* **2020**, 26, 10724-10728.
- [16] N. Iida, K. Tanaka, E. Tokunaga, H. Takahashi and N. Shibata, *ChemistryOpen* **2015**, 4, 102-106.

- [17] V. E. Pushkarev, V. V. Kalashnikov, A. Y. Tolbin, S. A. Trashin, N. E. Borisova, S. V. Simonov, V. B. Rybakov, L. G. Tomilova and N. S. Zefirov, *Dalton Transactions* **2015**, *44*, 16553-16564.
- [18] V. E. Pushkarev, E. V. Shulishov, Y. V. Tomilov and L. G. Tomilova, *Tetrahedron Letters* **2007**, *48*, 5269-5273.
- [19] T. Toshihiro, E. Ken and A. Yasuhiro, *Bulletin of the Chemical Society of Japan* **2001**, *74*, 907-916.
- [20] L. Yu, K. Muthukumaran, I. V. Sazanovich, C. Kirmaier, E. Hindin, J. R. Diers, P. D. Boyle, D. F. Bocian, D. Holten and J. S. Lindsey, *Inorganic Chemistry* **2003**, *42*, 6629-6647.
- [21] F. Ogasawara, H. Kasai, Y. Nagashima, T. Kawaguchi and A. Yoshizawa, *Ferroelectrics* **2008**, *365*, 48-57.

4. Appendix

Crystal data and structure refinement for 1-CH-cyclo-C₄H₃S,3-amino-isoindoline

—

Identification code	noraha1b
Elemental formula	C13 H10 N2 S
Formula weight	226.29
Crystal system, space group	Triclinic, P-1 (no. 2)
Unit cell dimensions	a = 12.0847(2) Å α =
95.9946(13) °	b = 13.8133(2) Å β =
102.3784(14) °	c = 13.9405(2) Å γ =
95.4710(13) °	
Volume	2243.89(6) Å ³
Z, Calculated density	8, 1.340 Mg/m ³
F(000)	944
Absorption coefficient	2.314 mm ⁻¹
Temperature	100.01(10) K
Wavelength	1.54184 Å
Crystal colour, shape	yellow plate
Crystal size	0.333 x 0.037 x 0.013 mm
Crystal mounting:	in a small loop, in oil, fixed in cold
N ₂ stream	
On the diffractometer:	
Theta range for data collection	3.241 to 69.999 °
Limiting indices	-14<=h<=13, -15<=k<=16,
-16<=l<=16	
Completeness to theta = 67.684	98.5 %
Absorption correction	Semi-empirical from
equivalents	
Max. and min. transmission	1.00000 and 0.82519

Reflections collected (not including absences) 23359

No. of unique reflections 8299 [R(int) for
equivalents = 0.031]

No. of 'observed' reflections ($I > 2\sigma_I$) 7729

Structure determined by: dual methods, in SHELXT

Refinement: Full-matrix least-squares on F^2 , in
SHELXL

Data / restraints / parameters 8299 / 0 / 617

Goodness-of-fit on F^2 1.065

Final R indices ('observed' data) $R_1 = 0.043$, $wR_2 = 0.126$

Final R indices (all data) $R_1 = 0.045$, $wR_2 = 0.128$

Reflections weighted:
 $w = [\sigma^2(\text{Fo}^2) + (0.0761P)^2 + 1.5555P]^{-1}$ where $P = (\text{Fo}^2 + 2\text{Fc}^2) / 3$

Extinction coefficient n/a

Largest diff. peak and hole 0.73 and -0.62 e.A-3

Location of largest difference peak near C(25)

Table 1. Atomic coordinates ($\times 10^5$) and equivalent isotropic displacement parameters ($\text{\AA}^2 \times 10^4$). $U(\text{eq})$ is defined as one third of the trace of the orthogonalized U_{ij} tensor. E.s.ds are in parentheses.

	x	y	z	$U(\text{eq})$
C(1)	66239(17)	51268(14)	89525(14)	206(4)
S(2)	68658(4)	39594(3)	85228(3)	225.1(13)
C(3)	83194(17)	42612(16)	88770(14)	254(4)
C(4)	86109(17)	52087(16)	93074(14)	253(4)
C(5)	76542(17)	57051(15)	93583(14)	231(4)
C(6)	55155(16)	54378(14)	89106(14)	212(4)
C(7)	44894(16)	49689(13)	84018(13)	193(4)
C(8)	33725(16)	53021(14)	84192(13)	199(4)
C(9)	25598(16)	45776(14)	78168(13)	194(4)
C(10)	13928(16)	46382(14)	76739(14)	221(4)
C(11)	10605(17)	54560(16)	81492(15)	256(4)

C (12)	18679 (18)	61906 (15)	87459 (15)	255 (4)
C (13)	30316 (18)	61216 (14)	88905 (14)	235 (4)
C (14)	32201 (16)	38483 (13)	74395 (13)	192 (4)
N (15)	43309 (13)	40713 (11)	77847 (11)	190 (3)
N (16)	27508 (14)	30413 (12)	68064 (12)	230 (3)
C (21)	83064 (17)	45206 (14)	52658 (15)	241 (4)
S (22)	82985 (4)	44165 (4)	64809 (4)	285.9 (14)
C (23)	74533 (17)	53158 (15)	65582 (16)	267 (4)
C (24)	71490 (20)	56982 (16)	56984 (17)	326 (5)
C (25)	76079 (17)	52767 (14)	48826 (15)	225 (4)
C (26)	89345 (18)	39561 (15)	46903 (15)	261 (4)
C (27)	94634 (17)	31657 (15)	49165 (15)	235 (4)
C (28)	100938 (16)	26181 (15)	42928 (15)	244 (4)
C (29)	104254 (16)	18212 (15)	47778 (14)	236 (4)
C (30)	110029 (17)	11205 (17)	43734 (16)	303 (5)
C (31)	112533 (19)	12425 (19)	34597 (17)	360 (5)
C (32)	109419 (19)	20445 (19)	29837 (17)	354 (5)
C (33)	103606 (19)	27421 (17)	33892 (16)	311 (5)
C (34)	100104 (16)	19327 (15)	56992 (14)	219 (4)
N (35)	94636 (14)	27135 (12)	57771 (12)	214 (3)
N (36)	101590 (15)	13157 (14)	63797 (13)	283 (4)
C (41)	113591 (16)	16495 (13)	96584 (13)	190 (4)
S (42)	117190 (4)	21835 (3)	86770 (3)	221.2 (13)
C (43)	131463 (16)	22328 (14)	91875 (14)	221 (4)
C (44)	133577 (17)	18650 (15)	100680 (15)	231 (4)
C (45)	123414 (16)	15273 (14)	103719 (17)	250 (4)
C (46)	102023 (16)	14135 (14)	97496 (14)	211 (4)
C (47)	92210 (16)	14836 (13)	90884 (14)	196 (4)
C (48)	80643 (16)	13033 (13)	92653 (14)	204 (4)
C (49)	73141 (16)	14898 (13)	84086 (14)	195 (4)
C (50)	61415 (17)	13899 (14)	83132 (15)	227 (4)
C (51)	57304 (17)	10929 (15)	91104 (16)	255 (4)
C (52)	64771 (18)	9272 (15)	99758 (16)	272 (4)
C (53)	76521 (17)	10313 (15)	100663 (16)	254 (4)
C (54)	80511 (16)	17840 (13)	77485 (14)	195 (4)
N (55)	91468 (13)	17725 (11)	81422 (12)	195 (3)
N (56)	76552 (14)	20265 (13)	68411 (12)	242 (4)
C (61)	30918 (15)	-590 (14)	59808 (14)	207 (4)
S (62)	31565 (4)	7241 (4)	70402 (4)	259.0 (3)
C (63)	24621 (18)	-1421 (16)	75505 (16)	281 (4)
C (64)	21801 (19)	-10046 (17)	69540 (17)	329 (5)
C (65)	25185 (15)	-10137 (14)	60112 (13)	187 (4)
C (66)	35295 (16)	2259 (14)	51551 (14)	202 (4)
C (67)	40731 (15)	11062 (14)	50797 (14)	192 (4)
C (68)	44648 (15)	13878 (14)	42086 (14)	202 (4)
C (69)	49917 (16)	23526 (14)	44703 (14)	210 (4)
C (70)	54477 (18)	28572 (16)	38009 (16)	280 (4)
C (71)	53620 (20)	23657 (17)	28592 (16)	331 (5)
C (72)	48355 (19)	14010 (17)	26000 (15)	301 (5)
C (73)	43815 (17)	9005 (15)	32667 (15)	247 (4)
C (74)	48906 (15)	26262 (14)	54905 (14)	204 (4)
N (75)	43537 (13)	19069 (12)	58377 (12)	203 (3)
N (76)	52877 (15)	35013 (13)	60189 (13)	266 (4)

Table 2. Molecular dimensions. Bond lengths are in Ångstroms, angles in degrees. E.s.ds are in parentheses.

C (1) -C (5)	C (23) -C (24)
1.387 (3)	1.353 (3)
C (1) -C (6)	C (24) -C (25)
1.436 (3)	1.460 (3)
C (1) -S (2)	C (26) -C (27)
1.7342 (19)	1.349 (3)
S (2) -C (3)	C (27) -N (35)
1.717 (2)	1.409 (3)
C (3) -C (4)	C (27) -C (28)
1.362 (3)	1.471 (3)
C (4) -C (5)	C (28) -C (33)
1.410 (3)	1.389 (3)
C (6) -C (7)	C (28) -C (29)
1.354 (3)	1.397 (3)
C (7) -N (15)	C (29) -C (30)
1.405 (2)	1.387 (3)
C (7) -C (8)	C (29) -C (34)
1.471 (3)	1.475 (3)
C (8) -C (13)	C (30) -C (31)
1.390 (3)	1.394 (3)
C (8) -C (9)	C (31) -C (32)
1.398 (3)	1.391 (4)
C (9) -C (10)	C (32) -C (33)
1.393 (3)	1.388 (3)
C (9) -C (14)	C (34) -N (35)
1.467 (3)	1.324 (3)
C (10) -C (11)	C (34) -N (36)
1.386 (3)	1.336 (3)
C (11) -C (12)	C (41) -C (45)
1.400 (3)	1.412 (3)
C (12) -C (13)	C (41) -C (46)
1.391 (3)	1.440 (3)
C (14) -N (15)	C (41) -S (42)
1.320 (2)	1.7350 (19)
C (14) -N (16)	S (42) -C (43)
1.342 (3)	1.7110 (19)
	C (43) -C (44)
C (21) -C (26)	1.360 (3)
1.439 (3)	C (44) -C (45)
C (21) -C (25)	1.435 (3)
1.477 (3)	C (46) -C (47)
C (21) -S (22)	1.355 (3)
1.717 (2)	C (47) -N (55)
S (22) -C (23)	1.405 (2)
1.691 (2)	C (47) -C (48)
	1.473 (3)

1.388 (3)	C (48) -C (53)	1.350 (3)	C (63) -C (64)
1.400 (3)	C (48) -C (49)	1.457 (3)	C (64) -C (65)
1.387 (3)	C (49) -C (50)	1.351 (3)	C (66) -C (67)
1.472 (3)	C (49) -C (54)	1.409 (2)	C (67) -N (75)
1.394 (3)	C (50) -C (51)	1.470 (3)	C (67) -C (68)
1.397 (3)	C (51) -C (52)	1.390 (3)	C (68) -C (73)
1.390 (3)	C (52) -C (53)	1.397 (3)	C (68) -C (69)
1.322 (3)	C (54) -N (55)	1.394 (3)	C (69) -C (70)
1.342 (3)	C (54) -N (56)	1.467 (3)	C (69) -C (74)
1.439 (3)	C (61) -C (65)	1.392 (3)	C (70) -C (71)
1.441 (3)	C (61) -C (66)	1.396 (3)	C (71) -C (72)
1.720 (2)	C (61) -S (62)	1.387 (3)	C (72) -C (73)
1.698 (2)	S (62) -C (63)	1.325 (3)	C (74) -N (75)
		1.336 (3)	C (74) -N (76)
125.23 (18)	C (5) -C (1) -C (6)	105.91 (16)	C (9) -C (8) -C (7)
110.05 (15)	C (5) -C (1) -S (2)	122.01 (18)	C (10) -C (9) -C (8)
124.71 (15)	C (6) -C (1) -S (2)	132.79 (17)	C (10) -C (9) -C (14)
92.08 (10)	C (3) -S (2) -C (1)	105.20 (16)	C (8) -C (9) -C (14)
111.85 (15)	C (4) -C (3) -S (2)	117.28 (18)	C (11) -C (10) -C (9)
112.82 (18)	C (3) -C (4) -C (5)	121.16 (19)	C (10) -C (11) -C (12)
113.20 (18)	C (1) -C (5) -C (4)	124.84 (17)	C (45) -C (41) -C (46)
128.12 (18)	C (7) -C (6) -C (1)	111.32 (15)	C (45) -C (41) -S (42)
124.74 (18)	C (6) -C (7) -N (15)	123.76 (14)	C (46) -C (41) -S (42)
125.83 (18)	C (6) -C (7) -C (8)	91.87 (9)	C (43) -S (42) -C (41)
109.42 (16)	N (15) -C (7) -C (8)	112.69 (15)	C (44) -C (43) -S (42)
120.32 (18)	C (13) -C (8) -C (9)	113.46 (18)	C (43) -C (44) -C (45)
133.77 (18)	C (13) -C (8) -C (7)	110.65 (19)	C (41) -C (45) -C (44)

128.25 (17)	C (47) -C (46) -C (41)	125.69 (19)	C (26) -C (27) -C (28)
125.49 (17)	C (46) -C (47) -N (55)	109.23 (17)	N (35) -C (27) -C (28)
125.20 (17)	C (46) -C (47) -C (48)	120.3 (2)	C (33) -C (28) -C (29)
109.27 (16)	N (55) -C (47) -C (48)	133.4 (2)	C (33) -C (28) -C (27)
120.51 (18)	C (53) -C (48) -C (49)	106.29 (17)	C (29) -C (28) -C (27)
133.31 (18)	C (53) -C (48) -C (47)	121.92 (19)	C (30) -C (29) -C (28)
106.16 (16)	C (49) -C (48) -C (47)	132.9 (2)	C (30) -C (29) -C (34)
122.00 (18)	C (50) -C (49) -C (48)	105.15 (17)	C (28) -C (29) -C (34)
132.97 (18)	C (50) -C (49) -C (54)	117.4 (2)	C (29) -C (30) -C (31)
105.03 (16)	C (48) -C (49) -C (54)	120.8 (2)	C (32) -C (31) -C (30)
117.24 (18)	C (49) -C (50) -C (51)	121.6 (2)	C (33) -C (32) -C (31)
120.97 (18)	C (50) -C (51) -C (52)	118.0 (2)	C (32) -C (33) -C (28)
121.23 (19)	C (13) -C (12) -C (11)	123.42 (18)	N (35) -C (34) -N (36)
118.00 (18)	C (8) -C (13) -C (12)	112.44 (17)	N (35) -C (34) -C (29)
123.32 (17)	N (15) -C (14) -N (16)	124.14 (18)	N (36) -C (34) -C (29)
112.79 (16)	N (15) -C (14) -C (9)	106.85 (16)	C (34) -N (35) -C (27)
123.89 (17)	N (16) -C (14) -C (9)	121.42 (19)	C (53) -C (52) -C (51)
106.65 (16)	C (14) -N (15) -C (7)	117.82 (19)	C (48) -C (53) -C (52)
123.71 (18)	C (26) -C (21) -C (25)	123.59 (18)	N (55) -C (54) -N (56)
124.39 (15)	C (26) -C (21) -S (22)	112.65 (16)	N (55) -C (54) -C (49)
111.89 (15)	C (25) -C (21) -S (22)	123.75 (17)	N (56) -C (54) -C (49)
93.03 (10)	C (23) -S (22) -C (21)	106.88 (16)	C (54) -N (55) -C (47)
112.97 (17)	C (24) -C (23) -S (22)	124.62 (17)	C (65) -C (61) -C (66)
115.36 (19)	C (23) -C (24) -C (25)	111.81 (14)	C (65) -C (61) -S (62)
106.74 (17)	C (24) -C (25) -C (21)	123.55 (15)	C (66) -C (61) -S (62)
128.31 (19)	C (27) -C (26) -C (21)	92.83 (10)	C (63) -S (62) -C (61)
125.05 (18)	C (26) -C (27) -N (35)	112.38 (17)	C (64) -C (63) -S (62)

C (63) -C (64) -C (65)	C (70) -C (69) -C (74)
114.86 (19)	133.29 (19)
C (61) -C (65) -C (64)	C (68) -C (69) -C (74)
108.12 (17)	105.29 (17)
C (67) -C (66) -C (61)	C (71) -C (70) -C (69)
127.52 (18)	117.7 (2)
C (66) -C (67) -N (75)	C (70) -C (71) -C (72)
124.74 (17)	120.8 (2)
C (66) -C (67) -C (68)	C (73) -C (72) -C (71)
126.19 (18)	121.45 (19)
N (75) -C (67) -C (68)	C (72) -C (73) -C (68)
109.07 (16)	118.00 (19)
C (73) -C (68) -C (69)	N (75) -C (74) -N (76)
120.68 (18)	123.14 (18)
C (73) -C (68) -C (67)	N (75) -C (74) -C (69)
133.02 (19)	112.48 (17)
C (69) -C (68) -C (67)	N (76) -C (74) -C (69)
106.29 (16)	124.38 (18)
C (70) -C (69) -C (68)	C (74) -N (75) -C (67)
121.40 (18)	106.87 (16)

Table 3. Anisotropic displacement parameters ($\text{\AA}^2 \times 10^4$) for the expression:

$$\exp \{-2\pi^2 (h^2 a^2 U_{11} + \dots + 2hka^* b^* U_{12})\}$$

E.s.ds are in parentheses.

	U ₁₁	U ₂₂	U ₃₃	U ₂₃	U ₁₃
U ₁₂					
C (1)	239 (9)	203 (9)	161 (9)	-10 (7)	35 (7)
6 (7)					
S (2)	252 (2)	208 (2)	193 (2)	-12 (2)	19 (2)
26 (2)					
C (3)	242 (10)	311 (11)	203 (9)	14 (8)	26 (8)
70 (8)					
C (4)	208 (9)	327 (11)	195 (9)	-9 (8)	15 (7)
6 (8)					
C (5)	236 (9)	240 (10)	201 (9)	-20 (7)	42 (7)
14 (8)					
C (6)	236 (9)	197 (9)	189 (9)	-13 (7)	48 (7)
1 (7)					
C (7)	224 (9)	190 (9)	158 (8)	14 (7)	47 (7)
1 (7)					
C (8)	225 (9)	219 (9)	158 (8)	41 (7)	56 (7)
5 (7)					

8 (7)	C (9)	236 (9)	197 (9)	153 (8)	45 (7)	50 (7)	
2 (7)	C (10)	206 (9)	255 (10)	199 (9)	45 (8)	43 (7)	
47 (8)	C (11)	227 (9)	326 (11)	246 (10)	91 (8)	92 (8)	
60 (8)	C (12)	312 (10)	246 (10)	234 (10)	22 (8)	115 (8)	
6 (8)	C (13)	280 (10)	224 (10)	197 (9)	6 (7)	71 (8)	-
0 (7)	C (14)	232 (9)	187 (9)	157 (8)	42 (7)	45 (7)	
0 (6)	N (15)	207 (8)	182 (8)	168 (7)	8 (6)	30 (6)	
14 (6)	N (16)	206 (8)	209 (8)	245 (8)	-21 (6)	28 (7)	-
6 (8)	C (21)	278 (10)	221 (10)	221 (9)	51 (8)	57 (8)	-
50 (2)	S (22)	290 (3)	310 (3)	264 (3)	46 (2)	66 (2)	
17 (8)	C (23)	261 (10)	246 (10)	285 (11)	6 (8)	77 (8)	-
81 (9)	C (24)	340 (11)	255 (11)	375 (12)	44 (9)	44 (9)	
27 (7)	C (25)	300 (10)	162 (9)	216 (9)	-26 (7)	86 (8)	
6 (8)	C (26)	338 (11)	243 (10)	217 (10)	57 (8)	102 (8)	-
41 (8)	C (27)	231 (9)	245 (10)	214 (9)	2 (8)	63 (8)	-
35 (8)	C (28)	204 (9)	278 (10)	231 (10)	-6 (8)	51 (8)	-
0 (8)	C (29)	156 (8)	326 (11)	193 (9)	-16 (8)	1 (7)	
90 (9)	C (30)	218 (10)	411 (12)	258 (10)	-2 (9)	9 (8)	
99 (10)	C (31)	259 (11)	510 (14)	311 (12)	-42 (10)	84 (9)	
0 (10)	C (32)	301 (11)	490 (14)	283 (11)	3 (10)	139 (9)	
19 (9)	C (33)	316 (11)	346 (12)	283 (11)	43 (9)	121 (9)	-
2 (7)	C (34)	163 (8)	279 (10)	176 (9)	-10 (7)	-15 (7)	-
2 (6)	N (35)	212 (8)	232 (8)	179 (8)	7 (6)	22 (6)	
134 (8)	N (36)	306 (9)	354 (10)	192 (8)	38 (7)	22 (7)	
33 (7)	C (41)	224 (9)	190 (9)	155 (8)	34 (7)	28 (7)	
10 (2)	S (42)	216 (2)	263 (3)	177 (2)	28 (2)	35 (2)	
29 (7)	C (43)	210 (9)	245 (10)	199 (9)	-1 (7)	41 (7)	

55 (8)	C (44)	198 (9)	268 (10)	224 (9)	22 (8)	32 (7)	
35 (7)	C (45)	176 (9)	194 (9)	390 (12)	48 (8)	72 (8)	
15 (7)	C (46)	238 (9)	218 (9)	183 (9)	61 (7)	54 (7)	
12 (7)	C (47)	208 (9)	184 (9)	204 (9)	46 (7)	58 (7)	
9 (7)	C (48)	212 (9)	170 (9)	231 (9)	26 (7)	56 (7)	
13 (7)	C (49)	218 (9)	150 (8)	219 (9)	22 (7)	58 (7)	
23 (7)	C (50)	215 (9)	187 (9)	265 (10)	22 (7)	29 (8)	
21 (8)	C (51)	202 (9)	240 (10)	335 (11)	33 (8)	94 (8)	
30 (8)	C (52)	279 (10)	282 (10)	295 (11)	83 (8)	135 (8)	
25 (8)	C (53)	264 (10)	262 (10)	249 (10)	84 (8)	66 (8)	
15 (7)	C (54)	222 (9)	163 (9)	196 (9)	20 (7)	42 (7)	
16 (6)	N (55)	205 (8)	192 (8)	185 (8)	38 (6)	35 (6)	
39 (7)	N (56)	199 (8)	314 (9)	215 (8)	76 (7)	26 (7)	
29 (7)	C (61)	160 (8)	242 (10)	203 (9)	38 (7)	1 (7)	
27 (2)	S (62)	291 (3)	267 (3)	236 (3)	55 (2)	90 (2)	
28 (8)	C (63)	257 (10)	354 (11)	255 (10)	117 (9)	77 (8)	
102 (9)	C (64)	283 (11)	354 (12)	319 (11)	107 (9)	34 (9)	-
35 (7)	C (65)	159 (8)	225 (9)	162 (8)	72 (7)	8 (7)	-
57 (7)	C (66)	194 (9)	225 (9)	181 (9)	12 (7)	22 (7)	
63 (7)	C (67)	168 (8)	242 (9)	166 (9)	24 (7)	21 (7)	
65 (7)	C (68)	183 (9)	240 (10)	188 (9)	51 (7)	26 (7)	
48 (7)	C (69)	195 (9)	252 (10)	182 (9)	34 (7)	26 (7)	
12 (8)	C (70)	318 (11)	289 (11)	251 (10)	70 (8)	95 (8)	
68 (10)	C (71)	435 (13)	393 (12)	215 (10)	113 (9)	141 (9)	
108 (9)	C (72)	385 (12)	380 (12)	156 (9)	44 (8)	72 (8)	
67 (8)	C (73)	275 (10)	275 (10)	186 (9)	19 (8)	29 (8)	
28 (7)	C (74)	174 (8)	249 (10)	182 (9)	31 (7)	23 (7)	

N(75)	200(8)	233(8)	169(8)	21(6)	33(6)	
16(6)						
N(76)	285(9)	284(9)	205(8)	-3(7)	63(7)	-
66(7)						

Table 4. Hydrogen coordinates ($\times 10^4$) and isotropic displacement parameters ($\text{\AA}^2 \times 10^3$). All hydrogen atoms were included in idealised positions with U(iso)'s refined freely.

	x	y	z	U(iso)
H(3)	8844	3830	8786	36(7)
H(4)	9361	5498	9543	25(6)
H(5)	7709	6355	9636	26(6)
H(6)	5501	6036	9279	28(6)
H(10)	859	4150	7276	28(6)
H(11)	288	5518	8070	33(7)
H(12)	1622	6735	9051	28(6)
H(13)	3565	6609	9290	23(6)
H(16A)	3180	2639	6606	29(6)
H(16B)	2021	2927	6601	39(7)
H(23)	7222	5526	7132	39(7)
H(24)	6681	6195	5632	43(8)
H(25)	7484	5451	4245	83(12)
H(26)	8982	4163	4085	43(7)
H(30)	11215	590	4700	27(6)
H(31)	11633	782	3165	37(7)
H(32)	11128	2115	2379	53(9)
H(33)	10156	3276	3066	42(7)
H(36A)	9893	1416	6902	53(9)
H(36B)	10521	818	6296	36(7)
H(43)	13716	2484	8895	34(7)
H(44)	14090	1835	10437	26(6)
H(45)	12331	1264	10958	5(4)
H(46)	10118	1184	10337	30(6)
H(50)	5650	1516	7741	25(6)
H(51)	4948	1004	9066	29(6)
H(52)	6182	743	10502	39(7)
H(53)	8146	922	10645	25(6)
H(56A)	8123	2186	6482	54(9)
H(56B)	6933	2023	6619	35(7)
H(63)	2295	-34	8171	33(7)
H(64)	1799	-1551	7131	52(8)
H(65)	2387	-1544	5515	69(11)
H(66)	3426	-251	4611	26(6)

H (70)	5797	3500	3977	29 (6)
H (71)	5658	2684	2397	41 (7)
H (72)	4789	1087	1966	43 (7)
H (73)	4032	258	3089	19 (5)
H (76A)	5199	3618	6614	35 (7)
H (76B)	5632	3947	5764	32 (7)

Table 5. Torsion angles, in degrees. E.s.ds are in parentheses.

C (5)-C (1)-S (2)-C (3)	-	C (9)-C (10)-C (11)-C (12)	
0.50 (15)		0.1 (3)	
C (6)-C (1)-S (2)-C (3)	-	C (10)-C (11)-C (12)-C (13)	-
179.29 (17)		0.6 (3)	
C (1)-S (2)-C (3)-C (4)		C (9)-C (8)-C (13)-C (12)	
0.21 (16)		0.3 (3)	
S (2)-C (3)-C (4)-C (5)		C (7)-C (8)-C (13)-C (12)	-
0.1 (2)		178.98 (19)	
C (6)-C (1)-C (5)-C (4)		C (11)-C (12)-C (13)-C (8)	
179.45 (18)		0.4 (3)	
S (2)-C (1)-C (5)-C (4)		C (10)-C (9)-C (14)-N (15)	-
0.7 (2)		178.61 (19)	
C (3)-C (4)-C (5)-C (1)	-	C (8)-C (9)-C (14)-N (15)	
0.5 (3)		1.5 (2)	
C (5)-C (1)-C (6)-C (7)		C (10)-C (9)-C (14)-N (16)	
169.2 (2)		1.7 (3)	
S (2)-C (1)-C (6)-C (7)	-	C (8)-C (9)-C (14)-N (16)	-
12.2 (3)		178.14 (17)	
C (1)-C (6)-C (7)-N (15)	-	N (16)-C (14)-N (15)-C (7)	
1.6 (3)		178.77 (17)	
C (1)-C (6)-C (7)-C (8)		C (9)-C (14)-N (15)-C (7)	-
177.21 (18)		0.9 (2)	
C (6)-C (7)-C (8)-C (13)		C (6)-C (7)-N (15)-C (14)	
1.4 (3)		178.91 (18)	
N (15)-C (7)-C (8)-C (13)	-	C (8)-C (7)-N (15)-C (14)	-
179.7 (2)		0.1 (2)	
C (6)-C (7)-C (8)-C (9)	-	C (26)-C (21)-S (22)-C (23)	
177.97 (18)		177.86 (18)	
N (15)-C (7)-C (8)-C (9)		C (25)-C (21)-S (22)-C (23)	-
1.0 (2)		0.95 (16)	
C (13)-C (8)-C (9)-C (10)	-	C (21)-S (22)-C (23)-C (24)	
0.7 (3)		0.86 (18)	
C (7)-C (8)-C (9)-C (10)		S (22)-C (23)-C (24)-C (25)	-
178.70 (17)		0.5 (3)	
C (13)-C (8)-C (9)-C (14)		C (23)-C (24)-C (25)-C (21)	-
179.15 (17)		0.2 (3)	
C (7)-C (8)-C (9)-C (14)	-	C (26)-C (21)-C (25)-C (24)	-
1.41 (19)		178.03 (19)	
C (8)-C (9)-C (10)-C (11)		S (22)-C (21)-C (25)-C (24)	
0.5 (3)		0.8 (2)	
C (14)-C (9)-C (10)-C (11)	-	C (25)-C (21)-C (26)-C (27)	-
179.34 (19)		170.0 (2)	

S (22) -C (21) -C (26) -C (27)	N (55) -C (47) -C (48) -C (53) -
11.4 (3)	178.3 (2)
C (21) -C (26) -C (27) -N (35)	C (46) -C (47) -C (48) -C (49)
2.3 (3)	178.01 (18)
C (21) -C (26) -C (27) -C (28)	N (55) -C (47) -C (48) -C (49)
179.96 (19)	0.1 (2)
C (26) -C (27) -C (28) -C (33)	C (53) -C (48) -C (49) -C (50) -
2.7 (4)	1.6 (3)
N (35) -C (27) -C (28) -C (33) -	C (47) -C (48) -C (49) -C (50)
179.3 (2)	179.82 (17)
C (26) -C (27) -C (28) -C (29) -	C (53) -C (48) -C (49) -C (54)
175.79 (19)	178.18 (17)
N (35) -C (27) -C (28) -C (29)	C (47) -C (48) -C (49) -C (54) -
2.2 (2)	0.4 (2)
C (33) -C (28) -C (29) -C (30) -	C (48) -C (49) -C (50) -C (51)
1.4 (3)	0.0 (3)
C (27) -C (28) -C (29) -C (30)	C (54) -C (49) -C (50) -C (51) -
177.31 (18)	179.71 (19)
C (33) -C (28) -C (29) -C (34)	C (49) -C (50) -C (51) -C (52)
179.59 (18)	1.5 (3)
C (27) -C (28) -C (29) -C (34) -	C (50) -C (51) -C (52) -C (53) -
1.7 (2)	1.4 (3)
C (28) -C (29) -C (30) -C (31)	C (49) -C (48) -C (53) -C (52)
0.5 (3)	1.7 (3)
C (34) -C (29) -C (30) -C (31)	C (47) -C (48) -C (53) -C (52)
179.2 (2)	179.8 (2)
C (29) -C (30) -C (31) -C (32)	C (51) -C (52) -C (53) -C (48) -
0.6 (3)	0.2 (3)
C (30) -C (31) -C (32) -C (33) -	C (50) -C (49) -C (54) -N (55) -
0.9 (4)	179.6 (2)
C (31) -C (32) -C (33) -C (28)	C (48) -C (49) -C (54) -N (55)
0.0 (3)	0.7 (2)
C (45) -C (41) -S (42) -C (43)	C (50) -C (49) -C (54) -N (56) -
0.73 (15)	0.3 (3)
C (46) -C (41) -S (42) -C (43)	C (48) -C (49) -C (54) -N (56)
177.63 (17)	179.96 (18)
C (41) -S (42) -C (43) -C (44) -	N (56) -C (54) -N (55) -C (47) -
0.17 (16)	179.91 (17)
S (42) -C (43) -C (44) -C (45) -	C (49) -C (54) -N (55) -C (47) -
0.4 (2)	0.7 (2)
C (46) -C (41) -C (45) -C (44) -	C (46) -C (47) -N (55) -C (54) -
177.94 (18)	177.57 (19)
S (42) -C (41) -C (45) -C (44) -	C (48) -C (47) -N (55) -C (54)
1.1 (2)	0.4 (2)
C (43) -C (44) -C (45) -C (41)	C (65) -C (61) -S (62) -C (63)
1.0 (2)	0.21 (15)
C (45) -C (41) -C (46) -C (47) -	C (66) -C (61) -S (62) -C (63)
178.0 (2)	178.35 (16)
S (42) -C (41) -C (46) -C (47)	C (61) -S (62) -C (63) -C (64)
5.6 (3)	0.02 (18)
C (41) -C (46) -C (47) -N (55)	S (62) -C (63) -C (64) -C (65) -
2.8 (3)	0.3 (3)
C (41) -C (46) -C (47) -C (48) -	C (66) -C (61) -C (65) -C (64) -
174.82 (18)	178.48 (18)
C (46) -C (47) -C (48) -C (53) -	S (62) -C (61) -C (65) -C (64) -
0.4 (3)	0.37 (19)

C (63) -C (64) -C (65) -C (61)	C (27) -C (28) -C (33) -C (32) -
0.4 (3)	177.2 (2)
C (65) -C (61) -C (66) -C (67)	C (30) -C (29) -C (34) -N (35) -
179.97 (18)	178.1 (2)
S (62) -C (61) -C (66) -C (67)	C (28) -C (29) -C (34) -N (35)
2.1 (3)	0.7 (2)
C (61) -C (66) -C (67) -N (75)	C (30) -C (29) -C (34) -N (36)
2.9 (3)	1.4 (3)
C (61) -C (66) -C (67) -C (68) -	C (28) -C (29) -C (34) -N (36) -
177.08 (17)	179.74 (18)
C (66) -C (67) -C (68) -C (73)	N (36) -C (34) -N (35) -C (27) -
2.1 (3)	178.90 (18)
N (75) -C (67) -C (68) -C (73) -	C (29) -C (34) -N (35) -C (27)
177.86 (19)	0.7 (2)
C (66) -C (67) -C (68) -C (69) -	C (26) -C (27) -N (35) -C (34)
179.12 (18)	176.22 (19)
N (75) -C (67) -C (68) -C (69)	C (28) -C (27) -N (35) -C (34) -
0.9 (2)	1.8 (2)
C (73) -C (68) -C (69) -C (70)	C (69) -C (68) -C (73) -C (72)
0.1 (3)	0.0 (3)
C (67) -C (68) -C (69) -C (70) -	C (67) -C (68) -C (73) -C (72)
178.90 (18)	178.63 (19)
C (73) -C (68) -C (69) -C (74)	C (70) -C (69) -C (74) -N (75)
178.42 (17)	178.0 (2)
C (67) -C (68) -C (69) -C (74) -	C (68) -C (69) -C (74) -N (75)
0.55 (19)	0.0 (2)
C (68) -C (69) -C (70) -C (71) -	C (70) -C (69) -C (74) -N (76) -
0.1 (3)	1.7 (3)
C (74) -C (69) -C (70) -C (71) -	C (68) -C (69) -C (74) -N (76) -
177.9 (2)	179.80 (18)
C (69) -C (70) -C (71) -C (72)	N (76) -C (74) -N (75) -C (67) -
0.0 (3)	179.61 (17)
C (70) -C (71) -C (72) -C (73)	C (69) -C (74) -N (75) -C (67)
0.1 (3)	0.6 (2)
C (71) -C (72) -C (73) -C (68)	C (66) -C (67) -N (75) -C (74)
0.0 (3)	179.11 (17)
C (29) -C (28) -C (33) -C (32)	C (68) -C (67) -N (75) -C (74) -
1.2 (3)	0.95 (19)

Table 6. Hydrogen bonds and other short intermolecular contacts, in Ångstroms and degrees.

D-H...A < (DHA)	d (D-H)	d (H...A)	d (D...A)
C (5) -H (5) ... S (42) #1	0.93	2.85	3.688 (2)
150.3			
N (16) -H (16A) ... S (62)	0.86	2.77	3.3228 (17)
123.1			

164.8	N(16)-H(16A)...N(75)	0.86	2.21	3.048(2)
144.1	C(25)-H(25)...N(16)#2	0.93	2.67	3.468(3)
111.9	N(36)-H(36A)...S(42)	0.86	2.96	3.3802(17)
174.6	N(36)-H(36A)...N(55)	0.86	2.15	3.007(2)
171.4	N(56)-H(56A)...N(35)	0.86	2.17	3.027(2)
131.1	N(76)-H(76A)...S(2)	0.86	2.94	3.5604(17)
156.8	N(76)-H(76A)...N(15)	0.86	2.19	3.001(2)
158.0	N(16)-H(16B)...C(34)#3	0.86	2.66	3.470
114.3	N(36)-H(36B)...C(30)#4	0.86	3.04	3.482
127.0	N(36)-H(36B)...S(62)#5	0.86	3.15	3.732
156.7	N(56)-H(56B)...C(74)	0.86	2.88	3.681
131.6	N(76)-H(76B)...C(23)	0.86	2.72	3.342

Symmetry transformations used to generate equivalent atoms:

#1 : 2-x, 1-y, 2-z #2 : 1-x, 1-y, 1-z #3 : x-1, y, z
 #4 : 2-x, -y, 1-z #5 : x+1, y, z

Crystal structure analysis of 1-CH-cyclo-C₄H₃S,3-amino-isoindoline

Crystal data: C₁₃H₁₀N₂S, M = 226.29. Triclinic, space group P-1 (no. 2), a = 12.0847(2), b = 13.8133(2), c = 13.9405(2) Å, α = 95.9946(13), β = 102.3784(14), γ = 95.4710(13) °, V = 2243.89(6) Å³. Z = 8, D_c = 1.340 g cm⁻³, F(000) = 944, T = 100.01(10) K, μ(Cu-Kα) = 23.14 cm⁻¹, λ(Cu-Kα) = 1.54184 Å.

The crystal was a yellow plate. From a sample under oil, one, *ca* 0.013 x 0.037 x 0.333 mm, was mounted on a small loop and fixed in the cold nitrogen stream on a Rigaku Oxford Diffraction XtaLAB Synergy diffractometer, equipped with Cu-Kα radiation, HyPix detector and mirror monochromator. Intensity data were measured by thin-slice ω-scans. Total no. of reflections recorded, to θ_{max} = 70.0°, was 23359 of which 8299 were unique (R_{int} = 0.031); 7729 were 'observed' with I > 2σ_I.

Data were processed using the CrysAlisPro-CCD and -RED (1) programs. The structure was determined by the intrinsic phasing routines in the SHELXT program (2A) and refined by full-matrix least-squares methods, on F²'s, in SHELXL (2B). There are four molecules in the asymmetric unit. The non-hydrogen atoms were refined with anisotropic thermal parameters. The hydrogen atoms were included in idealised positions and their U_{iso} values were refined freely. At the conclusion of the refinement, wR₂ = 0.128 and R₁ = 0.045 (2B) for all 8299 reflections weighted w = [σ²(F_o²) + (0.00761 P)² + 1.556 P]⁻¹ with P = (F_o² + 2F_c²)/3; for the 'observed' data only, R₁ = 0.043.

In the final difference map, the highest peak (*ca* 0.7 eÅ⁻³) was near C(25).

Scattering factors for neutral atoms were taken from reference (3). Computer programs used in this analysis have been noted above, and were run through WinGX (4) on a Dell Optiplex 780 PC at the University of East Anglia.

References

1. Programs CrysAlisPro, Rigaku Oxford Diffraction Ltd., Abingdon, UK (2018).
2. G. M. Sheldrick, Programs for crystal structure determination (SHELXT), *Acta Cryst.* (2015) **A71**, 3-8, and refinement (SHELXL), *Acta Cryst.* (2008) **A64**, 112-122 and (2015) **C71**, 3-8.
3. *International Tables for X-ray Crystallography*, Kluwer Academic Publishers, Dordrecht (1992). Vol. C, pp. 500, 219 and 193.

4. L. J. Farrugia, *J. Appl. Cryst.* (2012) **45**, 849–854.

Legends for Figures

Figure 1. View of one of the four essentially identical molecules of 1-CH-*cyclo*-C₄H₃S,3-amino-isoindoline, indicating the atom numbering scheme. Thermal ellipsoids are drawn at the 50% probability level.

Figure 2. Views of the four unique molecules, linked in dimer-pairs through hydrogen bonds.

Figure 3. View of the packing of molecules, along the *c* axis. Molecules are linked through N-H...X hydrogen bonds in an extensive 3-D network.

Notes on the structure

There are four independent molecules of the amino-isoindoline in this crystal and these are linked in pairs to form hydrogen bonded dimers. In each molecule, bond dimensions confirm (generally) that there are double bonds at C(3)-C(4), C(1)-C(5) and C(14)-N(15). All four molecules are close to planar, with the angle between the normals to the two ring groups at 12.67(6), 13.57(8), 7.66(6) and 5.15(7) °.

Table 6 shows clearly the four strong hydrogen bonds, as N(16)-H(16A)...N(75) that result in the dimer formation. The second H atom of each amine group forms a rather weaker contact, to a variety of acceptors, and there are other types of close intermolecular contacts also listed.

Crystal data and structure refinement for {C₈H₄N=CH-cyclo-(C₄H₃S)}-N-{C₈H₄NH=CH-cyclo-(C₄H₃S)}

Identification code	noraha3a		
Elemental formula	C ₂₆ H ₁₇ N ₃ S ₂		
Formula weight	435.54		
Crystal system, space group (no. 14)	Monoclinic, P 2 ₁ /c		
Unit cell dimensions 92.138 (4) °	a = 6.2874 (4) Å	α = 90 °	
	b = 14.8194 (4) Å	β =	
	c = 43.7886 (9) Å	γ = 90 °	
Volume	4077.2 (3) Å ³		
Z, Calculated density	8, 1.419 Mg/m ³		
F(000)	1808		
Absorption coefficient	2.513 mm ⁻¹		
Temperature	99.98 (13) K		
Wavelength	1.54184 Å		
Crystal colour, shape	dark orange rod		
Crystal size	0.070 x 0.018 x 0.016 mm		
Crystal mounting:	in a small loop, in oil, fixed in cold N ₂ stream		
On the diffractometer:			
Theta range for data collection	7.659 to 69.993 °		
Limiting indices 53<=l<=52	-7<=h<=7, -9<=k<=17, -		
Completeness to theta = 67.684	99.5 %		
Absorption correction equivalents	Semi-empirical from		
Max. and min. transmission	1.00000 and 0.76014		
Reflections collected (not including absences)	27022		

No. of unique reflections equivalents = 0.086]	7680 [R(int) for
No. of 'observed' reflections ($I > 2\sigma_I$)	6474
Structure determined by:	dual methods, in SHELXT
Refinement:	Full-matrix least-squares on F^2 , in SHELXL
Data / restraints / parameters	7680 / 0 / 561
Goodness-of-fit on F^2	1.089
Final R indices ('observed' data)	$R_1 = 0.066$, $wR_2 = 0.207$
Final R indices (all data)	$R_1 = 0.085$, $wR_2 = 0.235$
Reflections weighted:	
	$w = [\sigma^2(F_o^2) + (0.1252P)^2 + 12.0041P]^{-1}$ where $P = (F_o^2 + 2F_c^2) / 3$
Extinction coefficient	n/a
Largest diff. peak and hole	0.79 and $-0.60 \text{ e.}\text{\AA}^{-3}$
Location of largest difference peak	close to C(75)

Table 1. Atomic coordinates ($\times 10^4$) and equivalent isotropic displacement parameters ($\text{\AA}^2 \times 10^4$). $U(\text{eq})$ is defined as one third of the trace of the orthogonalized U_{ij} tensor. E.s.ds are in parentheses.

	x	y	z	$U(\text{eq})$
N(1)	6178 (5)	5509 (2)	6312.8 (7)	202 (6)
C(2)	7230 (6)	5600 (3)	6579.3 (8)	207 (7)
C(3)	6102 (5)	5204 (3)	6833.8 (8)	199 (7)
C(4)	6526 (6)	5213 (2)	7146.5 (8)	201 (7)
C(5)	4963 (6)	4869 (3)	7331.8 (8)	228 (8)
C(6)	3071 (6)	4511 (3)	7203.3 (9)	235 (8)
C(7)	2667 (6)	4504 (2)	6890.7 (9)	213 (7)
C(8)	4213 (6)	4865 (3)	6704.8 (8)	212 (7)
C(9)	4275 (6)	5053 (3)	6377.3 (8)	205 (7)
C(10)	2626 (6)	4893 (3)	6175.0 (8)	225 (8)
C(11)	2400 (6)	5092 (3)	5854.7 (9)	239 (8)
S(12)	4467.9 (16)	5351.7 (8)	5621.9 (2)	317 (3)
C(13)	2766 (8)	5485 (3)	5310.6 (10)	371 (10)
C(14)	702 (7)	5352 (3)	5381.9 (10)	370 (10)
C(15)	488 (6)	5129 (3)	5690.9 (10)	321 (9)

N(2)	9119 (5)	6036 (2)	6642.3 (7)	205 (6)
N(21)	9222 (5)	6830 (2)	6161.3 (7)	202 (6)
C(22)	9951 (5)	6575 (3)	6446.1 (8)	195 (7)
C(23)	11933 (5)	7069 (2)	6505.4 (8)	198 (7)
C(24)	13306 (6)	7057 (3)	6763.8 (8)	206 (7)
C(25)	15108 (6)	7591 (3)	6756.0 (9)	234 (8)
C(26)	15521 (6)	8121 (3)	6501.7 (9)	245 (8)
C(27)	14129 (6)	8136 (3)	6246.8 (9)	230 (8)
C(28)	12329 (6)	7591 (3)	6250.4 (8)	203 (7)
C(29)	10573 (6)	7452 (3)	6024.7 (8)	206 (7)
C(30)	10346 (6)	7855 (3)	5749.9 (8)	238 (8)
C(31)	8602 (6)	7778 (3)	5526.0 (8)	235 (8)
S(32)	90235 (16)	81621 (8)	5158.5 (2)	301 (3)
C(33)	6471 (7)	7908 (3)	5036.4 (9)	294 (9)
C(34)	5347 (6)	7557 (3)	5266.8 (9)	270 (8)
C(35)	6555 (6)	7483 (3)	5546.7 (8)	249 (8)
N(4)	4407 (5)	1442 (2)	6933.0 (7)	214 (6)
N(41)	4941 (5)	988 (2)	6409.6 (7)	203 (6)
C(42)	5482 (5)	1043 (2)	6705.6 (8)	192 (7)
C(43)	7470 (6)	571 (3)	6781.5 (8)	209 (7)
C(44)	8566 (6)	412 (3)	7057.8 (8)	211 (7)
C(45)	10396 (6)	-107 (3)	7051.5 (9)	245 (8)
C(46)	11137 (6)	-441 (3)	6775.5 (9)	250 (8)
C(47)	10042 (6)	-272 (3)	6500.5 (9)	244 (8)
C(48)	8196 (6)	234 (3)	6506.1 (8)	208 (7)
C(49)	6545 (6)	484 (2)	6273.4 (8)	199 (7)
C(50)	6475 (6)	189 (3)	5980.6 (8)	224 (8)
C(51)	4735 (6)	256 (3)	5757.1 (8)	246 (8)
S(52)	2357.5 (16)	781.0 (8)	5827.2 (2)	324 (3)
C(53)	1296 (7)	461 (3)	5478.2 (9)	325 (9)
C(54)	2685 (7)	-17 (3)	5310.7 (9)	342 (10)
C(55)	4739 (7)	-146 (3)	5460.6 (9)	260 (8)
N(61)	1624 (5)	2100 (2)	6605.4 (7)	204 (6)
C(62)	2648 (6)	1893 (3)	6878.6 (8)	200 (7)
C(63)	1351 (5)	2245 (2)	7119.5 (8)	194 (7)
C(64)	1682 (6)	2201 (3)	7434.5 (8)	211 (7)
C(65)	86 (6)	2538 (3)	7613.9 (9)	249 (8)
C(66)	-1770 (6)	2908 (3)	7477.5 (9)	235 (8)
C(67)	-2083 (6)	2959 (2)	7163.3 (9)	208 (7)
C(68)	-488 (5)	2618 (2)	6984.0 (8)	196 (7)
C(69)	-316 (5)	2543 (2)	6652.2 (8)	200 (7)
C(70)	-1733 (6)	2861 (3)	6438.2 (8)	208 (7)
C(71)	-1534 (6)	2860 (3)	6111.2 (9)	251 (8)
S(72)	-3753.3 (17)	2958.5 (9)	5872.8 (3)	411 (3)
C(73)	-2286 (8)	2959 (3)	5554.0 (10)	411 (11)
C(74)	-211 (8)	2892 (3)	5618.6 (10)	388 (11)
C(75)	260 (6)	2783 (3)	5932.5 (8)	264 (9)

Table 2. Molecular dimensions. Bond lengths are in Ångstroms, angles in degrees. E.s.ds are in parentheses.

N(1)-C(2)	C(25)-C(26)
1.327(5)	1.395(6)
N(1)-C(9)	C(26)-C(27)
1.412(5)	1.393(5)
C(2)-N(2)	C(27)-C(28)
1.370(5)	1.391(5)
C(2)-C(3)	C(28)-C(29)
1.466(5)	1.469(5)
C(3)-C(4)	C(29)-C(30)
1.385(5)	1.347(5)
C(3)-C(8)	C(30)-C(31)
1.390(5)	1.447(5)
C(4)-C(5)	C(31)-C(35)
1.394(5)	1.366(6)
C(5)-C(6)	C(31)-S(32)
1.401(5)	1.737(4)
C(6)-C(7)	S(32)-C(33)
1.383(5)	1.715(4)
C(7)-C(8)	C(33)-C(34)
1.397(5)	1.357(6)
C(8)-C(9)	C(34)-C(35)
1.463(5)	1.422(5)
C(9)-C(10)	N(4)-C(62)
1.359(5)	1.306(5)
C(10)-C(11)	N(4)-C(42)
1.435(5)	1.360(5)
C(11)-C(15)	N(41)-C(42)
1.378(5)	1.330(5)
C(11)-S(12)	N(41)-C(49)
1.726(4)	1.405(5)
S(12)-C(13)	C(42)-C(43)
1.713(4)	1.460(5)
C(13)-C(14)	C(43)-C(44)
1.361(7)	1.390(5)
C(14)-C(15)	C(43)-C(48)
1.404(6)	1.398(5)
N(2)-C(22)	C(44)-C(45)
1.298(5)	1.385(5)
N(21)-C(22)	C(45)-C(46)
1.366(5)	1.402(5)
N(21)-C(29)	C(46)-C(47)
1.402(5)	1.388(5)
C(22)-C(23)	C(47)-C(48)
1.460(5)	1.383(5)
C(23)-C(28)	C(48)-C(49)
1.389(5)	1.475(5)
C(23)-C(24)	C(49)-C(50)
1.397(5)	1.354(5)
C(24)-C(25)	C(50)-C(51)
1.384(5)	1.444(5)

1.429 (5)	C (51) -C (55)	1.402 (5)	C (65) -C (66)
1.723 (4)	C (51) -S (52)	1.385 (5)	C (66) -C (67)
1.712 (4)	S (52) -C (53)	1.392 (5)	C (67) -C (68)
1.360 (7)	C (53) -C (54)	1.465 (5)	C (68) -C (69)
1.440 (6)	C (54) -C (55)	1.354 (5)	C (69) -C (70)
1.372 (5)	N (61) -C (62)	1.442 (5)	C (70) -C (71)
1.407 (5)	N (61) -C (69)	1.401 (5)	C (71) -C (75)
1.454 (5)	C (62) -C (63)	1.718 (4)	C (71) -S (72)
1.389 (5)	C (63) -C (64)	1.702 (5)	S (72) -C (73)
1.394 (5)	C (63) -C (68)	1.328 (7)	C (73) -C (74)
1.390 (5)	C (64) -C (65)	1.404 (5)	C (74) -C (75)
105.8 (3)	C (2) -N (1) -C (9)	109.9 (3)	N (1) -C (9) -C (8)
128.7 (3)	N (1) -C (2) -N (2)	130.3 (4)	C (9) -C (10) -C (11)
112.9 (3)	N (1) -C (2) -C (3)	124.7 (4)	C (15) -C (11) -C (10)
118.4 (3)	N (2) -C (2) -C (3)	110.2 (3)	C (15) -C (11) -S (12)
122.4 (3)	C (4) -C (3) -C (8)	122.0 (3)	C (62) -N (4) -C (42)
131.8 (3)	C (4) -C (3) -C (2)	106.5 (3)	C (42) -N (41) -C (49)
105.4 (3)	C (8) -C (3) -C (2)	128.6 (3)	N (41) -C (42) -N (4)
117.3 (3)	C (3) -C (4) -C (5)	112.2 (3)	N (41) -C (42) -C (43)
120.7 (3)	C (4) -C (5) -C (6)	119.1 (3)	N (4) -C (42) -C (43)
121.5 (3)	C (7) -C (6) -C (5)	121.6 (3)	C (44) -C (43) -C (48)
117.9 (3)	C (6) -C (7) -C (8)	132.2 (3)	C (44) -C (43) -C (42)
120.3 (3)	C (3) -C (8) -C (7)	106.2 (3)	C (48) -C (43) -C (42)
106.0 (3)	C (3) -C (8) -C (9)	117.5 (3)	C (45) -C (44) -C (43)
133.5 (3)	C (7) -C (8) -C (9)	121.1 (4)	C (44) -C (45) -C (46)
125.8 (3)	C (10) -C (9) -N (1)	120.9 (4)	C (47) -C (46) -C (45)
124.0 (3)	C (10) -C (9) -C (8)	118.2 (3)	C (48) -C (47) -C (46)

120.7 (3)	C (47) -C (48) -C (43)	128.9 (3)	C (30) -C (29) -N (21)
133.9 (3)	C (47) -C (48) -C (49)	126.2 (4)	C (30) -C (29) -C (28)
105.2 (3)	C (43) -C (48) -C (49)	104.9 (3)	N (21) -C (29) -C (28)
125.1 (3)	C (50) -C (49) -N (41)	128.5 (4)	C (29) -C (30) -C (31)
124.8 (3)	C (50) -C (49) -C (48)	132.2 (3)	C (35) -C (31) -C (30)
109.8 (3)	N (41) -C (49) -C (48)	110.1 (3)	C (35) -C (31) -S (32)
128.1 (3)	C (49) -C (50) -C (51)	117.6 (3)	C (30) -C (31) -S (32)
124.1 (4)	C (55) -C (51) -C (50)	92.50 (19)	C (33) -S (32) -C (31)
125.0 (3)	C (10) -C (11) -S (12)	111.1 (3)	C (34) -C (33) -S (32)
92.0 (2)	C (13) -S (12) -C (11)	113.2 (4)	C (33) -C (34) -C (35)
111.9 (3)	C (14) -C (13) -S (12)	113.1 (3)	C (31) -C (35) -C (34)
112.5 (4)	C (13) -C (14) -C (15)	112.4 (3)	C (55) -C (51) -S (52)
113.4 (4)	C (11) -C (15) -C (14)	123.4 (3)	C (50) -C (51) -S (52)
121.7 (3)	C (22) -N (2) -C (2)	91.6 (2)	C (53) -S (52) -C (51)
112.5 (3)	C (22) -N (21) -C (29)	112.9 (3)	C (54) -C (53) -S (52)
130.1 (3)	N (2) -C (22) -N (21)	114.0 (4)	C (53) -C (54) -C (55)
123.6 (3)	N (2) -C (22) -C (23)	109.1 (4)	C (51) -C (55) -C (54)
106.2 (3)	N (21) -C (22) -C (23)	111.0 (3)	C (62) -N (61) -C (69)
122.3 (3)	C (28) -C (23) -C (24)	129.8 (3)	N (4) -C (62) -N (61)
108.3 (3)	C (28) -C (23) -C (22)	123.0 (3)	N (4) -C (62) -C (63)
129.4 (3)	C (24) -C (23) -C (22)	107.2 (3)	N (61) -C (62) -C (63)
117.0 (3)	C (25) -C (24) -C (23)	122.2 (3)	C (64) -C (63) -C (68)
121.2 (3)	C (24) -C (25) -C (26)	129.5 (3)	C (64) -C (63) -C (62)
121.2 (4)	C (27) -C (26) -C (25)	108.2 (3)	C (68) -C (63) -C (62)
118.0 (3)	C (28) -C (27) -C (26)	117.4 (3)	C (63) -C (64) -C (65)
120.2 (3)	C (23) -C (28) -C (27)	120.4 (3)	C (64) -C (65) -C (66)
108.0 (3)	C (23) -C (28) -C (29)	122.0 (3)	C (67) -C (66) -C (65)
131.7 (3)	C (27) -C (28) -C (29)	117.5 (3)	C (66) -C (67) -C (68)

C (67) -C (68) -C (63)	C (75) -C (71) -C (70)
120.5 (3)	131.0 (3)
C (67) -C (68) -C (69)	C (75) -C (71) -S (72)
132.0 (3)	108.7 (3)
C (63) -C (68) -C (69)	C (70) -C (71) -S (72)
107.5 (3)	120.3 (3)
C (70) -C (69) -N (61)	C (73) -S (72) -C (71)
127.8 (3)	92.6 (2)
C (70) -C (69) -C (68)	C (74) -C (73) -S (72)
126.1 (3)	112.6 (3)
N (61) -C (69) -C (68)	C (73) -C (74) -C (75)
106.0 (3)	112.8 (4)
C (69) -C (70) -C (71)	C (71) -C (75) -C (74)
127.4 (3)	113.1 (3)

Table 3. Anisotropic displacement parameters ($\text{\AA}^2 \times 10^4$) for the expression:

$$\exp \{-2\pi^2(h^2a^2U_{11} + \dots + 2hka^*b^*U_{12})\}$$

E.s.ds are in parentheses.

	U_{11}	U_{22}	U_{33}	U_{23}	U_{13}	
U_{12}						
N (1)	203 (14)	230 (16)	173 (14)	20 (12)	1 (11)	
5 (12)						
C (2)	193 (16)	248 (19)	182 (17)	29 (15)	34 (13)	
30 (14)						
C (3)	175 (16)	218 (18)	205 (17)	19 (14)	21 (13)	
8 (13)						
C (4)	198 (17)	216 (18)	188 (17)	8 (14)	-5 (13)	
16 (13)						
C (5)	269 (19)	245 (19)	170 (17)	16 (15)	24 (14)	
23 (15)						
C (6)	218 (17)	260 (20)	227 (18)	41 (15)	59 (14)	-
9 (14)						
C (7)	212 (17)	186 (18)	240 (18)	34 (15)	11 (14)	-
21 (14)						
C (8)	215 (17)	230 (19)	191 (17)	-13 (15)	17 (14)	-
2 (14)						
C (9)	198 (17)	226 (19)	193 (17)	-39 (14)	17 (13)	-
18 (14)						
C (10)	204 (17)	260 (20)	212 (18)	-15 (15)	36 (14)	
6 (14)						
C (11)	228 (18)	260 (20)	229 (19)	-40 (15)	-16 (14)	-
11 (14)						

S (12)	286 (5)	445 (6)	218 (5)	54 (4)	-17 (4)	-
68 (4)						
C (13)	480 (30)	430 (30)	191 (19)	-2 (18)	-76 (18)	-
50 (20)						
C (14)	420 (20)	440 (30)	240 (20)	-78 (19)	-138 (18)	
50 (20)						
C (15)	236 (19)	450 (30)	270 (20)	-125 (19)	-57 (16)	-
9 (17)						
N (2)	161 (14)	278 (17)	177 (14)	2 (13)	13 (11)	-
19 (12)						
N (21)	169 (14)	291 (17)	145 (14)	10 (12)	0 (11)	-
19 (12)						
C (22)	194 (16)	237 (19)	155 (16)	-30 (14)	24 (13)	
18 (14)						
C (23)	192 (17)	233 (19)	173 (17)	5 (14)	40 (13)	
24 (14)						
C (24)	207 (17)	228 (19)	186 (17)	10 (14)	23 (13)	
31 (14)						
C (25)	195 (17)	270 (20)	237 (18)	-23 (15)	-8 (14)	
19 (14)						
C (26)	186 (17)	270 (20)	280 (20)	-28 (16)	23 (15)	-
18 (14)						
C (27)	238 (18)	250 (20)	207 (18)	-9 (15)	56 (14)	-
6 (14)						
C (28)	220 (17)	209 (18)	180 (16)	-22 (14)	15 (13)	
28 (14)						
C (29)	196 (16)	260 (20)	160 (16)	-20 (14)	25 (13)	
7 (14)						
C (30)	232 (18)	290 (20)	192 (17)	11 (15)	30 (14)	-
25 (15)						
C (31)	283 (19)	280 (20)	142 (16)	35 (15)	23 (14)	
22 (15)						
S (32)	311 (5)	441 (6)	150 (4)	61 (4)	-9 (4)	-
88 (4)						
C (33)	330 (20)	360 (20)	185 (18)	23 (16)	-49 (15)	-
23 (17)						
C (34)	269 (19)	290 (20)	243 (19)	16 (16)	-29 (15)	-
18 (16)						
C (35)	294 (19)	270 (20)	182 (17)	21 (15)	17 (15)	-
4 (15)						
N (4)	179 (14)	276 (17)	189 (14)	7 (13)	18 (11)	
7 (12)						
N (41)	191 (14)	249 (16)	170 (14)	-13 (12)	21 (11)	-
15 (12)						
C (42)	199 (16)	174 (17)	203 (17)	42 (14)	14 (13)	-
12 (13)						
C (43)	194 (17)	241 (19)	194 (17)	0 (15)	26 (13)	-
42 (14)						
C (44)	210 (17)	236 (19)	188 (17)	-11 (14)	11 (13)	-
29 (14)						
C (45)	229 (18)	290 (20)	214 (18)	9 (16)	-5 (14)	-
19 (15)						
C (46)	194 (17)	260 (20)	290 (20)	25 (16)	7 (15)	
11 (14)						
C (47)	231 (18)	270 (20)	231 (18)	4 (15)	64 (14)	-
26 (15)						

48 (14)	C (48)	181 (16)	251 (19)	191 (17)	15 (15)	6 (13)	-
25 (13)	C (49)	194 (16)	219 (18)	183 (17)	2 (14)	15 (13)	-
12 (14)	C (50)	214 (17)	259 (19)	202 (18)	-19 (15)	30 (14)	-
44 (15)	C (51)	280 (19)	280 (20)	175 (17)	-18 (15)	32 (14)	-
6 (4)	S (52)	273 (5)	473 (7)	226 (5)	25 (4)	-11 (4)	
84 (18)	C (53)	310 (20)	440 (30)	218 (19)	47 (18)	-65 (16)	-
114 (19)	C (54)	440 (20)	360 (20)	214 (19)	45 (18)	-43 (17)	-
77 (15)	C (55)	370 (20)	198 (19)	202 (18)	-2 (15)	-117 (15)	-
9 (12)	N (61)	195 (14)	263 (17)	153 (14)	4 (12)	11 (11)	
49 (14)	C (62)	198 (17)	234 (19)	169 (17)	-3 (14)	4 (13)	-
15 (13)	C (63)	192 (17)	192 (18)	198 (17)	-5 (14)	-1 (13)	-
14 (14)	C (64)	222 (17)	227 (19)	183 (17)	-4 (14)	-7 (13)	-
20 (15)	C (65)	266 (19)	310 (20)	175 (17)	4 (15)	20 (14)	-
13 (15)	C (66)	215 (17)	280 (20)	215 (18)	-9 (15)	38 (14)	
11 (13)	C (67)	194 (17)	185 (18)	245 (18)	-11 (14)	-10 (14)	-
24 (13)	C (68)	197 (17)	188 (18)	200 (17)	5 (14)	-11 (13)	-
39 (13)	C (69)	181 (16)	214 (18)	204 (17)	-12 (14)	11 (13)	-
8 (14)	C (70)	194 (17)	226 (19)	202 (17)	-13 (14)	-14 (13)	-
4 (15)	C (71)	270 (19)	270 (20)	214 (19)	10 (15)	-44 (15)	-
16 (5)	S (72)	289 (5)	639 (8)	299 (6)	97 (5)	-63 (4)	-
90 (20)	C (73)	580 (30)	420 (30)	220 (20)	41 (19)	-110 (20)	-
60 (20)	C (74)	520 (30)	420 (30)	230 (20)	16 (19)	59 (19)	
55 (16)	C (75)	138 (16)	520 (30)	137 (16)	59 (16)	27 (13)	

Table 4. Hydrogen coordinates ($\times 10^4$) and isotropic displacement parameters ($\text{\AA}^2 \times 10^3$). All hydrogen atoms were included in idealised positions; for the C-H atoms, $U(\text{iso})$'s were set at $1.2 \cdot U(\text{eq})$ of the parent carbon atoms, but the N-H hydrogens were refined freely.

	x	y	z	U(iso)
H(4)	7801	5439	7229	24
H(5)	5179	4877	7543	27
H(6)	2064	4273	7331	28
H(7)	1406	4267	6807	26
H(10)	1459	4609	6257	27
H(13)	3201	5632	5116	44
H(14)	-439	5402	5242	44
H(15)	-818	5018	5777	39
H(21)	8062	6631	6075	29 (12)
H(24)	13021	6705	6933	25
H(25)	16062	7597	6924	28
H(26)	16750	8471	6502	29
H(27)	14395	8499	6079	28
H(30)	11454	8233	5697	29
H(33)	5928	7998	4838	35
H(34)	3929	7383	5244	32
H(35)	6007	7257	5726	30
H(44)	8089	645	7240	25
H(45)	11145	-236	7233	29
H(46)	12381	-781	6777	30
H(47)	10537	-492	6317	29
H(50)	7700	-92	5915	27
H(53)	-85	599	5410	39
H(54)	2338	-240	5117	41
H(55)	5885	-444	5378	31
H(61)	2105	1975	6429	70 (20)
H(64)	2923	1957	7522	25
H(65)	250	2518	7826	30
H(66)	-2822	3125	7602	28
H(67)	-3314	3212	7075	25
H(70)	-2977	3109	6510	25
H(73)	-2872	3001	5356	49
H(74)	818	2915	5472	47
H(75)	1623	2671	6013	32

Table 5. Torsion angles, in degrees. E.s.ds are in parentheses.

C (9) -N (1) -C (2) -N (2)	-	C (9) -C (10) -C (11) -C (15)	-
176.5 (4)		161.2 (4)	
C (9) -N (1) -C (2) -C (3)		C (9) -C (10) -C (11) -S (12)	
0.6 (4)		16.8 (6)	
N (1) -C (2) -C (3) -C (4)	-	C (15) -C (11) -S (12) -C (13)	-
173.8 (4)		1.0 (4)	
N (2) -C (2) -C (3) -C (4)		C (10) -C (11) -S (12) -C (13)	-
3.5 (6)		179.2 (4)	
N (1) -C (2) -C (3) -C (8)	-	C (11) -S (12) -C (13) -C (14)	
0.9 (4)		0.9 (4)	
N (2) -C (2) -C (3) -C (8)		S (12) -C (13) -C (14) -C (15)	-
176.4 (3)		0.6 (5)	
C (8) -C (3) -C (4) -C (5)	-	C (10) -C (11) -C (15) -C (14)	
0.4 (6)		179.0 (4)	
C (2) -C (3) -C (4) -C (5)		S (12) -C (11) -C (15) -C (14)	
171.5 (4)		0.8 (5)	
C (3) -C (4) -C (5) -C (6)		C (13) -C (14) -C (15) -C (11)	-
1.5 (6)		0.1 (6)	
C (4) -C (5) -C (6) -C (7)	-	N (1) -C (2) -N (2) -C (22)	
1.4 (6)		13.2 (6)	
C (5) -C (6) -C (7) -C (8)		C (3) -C (2) -N (2) -C (22)	-
0.2 (6)		163.7 (3)	
C (4) -C (3) -C (8) -C (7)	-	C (2) -N (2) -C (22) -N (21)	
0.9 (6)		1.1 (6)	
C (2) -C (3) -C (8) -C (7)	-	C (2) -N (2) -C (22) -C (23)	
174.6 (3)		178.6 (3)	
C (4) -C (3) -C (8) -C (9)		C (29) -N (21) -C (22) -N (2)	
174.6 (3)		178.2 (4)	
C (2) -C (3) -C (8) -C (9)		C (29) -N (21) -C (22) -C (23)	
0.8 (4)		0.4 (4)	
C (6) -C (7) -C (8) -C (3)		N (2) -C (22) -C (23) -C (28)	-
0.9 (6)		178.9 (3)	
C (6) -C (7) -C (8) -C (9)	-	N (21) -C (22) -C (23) -C (28)	-
173.0 (4)		0.9 (4)	
C (2) -N (1) -C (9) -C (10)		N (2) -C (22) -C (23) -C (24)	
173.4 (4)		1.6 (6)	
C (2) -N (1) -C (9) -C (8)		N (21) -C (22) -C (23) -C (24)	
0.0 (4)		179.6 (4)	
C (3) -C (8) -C (9) -C (10)	-	C (28) -C (23) -C (24) -C (25)	-
174.1 (4)		0.1 (5)	
C (7) -C (8) -C (9) -C (10)		C (22) -C (23) -C (24) -C (25)	
0.4 (7)		179.2 (4)	
C (3) -C (8) -C (9) -N (1)	-	C (23) -C (24) -C (25) -C (26)	
0.6 (4)		0.3 (5)	
C (7) -C (8) -C (9) -N (1)		C (24) -C (25) -C (26) -C (27)	
174.0 (4)		0.4 (6)	
N (1) -C (9) -C (10) -C (11)		C (25) -C (26) -C (27) -C (28)	-
3.0 (7)		1.3 (6)	
C (8) -C (9) -C (10) -C (11)		C (24) -C (23) -C (28) -C (27)	-
175.6 (4)		0.8 (5)	

C (22) -C (23) -C (28) -C (27)		C (42) -N (41) -C (49) -C (48)	-
179.7 (3)		1.1 (4)	
C (24) -C (23) -C (28) -C (29)	-	C (47) -C (48) -C (49) -C (50)	
179.4 (3)		4.2 (7)	
C (22) -C (23) -C (28) -C (29)		C (43) -C (48) -C (49) -C (50)	-
1.1 (4)		171.0 (4)	
C (26) -C (27) -C (28) -C (23)		C (47) -C (48) -C (49) -N (41)	
1.5 (5)		177.5 (4)	
C (26) -C (27) -C (28) -C (29)		C (43) -C (48) -C (49) -N (41)	
179.8 (4)		2.3 (4)	
C (22) -N (21) -C (29) -C (30)	-	N (41) -C (49) -C (50) -C (51)	-
178.9 (4)		5.3 (6)	
C (22) -N (21) -C (29) -C (28)		C (48) -C (49) -C (50) -C (51)	
0.2 (4)		167.0 (4)	
C (23) -C (28) -C (29) -C (30)		C (49) -C (50) -C (51) -C (55)	-
178.3 (4)		174.3 (4)	
C (49) -N (41) -C (42) -N (4)	-	C (49) -C (50) -C (51) -S (52)	
178.2 (4)		2.0 (6)	
C (49) -N (41) -C (42) -C (43)	-	C (55) -C (51) -S (52) -C (53)	
0.5 (4)		1.7 (3)	
C (62) -N (4) -C (42) -N (41)	-	C (50) -C (51) -S (52) -C (53)	-
4.1 (6)		175.0 (4)	
C (62) -N (4) -C (42) -C (43)		C (51) -S (52) -C (53) -C (54)	-
178.3 (3)		0.8 (4)	
N (41) -C (42) -C (43) -C (44)	-	S (52) -C (53) -C (54) -C (55)	-
176.2 (4)		0.3 (5)	
N (4) -C (42) -C (43) -C (44)		C (50) -C (51) -C (55) -C (54)	
1.7 (6)		174.6 (4)	
N (41) -C (42) -C (43) -C (48)		S (52) -C (51) -C (55) -C (54)	-
2.0 (4)		2.1 (4)	
N (4) -C (42) -C (43) -C (48)		C (53) -C (54) -C (55) -C (51)	
180.0 (3)		1.5 (5)	
C (48) -C (43) -C (44) -C (45)	-	C (42) -N (4) -C (62) -N (61)	-
1.0 (5)		4.0 (6)	
C (42) -C (43) -C (44) -C (45)		C (42) -N (4) -C (62) -C (63)	
176.9 (4)		173.3 (3)	
C (43) -C (44) -C (45) -C (46)		C (69) -N (61) -C (62) -N (4)	
1.5 (6)		175.7 (4)	
C (44) -C (45) -C (46) -C (47)	-	C (69) -N (61) -C (62) -C (63)	-
0.9 (6)		2.0 (4)	
C (45) -C (46) -C (47) -C (48)	-	N (4) -C (62) -C (63) -C (64)	
0.2 (6)		1.4 (6)	
C (46) -C (47) -C (48) -C (43)		N (61) -C (62) -C (63) -C (64)	
0.6 (6)		179.2 (4)	
C (46) -C (47) -C (48) -C (49)	-	N (4) -C (62) -C (63) -C (68)	-
174.0 (4)		174.9 (3)	
C (44) -C (43) -C (48) -C (47)		N (61) -C (62) -C (63) -C (68)	
0.0 (6)		2.9 (4)	
C (42) -C (43) -C (48) -C (47)	-	C (68) -C (63) -C (64) -C (65)	
178.4 (3)		0.7 (6)	
C (44) -C (43) -C (48) -C (49)		C (62) -C (63) -C (64) -C (65)	-
176.0 (3)		175.1 (4)	
C (42) -C (43) -C (48) -C (49)	-	C (63) -C (64) -C (65) -C (66)	-
2.5 (4)		0.2 (6)	
C (42) -N (41) -C (49) -C (50)		C (64) -C (65) -C (66) -C (67)	-
172.1 (4)		0.5 (6)	

C (65) -C (66) -C (67) -C (68)		C (31) -S (32) -C (33) -C (34)	
0.7 (6)		0.7 (4)	
C (66) -C (67) -C (68) -C (63)	-	S (32) -C (33) -C (34) -C (35)	-
0.2 (5)		0.4 (5)	
C (66) -C (67) -C (68) -C (69)		C (30) -C (31) -C (35) -C (34)	
178.3 (4)		177.8 (4)	
C (64) -C (63) -C (68) -C (67)	-	S (32) -C (31) -C (35) -C (34)	
0.5 (6)		0.7 (4)	
C (62) -C (63) -C (68) -C (67)		C (33) -C (34) -C (35) -C (31)	-
176.2 (3)		0.2 (5)	
C (64) -C (63) -C (68) -C (69)	-	C (63) -C (68) -C (69) -C (70)	-
179.4 (3)		177.0 (4)	
C (62) -C (63) -C (68) -C (69)	-	C (67) -C (68) -C (69) -N (61)	-
2.7 (4)		177.2 (4)	
C (62) -N (61) -C (69) -C (70)		C (63) -C (68) -C (69) -N (61)	
178.8 (4)		1.5 (4)	
C (62) -N (61) -C (69) -C (68)		N (61) -C (69) -C (70) -C (71)	-
0.3 (4)		3.4 (6)	
C (67) -C (68) -C (69) -C (70)		C (68) -C (69) -C (70) -C (71)	
4.3 (7)		174.9 (4)	
C (27) -C (28) -C (29) -C (30)	-	C (69) -C (70) -C (71) -C (75)	-
0.1 (7)		20.0 (7)	
C (23) -C (28) -C (29) -N (21)	-	C (69) -C (70) -C (71) -S (72)	
0.8 (4)		159.6 (3)	
C (27) -C (28) -C (29) -N (21)	-	C (75) -C (71) -S (72) -C (73)	-
179.2 (4)		3.1 (3)	
N (21) -C (29) -C (30) -C (31)		C (70) -C (71) -S (72) -C (73)	
2.4 (7)		177.2 (4)	
C (28) -C (29) -C (30) -C (31)	-	C (71) -S (72) -C (73) -C (74)	-
176.6 (4)		0.3 (4)	
C (29) -C (30) -C (31) -C (35)		S (72) -C (73) -C (74) -C (75)	
18.0 (7)		3.6 (6)	
C (29) -C (30) -C (31) -S (32)	-	C (70) -C (71) -C (75) -C (74)	-
165.1 (3)		174.7 (4)	
C (35) -C (31) -S (32) -C (33)	-	S (72) -C (71) -C (75) -C (74)	
0.8 (3)		5.6 (5)	
C (30) -C (31) -S (32) -C (33)	-	C (73) -C (74) -C (75) -C (71)	-
178.4 (3)		6.1 (6)	

Table 6. Hydrogen bonds, in Ångstroms and degrees.

D-H...A < (DHA)	d(D-H)	d(H...A)	d(D...A)
C (75) -H (75) ... S (72) #1	0.93	3.02	3.792 (4)
141.0			
N (21) -H (21) ... N (1)	0.86	2.31	2.834 (4)
119.3			

N(61)-H(61)...N(41)	0.86	2.31	2.817(4)
117.8			

Symmetry transformation used to generate equivalent atoms:

#1 : x+1, y, z

Crystal structure analysis of $\{C_8H_4N=CH-cyclo-(C_4H_3S)\}-N-\{C_8H_4NH=CH-cyclo-(C_4H_3S)\}$

Crystal data: $C_{26}H_{17}N_3S_2$, $M = 435.54$. Monoclinic, space group $P2_1/c$ (no. 14), $a = 6.2874(4)$, $b = 14.8194(4)$, $c = 43.7886(9)$ Å, $\beta = 92.138(4)^\circ$, $V = 4077.2(3)$ Å³. $Z = 8$, $D_c = 1.419$ g cm⁻³, $F(000) = 1808$, $T = 99.98(13)$ K, $\mu(Cu-K\alpha) = 25.1$ cm⁻¹, $\lambda(Cu-K\alpha) = 1.54184$ Å.

The crystal was a dark orange rod. From a sample under oil, one, *ca* 0.016 x 0.018 x 0.070 mm, was mounted on a small loop and fixed in the cold nitrogen stream on a Rigaku Oxford Diffraction XtaLAB Synergy diffractometer, equipped with Cu-K α radiation, HyPix detector and mirror monochromator. Intensity data were measured by thin-slice ω -scans. Total no. of reflections recorded, to $\theta_{max} = 70.0^\circ$, was 27022 of which 7680 were unique ($R_{int} = 0.086$); 6474 were 'observed' with $I > 2\sigma_I$.

Data were processed using the CrysAlisPro-CCD and -RED (1) programs. The structure was determined by the intrinsic phasing routines in the SHELXT program (2A) and refined by full-matrix least-squares methods, on F^2 's, in SHELXL (2B). There are two very similar molecules in this crystal. The non-hydrogen atoms were refined with anisotropic thermal parameters. The C-H hydrogen atoms were included in idealised positions and their Uiso values were set to ride on the Ueq values of the parent carbon atoms. Hydrogen atoms were also placed on all the nitrogen atoms; on refinement of their Uiso values, only one on each molecule gave an acceptable result, indicating the likely N-H groups. At the conclusion of the refinement, $wR_2 = 0.235$ and $R_1 = 0.085$ (2B) for all 7680 reflections weighted $w = [\sigma^2(F_o^2) + (0.1252 P)^2 + 12.00 P]^{-1}$ with $P = (F_o^2 + 2F_c^2)/3$; for the 'observed' data only, $R_1 = 0.066$.

In the final difference map, the highest peak (*ca* 0.8 eÅ⁻³) was close to C(75).

Scattering factors for neutral atoms were taken from reference (3). Computer programs used in this analysis have been noted above, and were run through WinGX (4) on a Dell Optiplex 780 PC at the University of East Anglia.

References

1. Programs CrysAlisPro, Rigaku Oxford Diffraction Ltd., Abingdon, UK (2018).

2. G. M. Sheldrick, Programs for crystal structure determination (SHELXT), *Acta Cryst.* (2015) **A71**, 3-8, and refinement (SHELXL), *Acta Cryst.* (2008) **A64**, 112-122 and (2015) **C71**, 3-8.
3. '*International Tables for X-ray Crystallography*', Kluwer Academic Publishers, Dordrecht (1992). Vol. C, pp. 500, 219 and 193.
4. L. J. Farrugia, *J. Appl. Cryst.* (2012) **45**, 849–854.

Legends for Figures

Figure 1. View of the two essentially identical molecules of $\{C_8H_4N=CH-cyclo-(C_4H_3S)\}-N-\{C_8H_4NH=CH-cyclo-(C_4H_3S)\}$, indicating the atom numbering scheme. Thermal ellipsoids are drawn at the 50% probability level.

Figure 2. View along the *a* axis of the packing of molecules,.

Notes on the structure

From a second crystal, the diffraction data were stronger, and produced an improved refinement with lower R-factors and more precise molecular dimensions. The preliminary coordinates, from the first crystal, were input into the SHELXL system and the refinement process was continued smoothly to convergence.

The assignment of the hydrogen atoms on N(21) and N(61) was confirmed; these are the donor atoms in intramolecular hydrogen bonds to N(1) and N(41) respectively, Figure 1. The arrangement of single and double bonds in the molecules was also confirmed as shown in the formula diagram.

The unit cell contents are shown in Figure 2. There is no extensive $\pi \dots \pi$ stacking in the crystal despite the variety of planar aromatic units.

Crystal data and structure refinement for [La₂ (phthal {(porph)-O(CH₂)₃OC₆H₄O(CH₂)₃O-(porph)})]

Identification code	noraha6
Elemental formula H ₂ C ₁₂)	C ₁₃₂ H ₈₆ La ₂ N ₁₆ O ₄ , 2(C
Formula weight	2407.83
Crystal system, space group	Triclinic, P-1 (no.2)
Unit cell dimensions 85.3515(14) °	a = 13.5286(2) Å α =
70.9603(17) °	b = 14.4358(2) Å β =
77.8062(14) °	c = 15.5074(3) Å γ =
Volume	2798.02(9) Å ³
Z, Calculated density	1, 1.429 Mg/m ³
F(000)	1220
Absorption coefficient	0.913 mm ⁻¹
Temperature	99.98(11) K
Wavelength	0.71073 Å
Crystal colour, shape	dark purple prism
Crystal size	0.600 x 0.123 x 0.072 mm
Crystal mounting: N ₂ stream	on a small loop, in oil, fixed in cold
On the diffractometer:	
Theta range for data collection	3.551 to 27.500 °
Limiting indices -20<=l<=20	-17<=h<=17, -18<=k<=18,
Completeness to theta = 25.242	99.7 %
Absorption correction equivalents	Semi-empirical from
Max. and min. transmission	1.00000 and 0.70769

Reflections collected (not including absences) 76444

No. of unique reflections 12788 [R(int) for
equivalents = 0.069]

No. of 'observed' reflections ($I > 2\sigma_I$) 11478

Structure determined by: dual methods, in SHELXT

Refinement: Full-matrix least-squares on F^2 , in
SHELXL

Data / restraints / parameters 12788 / 0 / 811

Goodness-of-fit on F^2 1.101

Final R indices ('observed' data) $R_1 = 0.061$, $wR_2 = 0.164$

Final R indices (all data) $R_1 = 0.068$, $wR_2 = 0.167$

Reflections weighted:
 $w = [\sigma^2(F_o^2) + (0.0770P)^2 + 14.679P]^{-1}$ where $P = (F_o^2 + 2F_c^2) / 3$

Extinction coefficient n/a

Largest diff. peak and hole 3.30 and $-1.22 \text{ e.}\text{\AA}^{-3}$

Location of largest difference peak close to Cl(91)

Table 1. Atomic coordinates ($\times 10^4$) and equivalent isotropic displacement parameters ($\text{\AA}^2 \times 10^4$). $U(\text{eq})$ is defined as one third of the trace of the orthogonalized U_{ij} tensor. E.s.ds are in parentheses.

S.o.f.#	x	y	z	U(eq)
La	6220.4(2)	4330.6(2)	5359.8(2)	171.3(9)
N(1)	5823(3)	4743(3)	3720(3)	198(7)
C(2)	6455(4)	5310(3)	3134(3)	211(9)
C(3)	6911(4)	4884(3)	2235(3)	243(10)
C(4)	7598(4)	5180(4)	1417(3)	311(11)
C(5)	7903(5)	4599(5)	671(4)	423(14)
C(6)	7528(6)	3739(5)	737(4)	511(18)
C(7)	6849(5)	3458(4)	1549(4)	415(14)
C(8)	6546(4)	4041(4)	2296(3)	259(10)
C(9)	5858(4)	3974(3)	3234(3)	208(9)

N(10)	5329 (3)	3264 (3)	3537 (3)	234 (8)	
N(11)	4495 (3)	3816 (3)	5094 (3)	208 (8)	
C(12)	4685 (4)	3209 (3)	4389 (3)	228 (9)	
C(13)	4048 (4)	2482 (3)	4694 (3)	243 (10)	
C(14)	3896 (5)	1755 (4)	4234 (4)	304 (11)	
C(15)	3164 (5)	1229 (4)	4714 (4)	369 (13)	
C(16)	2590 (5)	1385 (4)	5641 (4)	362 (12)	
C(17)	2734 (5)	2103 (4)	6109 (4)	308 (11)	
C(18)	3471 (4)	2654 (3)	5612 (3)	242 (10)	
C(19)	3765 (4)	3495 (3)	5847 (3)	215 (9)	
N(20)	6655 (3)	6119 (3)	3328 (3)	228 (8)	
N(21)	7983 (3)	3695 (3)	4248 (3)	213 (8)	
C(22)	8694 (4)	4256 (3)	3772 (3)	239 (9)	
C(23)	9355 (5)	3801 (4)	2917 (4)	348 (12)	
C(24)	9032 (5)	2980 (4)	2889 (4)	369 (13)	
C(25)	8184 (4)	2901 (3)	3730 (3)	257 (10)	
C(26)	7655 (4)	2129 (3)	3984 (3)	240 (9)	
N(27)	6585 (3)	2593 (3)	5576 (3)	211 (8)	
C(28)	6905 (4)	2000 (3)	4842 (3)	226 (9)	
C(29)	6421 (4)	1172 (3)	5108 (3)	267 (10)	
C(30)	5831 (4)	1264 (3)	5998 (3)	260 (10)	
C(31)	5937 (4)	2148 (3)	6302 (3)	216 (9)	
C(32)	5492 (4)	2489 (3)	7198 (3)	227 (9)	
N(33)	6147 (3)	3999 (3)	6973 (3)	194 (7)	
C(34)	5613 (4)	3334 (3)	7513 (3)	218 (9)	
C(35)	5241 (5)	3621 (4)	8453 (3)	319 (12)	
C(36)	5550 (5)	4450 (4)	8481 (3)	298 (11)	
C(37)	6134 (4)	4678 (3)	7553 (3)	208 (9)	
C(38)	6658 (4)	5451 (3)	7289 (3)	235 (9)	
N(39)	7545 (3)	5112 (3)	5643 (3)	207 (8)	
C(40)	7331 (4)	5632 (3)	6410 (3)	228 (9)	
C(41)	7942 (4)	6378 (3)	6189 (3)	268 (10)	
C(42)	8528 (4)	6301 (3)	5293 (3)	257 (10)	
C(43)	8304 (4)	5489 (3)	4953 (3)	214 (9)	
C(44)	8806 (4)	5118 (3)	4068 (3)	227 (9)	
C(261)	7951 (4)	1341 (3)	3313 (3)	279 (10)	
C(262)	7208 (5)	1162 (4)	2936 (4)	358 (12)	
C(263)	7454 (6)	388 (5)	2371 (4)	450 (15)	
C(264)	8438 (6)	-196 (4)	2161 (4)	430 (15)	
C(265)	9188 (5)	-23 (4)	2522 (4)	407 (14)	
C(266)	8935 (5)	752 (4)	3102 (4)	352 (12)	
C(321)	4871 (5)	1864 (4)	7890 (3)	293 (11)	
C(322)	3765 (5)	2083 (5)	8203 (4)	380 (13)	
C(323)	3190 (7)	1482 (6)	8819 (4)	567 (20)	
C(324)	3715 (11)	667 (6)	9137 (4)	811 (40)	
C(325)	4794 (10)	444 (5)	8834 (5)	633 (30)	
C(326)	5376 (7)	1042 (4)	8210 (4)	465 (16)	
O(327)	2776 (7)	261 (6)	9720 (6)	432 (20)	
0.5					
	C(328)	3160 (10)	-710 (9)	9908 (10)	428 (30)
0.5					
	C(329)	2163 (6)	-1122 (5)	10416 (5)	461 (15)
0.5					
	C(330)	1461 (12)	-1107 (10)	9872 (10)	475 (30)
0.5					

	O (331)	632 (7)	-1576 (6)	10319 (6)	429 (20)
0.5	C (332)	-141 (16)	-1505 (17)	9948 (9)	593 (50)
0.5	C (333)	-703 (10)	-610 (9)	9735 (8)	390 (30)
0.5	C (334)	-1415 (10)	-561 (10)	9263 (8)	421 (30)
0.5	C (335)	-1542 (10)	-1361 (9)	8818 (12)	557 (40)
0.5	C (336)	-985 (9)	-2238 (9)	9114 (8)	396 (30)
0.5	C (337)	-302 (10)	-2352 (8)	9568 (8)	356 (30)
0.5	O (451)	-2039 (7)	300 (7)	9097 (6)	429 (20)
0.5	C (450)	-2163 (6)	1122 (5)	9584 (5)	461 (15)
0.5	C (449)	-2846 (9)	1929 (9)	9322 (8)	367 (30)
0.5	C (448)	-2300 (9)	2408 (8)	8433 (8)	323 (20)
0.5	O (447)	-1471 (6)	2754 (6)	8594 (5)	314 (16)
0.5	C (381)	6515 (4)	6137 (4)	8020 (3)	263 (10)
	C (382)	5815 (5)	6998 (4)	8065 (4)	409 (14)
	C (383)	5673 (6)	7649 (5)	8729 (5)	507 (17)
	C (384)	6203 (6)	7459 (4)	9342 (4)	437 (15)
0.75	C (385)	6806 (8)	6604 (7)	9355 (6)	378 (19)
0.75	C (386)	6981 (7)	5940 (6)	8683 (6)	316 (16)
0.75	C (884)	6203 (6)	7459 (4)	9342 (4)	437 (15)
0.25	C (885)	7240 (30)	6620 (30)	9100 (30)	604 (110) *
0.25	C (886)	7430 (30)	6010 (30)	8440 (20)	506 (90) *
0.25	C (441)	9547 (4)	5662 (3)	3387 (3)	238 (9)
	C (442)	9328 (4)	5999 (4)	2587 (4)	312 (11)
	C (443)	9980 (5)	6526 (4)	1947 (4)	360 (12)
	C (444)	10870 (4)	6718 (4)	2096 (4)	324 (11)
	C (445)	11105 (4)	6383 (4)	2884 (4)	345 (12)
	C (446)	10455 (4)	5858 (4)	3519 (4)	308 (11)
	C1 (91)	-1500 (5)	739 (10)	16513 (8)	2227 (70)
0.5	C (92)	-480 (30)	1620 (20)	15649 (12)	1431 (160)
0.5	C1 (93)	223 (4)	1407 (5)	15009 (10)	1608 (50)
0.5	C1 (95)	135 (8)	1618 (9)	10545 (9)	1597 (40)
0.5	C1 (97)	578 (11)	3487 (12)	10355 (9)	2032 (60)

- site occupancy, if different from 1.
* - U(iso) ($\text{\AA}^2 \times 10^4$)

Table 2. Molecular dimensions. Bond lengths are in Ångstroms, angles in degrees. E.s.ds are in parentheses.

La-N(27)	La-N(11)
2.470 (4)	2.753 (4)
La-N(39)	La-N(1)
2.475 (4)	2.760 (4)
La-N(21)	La-N(11) #1
2.480 (4)	2.764 (4)
La-N(33)	La-N(1) #1
2.482 (4)	2.764 (4)
	La-La#1
	3.9041 (5)
N(27)-La-N(39)	N(39)-La-N(11) #1
113.36 (13)	79.59 (12)
N(27)-La-N(21)	N(21)-La-N(11) #1
72.41 (13)	109.97 (12)
N(39)-La-N(21)	N(33)-La-N(11) #1
72.51 (13)	116.88 (12)
N(27)-La-N(33)	N(11)-La-N(11) #1
72.31 (13)	89.91 (11)
N(39)-La-N(33)	N(1)-La-N(11) #1
72.61 (12)	59.97 (11)
N(21)-La-N(33)	N(27)-La-N(1) #1
113.46 (13)	115.73 (12)
N(27)-La-N(11)	N(39)-La-N(1) #1
77.43 (13)	110.14 (12)
N(39)-La-N(11)	N(21)-La-N(1) #1
168.61 (12)	167.69 (12)
N(21)-La-N(11)	N(33)-La-N(1) #1
115.75 (12)	78.50 (12)
N(33)-La-N(11)	N(11)-La-N(1) #1
108.93 (12)	60.06 (11)
N(27)-La-N(1)	N(1)-La-N(1) #1
108.79 (12)	90.06 (11)
N(39)-La-N(1)	N(11) #1-La-N(1) #1
116.88 (12)	59.87 (11)
N(21)-La-N(1)	N(27)-La-La#1
78.28 (12)	122.35 (10)
N(33)-La-N(1)	N(39)-La-La#1
167.42 (12)	124.29 (9)
N(11)-La-N(1)	N(21)-La-La#1
60.05 (11)	123.24 (9)
N(27)-La-N(11) #1	N(33)-La-La#1
166.54 (13)	123.29 (9)

N(11)-La-La#1	N(11)#1-La-La#1
45.07(8)	44.84(8)
N(1)-La-La#1	N(1)#1-La-La#1
45.07(8)	44.99(8)
N(1)-C(9)	N(21)-C(25)
1.376(6)	1.381(6)
N(1)-C(2)	C(22)-C(44)
1.378(6)	1.413(7)
C(2)-N(20)	C(22)-C(23)
1.331(6)	1.452(7)
C(2)-C(3)	C(23)-C(24)
1.456(6)	1.355(8)
C(3)-C(8)	C(24)-C(25)
1.393(7)	1.444(7)
C(3)-C(4)	C(25)-C(26)
1.401(7)	1.411(7)
C(4)-C(5)	C(26)-C(28)
1.383(8)	1.412(7)
C(5)-C(6)	C(26)-C(261)
1.421(9)	1.506(7)
C(6)-C(7)	N(27)-C(28)
1.383(9)	1.377(6)
C(7)-C(8)	N(27)-C(31)
1.386(7)	1.387(6)
C(8)-C(9)	C(28)-C(29)
1.456(6)	1.448(7)
C(9)-N(10)	C(29)-C(30)
1.340(6)	1.351(7)
N(10)-C(12)	C(30)-C(31)
1.332(6)	1.446(6)
N(11)-C(12)	C(31)-C(32)
1.381(6)	1.406(7)
N(11)-C(19)	C(32)-C(34)
1.381(6)	1.409(6)
C(12)-C(13)	C(32)-C(321)
1.450(7)	1.500(7)
C(13)-C(18)	N(33)-C(37)
1.397(7)	1.378(6)
C(13)-C(14)	N(33)-C(34)
1.399(7)	1.383(6)
C(14)-C(15)	C(34)-C(35)
1.362(8)	1.443(7)
C(15)-C(16)	C(35)-C(36)
1.404(9)	1.357(7)
C(16)-C(17)	C(36)-C(37)
1.392(8)	1.447(7)
C(17)-C(18)	C(37)-C(38)
1.398(7)	1.408(6)
C(18)-C(19)	C(38)-C(40)
1.462(7)	1.411(7)
C(19)-N(20)#1	C(38)-C(381)
1.332(6)	1.503(6)
N(21)-C(22)	N(39)-C(40)
1.377(6)	1.375(6)

N (39) -C (43)	C (333) -C (334)
1.387 (6)	1.375 (18)
C (40) -C (41)	C (334) -C (335)
1.446 (6)	1.461 (19)
C (41) -C (42)	C (335) -C (336)
1.357 (7)	1.45 (2)
C (42) -C (43)	C (336) -C (337)
1.449 (7)	1.310 (19)
C (43) -C (44)	O (451) -C (450)
1.411 (7)	1.408 (11)
C (44) -C (441)	C (450) -C (449)
1.498 (6)	1.445 (15)
C (261) -C (266)	C (449) -C (448)
1.374 (8)	1.523 (14)
C (261) -C (262)	C (448) -O (447)
1.391 (8)	1.419 (13)
C (262) -C (263)	C (381) -C (386)
1.392 (8)	1.354 (9)
C (263) -C (264)	C (381) -C (382)
1.370 (10)	1.386 (8)
C (264) -C (265)	C (381) -C (886)
1.380 (10)	1.55 (4)
C (265) -C (266)	C (382) -C (383)
1.407 (8)	1.390 (8)
C (321) -C (326)	C (383) -C (884)
1.379 (8)	1.345 (10)
C (321) -C (322)	C (383) -C (384)
1.388 (9)	1.345 (10)
C (322) -C (323)	C (384) -C (385)
1.390 (8)	1.331 (12)
C (323) -C (324)	C (385) -C (386)
1.383 (14)	1.402 (11)
C (324) -C (325)	C (884) -C (885)
1.354 (15)	1.62 (4)
C (325) -C (326)	C (885) -C (886)
1.399 (10)	1.32 (5)
O (327) -C (328)	C (441) -C (442)
1.430 (15)	1.395 (7)
C (328) -C (329)	C (441) -C (446)
1.537 (13)	1.397 (7)
C (329) -C (330)	C (442) -C (443)
1.457 (15)	1.390 (7)
C (330) -O (331)	C (443) -C (444)
1.390 (15)	1.384 (8)
O (331) -C (332)	C (444) -C (445)
1.33 (2)	1.386 (8)
C (332) -C (333)	C (445) -C (446)
1.43 (3)	1.383 (7)
C (332) -C (337)	
1.49 (2)	
C (9) -N (1) -C (2)	C (2) -N (1) -La
107.4 (4)	114.8 (3)
C (9) -N (1) -La	C (9) -N (1) -La#1
115.7 (3)	113.9 (3)

114.6 (3)	C (2) -N (1) -La#1	120.9 (5)	C (18) -C (13) -C (14)
89.94 (11)	La-N (1) -La#1	106.7 (4)	C (18) -C (13) -C (12)
127.2 (4)	N (20) -C (2) -N (1)	132.3 (5)	C (14) -C (13) -C (12)
123.3 (4)	N (20) -C (2) -C (3)	117.6 (5)	C (15) -C (14) -C (13)
109.5 (4)	N (1) -C (2) -C (3)	122.2 (5)	C (14) -C (15) -C (16)
121.5 (5)	C (8) -C (3) -C (4)	121.0 (5)	C (17) -C (16) -C (15)
107.0 (4)	C (8) -C (3) -C (2)	116.9 (5)	C (16) -C (17) -C (18)
131.5 (5)	C (4) -C (3) -C (2)	121.5 (5)	C (13) -C (18) -C (17)
117.3 (5)	C (5) -C (4) -C (3)	106.2 (4)	C (13) -C (18) -C (19)
120.9 (5)	C (4) -C (5) -C (6)	132.1 (5)	C (17) -C (18) -C (19)
121.0 (5)	C (7) -C (6) -C (5)	127.2 (4)	N (20) #1 -C (19) -N (11)
117.9 (6)	C (6) -C (7) -C (8)	122.9 (4)	N (20) #1 -C (19) -C (18)
121.2 (5)	C (7) -C (8) -C (3)	109.9 (4)	N (11) -C (19) -C (18)
132.8 (5)	C (7) -C (8) -C (9)	123.0 (4)	C (2) -N (20) -C (19) #1
106.0 (4)	C (3) -C (8) -C (9)	107.2 (4)	C (22) -N (21) -C (25)
127.0 (4)	N (10) -C (9) -N (1)	123.2 (3)	C (22) -N (21) -La
122.8 (4)	N (10) -C (9) -C (8)	123.7 (3)	C (25) -N (21) -La
110.1 (4)	N (1) -C (9) -C (8)	126.5 (4)	N (21) -C (22) -C (44)
123.0 (4)	C (12) -N (10) -C (9)	108.8 (4)	N (21) -C (22) -C (23)
107.0 (4)	C (12) -N (11) -C (19)	124.6 (4)	C (44) -C (22) -C (23)
118.1 (3)	C (12) -N (11) -La	107.4 (5)	C (24) -C (23) -C (22)
117.3 (3)	C (19) -N (11) -La	107.3 (5)	C (23) -C (24) -C (25)
111.5 (3)	C (12) -N (11) -La#1	125.6 (4)	N (21) -C (25) -C (26)
112.0 (3)	C (19) -N (11) -La#1	109.2 (4)	N (21) -C (25) -C (24)
90.09 (11)	La-N (11) -La#1	125.2 (5)	C (26) -C (25) -C (24)
127.0 (4)	N (10) -C (12) -N (11)	125.6 (4)	C (25) -C (26) -C (28)
122.8 (4)	N (10) -C (12) -C (13)	118.2 (4)	C (25) -C (26) -C (261)
110.2 (4)	N (11) -C (12) -C (13)	116.2 (4)	C (28) -C (26) -C (261)

106.6 (4)	C (28) -N (27) -C (31)	106.6 (4)	C (40) -N (39) -C (43)
120.7 (3)	C (28) -N (27) -La	123.0 (3)	C (40) -N (39) -La
121.6 (3)	C (31) -N (27) -La	123.2 (3)	C (43) -N (39) -La
125.8 (4)	N (27) -C (28) -C (26)	125.8 (4)	N (39) -C (40) -C (38)
109.4 (4)	N (27) -C (28) -C (29)	109.5 (4)	N (39) -C (40) -C (41)
124.6 (4)	C (26) -C (28) -C (29)	124.6 (4)	C (38) -C (40) -C (41)
107.4 (4)	C (30) -C (29) -C (28)	107.5 (4)	C (42) -C (41) -C (40)
107.4 (4)	C (29) -C (30) -C (31)	106.9 (4)	C (41) -C (42) -C (43)
125.0 (4)	N (27) -C (31) -C (32)	125.1 (4)	N (39) -C (43) -C (44)
109.2 (4)	N (27) -C (31) -C (30)	109.4 (4)	N (39) -C (43) -C (42)
125.7 (4)	C (32) -C (31) -C (30)	125.5 (4)	C (44) -C (43) -C (42)
126.5 (4)	C (31) -C (32) -C (34)	125.5 (4)	C (43) -C (44) -C (22)
116.1 (4)	C (31) -C (32) -C (321)	117.7 (4)	C (43) -C (44) -C (441)
117.3 (4)	C (34) -C (32) -C (321)	116.8 (4)	C (22) -C (44) -C (441)
106.5 (4)	C (37) -N (33) -C (34)	118.8 (5)	C (266) -C (261) -C (262)
123.5 (3)	C (37) -N (33) -La	120.6 (5)	C (266) -C (261) -C (26)
123.2 (3)	C (34) -N (33) -La	120.4 (5)	C (262) -C (261) -C (26)
125.2 (4)	N (33) -C (34) -C (32)	120.4 (6)	C (261) -C (262) -C (263)
109.3 (4)	N (33) -C (34) -C (35)	120.6 (6)	C (264) -C (263) -C (262)
125.4 (4)	C (32) -C (34) -C (35)	119.7 (5)	C (263) -C (264) -C (265)
107.7 (4)	C (36) -C (35) -C (34)	119.7 (6)	C (264) -C (265) -C (266)
106.8 (4)	C (35) -C (36) -C (37)	120.8 (6)	C (261) -C (266) -C (265)
125.1 (4)	N (33) -C (37) -C (38)	118.2 (6)	C (326) -C (321) -C (322)
109.7 (4)	N (33) -C (37) -C (36)	121.3 (6)	C (326) -C (321) -C (32)
125.1 (4)	C (38) -C (37) -C (36)	120.5 (5)	C (322) -C (321) -C (32)
126.5 (4)	C (37) -C (38) -C (40)	120.4 (7)	C (321) -C (322) -C (323)
117.1 (4)	C (37) -C (38) -C (381)	120.4 (8)	C (324) -C (323) -C (322)
116.5 (4)	C (40) -C (38) -C (381)	119.8 (6)	C (325) -C (324) -C (323)

120.1 (8)	C (324) -C (325) -C (326)	120.6 (14)	C (382) -C (381) -C (886)
121.2 (8)	C (321) -C (326) -C (325)	116.6 (14)	C (38) -C (381) -C (886)
105.8 (9)	O (327) -C (328) -C (329)	120.2 (6)	C (381) -C (382) -C (383)
113.3 (8)	C (330) -C (329) -C (328)	121.2 (7)	C (884) -C (383) -C (382)
111.4 (10)	O (331) -C (330) -C (329)	121.2 (7)	C (384) -C (383) -C (382)
117.1 (12)	C (332) -O (331) -C (330)	119.0 (6)	C (385) -C (384) -C (383)
122.1 (16)	O (331) -C (332) -C (333)	120.8 (7)	C (384) -C (385) -C (386)
120.4 (19)	O (331) -C (332) -C (337)	121.2 (7)	C (381) -C (386) -C (385)
116.4 (13)	C (333) -C (332) -C (337)	116.7 (16)	C (383) -C (884) -C (885)
120.6 (13)	C (334) -C (333) -C (332)	121 (3)	C (886) -C (885) -C (884)
124.7 (13)	C (333) -C (334) -C (335)	114 (3)	C (885) -C (886) -C (381)
109.5 (14)	C (336) -C (335) -C (334)	117.8 (4)	C (442) -C (441) -C (446)
128.7 (12)	C (337) -C (336) -C (335)	119.3 (4)	C (442) -C (441) -C (44)
118.7 (13)	C (336) -C (337) -C (332)	122.9 (4)	C (446) -C (441) -C (44)
112.6 (8)	O (451) -C (450) -C (449)	121.3 (5)	C (443) -C (442) -C (441)
114.0 (9)	C (450) -C (449) -C (448)	119.8 (5)	C (444) -C (443) -C (442)
105.7 (9)	O (447) -C (448) -C (449)	119.7 (5)	C (443) -C (444) -C (445)
117.1 (5)	C (386) -C (381) -C (382)	120.3 (5)	C (446) -C (445) -C (444)
123.7 (5)	C (386) -C (381) -C (38)	121.1 (5)	C (445) -C (446) -C (441)
119.0 (5)	C (382) -C (381) -C (38)		
2.14 (3)	Cl (91) -C (92)	128 (2)	Cl (93) -C (92) -Cl (91)
1.14 (3)	C (92) -Cl (93)		

Symmetry transformations used to generate equivalent atoms:
 #1 : 1-x, 1-y, 1-z

Table 3. Anisotropic displacement parameters ($\text{\AA}^2 \times 10^4$) for the expression:

$$\exp \{-2\pi^2 (h^2 a^2 U_{11} + \dots + 2hka^* b^* U_{12})\}$$

E.s.ds are in parentheses.

	U_{11}	U_{22}	U_{33}	U_{23}	U_{13}	
La	212.1 (14)	140.2 (13)	158.0 (13)	-4.4 (8)	-57.1 (9)	-
28.2 (9)						
N(1)	236 (19)	174 (18)	177 (18)	6 (14)	-74 (15)	-
17 (14)						
C(2)	210 (20)	220 (20)	180 (20)	8 (17)	-44 (17)	-
36 (17)						
C(3)	260 (20)	240 (20)	200 (20)	-38 (18)	-53 (19)	-
18 (19)						
C(4)	360 (30)	300 (30)	230 (20)	0 (20)	-40 (20)	-
50 (20)						
C(5)	520 (40)	440 (30)	210 (30)	-40 (20)	40 (20)	-
110 (30)						
C(6)	740 (50)	430 (40)	240 (30)	-130 (30)	60 (30)	-
160 (30)						
C(7)	540 (40)	370 (30)	290 (30)	-140 (20)	-20 (30)	-
110 (30)						
C(8)	270 (20)	270 (20)	200 (20)	-14 (18)	-54 (19)	-
6 (19)						
C(9)	230 (20)	220 (20)	170 (20)	-4 (17)	-68 (17)	-
33 (17)						
N(10)	280 (20)	194 (19)	211 (19)	-25 (15)	-67 (16)	-
15 (16)						
N(11)	245 (19)	190 (18)	189 (18)	-5 (14)	-72 (15)	-
31 (15)						
C(12)	280 (20)	190 (20)	210 (20)	9 (17)	-95 (19)	-
13 (18)						
C(13)	300 (20)	180 (20)	250 (20)	5 (18)	-97 (19)	-
24 (18)						
C(14)	420 (30)	190 (20)	310 (30)	-9 (19)	-130 (20)	-
50 (20)						
C(15)	510 (30)	220 (30)	440 (30)	-10 (20)	-190 (30)	-
120 (20)						
C(16)	490 (30)	230 (30)	390 (30)	40 (20)	-130 (30)	-
170 (20)						
C(17)	390 (30)	230 (20)	310 (30)	40 (20)	-100 (20)	-
110 (20)						
C(18)	310 (30)	180 (20)	250 (20)	47 (18)	-110 (20)	-
57 (18)						
C(19)	230 (20)	210 (20)	200 (20)	38 (17)	-65 (18)	-
52 (17)						
N(20)	250 (20)	218 (19)	213 (19)	4 (15)	-79 (16)	-
42 (16)						

N(21)	240 (20)	179 (18)	198 (18)	-3 (14)	-49 (15)	-
34 (15)						
C (22)	260 (20)	210 (20)	200 (20)	-2 (17)	-21 (18)	-
32 (18)						
C (23)	400 (30)	260 (30)	280 (30)	-40 (20)	70 (20)	-
120 (20)						
C (24)	440 (30)	290 (30)	260 (30)	-50 (20)	70 (20)	-
100 (20)						
C (25)	310 (30)	210 (20)	220 (20)	-8 (18)	-45 (19)	-
44 (19)						
C (26)	300 (20)	190 (20)	210 (20)	-22 (17)	-57 (19)	-
29 (18)						
N(27)	260 (20)	169 (18)	170 (18)	-2 (14)	-31 (15)	-
27 (15)						
C (28)	290 (20)	150 (20)	220 (20)	-10 (17)	-76 (19)	-
10 (18)						
C (29)	390 (30)	160 (20)	260 (20)	-25 (18)	-110 (20)	-
71 (19)						
C (30)	350 (30)	190 (20)	250 (20)	22 (18)	-90 (20)	-
80 (19)						
C (31)	300 (20)	140 (20)	220 (20)	13 (16)	-95 (19)	-
35 (17)						
C (32)	300 (20)	180 (20)	200 (20)	19 (17)	-75 (19)	-
61 (18)						
N(33)	245 (19)	184 (18)	158 (17)	-6 (14)	-57 (15)	-
57 (15)						
C (34)	270 (20)	190 (20)	170 (20)	15 (17)	-42 (18)	-
59 (18)						
C (35)	490 (30)	270 (30)	170 (20)	10 (19)	-20 (20)	-
170 (20)						
C (36)	420 (30)	280 (30)	180 (20)	-30 (19)	-40 (20)	-
120 (20)						
C (37)	250 (20)	210 (20)	180 (20)	-9 (17)	-71 (18)	-
70 (18)						
C (38)	290 (20)	200 (20)	220 (20)	-15 (17)	-81 (19)	-
47 (18)						
N(39)	241 (19)	186 (18)	191 (18)	20 (14)	-63 (15)	-
51 (15)						
C (40)	280 (20)	210 (20)	230 (20)	9 (17)	-115 (19)	-
74 (18)						
C (41)	350 (30)	210 (20)	260 (20)	-16 (18)	-80 (20)	-
110 (20)						
C (42)	280 (20)	210 (20)	290 (20)	30 (19)	-80 (20)	-
87 (19)						
C (43)	210 (20)	180 (20)	230 (20)	33 (17)	-65 (18)	-
22 (17)						
C (44)	230 (20)	220 (20)	200 (20)	29 (17)	-41 (18)	-
21 (18)						
C (261)	390 (30)	190 (20)	200 (20)	-5 (18)	-10 (20)	-
70 (20)						
C (262)	530 (40)	270 (30)	280 (30)	-40 (20)	-170 (20)	-
10 (20)						
C (263)	690 (40)	380 (30)	330 (30)	-90 (30)	-220 (30)	-
90 (30)						
C (264)	690 (40)	270 (30)	250 (30)	-80 (20)	0 (30)	-
120 (30)						

40 (20)	C (265)	450 (30)	280 (30)	350 (30)	-100 (20)	60 (30)	-
100 (20)	C (266)	370 (30)	300 (30)	310 (30)	-80 (20)	30 (20)	-
170 (20)	C (321)	500 (30)	230 (20)	190 (20)	-2 (18)	-90 (20)	-
290 (30)	C (322)	530 (40)	420 (30)	240 (30)	0 (20)	-60 (20)	-
590 (40)	C (323)	840 (50)	700 (50)	260 (30)	-50 (30)	-20 (30)	-
880 (60)	C (324)	1710 (110)	620 (50)	200 (30)	-10 (30)	-30 (50)	-
340 (40)	C (325)	1560 (100)	250 (30)	270 (30)	90 (30)	-250 (50)	-
110 (30)	C (326)	890 (50)	220 (30)	280 (30)	50 (20)	-190 (30)	-
150 (40)	O (327)	470 (50)	310 (40)	430 (50)	30 (40)	20 (40)	-
180 (50)	C (328)	420 (70)	390 (70)	510 (70)	140 (60)	-170 (60)	-
330 (30)	C (329)	550 (40)	480 (40)	400 (30)	130 (30)	-110 (30)	-
180 (60)	C (330)	540 (80)	410 (70)	540 (80)	90 (60)	-230 (60)	-
180 (40)	O (331)	480 (50)	440 (50)	380 (50)	80 (40)	-120 (40)	-
340 (100)	C (332)	670 (100)	1040 (150)	150 (60)	-120 (70)	-110 (60)	-
200 (60)	C (333)	500 (70)	420 (70)	270 (50)	20 (50)	-90 (50)	-
170 (60)	C (334)	390 (60)	590 (80)	250 (50)	100 (50)	-30 (50)	-
200 (50)	C (335)	230 (60)	370 (70)	1010 (120)	-120 (70)	10 (60)	-
100 (50)	C (336)	280 (60)	470 (70)	340 (60)	-190 (50)	90 (50)	-
150 (50)	C (337)	480 (70)	230 (50)	310 (60)	-10 (40)	-20 (50)	-
260 (40)	O (451)	480 (50)	570 (60)	330 (40)	80 (40)	-170 (40)	-
330 (30)	C (450)	550 (40)	480 (40)	400 (30)	130 (30)	-110 (30)	-
260 (50)	C (449)	340 (60)	490 (70)	290 (50)	70 (50)	-30 (40)	-
120 (40)	C (448)	280 (50)	360 (60)	310 (50)	30 (40)	-40 (40)	-
170 (30)	O (447)	300 (40)	360 (40)	280 (40)	70 (30)	-40 (30)	-
150 (20)	C (381)	370 (30)	240 (20)	200 (20)	0 (18)	-70 (20)	-
60 (30)	C (382)	550 (40)	310 (30)	410 (30)	-130 (20)	-190 (30)	-
120 (30)	C (383)	750 (50)	330 (30)	460 (40)	-170 (30)	-170 (30)	-
270 (30)	C (384)	700 (40)	360 (30)	270 (30)	-80 (20)	-60 (30)	-

C (385)	390 (50)	570 (60)	220 (40)	-120 (30)	-120 (40)	-
130 (40)						
C (386)	320 (40)	360 (40)	310 (40)	-60 (30)	-150 (40)	-
40 (30)						
C (884)	700 (40)	360 (30)	270 (30)	-80 (20)	-60 (30)	-
270 (30)						
C (441)	240 (20)	220 (20)	220 (20)	16 (18)	-19 (18)	-
60 (18)						
C (442)	300 (30)	400 (30)	250 (20)	50 (20)	-80 (20)	-
150 (20)						
C (443)	380 (30)	450 (30)	250 (30)	100 (20)	-80 (20)	-
150 (30)						
C (444)	310 (30)	310 (30)	310 (30)	50 (20)	-20 (20)	-
100 (20)						
C (445)	240 (20)	390 (30)	390 (30)	70 (20)	-70 (20)	-
100 (20)						
C (446)	260 (30)	320 (30)	310 (30)	70 (20)	-80 (20)	-
40 (20)						
C1 (91)	480 (30)	3850 (160)	2270 (100)	-1830 (110)	-800 (50)	
990 (60)						
C (92)	3100 (400)	1500 (200)	360 (90)	230 (120)	-620 (160)	-
1700 (300)						
C1 (93)	450 (30)	1010 (50)	3370 (140)	-810 (70)	-590 (50)	
110 (30)						
C1 (95)	1140 (60)	1600 (90)	1750 (100)	-260 (90)	110 (70)	-
410 (60)						
C1 (97)	1830 (110)	2760 (160)	1650 (100)	-610 (100)	-640 (80)	-
400 (100)						

Table 4. Hydrogen coordinates ($\times 10^4$) and isotropic displacement parameters ($\text{Å}^2 \times 10^3$). All hydrogen atoms were included in idealised positions with $U(\text{iso})$'s set at $1.2 \times U(\text{eq})$ of the parent carbon atoms.

S.o.f.#	x	y	z	U(iso)
H (4)	7839	5744	1378	37
H (5)	8360	4773	119	51
H (6)	7743	3359	227	61
H (7)	6604	2895	1593	50
H (14)	4280	1636	3623	36
H (15)	3041	751	4417	44
H (16)	2107	1002	5947	43
H (17)	2357	2211	6723	37
H (23)	9899	4031	2471	42
H (24)	9306	2547	2416	44
H (29)	6502	671	4734	32

	H (30)	5431	837	6350	31
	H (35)	4859	3297	8950	38
	H (36)	5413	4804	8997	36
	H (41)	7935	6828	6589	32
	H (42)	8986	6695	4961	31
	H (262)	6543	1562	3062	43
	H (263)	6945	266	2134	54
	H (264)	8600	-708	1777	52
	H (265)	9858	-417	2381	49
	H (266)	9440	866	3347	42
	H (322)	3406	2634	8000	46
	H (323)	2449	1630	9019	68
	H (324)	3328	274	9558	97
0.5					
	H (325)	5149	-107	9042	83
	H (326)	6116	883	8007	56
	H (32A)	3618	-757	10285	51
0.5					
	H (32B)	3561	-1047	9346	51
0.5					
	H (32C)	2385	-1771	10597	55
0.5					
	H (32D)	1767	-762	10966	55
0.5					
	H (33A)	1168	-455	9750	57
0.5					
	H (33B)	1870	-1407	9292	57
0.5					
	H (333)	-587	-55	9917	47
0.5					
	H (335)	-1922	-1317	8408	67
0.5					
	H (336)	-1131	-2792	8960	48
0.5					
	H (337)	73	-2953	9651	43
0.5					
	H (45A)	-1468	1273	9480	55
0.5					
	H (45B)	-2462	996	10232	55
0.5					
	H (44C)	-3107	2391	9806	44
0.5					
	H (44D)	-3457	1724	9261	44
0.5					
	H (44A)	-2011	1957	7939	39
0.5					
	H (44B)	-2801	2924	8275	39
0.5					
	H (382)	5438	7140	7650	49
	H (383)	5204	8226	8750	61
	H (384)	6149	7920	9750	52
0.75					
	H (385)	7114	6445	9815	45
0.75					
	H (386)	7424	5354	8692	38
0.75					

0.25	H(884)	5981	7797	9880	52
0.25	H(885)	7721	6556	9424	72
0.25	H(886)	8051	5557	8249	61
0.5	H(442)	8733	5869	2480	37
	H(443)	9818	6750	1419	43
	H(444)	11309	7070	1670	39
0.5	H(445)	11703	6511	2986	41
	H(446)	10625	5633	4043	37
0.5	H(92A)	-947	2143	15464	172
0.5	H(92B)	-189	1887	16048	172

- site occupancy, if different from 1.

Table 5. Torsion angles, in degrees. E.s.ds are in parentheses.

C(9)-N(1)-C(2)-N(20)	-	C(6)-C(7)-C(8)-C(3)	
179.0(5)		0.0(9)	
La-N(1)-C(2)-N(20)	-	C(6)-C(7)-C(8)-C(9)	
48.7(6)		179.9(6)	
La#1-N(1)-C(2)-N(20)		C(4)-C(3)-C(8)-C(7)	
53.4(6)		0.1(8)	
C(9)-N(1)-C(2)-C(3)		C(2)-C(3)-C(8)-C(7)	-
0.1(5)		179.3(5)	
La-N(1)-C(2)-C(3)		C(4)-C(3)-C(8)-C(9)	-
130.3(3)		179.8(5)	
La#1-N(1)-C(2)-C(3)	-	C(2)-C(3)-C(8)-C(9)	
127.6(3)		0.7(5)	
N(20)-C(2)-C(3)-C(8)		C(2)-N(1)-C(9)-N(10)	-
178.6(5)		177.7(5)	
N(1)-C(2)-C(3)-C(8)	-	La-N(1)-C(9)-N(10)	
0.5(5)		52.7(6)	
N(20)-C(2)-C(3)-C(4)	-	La#1-N(1)-C(9)-N(10)	-
0.8(9)		49.6(6)	
N(1)-C(2)-C(3)-C(4)	-	C(2)-N(1)-C(9)-C(8)	
179.9(5)		0.4(5)	
C(8)-C(3)-C(4)-C(5)	-	La-N(1)-C(9)-C(8)	-
0.2(8)		129.3(3)	
C(2)-C(3)-C(4)-C(5)		La#1-N(1)-C(9)-C(8)	
179.1(6)		128.5(3)	
C(3)-C(4)-C(5)-C(6)		C(7)-C(8)-C(9)-N(10)	-
0.2(10)		2.5(9)	
C(4)-C(5)-C(6)-C(7)	-	C(3)-C(8)-C(9)-N(10)	
0.1(12)		177.4(4)	
C(5)-C(6)-C(7)-C(8)		C(7)-C(8)-C(9)-N(1)	
0.0(11)		179.3(6)	

C (3) -C (8) -C (9) -N (1) 0.7 (5)	-	La#1-N (11) -C (19) -N (20) #1 56.2 (6)	-
N (1) -C (9) -N (10) -C (12) 0.9 (8)	-	C (12) -N (11) -C (19) -C (18) 0.3 (5)	-
C (8) -C (9) -N (10) -C (12) 178.8 (5)	-	La-N (11) -C (19) -C (18) 135.7 (3)	-
C (9) -N (10) -C (12) -N (11) 3.4 (8)	-	La#1-N (11) -C (19) -C (18) 122.2 (3)	-
C (9) -N (10) -C (12) -C (13) 174.9 (4)	-	C (13) -C (18) -C (19) -N (20) #1 178.4 (4)	-
C (19) -N (11) -C (12) -N (10) 179.2 (5)	-	C (17) -C (18) -C (19) -N (20) #1 2.4 (9)	-
La-N (11) -C (12) -N (10) 45.9 (6)	-	C (13) -C (18) -C (19) -N (11) 0.1 (5)	-
La#1-N (11) -C (12) -N (10) 56.4 (6)	-	C (17) -C (18) -C (19) -N (11) 176.1 (5)	-
C (19) -N (11) -C (12) -C (13) 0.7 (5)	-	N (1) -C (2) -N (20) -C (19) #1 1.1 (8)	-
La-N (11) -C (12) -C (13) 135.6 (3)	-	C (3) -C (2) -N (20) -C (19) #1 180.0 (4)	-
La#1-N (11) -C (12) -C (13) 122.1 (3)	-	C (25) -N (21) -C (22) -C (44) 176.9 (5)	-
N (10) -C (12) -C (13) -C (18) 179.3 (4)	-	La-N (21) -C (22) -C (44) 29.5 (7)	-
N (11) -C (12) -C (13) -C (18) 0.7 (5)	-	C (25) -N (21) -C (22) -C (23) 0.9 (6)	-
N (10) -C (12) -C (13) -C (14) 3.7 (9)	-	La-N (21) -C (22) -C (23) 152.8 (4)	-
N (11) -C (12) -C (13) -C (14) 174.8 (5)	-	N (21) -C (22) -C (23) -C (24) 0.2 (7)	-
C (18) -C (13) -C (14) -C (15) 0.3 (8)	-	C (44) -C (22) -C (23) -C (24) 178.0 (5)	-
C (12) -C (13) -C (14) -C (15) 174.7 (5)	-	C (22) -C (23) -C (24) -C (25) 1.1 (7)	-
C (13) -C (14) -C (15) -C (16) 1.3 (9)	-	C (22) -N (21) -C (25) -C (26) 177.8 (5)	-
C (14) -C (15) -C (16) -C (17) 1.2 (9)	-	La-N (21) -C (25) -C (26) 28.7 (7)	-
C (15) -C (16) -C (17) -C (18) 0.0 (9)	-	C (22) -N (21) -C (25) -C (24) 1.6 (6)	-
C (14) -C (13) -C (18) -C (17) 0.9 (8)	-	La-N (21) -C (25) -C (24) 151.9 (4)	-
C (12) -C (13) -C (18) -C (17) 177.0 (5)	-	C (23) -C (24) -C (25) -N (21) 1.7 (7)	-
C (14) -C (13) -C (18) -C (19) 175.7 (5)	-	C (23) -C (24) -C (25) -C (26) 177.6 (6)	-
C (12) -C (13) -C (18) -C (19) 0.5 (5)	-	N (21) -C (25) -C (26) -C (28) 6.2 (8)	-
C (16) -C (17) -C (18) -C (13) 1.0 (8)	-	C (24) -C (25) -C (26) -C (28) 173.0 (5)	-
C (16) -C (17) -C (18) -C (19) 174.5 (5)	-	N (21) -C (25) -C (26) -C (261) 177.5 (5)	-
C (12) -N (11) -C (19) -N (20) #1 178.7 (5)	-	C (24) -C (25) -C (26) -C (261) 3.3 (8)	-
La-N (11) -C (19) -N (20) #1 45.9 (6)	-	C (31) -N (27) -C (28) -C (26) 173.4 (5)	-

La-N(27) -C(28) -C(26)		N(33) -C(34) -C(35) -C(36)	-
42.3(6)		0.2(6)	
C(31) -N(27) -C(28) -C(29)		C(32) -C(34) -C(35) -C(36)	
1.6(5)		177.3(5)	
La-N(27) -C(28) -C(29)	-	C(34) -C(35) -C(36) -C(37)	-
142.7(3)		0.8(6)	
C(25) -C(26) -C(28) -N(27)	-	C(34) -N(33) -C(37) -C(38)	
1.6(8)		175.2(5)	
C(261) -C(26) -C(28) -N(27)		La-N(33) -C(37) -C(38)	-
174.8(5)		33.2(6)	
C(25) -C(26) -C(28) -C(29)	-	C(34) -N(33) -C(37) -C(36)	-
175.9(5)		1.7(5)	
C(261) -C(26) -C(28) -C(29)		La-N(33) -C(37) -C(36)	
0.4(7)		149.9(3)	
N(27) -C(28) -C(29) -C(30)	-	C(35) -C(36) -C(37) -N(33)	
1.0(6)		1.6(6)	
C(26) -C(28) -C(29) -C(30)		C(35) -C(36) -C(37) -C(38)	-
174.1(5)		175.3(5)	
C(28) -C(29) -C(30) -C(31)		N(33) -C(37) -C(38) -C(40)	-
0.0(6)		4.1(8)	
C(28) -N(27) -C(31) -C(32)		C(36) -C(37) -C(38) -C(40)	
176.0(5)		172.4(5)	
La-N(27) -C(31) -C(32)	-	N(33) -C(37) -C(38) -C(381)	
40.1(6)		177.8(4)	
C(28) -N(27) -C(31) -C(30)	-	C(36) -C(37) -C(38) -C(381)	-
1.7(5)		5.7(7)	
La-N(27) -C(31) -C(30)		C(43) -N(39) -C(40) -C(38)	-
142.3(3)		175.3(5)	
C(29) -C(30) -C(31) -N(27)		La-N(39) -C(40) -C(38)	
1.1(6)		33.6(6)	
C(29) -C(30) -C(31) -C(32)	-	C(43) -N(39) -C(40) -C(41)	
176.6(5)		2.1(5)	
N(27) -C(31) -C(32) -C(34)		La-N(39) -C(40) -C(41)	-
0.6(8)		149.0(3)	
C(30) -C(31) -C(32) -C(34)		C(37) -C(38) -C(40) -N(39)	
177.9(5)		3.9(8)	
N(27) -C(31) -C(32) -C(321)	-	C(381) -C(38) -C(40) -N(39)	-
176.3(5)		178.1(5)	
C(30) -C(31) -C(32) -C(321)		C(37) -C(38) -C(40) -C(41)	-
1.0(7)		173.2(5)	
C(37) -N(33) -C(34) -C(32)	-	C(381) -C(38) -C(40) -C(41)	
176.3(5)		4.9(7)	
La-N(33) -C(34) -C(32)		N(39) -C(40) -C(41) -C(42)	-
32.0(6)		0.4(6)	
C(37) -N(33) -C(34) -C(35)		C(38) -C(40) -C(41) -C(42)	
1.2(5)		177.0(5)	
La-N(33) -C(34) -C(35)	-	C(40) -C(41) -C(42) -C(43)	-
150.5(4)		1.3(6)	
C(31) -C(32) -C(34) -N(33)		C(40) -N(39) -C(43) -C(44)	
3.9(8)		175.0(4)	
C(321) -C(32) -C(34) -N(33)	-	La-N(39) -C(43) -C(44)	-
179.1(5)		34.0(6)	
C(31) -C(32) -C(34) -C(35)	-	C(40) -N(39) -C(43) -C(42)	-
173.2(5)		2.9(5)	
C(321) -C(32) -C(34) -C(35)		La-N(39) -C(43) -C(42)	
3.7(8)		148.1(3)	

C (41) -C (42) -C (43) -N (39)		C (321) -C (322) -C (323) -C (324)	
2.7 (6)		0.9 (9)	
C (41) -C (42) -C (43) -C (44)	-	C (322) -C (323) -C (324) -C (325)	-
175.3 (5)		1.2 (10)	
N (39) -C (43) -C (44) -C (22)	-	C (323) -C (324) -C (325) -C (326)	
6.6 (8)		0.7 (10)	
C (42) -C (43) -C (44) -C (22)		C (322) -C (321) -C (326) -C (325)	-
171.1 (5)		0.1 (9)	
N (39) -C (43) -C (44) -C (441)		C (32) -C (321) -C (326) -C (325)	-
175.5 (4)		178.0 (5)	
C (42) -C (43) -C (44) -C (441)	-	C (324) -C (325) -C (326) -C (321)	-
6.9 (7)		0.1 (10)	
N (21) -C (22) -C (44) -C (43)		O (327) -C (328) -C (329) -C (330)	
9.0 (8)		62.6 (13)	
C (23) -C (22) -C (44) -C (43)	-	C (328) -C (329) -C (330) -O (331)	
168.4 (5)		173.6 (10)	
N (21) -C (22) -C (44) -C (441)	-	C (329) -C (330) -O (331) -C (332)	
173.1 (5)		171.4 (13)	
C (23) -C (22) -C (44) -C (441)		C (330) -O (331) -C (332) -C (333)	-
9.6 (8)		53.7 (19)	
C (25) -C (26) -C (261) -C (266)		C (330) -O (331) -C (332) -C (337)	
68.7 (7)		113.8 (16)	
C (28) -C (26) -C (261) -C (266)	-	O (331) -C (332) -C (333) -C (334)	
108.0 (6)		172.9 (12)	
C (25) -C (26) -C (261) -C (262)	-	C (337) -C (332) -C (333) -C (334)	
115.2 (6)		5 (2)	
C (28) -C (26) -C (261) -C (262)		C (332) -C (333) -C (334) -C (335)	-
68.2 (6)		10.2 (19)	
C (266) -C (261) -C (262) -C (263)		C (333) -C (334) -C (335) -C (336)	
1.3 (8)		12.4 (17)	
C (26) -C (261) -C (262) -C (263)	-	C (334) -C (335) -C (336) -C (337)	-
175.0 (5)		11.9 (18)	
C (261) -C (262) -C (263) -C (264)	-	C (335) -C (336) -C (337) -C (332)	
1.5 (9)		8.3 (19)	
C (262) -C (263) -C (264) -C (265)		O (331) -C (332) -C (337) -C (336)	-
0.8 (10)		172.0 (12)	
C (263) -C (264) -C (265) -C (266)		C (333) -C (332) -C (337) -C (336)	-
0.1 (9)		3.9 (19)	
C (262) -C (261) -C (266) -C (265)	-	O (451) -C (450) -C (449) -C (448)	-
0.4 (8)		78.7 (10)	
C (26) -C (261) -C (266) -C (265)		C (450) -C (449) -C (448) -O (447)	-
175.8 (5)		63.0 (12)	
C (264) -C (265) -C (266) -C (261)	-	C (37) -C (38) -C (381) -C (386)	
0.3 (9)		73.1 (8)	
C (31) -C (32) -C (321) -C (326)		C (40) -C (38) -C (381) -C (386)	-
73.2 (6)		105.2 (7)	
C (34) -C (32) -C (321) -C (326)	-	C (37) -C (38) -C (381) -C (382)	-
104.0 (6)		102.4 (6)	
C (31) -C (32) -C (321) -C (322)	-	C (40) -C (38) -C (381) -C (382)	
104.6 (6)		79.3 (6)	
C (34) -C (32) -C (321) -C (322)		C (37) -C (38) -C (381) -C (886)	
78.2 (6)		99.3 (15)	
C (326) -C (321) -C (322) -C (323)	-	C (40) -C (38) -C (381) -C (886)	-
0.3 (8)		78.9 (15)	
C (32) -C (321) -C (322) -C (323)		C (386) -C (381) -C (382) -C (383)	
177.6 (5)		4.7 (10)	

C (38) -C (381) -C (382) -C (383)	-	C (38) -C (381) -C (886) -C (885)	-
179.5 (6)		178 (3)	
C (886) -C (381) -C (382) -C (383)	-	C (43) -C (44) -C (441) -C (442)	-
22.1 (18)		119.7 (5)	
C (381) -C (382) -C (383) -C (884)	-	C (22) -C (44) -C (441) -C (442)	
0.4 (11)		62.1 (6)	
C (381) -C (382) -C (383) -C (384)	-	C (43) -C (44) -C (441) -C (446)	
0.4 (11)		59.6 (7)	
C (382) -C (383) -C (384) -C (385)	-	C (22) -C (44) -C (441) -C (446)	-
5.4 (11)		118.5 (6)	
C (383) -C (384) -C (385) -C (386)		C (446) -C (441) -C (442) -C (443)	-
6.7 (13)		0.9 (8)	
C (382) -C (381) -C (386) -C (385)	-	C (44) -C (441) -C (442) -C (443)	
3.5 (12)		178.5 (5)	
C (38) -C (381) -C (386) -C (385)	-	C (441) -C (442) -C (443) -C (444)	
179.1 (7)		0.5 (9)	
C (384) -C (385) -C (386) -C (381)	-	C (442) -C (443) -C (444) -C (445)	
2.2 (15)		0.0 (9)	
C (382) -C (383) -C (884) -C (885)		C (443) -C (444) -C (445) -C (446)	
18.0 (19)		0.0 (9)	
C (383) -C (884) -C (885) -C (886)	-	C (444) -C (445) -C (446) -C (441)	-
14 (4)		0.5 (9)	
C (884) -C (885) -C (886) -C (381)	-	C (442) -C (441) -C (446) -C (445)	
6 (5)		1.0 (8)	
C (382) -C (381) -C (886) -C (885)		C (44) -C (441) -C (446) -C (445)	-
24 (4)		178.4 (5)	

Symmetry transformation used to generate equivalent atoms:

#1 : 1-x, 1-y, 1-z

Crystal structure analysis of the [La₂ (phthal {(porph)-O(CH₂)₃OC₆H₄O(CH₂)₃O-(porph)})].2(CH₂Cl₂)] complex

Crystal data: C₁₃₂H₈₆La₂N₁₆O₄, 2(CH₂Cl₂), M = 2407.83. Triclinic, space group P-1 (no. 2), a = 13.5286(2), b = 14.4358(2), c = 15.5074(3) Å, α = 85.3515(14), β = 70.9603(17), γ = 77.8062(14)°, V = 2798.02(9) Å³. Z = 1, D_c = 1.429 g cm⁻³, F(000) = 1220, T = 99.98(11) K, μ(Mo-Kα) = 9.13 cm⁻¹, λ(Mo-Kα) = 0.71073 Å.

The crystal was a dark purple prism. From a sample under oil, one, *ca* 0.072 x 0.123 x 0.600 mm, was mounted on a small loop and fixed in the cold nitrogen stream on a Rigaku Oxford Diffraction XtaLAB Synergy diffractometer, equipped with Mo-Kα radiation, HyPix detector and mirror monochromator. Intensity data were measured by thin-slice ω-scans. Total no. of reflections recorded, to θ_{max} = 27.5°, was 76444 of which 12788 were unique (R_{int} = 0.069); 11478 were 'observed' with I > 2σ_I.

Data were processed using the CrysAlisPro-CCD and -RED (1) programs. The structure was determined principally by the intrinsic phasing routines in the SHELXT program (2A), with addition of some atoms in the bridging group located using the difmap option; refinement by full-matrix least-squares methods, on F²'s, in SHELXL (2B) followed. The triple-deck porph-phthal-porph group was clearly identified, but the bridging group between the two porph rings was disordered on either side of the triple-deck unit and was less well-resolved. There were also two solvent CH₂Cl₂ molecules included in the disordered regions. The non-hydrogen atoms were refined with anisotropic thermal parameters. The hydrogen atoms were included in idealised positions and their U_{iso} values were set to ride on the U_{eq} values of the parent carbon atoms. At the conclusion of the refinement, there were still fragments of unidentified 'solvent' molecules in the lattice, but wR₂ = 0.167 and R₁ = 0.068 (2B) for all 12788 reflections weighted w = [σ²(F_o²) + (0.0770 P)² + 14.68 P]⁻¹ with P = (F_o² + 2F_c²)/3; for the 'observed' data only, R₁ = 0.061.

In the final difference map, the highest peak (*ca* 3.3 eÅ⁻³) was close to Cl(91).

Scattering factors for neutral atoms were taken from reference (3). Computer programs used in this analysis have been noted above, and were run through WinGX (4) on a Dell Optiplex 780 PC at the University of East Anglia.

References

1. Programs CrysAlisPro, Rigaku Oxford Diffraction Ltd., Abingdon, UK (2021).
2. G. M. Sheldrick, Programs for crystal structure determination (SHELXT), *Acta Cryst.* (2015) **A71**, 3-8, and refinement (SHELXL), *Acta Cryst.* (2008) **A64**, 112-122 and (2015) **C71**, 3-8.
3. *International Tables for X-ray Crystallography*, Kluwer Academic Publishers, Dordrecht (1992). Vol. C, pp. 500, 219 and 193.
4. L. J. Farrugia, *J. Appl. Cryst.* (2012) **45**, 849–854.

Legends for Figures

Figure 1. An initial view of a molecule of the centrosymmetrical $[\text{La}_2(\text{phthal})\{(\text{porph})\text{O}(\text{CH}_2)_3\text{OC}_6\text{H}_4\text{O}(\text{CH}_2)_3\text{O}-(\text{porph})\}]$ complex, indicating the atom numbering scheme. Thermal ellipsoids are drawn, for clarity, at the 20% probability level.

Figure 2. A view of the refined molecule of the $[\text{La}_2(\text{phthal})\{(\text{porph})\text{O}(\text{CH}_2)_3\text{OC}_6\text{H}_4\text{O}(\text{CH}_2)_3\text{O}-(\text{porph})\}]$ complex.

Figure 3, The linking of the “centrosymmetrical” molecules, through shared atoms, in a polymeric chain.

Figure 4. View showing detail of the triple-decker section of the molecule.

Figure 5. View of the eclipsed rings of the triple-decker section of the molecule.

Notes on the structure

The crystal appears to be centrosymmetrical, space group P-1, with the molecule lying around a centre of symmetry at the mid-point between the two lanthanum atoms, Figure 1. On closer inspection, however, the atoms of the two bridging units are less well-defined than those of the central triple-decker structure and are, I believe, units of disorder, of half-occupancy – for each triple-decker unit, there is only one bridging unit between the outer porph ring systems, Figure 2; this bridging unit is on one side of the triple-decker unit or on the other side, not on both sides.

If these links were of full occupancy atoms, the picture would be as Figure 3, showing overlapping bridging groups, including two atoms common to each of the bridging groups (and a polymeric product of a remarkable preparation!). However, the refinement of the bridging group atoms with half-occupancy gives far lower R values, and shows the unique molecule, Figure 1, as the expected product and a more acceptable result!

The actual molecule (with one bridging unit) has constraints in its packing formation, *viz* as Figure 2, where adjacent molecules are aligned in long columns in the same orientation; of course, the arrangement in neighbouring columns can take the same or the opposite orientation, and, overall, this randomness of orientation yields a centrosymmetric crystal.

Figure 4 shows a different view of the unique molecule and an indication of the atom numbering scheme.

The lanthanum atoms are eight-coordinate with a square-prismatic conformation, Figure 5. For the central, phthalocyanine, ligand, the La–N distances are in the range 2.753(4) and 2.764(4) Å, whereas for the outer, porphyrin rings, the La–N distances lie in the range 2.470(4) – 2.482(4) Å. The lanthanum atoms are 3.9041(5) Å apart, 1.9521(3) Å from the plane of the four phthal N atoms and 1.3595 Å from the mean-plane of the central N₄ atoms of the porph rings. The three ring systems are essentially parallel, about 3.40 Å apart and eclipsed, Figure 5.

There are, also, two distinct solvent molecules (CH₂Cl₂), disordered, in the structure; the methylene carbon was clearly identified in one molecule but was not observed (further disorder?) in the second molecule